

# THE INFLUENCE OF MECHANICAL CONDITIONS ON THE HEALING OF EXPERIMENTAL FRACTURES IN THE RABBIT: A MICROSCOPICAL STUDY

BY DOREEN E. ASHHURST

*Department of Anatomy, St George's Hospital Medical School, Cranmer Terrace,  
London SW17 0RE, U.K.*

*(Communicated by Dame Honor Fell, F.R.S. – Received 4 March 1985)*

[Plates 1–28]

## CONTENTS

|  | PAGE |
|--|------|
| I. INTRODUCTION  | 273  |
| II. MATERIALS AND METHODS                                      | 275  |
| 1. Experimental fractures                                      | 275  |
| 2. Preparation for microscopy                                  | 275  |
| III. RESULTS   | 277  |
| 1. Fractures healing under stable mechanical conditions        | 277  |
| (a) Radiological studies                                       | 277  |
| (b) Microscopical studies                                      | 278  |
| 2. Fractures healing under unstable mechanical conditions      | 282  |
| (a) Radiological studies                                       | 282  |
| (b) Microscopical studies                                      | 283  |
| IV. DISCUSSION   | 287  |
| 1. Formation of the periosteal callus                          | 288  |
| 2. The endosteal callus  | 289  |
| 3. Healing of fractures under stable mechanical conditions     | 289  |
| 4. Healing of fractures under unstable mechanical conditions   | 290  |
| 5. Variation in the healing process                            | 290  |
| 6. Resorption of the periosteal callus                         | 291  |
| 7. The significance of the size of the periosteal callus       | 291  |
| 8. Remodelling of the cortical bone                            | 292  |
| 9. Fate of the cells in the cortical bone and the blood supply | 292  |
| 10. Cartilage and the fracture callus                          | 293  |
| 11. The cells involved in healing                              | 293  |
| 12. Factors involved in the differentiation of cartilage cells | 294  |
| 13. Conclusions  | 295  |
| REFERENCES   | 296  |

To examine in detail the events that lead to healing under different mechanical conditions, experimental fractures of the rabbit tibia were immobilized with either a metal compression plate or a plastic plate, to produce stable or unstable mechanical conditions respectively. To fracture the bone, a small saw cut is made in the medial cortex and three-point pressure is then applied to fracture the remaining cortical bone. A small amount of bone is removed by the saw cut. This is of no consequence when a plastic plate is used because the plate is designed so that a small gap remains between the fractured surfaces. When a compression plate is used, a gap approximately 100  $\mu\text{m}$  wide remains under the plate. In addition, despite the use of compression, only part of the fractured surfaces are normally in contact, so other narrow fracture gaps may remain. The fractures were examined at experimental times from 4 days to 1 year by both light and electron microscopy.

In stable mechanical conditions, a thin layer of periosteal callus starts to form within 4 days and healthy mesenchymal cells and capillaries are adjacent to the fracture. By 7 days the callus is fully developed and is covered by a new periosteum. Over the following weeks it becomes more compact as the cavities are filled by bone. The endosteal callus, if formed, is small.

From 9 days onwards the fracture gaps of between 30 and 100  $\mu\text{m}$  are invaded by mesenchymal cells; macrophages remove the debris and fibroblasts lay down a collagenous matrix. Capillaries are numerous. By 2 weeks, these gaps are lined by osteoblasts producing transverse layers of new bone on the fractured surfaces. The gap is rapidly filled by transversely orientated bone to achieve union by 3–4 weeks. Resorption is limited to very small, isolated regions of the fractured surfaces.

The gaps between 10 and 30  $\mu\text{m}$  wide appear to be too narrow for cells and capillaries to enter, and they are widened by osteoclastic action. Mesenchymal cells and capillaries then enter and bone is laid down on the surfaces of the newly excavated cavities. After union, the region is recognized as a wide band of irregularly organized bone.

In compressed regions, areas of actual contact are very few, and narrow gaps can be seen. Union is achieved by direct Haversian remodelling across gaps up to 9  $\mu\text{m}$  wide. Remodelling starts at about 3 weeks and it is part of the normal process that occurs after union of a fractured cortex.

The events in the fractures healing under unstable mechanical conditions diverge immediately. The initial periosteal reaction is similar, but cancellous bone forms only away from the fracture gap. Mesenchymal cells in a fibrous matrix, but with very few, if any, associated capillaries, persist as a thick layer over the fracture gap. At 6 days islands of cartilage begin to develop, and by 12 days the whole central area is filled by a cartilaginous matrix containing thick and thin collagen fibrils and elastic fibres. The cartilage is replaced by bone by 3–4 weeks. At this point, healthy cells and capillaries are found near the fracture gap. A small endosteal callus may form in a similar way.

The fracture gaps are now invaded. The debris is removed by macrophages, and fibroblasts produce a collagenous matrix. Osteoclasts cover the fractured surfaces, but the amount of resorption is minimal. Capillaries also enter the gap. Within 1–2 weeks the gap is filled by transverse lamellae of bone.

Once the fractured cortex is united, the events are similar in both series of fractures. Resorption of any callus starts. In the periosteal callus, large cavities form particularly along the callus-cortex junction. Over the next 3 months the callus is resorbed and the cortex is extensively remodelled. By 18 weeks no callus remains. The cortical bone is compact, but large cavities filled with fat cells may occur. The overall dimensions of the bone may be larger than that of the contralateral normal tibia, but the layer of cortical bone is thinner. Thus the plate, whether of metal or plastic, affects the structure of the bone.

This study serves to emphasize that the mechanical stability of a healing fracture determines the composition and size of the periosteal callus and the time at which



union across a fracture gap is achieved. The fracture fragments must be mechanically stable, so that there is no movement at the fracture gap before cells can enter and lay down new bone. This may be achieved immediately, though artificially, by a metal compression plate, or slowly, though naturally, by the formation of a large callus of cancellous bone.

The movements and differentiation of the cells involved in healing are discussed. This experimental fracture model will form a basis for future experimental studies of healing fractures.

#### INTRODUCTION

It has been recognized for many centuries that the healing and subsequent alignment of a fractured bone are facilitated by immobilizing the fragments and associated joints. To this end, simple external splintage with wooden boards was used from the 3rd millennium B.C. (Elliot-Smith 1908), until in the 19th century casts of plaster of Paris were made (Mathijssen 1852). Other methods, such as traction, were also developed. Although a fracture usually heals by bony union, other disorders frequently ensue; these are joint stiffness, muscle wasting and fibrosis, and shortening of the healed bone, which together are often referred to as 'fracture disease'. Despite treatment by physiotherapy, reduced mobility – and hence disability – may be permanent. Indeed some orthopaedic surgeons today do not consider this situation to be unacceptable (Haines *et al.* 1984).

During the late 19th century, experiments were started on the internal fixation of fractures by means of plates and screws, or medullary nails (Hansmann 1886). Many types of plates and screws have been used. They all permit a more accurate reduction, or alignment, of the fracture fragments, but with many systems of internal fixation, the fixation of the fragments does not provide sufficient strength, or stability, and further external stabilization with a plaster cast may be required. Thus problems of fracture disease persist.

In the late 1940s Danis (1949) experimented with the use of a compressive force across the fragments to increase the stability of the fracture. His results were encouraging but his ideas were not developed further at that time. In the 1950s a group of Swiss surgeons, who felt that the amount of residual permanent disability due to fractures, particularly among young patients, was unacceptable, decided to experiment further with the use of compression applied either through specially designed plates or through lag screws. The techniques they developed proved successful and make external stabilization of the fracture unnecessary. Hence the associated joints are not immobilized; indeed post-operative mobilization is an integral part of the treatment. Permanent disability is reduced to a minimum and fracture disease is virtually eliminated. This Swiss (AO) system of fracture fixation is now widely used in both human and veterinary medical practice (Müller *et al.* 1969).

With the advent of the use of compression, it became apparent that the mechanical stability at the fracture site affects the healing process. The initial reaction to a fracture, i.e. the formation of a haematoma followed by the invasion of the fracture area by mesenchymal cells, is independent of the stability of the fracture. It is immediately after this initial response that differences occur. If a fracture is treated by a method that leaves it in a mechanically unstable condition, i.e. movement between the fragments is possible, a large periosteal callus of cancellous bone† and cartilage is produced that bridges the fracture fragments externally. The cartilage is gradually replaced by bone and the gap is filled by new bone in a transverse

† The types of bone are classified and named according to the descriptions and nomenclature of Enlow (1975).

orientation. The bone can then resume its normal function. Subsequently the callus is resorbed and the normal structure of the cortical bone is restored by Haversian remodelling.

If, however, a lag screw or plate system that produces compression between the fragments is used, the fracture is mechanically stable and the healing process is greatly changed. Only a very thin, radiographically indistinct, layer of callus composed of bone is produced. Healing across the compressed fracture occurs as a direct result of Haversian remodelling, and any wider gaps are filled with transverse lamellae of bone. This direct healing process has been named 'primary' healing, as opposed to the indirect healing process, or 'secondary' healing described earlier (Schenk & Willenegger 1967).

The processes involved in healing are superimposed upon the normal remodelling, or regenerative, process within the bone. The cortical bone of the diaphyses of the long bones is organized into osteons, or Haversian systems, around a central canal containing blood vessels. Channels are made in old bone by osteoclasts and new osteons are formed within them. Remodelling is accelerated after a fracture and it can be directly responsible for cortical healing (see above). Later it restores the normal structure of the bone. One consequence of this constant remodelling is that all traces of a fracture may eventually be obliterated.

Despite the obvious advantages of stable fixation in the alleviation of fracture disease and the reduction of the incidence of non-union that results from its use (Karström & Olerud 1974), there is still much dispute about its widespread use because the plate, which is commonly made of stainless steel or titanium, protects the bone from some of its normal stress and this is thought to lead, over a period of months, to weakening of the cortical bone due to alterations in its microscopical structure and thickness. When healing is complete, the plate is removed and the normal structure is gradually restored by Haversian remodelling; in the months immediately after removal, refracture may be a hazard. Many surgeons dismiss stable fixation by means of compression systems because they consider that the strength of a healing fracture lies in the callus (McKibbin 1978), and favour methods of stabilization that lead to the production of a large amount of periosteal callus.

Previous studies of both 'primary' and 'secondary' fracture healing (Cruess & Dumont 1975; Ham & Harris 1971; McKibbin 1978; Schenk & Willenegger 1967) are light microscopical and were not designed to provide details of cell migrations and differentiation. Furthermore, the most detailed of these studies, that of Ham (1930), used a rib fracture of the rabbit as a model; the rib is not a typical long bone either structurally or with respect to its mechanical loading. Only Aho (1966) attempted a study using the electron microscope; he made fractures of the rat femur which were not immobilized. The misalignment of such fractures, together with the technical difficulties of specimen preparation, make it difficult to form a coherent picture of the cell movements and differentiation during healing.

It is apparent that much more information about the movements and behaviour of the cells involved in fracture healing is necessary for a better understanding of the effects of mechanical stability on the healing process and to provide a basis for future experimental work. It was therefore decided to embark upon a comparative light and electron microscopical study of healing under stable and unstable mechanical conditions. To remove the ambiguities inherent in many studies because of the inability to relate the position of the tissue shown in electron micrographs to the fracture as a whole, it is essential that the experimental fracture chosen can be well aligned and is amenable to preparation so that sections of the whole fracture might be examined and sites for study by electron microscopy selected.

As a prerequisite to these studies a fracture model was developed with the tibia of the rabbit as the experimental bone (Ashhurst *et al.* 1982). The rabbit is preferred because the cortical bone is thin enough to allow the whole fracture area to be prepared for electron microscopy, and the structure of the cortical bone is Haversian. The fractures are made by three-point pressure around an initial saw cut through the medial cortex. One series of fractures was accurately reduced and plated with rigid metal plates using compression so that the fractures were stable, while another series of fractures was immobilized with deformable plastic plates designed to leave a small gap between the fractured surfaces so that the fractures were unstable. The healing processes in the two series of fractures were predictable and enabled the detailed study described in this paper to be made.

The aim of this comparative study is to elucidate the detailed sequence of cellular events that lead to healing of fractures under different conditions of mechanical stability and that might contribute to the understanding of the relative merits of different types of stabilization. Fracture healing involves the differentiation of mesenchymal cells into fibroblasts, osteoblasts and chondroblasts, as well as the differentiation of monocytes into macrophages, multinucleated giant cells and osteoclasts. Furthermore, mechanical stability affects the differentiation of osteoprogenitor cells into chondroblasts and determines whether or not cartilage is present in the callus. Hence the healing fracture is a site at which some of the factors that control the differentiation of osteoprogenitor and other cells can be studied *in vivo*.

## II. MATERIALS AND METHODS

### 1. *Experimental fractures*

Male New Zealand White rabbits weighing between 3 and 4 kg, i.e. approximately 3 months old, were used for all the experiments. Experimental fractures were made in the left tibia by the method of Ashhurst *et al.* (1982). The medial surface of the tibia is exposed and the periosteum removed. To fracture the bone a cut is made through the medial cortex by using an oscillating saw with a blade 100  $\mu\text{m}$  thick. The bone is fractured from the saw cut by applying pressure on the cortex opposite the cut and at two points on the medial surface away from the saw cut with a specially designed fracture device (figure 1). The fractures were stabilized by means of plates and screws. In one series of 27 rabbits the fractures were stabilized with six-hole, stainless steel, dynamic compression plates (figure 2*a*), which were pre-bent (Bagby & Janes 1958), while in another series of 20 rabbits, the fractures were stabilized with plastic plates of the same dimensions but with round screw holes (figure 2*b*), which were designed so that a gap of 0.5 mm remains between the fracture fragments (Ashhurst *et al.* 1982). The rabbits were kept after operation for experimental periods of 4 days to 1 year; weight-bearing was unrestricted.

### 2. *Preparation for microscopy*

At the predetermined post-operative times, the rabbits were anaesthetized and perfused with heparinized saline (400 ml) followed by fixative. The fixative was glutaraldehyde in 0.1 M phosphate buffer, pH 7.2, to which sucrose was added to give a molarity of 1.5 M; the osmolarity of the buffer plus sucrose was between 340 and 350 mosmol  $\text{l}^{-1}$ . The rabbits were perfused with 100 ml of a solution containing 20% glutaraldehyde by volume, followed by

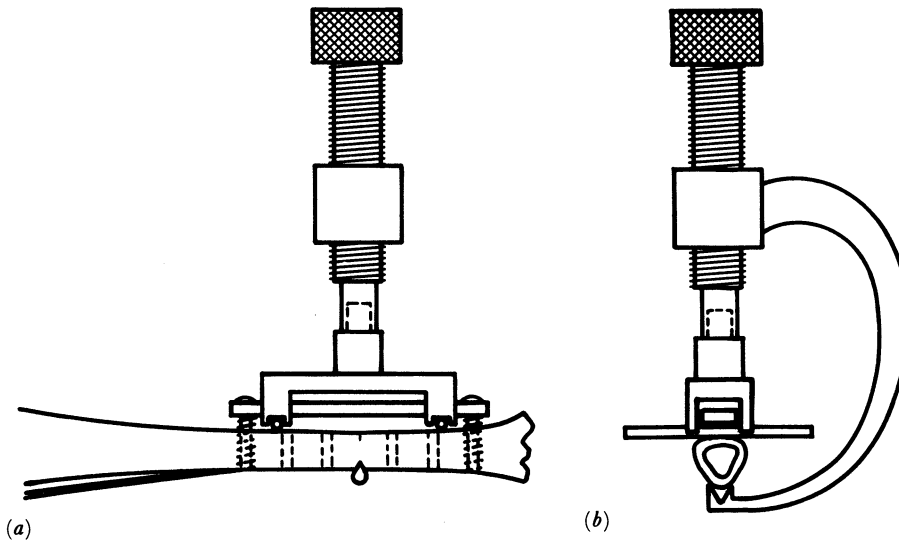


FIGURE 1. Diagrams to show the instruments used to make the fracture in position on a tibia; (a) front view, (b) side view. The plate is attached to the tibia by the two end screws and held off the bone by two rods. The fracture device fits over the plate and rests on the rods. By tightening the clamp, which holds the device in position, three-point pressure is exerted on the bone via the rods and clamp. (From Ashhurst *et al.* (1982), with permission.)

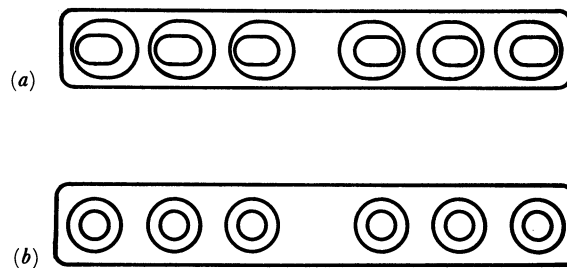


FIGURE 2. Diagram to show the plates used to stabilize the fractures; (a) the stainless steel, dynamic compression plate, (b) the plastic plate. (Magn.  $\times 1\frac{1}{3}$ .) (From Ashhurst *et al.* (1982), with permission.)

400 ml of 5% glutaraldehyde. The fractured bone was then removed and immersed in fixative containing 5% glutaraldehyde. After removal of the plate, the fracture region between the two central screws was removed and cut longitudinally into five or six segments with a circular saw. The pieces were left in fixative to make a total fixation time of 4 h, after which they were washed overnight in several changes of phosphate buffer plus sucrose. They were then decalcified at 4 °C in aqueous EDTA (41 g l<sup>-1</sup>) adjusted to pH 7.2 with sodium hydroxide (Warshawsky & Moore 1967). The completion of decalcification was determined radiologically; depending on their size the segments required between 3 and 6 weeks in EDTA. The decalcified segments were washed in 0.1 M phosphate buffer without sucrose for at least 24 h at 4 °C. They were then postfixed in osmium tetroxide (10 g l<sup>-1</sup>) in 0.1 M phosphate buffer, pH 7.2, for 2 h at room temperature. They were washed briefly in phosphate buffer and dehydrated through graded ethanols for a total period of 4 h. The segments were then transferred to propylene oxide for 10 min before they were placed in a 1:1 mixture of propylene oxide and Spurr's epoxy resin and left overnight at room temperature. The segments were then infiltrated in two changes

of fresh Spurr's resin for at least 3 h before they were embedded in the resin, which was polymerized at 60 °C for at least 48 h. Throughout the decalcification and subsequent preparative procedures each segment was handled individually and the bathing fluids were constantly agitated.

Semi-thin, longitudinal sections of the whole fracture area were cut with glass knives and stained with alkaline Toluidine Blue. Subsequently mesas, about 1 mm square, were made of the area chosen for examination with the electron microscope. Thin sections of silver-gold interference colour were cut from the mesas by using diamond knives (Dupont) with a 55–60° cutting angle. A Reichert OmU4 Ultracut ultramicrotome was used throughout. Thin sections were stained with uranyl acetate and lead citrate and examined with a Philips 301 electron microscope.

All the photomicrographs in this paper were prepared from sections of the blocks used for electron microscopy. Some sections are creased and this is apparent in the photomicrographs. It proved impossible to obtain a perfect large semi-thin section because the tissue is of varying densities.

### III. RESULTS

Two series of fractures were examined: in one series the fractures were immobilized with a stainless steel, dynamic compression plate, and so healed under stable mechanical conditions, whereas in the second they were immobilized with a plastic plate and so healed under unstable conditions. The fractures consist of two regions: the saw cut through the medial cortex, which is under the plate, and the true fracture, which is through the lateral and posterior cortices. The rabbits were not fully grown at the time of operation because the epiphyseal plates were not closed (see figures 3 and 56); comparison of the tibial length at the beginning and end of the experimental times (compare figures 3 and 7, and figures 56 and 60) shows that the operation and plates do not prevent further growth of the bone.

The results reported below are based on observations of at least two fractures at each experimental time. Although the healing process follows a set pattern of cellular events, there is some variation in the precise timing of these events in different animals.

#### 1. *Fractures healing under stable mechanical conditions*

When a dynamic compression plate is applied properly to a fractured bone, a large part of the opposing fractured surfaces of the bone are compressed together so that there is no movement between the fragments and a stable biomechanical environment is created around the fracture. Since the saw cut used to 'start' the fracture necessarily involves the removal of some cortical bone, a narrow gap is always present in the cortex under the plate. In the true fracture region, the fractured surfaces are for the most part in contact, or very close together, but small gaps may exist in some regions due to slight misalignment during the reduction of the fracture. For this reason the healing process varies in different parts of the fracture, as described below.

##### (a) *Radiological studies*

Immediately after the operation, the fracture is visible only as a faint line extending from the saw cut under the plate (figure 3). At 2 weeks the fracture line may be more distinct

(figure 4); the reason for this is not apparent. A very thin irregular layer of callus may be seen at one week, but at two weeks (figure 4) it forms a thin layer of uniform thickness over the whole plated area. The fracture line disappears between 4 and 8 weeks (figures 5 and 6), and when this occurs a less dense area can be seen between the callus and the cortex (figure 6). This appearance persists up to 26 weeks (figures 7 and 8), and thereafter there is no distinction between the callus and the cortex.

(b) *Microscopical studies*

(i) *Fractures less than one week after operation.* The initial reaction to the fracture is the development of a haematoma. At 1 day the only activity is on the endosteal surface where a few monocytes are present on the cortical surface near the fracture, but by 4 days the debris from the haematoma has dispersed and the periosteal reaction has started. This reaction does not occur simultaneously over the whole periosteal surface; it starts on the cortex opposite the plate and gradually extends round the tibia to include the medial cortex, which is covered by the plate. This gradient in the timing of the cellular events from the cortex opposite to that under the plate is apparent throughout the first four weeks as the periosteal callus develops.

Opposite the plate, the cortex is covered by a thick layer of cells (figure 9). Peripherally, a new periosteum is forming, while underneath cancellous bone is being laid down to form the callus. The periosteal layer consists of flattened fibroblasts in a matrix containing bundles of collagen fibrils and elastic fibres orientated longitudinally (figure 11). Beneath the developing periosteum and away from the fracture, the cells are rounded and a matrix containing collagen fibrils is found between them. These cells have the characteristic structure of osteoblasts and they overlie a region in which small trabeculae of cancellous bone have been produced (figure 12). The trabeculae are covered by osteoblasts, and capillaries are found in the spaces. This cancellous bone is attached to the cortical bone of the tibia and already may be continuous over the fracture in some regions (figure 9). Thus, healthy cells are adjacent to the fracture gap by 4 days. Occasional macrophages or fat cells may also be present. Under the plate, the cortex is still covered by the remains of the haematoma.

Endosteal callus formation over the fracture gap was first seen at 6 days; it appears as a cone of cancellous bone. The trabeculae are much thinner than those of the periosteal cancellous bone (figure 10) and the large cavities are confluent with the medullary cavity.

The gap between the fractured surfaces of the bone, irrespective of its width, is filled by cell debris during the first week (figures 9 and 10).

(ii) *Fractures between 1 and 2 weeks old.* The periosteal layer of cancellous bone continues to develop so that by 9 days it covers the cortex away from the plate (figure 13). Its structure is seen in figure 17: the cavities in the bone are lined by osteoblasts and contain numerous capillaries, fibroblasts, macrophages and monocytes in a loose collagenous matrix (figure 19). Over the fracture gap, a small area of fibrous tissue with capillaries remains under the cancellous bone (figure 14). By 12 days the layer of callus covers the whole periosteal surface and varies in thickness from about 0.2 mm under the plate to 1.5 mm elsewhere. It should be noted that the callus is not confined to the area immediately adjacent to the fracture; it covers the whole surface of the bone in the plated region from which the periosteum was stripped. The new periosteum is very well developed at this stage (figures 13 and 17).

The endosteal callus continues to develop in the region over and around the fracture gap

(figure 15). The lamellae are still thinner than those of the cancellous bone of the periosteal callus. Endosteal callus was not produced in all the fractures.

Between 7 and 14 days, a very small island of cartilage is occasionally seen in the space in the cancellous bone adjacent to either the endosteal or periosteal end of the fracture (figure 15); it may persist through only a few 1  $\mu\text{m}$  sections. Cartilage is not seen in association with either callus at later experimental times.

At this stage cells from either or both the periosteal and endosteal surfaces begin to invade the fracture gaps over 75  $\mu\text{m}$  (0.075 mm) wide, i.e. mainly the saw cuts. An example is seen in figure 15. The saw cuts are first invaded by macrophages, monocytes and fibroblasts; the former remove the debris, and the latter lay down a collagenous matrix. As these cells migrate further into the gap, more cells and then capillaries enter (figure 15). The tissue becomes more organized (figure 16); many of the fibroblasts are flattened and form a layer several cells thick along the fracture surfaces, whereas the macrophages, monocytes, fat cells and red cells are more centrally placed among the capillaries (figure 18). Osteoclasts are rarely seen and areas of their activity, recognized by the interruption of the straight walls of a saw cut, are infrequent. Macrophages and other mononuclear cells occur in the matrix, but none are seen along the fractured surfaces. There is no change in the narrower and compressed gaps, which are still full of debris (figure 13).

(iii) *Two-week fractures.* The periosteal callus is becoming more compact because new lamellae of bone are being laid down by the osteoblasts lining the cavities (figure 20). There is no change in the appearance of the endosteal callus.

In the fracture gaps and saw cuts more than 75  $\mu\text{m}$  wide, which were invaded by cells between 1 and 2 weeks, a layer of new bone may now be present on the fractured or cut surfaces (figure 23). It is apparent that the new bone is laid down on surfaces that have undergone little osteoclastic resorption. This is deduced from the correspondence of the contours of the two opposing surfaces which are covered by new bone and the infrequency with which osteoclasts are seen. The new bone is covered by a continuous layer of osteoblasts (figures 23 and 24); a few of these cells have already been trapped in the new bone. Processes of these osteocytes extend towards the osteoblasts (figure 24). The osteoblasts are more rounded in shape than the fibroblasts, and the cell membranes adjacent to the new bone and between the osteoblasts form numerous processes (figure 25); the processes of adjacent cells may be joined by cell junctions. The osteoblasts are filled by abundant rough endoplasmic reticulum and have large Golgi complexes (figure 25). The central region of the gap is usually filled by a matrix containing collagen fibrils (figures 24 and 26) in which capillaries, macrophages and fibroblasts are found.

At this time cells begin to migrate into the gaps between 30 and 75  $\mu\text{m}$  wide. The pattern of the cellular invasion is similar to that in the wider gaps (figures 21 and 22). It was frequently noticed that osteoclasts are found on the cortical surface adjacent to the gap (figures 21 and 22). They widen the opening of the gap periosteally, but they are rarely seen within the gap. The gaps less than 30  $\mu\text{m}$  wide are still filled by debris.

(iv) *Three-week fractures.* The periosteal layer of bone appears still more compact as the cavities continue to be filled by layers of new bone (figure 31). In one fracture the cortical bone is already united across the saw cut (see below) and the periosteal callus is compact

peripherally, but adjacent to the cortical bone large cavities are developing (figure 27). These cavities are distinct from those in the developing callus by virtue both of their large size and their contents; they are not completely lined by osteoblasts and they contain some fat cells (figure 30). The endosteal callus is still confined to a small area at the fracture gap and appears as a loose network of cancellous bone (figure 27); the cavities are not filled in. The endosteal end of the fracture gap is frequently closed by the trabeculae of the callus (figure 27).

The wide gaps are now almost filled by transverse lamellae of bone; in some regions there is continuity of bone across the gap to unite the cortex (figures 27–29), though such regions are not frequent at this 3-week stage. The boundaries between the cortical and new bone in the saw cuts are often straight with only small indentations into the old bone (figure 27–29); these small indentations, or Howship's lacunae, which are less than 40  $\mu\text{m}$  in depth, are the only regions in which resorption of the fractured surfaces has occurred. The cavities that remain between the transverse lamellae are lined by osteoblasts, and contain capillaries, fibroblasts and other cells in a collagenous matrix. The examples illustrated in figures 28 and 29 are different regions of the same saw cut; one (figure 29) shows the saw cut under the plate, the other (figure 28) shows the end of the saw cut and beginning of the fracture; the pattern of the cavities changes completely over a very short distance.

The narrow gaps observed at 3 weeks are of complex structure. In one fracture, owing to a slight inaccuracy in its reduction, parts of the central region are in contact, so that the gap is occluded, while a gap up to 60  $\mu\text{m}$  wide occurs at both the periosteal and endosteal ends (figure 33). The periosteal end of the latter gap is being invaded by fibroblasts and macrophages, although they have not yet penetrated the full depth, but the endosteal end is filled by chondrocytes in a cartilaginous matrix (figures 34 and 35); it must be emphasized that the endosteal end of this gap is sealed by bone of the endosteal callus and the other end by the compressed surfaces of the fracture (figure 33). Thus the tissue in this gap is deprived of a blood supply, which may account for the differentiation of the osteoprogenitor cells into chondroblasts. This is another region of the fracture seen in figures 27 and 29.

In the compressed regions the fracture may be difficult to distinguish, or it may be marked by a line of debris in a gap which can be up to 9  $\mu\text{m}$  wide (figure 31). Haversian remodelling has now started in the cortical bone, and remodelling cavities are crossing these regions of the fractures (figure 32). Some remodelling cavities originate in the cancellous bone of the endosteal or periosteal callus, enter the cortical bone in a transverse direction, and then turn into a longitudinal orientation (figures 27 and 31).

(v) *Four-week fractures.* The periosteal callus resorption, seen occasionally at 3 weeks, now occurs in most fractures. The very large cavities that are produced tend to have a longitudinal orientation and to be located preferentially along the junction with the cortical bone.

The wide fracture gaps and saw cuts continue to be filled by transverse lamellae of bone, which now bridge most regions of the gaps. The cavities remaining in these gaps may veer longitudinally into the old cortical bone; whether this process starts from the gap or whether remodelling cavities penetrate from the cortex to join with those in the gap cannot be determined (figure 40).

In the cortex away from the plate, large remodelling cavities may be present (figures 36 and 38); close examination reveals that these cavities are linked by narrow fracture gaps (figures 37–39) between 10 and 18  $\mu\text{m}$  wide. The orientation of the cavities suggests that they follow



the original fracture line. Some cavities may be partly filled by lamellae of new bone laid down around their periphery (figures 37 and 39), whereas others are at their maximal size (figure 39). Their inner surface is lined for the most part by osteoblasts, but osteoclasts occur where resorption is still active (figure 37). The cavity is filled by capillaries, together with fibroblasts and macrophages (figures 37 and 39). The narrow fracture gaps that remain between the cavities contain debris, but a few cells are beginning to penetrate them. The upper region of the fracture in figure 36 shows the end of this process: a wide area of transversely orientated bone unites the fracture. Figures 36 and 38 are from the same fracture; the regions sampled are less than 1 mm apart. This example illustrates the wide variation in the time course of the healing and the appearance of the fracture sites within one healing fracture. Other gaps between 10 and 30  $\mu\text{m}$  are unchanged at four weeks, but some widening of the gap has usually started at the periosteal end to form a cavity with contents similar to those described earlier. It appears that gaps of less than about 30  $\mu\text{m}$  wide are too narrow for cells to penetrate and that the gap must be widened before the healing process can start. Despite the amount of bone resorbed, few osteoclasts are seen.

The compressed areas of the fracture are now frequently crossed by remodelling cavities (figures 40–42). These may be quite large and cause difficulty in tracing the complete path of the fracture across the cortex, especially where its orientation is oblique. The cavities are longitudinally orientated within the cortex in contrast to those described in association with the 10–30  $\mu\text{m}$  gaps. Osteoclasts and debris are found at the leading end of these cavities (figures 41 and 43). A later stage in this process is seen in figure 44; the leading end of the remodelling cavity has passed beyond the fracture, which is bridged by new bone. Although in photomicrographs the fractured surfaces may appear to be in contact, a small gap of 1  $\mu\text{m}$  or less is nevertheless seen in electron micrographs (figures 43 and 44).

(vi) *Six-week and eight-week fractures.* The healing processes under way at 4 weeks continue. The periosteal callus is further eroded, particularly adjacent to the cortex (figure 45). Osteoclasts are frequently seen along the surfaces of the bone within the cavities, though some parts are still covered by a layer of osteoblasts. The large spaces contain capillaries and many fat cells (figure 45). Erosion of any endosteal callus starts at this time. In all fractures, remodelling cavities enter the cortical bone from both the periosteal and endosteal callus.

The saw cuts and other wide gaps are now filled by transverse lamellae and osteons of new bone; remodelling to replace the transverse bone with longitudinally orientated osteons has started (figures 46 and 47). The regions of transverse bone show an irregular arrangement of lamellae, with differing orientations of collagen fibrils (figure 50); each new lamella of bone is bounded by a lamina limitans. The large cavities are lined by osteoblasts and spindle-shaped cells, which will presumably differentiate into osteoblasts (figure 50). Centrally there is a collagenous matrix, populated by macrophages, monocytes and fibroblasts, through which the capillaries pass.

The situation with the gaps between 10 and 30  $\mu\text{m}$  wide is variable. Some remain unaltered and filled with debris, while in other fractures, large cavities may still be joined across the cortex by narrow gaps, again still filled by debris (figure 46). Other fractures may be identified only by a wide band of transversely orientated osteons making an irregular pathway across the cortex. The overall width of the band may be over 200  $\mu\text{m}$ , so the region of transverse lamellae is much wider than in the healed saw cuts, and this fact, together with their irregular course,

leads to the suggestion that they are the final stage in the healing of the narrow gaps. An occasional gap around 30 to 35  $\mu\text{m}$  wide, filled by a few cells in a collagenous matrix, was seen (figure 48). On more detailed examination these cells appear as rather unhealthy osteoblasts in a bone-like matrix (figure 49). It is possible that after these gaps were invaded by cells their ends were sealed by new bone from the large remodelling cavities (see figure 48), so that the cells are effectively cut off from any source of nutrition.

The compressed regions of the fractures are now crossed by numerous remodelling cavities, which reflects the increased remodelling activity throughout the cortical bone.

(vii) *Twelve-week and eighteen-week fractures.* By this time both the endosteal and periosteal calluses are very thin and may be difficult to distinguish from the cortex, because, owing to the extensive remodelling, the orientation of the Haversian systems is disrupted (figures 51 and 52). Frequently, the original cortex, which can be distinguished by the longitudinal orientation of the osteons, is reduced to a thin layer (figure 51). Large cavities containing fat cells are present, particularly in the old cortical bone and along the endosteal surface; some are confluent with the medullary cavity. The total width of this bone is approximately that of the uninjured cortex.

The saw cuts are fully healed; in most instances, the position of the true fracture is apparent only as an area of remodelling. In some instances, the area of remodelling is interrupted by a length of narrow gap that is still not united. Similarly, compressed regions that have not been traversed by remodelling cavities may be seen at both 12 and 18 weeks (figures 52 and 53). It must be noted that the sections are very thin and hence only a very small portion of the total fracture is being sampled; thus large areas of the fracture will be united and, hence, healed.

(viii) *Twenty-six-week and one-year fractures.* The total thickness of the bone plus callus is now very much reduced, so that it is thinner than the original cortex. The orientation of the osteons is still mostly random. A few large cavities filled by fat cells occur, especially under the plate (figures 54 and 55); many of these are confluent with the medullary cavity, thus making the endosteal surface very irregular (figure 55). The result of these changes is that the diameter of the medullary cavity, and hence of the tibia, is increased. The sites of the fractures can no longer be seen.

## 2. *Fractures healing under unstable mechanical conditions*

The plastic plates used to immobilize these fractures are designed so that a gap of 0.5 mm is left between the fractured surfaces in the region under the plate. Thus both the material of the plate and the gap contribute to the mechanical instability of the fracture. Because of the flexibility of the plate and the weight-bearing permitted, the gap opposite the plate tends to close; in some instances the ends touch and comminution of the fracture may occur during the first few days (see figure 70). Any variation in the width of the fracture gap is not of significance, since all are wide compared with those of the compression-plated fractures.

### (a) *Radiological studies*

A gap is clearly visible in the X-ray of a plastic-plated fracture immediately after operation (figure 56). By 1 week, callus is developing on either side of the fracture, but a large lucent

area develops over the fracture itself. At two weeks, this lucent area is narrower and the callus is seen as a distinct swelling (figure 57). By 3–4 weeks, the lucent region is reduced to a thin line continuous with the fracture gap (figure 58). The callus here is now about 3–4 mm thick. The fracture gap disappears between 6 and 8 weeks (figure 59 and 60), and from this stage onwards the callus gradually becomes thinner and is of uniform thickness along the bone; in most tibiae the periphery of the callus now appears to be denser than the region along the cortex (arrow, figure 60). Thereafter there is little change in the appearance of the radiographs, over the period up to one year (figure 61).

(b) *Microscopical studies*

(i) *Fractures less than one week after operation.* During the first 4 days after fracture there is little reaction apart from the removal of the haematoma. No callus is visible and the fracture gap is filled by debris. By 6 days, a periosteal reaction has started. Cancellous bone develops on the surface of the cortex, but it does not reach the fracture (figure 62). Between and covering this cancellous bone there is an area of loose fibrous tissue (figures 62 and 63). Small areas of cartilage are developing on the periosteal surface of the cancellous bone and over the fibrous tissue (figure 62). While the newly developed bone is well vascularized, the fibrous tissue is not (figure 63). Peripherally a new periosteum is forming.

A detailed examination of the fibrous tissue reveals that its organization varies (figure 63). Debris protrudes from the fracture gap and this is met by an area of macrophages, monocytes and fibroblasts interspersed with erythrocytes lying in the collagenous matrix (figure 65). This region extends for about 400  $\mu\text{m}$ . In the next region, fibroblasts predominate; the cells may show some signs of a preferred orientation and are more widely spaced. Bundles of collagen fibrils occur in the matrix (figure 66). Farther away from the fracture gap, the fibrous tissue merges into regions of bone or cartilage; around the areas of cartilage, the cells appear to be degenerating. The chondrocytes are large and rounded, but they also appear to be degenerating (figure 67). The cartilaginous matrix contains both thick and thin collagen fibrils and elastic fibres. The elastic fibres may be very long and extend from regions of fibrous tissue into the cartilage (figure 64). The cells bordering areas of bone appear healthy and here the matrix contains densely packed, large-diameter collagen fibrils. No blood vessels were seen in either the fibrous region or the cartilage.

No endosteal callus was seen in these early fractures. The fracture gap is either filled by debris or empty (figure 62).

(ii) *Fractures between 1 and 2 weeks old.* During this period the periosteum is reformed and the periosteal callus continues to develop. The cancellous bone grows towards the fracture; the rate of growth is greatest along the cortical surface. Farther outwards, regions of cartilage now separate the cancellous bone from the fibrous tissue (figure 68). The areas of cartilage increase in size over the next few days, so that by 12 days the space between the cancellous bone is filled by cartilage (figure 70); this is the lucent area over the fracture in the radiographs taken at 2 weeks (figure 57). The cartilage forms a roughly triangular area with the apex of the triangle towards the fracture gap.

Ahead of the advancing cancellous bone as the callus approaches the fracture, osteoclasts are occasionally seen forming small lacunae (figures 70 and 74), but the straightness of much of the edge of the cortical bone behind them suggests that only part of the surface of the cortex

is modified by these cells. The areas adjacent to osteoclasts may have many osteoblasts in a matrix containing bundles of collagen fibrils. Farther from the fracture, osteoblasts are laying down bone on the cortical surface and also producing the trabeculae of the callus. These areas are well vascularized.

At the periphery of the callus there is a more rapid development of new trabeculae, which results in the formation of a layer of cancellous bone between the cartilage and periosteum (figures 72 and 73); this represents the first external bridging of the fracture by new bone and is seen at approximately 12 days. These new trabeculae appear in electron micrographs as dense aggregations of collagen fibrils, many of which are aligned in parallel in the matrix. These areas may contain some osteocytes and they are surrounded by an almost continuous layer of osteoblasts. These are active, synthetic cells, filled with cisternae of rough endoplasmic reticulum.

The new periosteum consists of layers of fibroblasts orientated with their long axes parallel to that of the bone. The matrix between the cells contains bundles of collagen fibrils in differing orientations, and some elastic fibres (figure 76). The region of the periosteum examined is over an area in which cancellous bone is just beginning to develop over the cartilage (figures 70 and 71). Deep to the periosteum, there is a layer of fibrous tissue with longitudinally orientated cells (figure 77), then a thicker layer in which osteoblasts predominate and are laying down the first small trabeculae of bone (figure 78). The developing bone contains an area of densely packed matrix with a variety of mesenchymal cells and many capillaries. Beneath the bone there is another region of longitudinally orientated, spindle-shaped fibroblasts (figure 79). The matrix here contains many elastic fibres (figure 80). This layer merges into the outer regions of the cartilage, where again there are many elastic fibres in the matrix (figure 81). Regions such as this suggest that the chondrocytes are recruited from the fibroblasts, because there is a progressive change in the shape of the cells from long spindle-shaped cells in the fibrous tissue and periphery of the cartilage to rounded cells in the deeper regions of the cartilage. The chondrocytes here appear healthy (figure 81). Similarly there is a gradual change in the matrix in the cartilage; it contains thin cartilage-type collagen fibrils, bundles of thicker collagen fibrils and elastic fibres (figure 81). It is conceivable that little cell movement is involved: a change in the type of collagen and other matrix macromolecules synthesized, and an increase in the amount secreted, could account for the increased area of the matrix and the change in the shape of the cells.

If the region of the developing callus immediately over the fracture is examined in more detail, several regions can be distinguished (figures 68 and 69). Debris still protrudes from the fracture gap and at 7–9 days it is surrounded and sometimes penetrated by macrophages, monocytes and a few fibroblasts: only occasional red cells are now seen (figures 68, 69 and 82). Droplets of fat are seen both among the debris and in the adjacent region of the fracture, which is populated by fibroblasts and macrophages (figure 83); a collagenous matrix is present. The next region consists primarily of fibroblasts in a well organized matrix (figure 84). The cells and fibrils tend to be orientated around a semi-circle with its centre at the fracture gap. Some elastic fibres are present in the peripheral regions (figures 84 and 85). Only occasional capillaries penetrate this fibrous layer, but despite the lack of vascularization the cells appear to be healthy. Between 9 and 12 days the areas of cartilage increase in size to replace all the fibrous tissue in the central region (figures 72 and 74). The cartilage abuts directly on to the debris in the fracture gap (figure 86). The structure of both the cells and the matrix of this

cartilage is very variable. Large areas contain chondrocytes of healthy appearance (figures 81 and 86): these are round or oval cells with an irregular outline formed by many microvilli. Their cytoplasm is filled by rough endoplasmic reticulum, Golgi complexes and other organelles. There is no differentiation of the matrix to form lacunae around these cells, although the matrix may not be homogeneous. In some regions (figure 86) it is composed entirely of thin collagen fibrils in a random network, i.e. it is a typical cartilaginous matrix, whereas in other regions (figure 81) the matrix is interrupted by the presence of larger diameter, clearly banded, collagen fibrils and long elastic fibres. The central region of the triangle of cartilage contains degenerating chondrocytes in a very heterogeneous matrix containing bundles of thick collagen fibrils (figure 87). Some large sinusoid-like blood vessels may occasionally occur in this region (figure 74). The peripheral regions of the cartilage are also populated by degenerating and hypertrophied chondrocytes (figures 88 and 89): some of these cells are in a late stage of disintegration. The matrix in these areas is again very diverse. The cells are surrounded by a less dense region of matrix and a lacuna is formed as the cell shrinks. The interlacunar matrix may contain thicker collagen fibrils and elastic fibres in addition to the thin cartilage-type fibrils (figures 88 and 89).

The junctions between the cancellous bone and cartilage may be quite abrupt. In some peripheral areas (figures 72 and 73) the two tissues are separated by a narrow region of very flattened cells: it is pertinent to note that in such areas there is only a very short distance between the healthy osteocytes of the bone and the hypertrophied and degenerating chondrocytes (figure 88). In other regions a process akin to endochondral ossification is in progress. The cartilage is invaded by chondroclasts and mononuclear cells, followed by capillaries, osteoblasts and fibroblasts (figures 75 and 90). Large spaces are made in the cartilage so that only thin spicules remain. These are then covered by osteoblasts, which lay down bone on their surface. In this way, the cartilage is progressively replaced by bone from the peripheral regions towards the centre over the fracture gap.

A developing endosteal callus is present in some fractures. It is thick over the fracture gap and rapidly decreases in size laterally. The trabeculae are thinner than in the periosteal callus, and they do not form a compact network. Very little cartilage may be present in the callus at this time.

The fracture gap is unchanged during this period (figures 68, 70, 72 and 74); in one fracture, a few trabeculae from the endosteal callus are penetrating into the gap under the plate, but this is not occurring in other regions of the same fracture.

(iii) *Three-week to four-week fractures.* The periosteal callus is now fully developed (figure 91); over the fracture it may be 4 mm thick. The cancellous bone is more compact because further layers of bone have been secreted onto the original trabeculae by the osteoblasts. The cancellous bone forms a complete layer peripherally, but remnants of cartilage may remain immediately in line with the fracture gap; this is seen as a lucent line continuous with the gap on the radiograph (figure 58). In some 4-week fractures the cartilage has been completely replaced by cancellous bone, and the callus has consolidated with the result that its width over the fracture is reduced to about 2 mm. Immediately over the gap there is now an area of well-vascularized fibrous tissue; mesenchymal cells and capillaries have moved into this region from the cancellous bone (figure 92). Thus the fracture is bridged externally by a thick layer of cancellous bone.

Cells and capillaries now begin to penetrate the fracture gap from the periosteal callus (figures 91 and 92). The macrophages and monocytes remove the debris, and other cells and capillaries follow. The gap in figure 92 illustrates the different phases in this process. Towards the endosteal end of the gap, debris remains, but it is being removed by macrophages, monocytes and multinucleated giant cells, which are moving in a collagenous matrix secreted by the fibroblasts nearby (figure 93). More periosteally in the centre of the gap, fibroblasts are orientated along its axis and are found with monocytes and capillaries in an ordered matrix (figure 95), but along the sides of the gap there is still some debris and an array of macrophages and monocytes (figure 94). Osteoclasts lie on the bone and they are eroding its surface. This is the first time that any alteration in the width of the gap has been possible and measurements suggest that the amount of bone resorbed is minimal (see next subsection). The cells in the gap are quickly organized and the bone surfaces covered by osteoblasts, which secrete transverse lamellae of new bone. A network of lamellae is formed to unite the cortical bone across the gap.

(iv) *Five-week to eight-week fractures.* Over this period the fracture is united and immediately changes occur in the periosteal callus. Firstly, the cancellous bone is very compact and the layer is now between 1 and 2 mm thick; it no longer forms the distinct bulge over the fracture seen in radiographs at the earlier stages (figures 59 and 60). Over the fracture a few small islands of cartilage may still be found within the trabeculae of the cancellous bone. The most important change during this period is that large resorption cavities develop and are especially frequent along the original cortex (figure 98). The cavities may be very large and some are filled by fat cells. The amount of resorption varies greatly in different regions of the callus. The endosteal callus is now compact, but it is gradually eroded from the medullary cavity so that by 8 weeks little remains.

The fracture gaps are filled by irregularly arranged lamellae of compact bone (figures 97 and 98). Measurements taken from healed saw cuts indicate that osteoclastic resorption leads only to an increase in gap width of between 150 and 400  $\mu\text{m}$ ; this is also illustrated by the straight sides in parts of the saw cut in figure 97. Occasionally a gap that had not been invaded by cells was seen (figure 96); these were narrow gaps, less than 50  $\mu\text{m}$  wide, and occurred in only two of the fractures examined. In both instances the fractures were slightly misaligned and the flexible plate presumably allowed the fracture gap to close slightly away from the plate. Where the fracture is united, remodelling is in progress; the transverse lamellae are being replaced by longitudinal osteons (figures 97 and 98). There are remodelling cavities in the cortex on both sides of the fracture and cavities enter the cortex both from the periosteal callus and the endosteal surface.

(v) *Twelve-week and eighteen-week fractures.* The layer of periosteal callus is gradually removed. Resorption is still most rapid along the junction with the original cortex (figure 99). By 18 weeks the periosteal callus cannot be distinguished from the cortical bone (figure 100).

The site of the fracture is now identified by the presence of transverse lamellae across the cortex. In the region of a fracture shown in figure 99 these lamellae are clearly visible, and there has been no remodelling, but in another region of the same fracture a large part of the cortex at the fracture site has been eroded and a large cavity is present. At 12 weeks the cortex contains many large cavities, and these may be confluent with the medullary cavity (figure 99).

By 18 weeks there is a single layer of compact bone with osteons in varying orientations. It is impossible to distinguish any callus from the cortical bone (figure 100).

(vi) *Twenty-six-week and one-year fractures.* At 26 weeks (figure 101) the appearance of the bone is similar to that at 18 weeks; there may be layers of longitudinally orientated bone, but most of the cortex consists of irregularly orientated osteons. At one year (figure 102) resorption cavities are again seen in the bone; these are filled by fat cells and may be confluent with either the periosteal or endosteal surface of the bone (figure 102). The site of the fracture is no longer visible.

#### IV. DISCUSSION

There have been many studies of fracture healing in both stable and unstable mechanical conditions (see, for example, Aho 1966; Crelin *et al.*, 1978; Grieff 1978; Ham 1930; Schenk & Willenegger 1967), but none of these has provided detailed information about the cell movements and extracellular matrices formed during the healing process. The reasons are primarily the fracture models used and, with the exception of that of Aho (1966), the absence of electron microscopical studies. In the work reported here, a true reproducible fracture is made that can be immobilized so that it is either mechanically stable or unstable, simply by the use of different plates. Thus a direct comparison of the effects of mechanical stability on the healing process is possible. The fractures are well aligned, so the arrangement of the different cells and matrices involved follows a well-defined pattern around the fracture; this is particularly important in unstable conditions since misalignment of the fractured cortices leads to considerable variation in the distribution of the cells and matrices, in the width of the fracture gap, and in the timing of the various stages of healing. It has therefore been possible to make a direct, timed comparison of the effects of the mechanical conditions on fracture healing and these observations have served to emphasize various points.

The more significant findings which are discussed below, may be summarized as follows.

1. Fibrous matrices containing collagen fibrils are produced on the periosteal surface of a fractured bone as soon as mesenchymal cells move into the fracture area. In stable conditions the only other matrix produced is that of bone, but in unstable conditions a cartilaginous matrix is laid down on the pre-existing fibrous matrix, which is incorporated into the new matrix. When cells invade a fracture gap, a fibrous matrix is produced, which is later replaced by bone.

2. The fracture must be mechanically stable before either (a) the regions immediately adjacent to the ends of the fracture gap can be populated by mesenchymal cells, and more importantly, by capillaries, which are essential for new bone formation, or (b) the gap can be invaded by these mesenchymal cells and capillaries and the processes leading to union of the cortex can commence.

3. Although fixation with compression implies that the fractured surfaces are in contact, in practice the regions of actual contact may be very limited, as shown here by the electron micrographs.

4. Narrow gaps between 10 and 30  $\mu\text{m}$  wide in compression-plated fractures are not invaded by cells; they are first widened by osteoclasts and large remodelling cavities are formed along the fracture. This process has not been described previously.

5. Although resorption of the old cortical bone does occur during fracture healing, the

amount resorbed is very small. Because the width of the gap is maintained by the plates, it is possible to estimate the amount of resorption. Resorption is *essential* only in the narrow gaps described in (4) above.

6. The resorption of the periosteal callus starts immediately the fractured cortex is reunited, and the resorption cavities are found initially along the callus-cortex junction.

#### 1. *The formation of the periosteal callus*

The first reaction to a fracture is a proliferation of mesenchymal cells which remove the haematoma, produce a collagenous matrix on the periosteal surface of the bone and form a new periosteum. The cells include fibroblasts, macrophages, monocytes and osteoprogenitor cells, and the area is invaded by capillaries. The source of these cells was not investigated, but there is evidence that some migrate from the surrounding connective tissues while others are blood-borne (Kernek & Wray 1973; Simmons & Kahn 1979). In stable mechanical conditions, a uniformly thin layer of cancellous bone develops over the entire periosteal surface of the cortical bone during the first week, and healthy cells and capillaries are adjacent to the fracture gap. In contrast, in unstable mechanical conditions, cancellous bone is formed on the periosteal surface of the cortical bone away from the fracture leaving a fibrous matrix with few, if any, capillaries over the fracture gap. This fibrous tissue is replaced by a cartilaginous matrix that is heterogeneous in that it contains typical, thin, cartilage-type collagen fibrils, together with bundles of thicker, clearly banded collagen fibrils and elastic fibres. The cells in the cartilage are also heterogeneous: they include healthy, hypertrophied and degenerating chondrocytes, necrotic fibroblasts and macrophages. These observations suggest that the original cells and matrix are not removed before the cartilaginous matrix is secreted; this contrasts with the removal of type I collagen during chondrogenesis in developing chick limb buds (Dessau *et al.* 1980). The cartilage forms a ring around the fracture and it is completely isolated from the other tissues by cancellous bone. Only the peripheral regions of the cartilage are calcified (M. Page & D. E. Ashhurst, unpublished observation) and the cartilage is replaced by bone by a process similar to that of endochondral ossification.

It is often said that fracture healing is similar to endochondral ossification (Ketenjian *et al.* 1978; Lane *et al.* 1979, 1982); this comparison is only partly valid. The cells on the epiphyseal side of the growth plate divide and secrete new matrix continuously and then hypertrophy only when the matrix is calcified, but those in the callus are not dividing and secrete the matrix within a few days and then degenerate almost immediately. The cells in the uncalcified cartilage of a developing limb and growth plate are alive and receive nutrients from the surrounding vascularized tissues (Keuttner & Pauli 1983), whereas all the cells in the callus cartilage are isolated from potential sources of nutrition by the peripheral calcified layer. Any similarities between the two processes are therefore restricted to the replacement of cartilage by bone. The bridging of the fracture gaps described in the present paper involves completely different processes.

The periosteal callus produced under stable mechanical conditions is clearly not a response to mechanical instability. It is very thin; indeed it is often found that in man and some other animals no radiologically visible callus is formed, but it has been observed in the dog (Olerud & Danckwardt-Lillieström 1971). In the present experiments, the periosteum was removed and this might provide a stimulus for callus production in the rabbit (Rahn *et al.* 1971); there is some evidence, however, that intact rabbit bones that have been plated without disturbing the



periosteum also produce a thin layer of periosteal cancellous bone. It therefore appears that any surgical procedure may stimulate the production of periosteal cancellous bone. The fact that implants on human bones are frequently encased in bone at the time of removal suggests that there is often a periosteal reaction in man. Thus any difference between the periosteal reaction in man and the rabbit may be simply one of degree.

### 2. *The endosteal callus*

Endosteal callus is readily distinguished from periosteal callus because it is composed of thinner lamellae of cancellous bone, and in longitudinal section it forms a cone, the apex of which is over the fracture. The amount of callus produced is much more variable than is the case with the periosteal callus and in many fractures none is formed. After union, the endosteal callus is resorbed. It has been suggested (Ashton *et al.* 1980) that the osteoprogenitor cells in the bone marrow might contribute to fracture healing, but in the present experiments the fracture gap was rarely invaded from the endosteal side.

### 3. *Healing of fractures under stable mechanical conditions*

To obtain absolute stability, the fractured surfaces must be in contact and compressed together. These criteria determine the design of the metal compression plates used and require that the fracture be perfectly reduced. In practice this latter condition is not achieved since fractured surfaces are rough and a very small displacement of the proximal and distal fragments relative to each other will disturb the perfect reduction. Further disturbance will also be caused by small fragments of bone produced at the time of fracture. Hence, both in the accurately reduced, experimental fractures described here, and in clinical practice where accurate reduction is more difficult to achieve, the relationship of the fractured surfaces will be variable. In some areas the surfaces will be closely apposed, though actual contact may be much more limited than has been previously suspected (Perren 1979). This is demonstrated very clearly by the electron micrographs of the 'contact' areas; a gap of about 1  $\mu\text{m}$  is seen. Some contact between the opposing fractured surfaces is essential for complete stability, but it has been calculated that this can be achieved in the present conditions if only 0.5% of the area of the opposing surfaces is in contact (J. Cordey, personal communication). In other areas, gaps of up to 100  $\mu\text{m}$  may remain between the fractured surfaces. The mechanical conditions in a fracture are variable. Bending and torque will result in different amounts of force. These forces will deform the bone at points of contact but will tend to open or close the gap in neighbouring regions. Since loading is dynamic, it will change with time and lead to changing conditions.

The way in which cortical bone healing is achieved differs with the width of the gap at the fracture. In regions in which the gap is less than 10  $\mu\text{m}$  wide, direct Haversian remodelling occurs across the gap; this starts at about 3 weeks after fracture, which is the time required for the remodelling processes to be stimulated.

In contrast, the gaps of between 30 and 100  $\mu\text{m}$  are invaded by cells from the periosteal callus between 9 and 14 days after fracture. Any debris is rapidly removed and the cells form an organized tissue with a collagenous matrix. New bone is laid down on the fractured surfaces by 14 days. This follows the general pattern described by Schenk & Willenegger (1967), although Schenk (1978) states that connective tissue is not present before bone is laid down in these gaps. Osteoclasts are rarely seen in these gaps, so there is little resorption of the fractured cortical surfaces. A measure of the amount of resorption is provided by the saw cut

regions because indentations are seen where osteoclastic activity has occurred. This limited resorption was also observed in rabbit fractures by Greiff (1978). Subsequently, the gaps are rapidly filled by transverse lamellae of bone so that union of the cortex may be achieved as early as 3 weeks after fracture.

If the fracture gap is between 10 and 30  $\mu\text{m}$  wide, it is not invaded by mesenchymal cells; the reason for this is not obvious. It is unlikely to be due to a lack of gross mechanical stability, since in the saw cut region of the same fracture healing has proceeded. Very small or localized instability will, however, affect narrower gaps to a greater degree than wider gaps and the higher strain induced in the narrow gap may inhibit the movement of, or not be tolerated by, the cells. A further possibility is that the gap is simply of insufficient width to allow the invasion of cells and capillaries in rapid succession. So these gaps are widened by osteoclastic activity with the resulting formation of large remodelling cavities along the fracture line. The arrangement of the cavities is determined by the route taken along the fracture by the osteoclasts; this appears to be random, because with sections only a few micrometres apart one may show only large cavities along the fracture line, whereas another may show an unaltered fracture gap. Thus the timing of the resorption is variable and the process may take several weeks to complete. The result is a wide band of transverse lamellae across the cortex. Thus osteoclastic resorption is of utmost importance in facilitating the healing of these narrow gaps. This healing process has not been described previously.

Under stable mechanical conditions, union of both contact and gap regions of a fractured cortex may be complete by 6 weeks, but the persistence of narrow gaps and unbridged contact regions as late as 18 weeks suggests that there is no mechanism to ensure that union occurs throughout the whole cortex at the same time.

#### 4. *Healing of fractures under unstable mechanical conditions*

The plastic plates used in these experiments are designed to leave a gap between the fractured cortical surfaces which is about 0.5 mm wide under the plate. Away from the plate the width is variable, due partly to the permitted weight-bearing and partly to the flexibility of the plate. There is only debris in these gaps until the fracture is stabilized externally. This is achieved by 3–4 weeks and the area adjacent to the gap is then populated by healthy mesenchymal cells and capillaries, which invade the fracture gap. There is some osteoclastic activity along the fractured surfaces of the bone, but the amount of resorption is minimal. The gap is filled over the next 1–2 weeks by transverse lamellae of new bone. This emphasizes the fact that only when the external bridging callus is sufficiently strong to eliminate movement between the fracture fragments and provide complete stability, can cells invade the gap.

#### 5. *Variation in the healing process*

This study shows that fracture healing is a heterogeneous and very variable process. Not only is there variation in the timing of the events in different animals, there are variations in the timing in different regions of the same fracture. Added to this, the method by which the fractured cortex is reunited clearly depends on the width of the gap between the fracture surfaces. Neither cartilage nor cancellous bone was normally present in the fracture gap, although it has been described by other workers (Crelin *et al.* 1978; Greiff 1978). The reason is almost certainly that the fracture gaps in the present experiments are too narrow; Greiff (1978) found cancellous bone only in gaps wider than 750  $\mu\text{m}$ , i.e. 0.75 mm, in the rabbit tibia.

In fracture gaps more than 1 mm wide and in displaced fractures, the healing pattern differs greatly from that described here (Aho 1966; Crelin *et al.* 1978; Greiff 1978).

#### 6. *Resorption of the periosteal callus*

In both series of experimental fractures, as soon as the fracture gap is bridged by bone, changes occur in the periosteal callus; it must be emphasized that union may have occurred between only small areas of the fracture surfaces when these changes start. Large resorption cavities develop preferentially along the junction between the cortex and the callus. The thickness of the callus decreases rapidly; by 12 weeks it may be simply a thin shell attached randomly to the cortex. These observations support the hypothesis that the main function of the periosteal callus, when the fracture is unstable, is to provide the complete stability necessary to enable mesenchymal cells to invade the gap. As soon as union by bone is achieved, the mechanical loading of the callus is greatly reduced rendering it redundant.

The large resorption cavities immediately peripheral to the cortex can be identified on the radiographs as a lighter region. The initiation of resorption here may be explained as follows: the mechanical effects of the external bridging callus increase with the cube of the radial distance from the neutral axis of bending, so that the external layers of bone contribute more to overall stiffness and hence decrease the strain at the gap more than those adjacent to it. Thus, after union, the bone adjacent to the cortex is mechanically less efficient and hence is redundant and removed first.

The control of, or stimulus for, callus resorption is not known. Once there is union across even a small part of the fractured cortex, the mechanical loading within the callus is reduced and its resorption starts. Various suggestions have been put forward to explain the control of such mechanisms in bone; these include piezoelectric currents and mechanical signals (Bassett 1968; Jaffe 1981). Recent work shows that mechanical stimulation leads to the increased synthesis of prostaglandin E (PGE) by osteoblasts (Binderman *et al.* 1984; Davidovitch *et al.* 1984; Yeh & Rodan 1984); PGE stimulates bone remodelling and turnover. It is interesting that orthopaedic surgeons report that patients may say that a fracture has healed, and that this claim is subsequently confirmed by the radiographs. It is suggested that this may be associated with the changed mechanical conditions which result from the continuity between the proximal and distal ends of the bone.

#### 7. *The significance of the size of the periosteal callus*

That stability at the fracture site is one of the factors on which the size of the periosteal callus depends has been discussed earlier. Thus stable conditions lead to a minimal amount of periosteal callus, whereas unstable conditions lead to the production of a large callus. It follows, therefore, that the size of the callus may be an indication of the mechanical stability at the fracture site; i.e. the larger the callus, the greater the instability (or the less the stability) at the fracture site. Furthermore, it follows from the observation that resorption of the callus starts as soon as the fracture gap is bridged by bone, that the persistence of a large callus indicates that the fractured cortical bone has not yet united. Clinically, a fracture may be considered to be united when the periosteal callus forms a continuous layer of cancellous bone over the fracture.

### 8. *Remodelling of the cortical bone*

The second phase of fracture healing is the remodelling of the bone to re-establish the original histology. Increased remodelling activity begins at 3–4 weeks irrespective of the initial stability of the fracture. Cavities enter the cortical bone from either the endosteal or periosteal surfaces. It is particularly noticeable that immediately a fracture gap has been bridged by transverse lamellae of bone, it is invaded by longitudinally orientated remodelling cavities. Again, there must be a signal or coordinating system in the bone that initiates and maintains this lengthy process. In the rabbit bones studied, the remodelling phase continues for at least 9 months. Initially only the cortex is remodelled, while the callus is resorbed, but later the remaining callus and cortex are remodelled to form a single layer of compact bone consisting of irregularly orientated osteons; these are replaced gradually by longitudinal osteons. The cortex may now be thinner than the original cortex, but the overall dimensions of the tibia may be greater than those of the contralateral intact bone. The dimensions and structure of the tibiae in these later stages of healing and remodelling is undoubtedly affected by the plates which are still on the bones; a detailed analysis of the effects of the plates on the bone will be the subject of another paper. The original structure of the bone cannot be restored while a plate is attached to the bone, because any plate, irrespective of the material of which it is made, will have a mechanical effect on the bone.

### 9. *Fate of the cells in the cortical bone and the blood supply*

A fracture inevitably disrupts the blood supply to the bone and this will lead to the death of osteocytes, particularly those adjacent to the fracture; Ham (1930) found that 1–5 mm of 'dead' bone is present on either side of a fracture of the rabbit rib, but more recently Rhineland (1980) suggested that in the dog the zone of osteocytic necrosis is much narrower. Many workers consider that this bone is removed and the fracture gap widened before the cortices are reunited (Ham & Harris 1971), but the evidence presented here shows little resorption along the fracture surfaces (except in the 10–30  $\mu\text{m}$  gaps) and that the 'dead' bone remains after union; this view is supported by other workers (McKibbin 1978). The 'dead' bone is removed during the normal remodelling processes. There is no reason why this bone should be removed before union, since the mechanical properties of the bone matrix are not adversely affected by the death of the cells. It is pertinent to point out here that the cells in some parts of all compact bone are dead (Luk *et al.* 1974). Once an osteoblast has passed into the bone matrix it becomes a formative osteocyte involved in matrix formation. As the further deposition of new bone pushes the cell farther from the Haversian canal it becomes a resorptive osteocyte and it lies in a larger lacuna. Finally it becomes a degenerative osteocyte and lies at the periphery of the osteon or in the interstitial bone far from a blood supply, where it may undergo complete lysis to leave a very large empty lacuna containing only flocculent material. Remodelling starts preferentially in the interstitial areas, and Luk *et al.* (1974) suggest that the flocculent material, which is thought to be rich in glycosaminoglycans (Jande 1971), might enhance the remodelling activity. Jee (1964) found that damage to blood vessels and bone cells increases the remodelling rate of Haversian bone. Thus the dead bone at the ends of the fracture fragments might stimulate the remodelling activity.

A further disruption to the blood supply to the bone, which presumably results in some osteocytic death, is produced by the plate. Gunst (1980) found that within 10 min after plating,

the vessels under the plate are occluded, but that normal circulation is re-established within four weeks. This should not interfere with healing because most of the vessels involved in producing new bone in the fracture gap originate outside the cortical bone (see below). It has been suggested recently that much of the porosity seen in plated bone can be attributed to remodelling to repair the initial vascular damage rather than to stress protection (Gautier *et al.* 1984).

The flow of blood through intact cortical bone is centrifugal from the medullary arteries towards the periosteum (Rhineland 1980). The findings reported here emphasize the importance of the blood supply for the development of the new bone essential for healing. They confirm the findings of Rhineland (1980) and Schweiberer & Schenk (1977) that periosteal callus is well vascularized by an extraosseous blood supply, while endosteal callus is vascularized from the medullary arterioles. The fracture gap can be vascularized from either supply, and it was noted that remodelling channels also may enter the cortical bone from either surface. Once the periosteal callus has been resorbed, the remodelling cavities originate endosteally, which suggests that the normal endosteal blood supply has been restored.

#### 10. *Cartilage and the fracture callus*

The cartilage in the fracture callus is usually described as fibrocartilage (Ham & Harris 1971), though this term was used only for initial fibrous tissue around the fracture by Ketenjian *et al.* (1978). Fibrocartilage has a well-organized matrix in which thick collagen fibrils occur in bundles with a preferred orientation (Bloom & Fawcett 1975). The thicker collagen fibrils in the callus cartilage are irregularly arranged and are the remnants of a previous matrix, and the long fibres, seen in the photomicrographs, are elastic fibres that are also present before the cartilaginous matrix is produced. An interlacunar network, as described in fracture callus cartilage by Cole (1981), was not seen. It is therefore suggested that the description of the callus cartilage as fibrocartilage is inaccurate.

The presence of elastic fibres in fracture callus has not been reported previously; it may be significant that elastic fibres are said to occur in regions with a high rate of change of tension or stretching forces (Weiss & Amprino 1941, quoted by Mindell *et al.* 1971). Elastic fibres were not observed in the callus of fractures healing in stable mechanical conditions.

#### 11. *The cells involved in healing*

It was pointed out by Ham in 1930 that the cells responsible for fracture healing originate outside the bone, because once a cell has entered the bone matrix and become an osteocyte it cannot divide or revert to its actively synthetic precursor, the osteoblast. The mesenchymal cells that migrate to the periosteal surface around the fracture in the first 4 days include osteoprogenitor cells and fibroblasts, which presumably migrate from the remains of the periosteum and other surrounding connective tissues, and monocytes, macrophages and an occasional osteoclast, which are haematogenously derived and blood-borne (Kernek & Wray 1973; Simmons & Kahn 1979); mast cells, though reported by Duthie & Barker (1955) to be present near fractures, were never seen. These cells clear the debris of the haematoma, initiate periosteal callus formation and later provide the cells that enter the fracture gap. The invasion of a gap from the endosteal surface was rarely seen. Thus healing depends primarily on cells from outside the bone rather than on cells from the medullary cavity. That osteoprogenitor cells are present in the haemopoietic tissue in the cavity has been demonstrated by Ashton

*et al.* (1980) and Friedenstein (1980); their presence in the medullary cavity is consistent with the fact that during normal remodelling, the newly excavated channels, blood vessels and associated cells enter the cortical bone through the endosteal surface.

In the initial stages of healing monocytes and macrophages remove the debris of the haematoma. Later, mononucleated and multinucleated cells erode the cartilage in the callus of the unstable fractures before its replacement by bone. The role of mononuclear cells, either monocytes or macrophages, in bone resorption has been described by several workers (Teitelbaum *et al.* 1979; Tran Van *et al.* 1982). Typical multinucleated osteoclasts were observed only within the remodelling cavities or on the original cortical bone. The observations presented in this paper in no way conflict with the evidence that blood-borne monocytes are the precursor cells of both macrophages (Volkman & Gowans 1965) and osteoclasts (Burger *et al.* 1982; Hanaoka 1979; Jotereau & Le Douarin 1978; Ko & Bernard 1981; Touw *et al.* 1980).

The role of the osteoclasts is twofold: firstly, they modify surfaces to which new bone is to be attached, and secondly, they excavate the remodelling cavities. They are frequently seen along the periosteal surface of the cortical bone and on the fractured surfaces in the gaps of unstable fractures, but they are rarely present on the fractured surfaces in the wide gaps of the stable fractures. Their role is greater in the healing of the 10–30  $\mu\text{m}$  stable gaps, since resorption is essential before the cells can enter. Osteoclasts resorb only part of the surfaces to which new bone is to be attached. In doing so they produce irregularities in these surfaces that will promote firm attachment of the new bone; Greiff (1978) described ‘plugging’ of the old cortical bone by the new bone. Thus most of the dead bone remains during healing and is removed during the remodelling phase.

The interplay between the macrophages, monocytes and fibroblasts seen in healing skin wounds (Leibovich & Ross 1975) is also exhibited in healing fractures. The macrophages enter a fracture gap first, or are in close proximity to an area of debris, but fibroblasts are always immediately behind them laying down a collagenous matrix in which other cells and capillaries can migrate. It is known that macrophages produce a fibroblast-stimulating factor (Leibovich & Ross 1976), and now a growth factor for osteoblast-like cells and chondrocytes has been isolated from the incubation medium of rat peritoneal macrophages (Rifas *et al.* 1984). This factor is a mitogen and the authors suggest that it may be active in bone and cartilage growth, remodelling and repair. The prevalence of monocytes and macrophages in the fracture areas, especially in the early stages, certainly lends support to the possibility that macrophages have an important role, in addition to that of removing debris.

#### 12. *Factors involved in the differentiation of cartilage cells*

A number of questions arise that concern the factors which inhibit the formation of cancellous bone over the fracture and lead instead to the formation of elastic fibres and later cartilage when the mechanical conditions are unstable; this correlation between mechanical instability and cartilage production in fractures has been noted by other workers (Hall & Jacobson 1975; Pritchard 1964). The problem is especially significant because initially the population of cells over the fracture is the same as in stable mechanical conditions.

One question concerns the stimulus that causes the osteoprogenitor cells over the fracture to differentiate into chondrocytes. The generally accepted hypothesis is that differentiation into osteoblasts occurs where there is a high oxygen tension, whereas differentiation into chondrocytes occurs where the oxygen tension is low (Bassett & Herrman 1961; Jargiello &

Caplan 1983). The availability of oxygen is dependent on the blood supply to the tissue, and the region over the fracture, in which the cartilage is produced, is devoid of capillaries; Ham (1930) also noticed the absence of capillaries in regions of cartilage formation in healing fractures. Thus the primary factors leading to the production of cartilage or bone may act, not directly on the osteoprogenitor cells, but on the endothelial cells of the developing capillary network. That the mechanical stability of the fracture affects capillary ingrowth is illustrated by the numerous capillaries adjacent to the stable fractures but the absence of capillaries in the same region adjacent to unstable fractures. That such effects may be localized is shown by the close juxtaposition of the well-vascularized bone and the avascular cartilage in the callus.

The mechanical conditions may be implicated since they will vary in the different regions of the periosteal callus. When there is movement between the fractured surfaces of the cortical bone, it will impose strain on those cells of the callus that bridge the gap. The strain will be greater centrally over the gap and decrease laterally towards the cancellous bone. The effect of this strain will be minimal on the cancellous bone, but at the boundary between the bone and the soft tissue the strain and/or micromovement may be sufficient to affect adversely the growth of capillaries into the central region and hence result in hypoxic conditions and the differentiation of the osteoprogenitor cells into chondroblasts.

Recently, many factors that affect angiogenesis and the differentiation of chondrocytes and osteoblasts have been described. Many cells, such as macrophages and platelets, produce angiogenic factors, and their production may be stimulated by hypoxic or injured tissue (Hunt *et al.* 1984). Chondrocytes produce an anti-angiogenic factor, which prevents the vascularization of the cartilaginous matrix (Langer *et al.* 1980; Sorgente *et al.* 1975), but as this is effective after cartilage is produced it cannot be involved in the initial inhibition of the vascularization of an undifferentiated region, such as that over the unstable fractures. The matrix components may be implicated because hyaluronate inhibits angiogenesis (Feinberg & Beebe 1983) and the expression of the chondrocytic phenotype (Toole 1972). A number of factors of low molecular mass derived from bone and cartilage matrices has recently been described; these may be chemotaxic and mitogenic for mesenchymal cells, chondrocytes and osteoblasts, and may also stimulate collagen and proteoglycan production (Canalis *et al.* 1984; Kato *et al.* 1982; Mohan *et al.* 1984; Reddi 1983). The role of these factors in the differentiation of the mesenchymal cells into chondrocytes and osteoblasts in healing fractures cannot be assessed on the basis of our present knowledge.

### 13. Conclusions

The main conclusions derived from this study of the effects of mechanical stability on fracture healing in the rabbit are summarized below.

1. Mechanical stability affects the composition of the developing periosteal callus; cartilage is found only where there is instability, or movement, at the fracture site.

2. The inhibition of angiogenesis, which is caused by localized movement within the developing callus, leads to hypoxic conditions, which in turn initiate the differentiation of mesenchymal cells into chondrocytes.

3. Mechanical stability of the fracture fragments is essential before the cell migrations, which subsequently lead to union of the fractured cortex, can take place.

4. The use of a compressive force provides immediate mechanical stability at the fracture site and leads to early cortical union. The development of a large bridging callus of cancellous bone and cartilage as a result of unstable mechanical conditions delays cortical union.

5. Resorption of any periosteal callus starts immediately cortical union is achieved; the area of cortical union at this time may be very limited.
6. Both metal and plastic plates affect the remodelling of the cortical bone after union and lead to changes in its structure.
7. The healing fracture is a site at which the differentiation and migrations of mesenchymal cells may be observed *in vivo*.

I should like to express my gratitude to Mr R. L. Batten, without whose enthusiastic interest and help this project could not have been attempted. I am very grateful to Professor S. M. Perren for inviting me to visit the Laboratory for Experimental Surgery, Davos, Switzerland, to learn the operative techniques; I have benefited greatly from many discussions with him. My thanks are due to Miss Y. Bland, Mrs J. Hogg, Mrs M. Naylor and Mr J. Hynd for their technical assistance and to Mrs M. Coulton for her patience while preparing the typescript. Finally, I am grateful to Dame Honor Fell, F.R.S., for agreeing to communicate this paper for me, and for her valuable comments on the typescript; sadly Dame Honor died on 22 April 1986, before seeing this paper in its final form.

The surgical instruments and implants were provided by AO International and Straumann (Great Britain) Ltd. The work was supported by a project grant from the Medical Research Council.

#### REFERENCES

- Aho, A. J. 1966 Electron microscopic and histological observations on fracture repair in young and old rats. *Acta path. microbiol. scand.* Suppl. **184**, 1–96.
- Ashhurst, D. E., Hogg, J. & Perren, S. M. 1982 A method for making reproducible experimental fractures of the rabbit tibia. *Injury* **14**, 236–242.
- Ashton, B. A., Allen, T. D., Howlett, C. R., Eaglesom, C. C., Hattori, A. & Owen, M. 1980 Formation of bone and cartilage by marrow stromal cells in diffusion chambers *in vivo*. *Clin. Orthop.* **151**, 294–307.
- Bagby, G. W. & Janes, J. M. 1958 The effect of compression on the rate of fracture healing using a special plate. *Am. J. Surg.* **95**, 761–771.
- Bassett, C. A. L. 1968 Biologic significance of piezoelectricity. *Calcif. Tiss. Res.* **1**, 252–272.
- Bassett, C. A. L. & Herrmann, I. 1961 Influence of oxygen concentration and mechanical factors on differentiation of connective tissues *in vitro*. *Nature, Lond.* **190**, 460–461.
- Binderman, I., Shimshoni, Z. & Somjen, D. 1984 Biochemical pathways involved in the translation of physical stimulus into biological message. *Calcif. Tissue int.* **36**, S82–S85.
- Bloom, W. & Fawcett, D. W. 1975 *A textbook of histology*, 10th edn. (1033 pages.) Philadelphia, London and Toronto: W. B Saunders.
- Burger, E. H., Van Der Meer, J. W. M., Van De Gevel, J. S., Gribnau, J. C., Thesingh, C. W. & Van Furth, R. 1982 In vitro formation of osteoclasts from long-term cultures of bone marrow mononuclear phagocytes. *J. exp. Med.* **156**, 1604–1614.
- Canalis, E., Kato, Y., Hiraki, Y. & Suzuki, F. 1984 Effect of cartilage-derived factor on DNA and protein synthesis in cultured rat calvariae. *Calcif. Tissue int.* **36**, 102–107.
- Cole, M. B. 1981 An interlacunar network in fracture callus cartilage. In *The chemistry and biology of mineralized connective tissues* (ed. A. Veis), pp. 363–365. New York: Elsevier, North-Holland.
- Crelin, E. S., White, A. A., Panjabi, M. M. & Southwick, W. O. 1978 Microscopic changes in fractured rabbit tibias. *Connecticut Med.* **42**, 561–569.
- Cruess, R. L. & Dumont, J. 1975 Fracture healing. *Can. J. Surg.* **18**, 403–413.
- Danis, R. 1949 *Théorie et pratique de l'ostéosynthèse*. (296 pages.) Paris: Masson.
- Davidovitch, Z., Shanfeld, J. L., Montgomery, P. C., Lally, E., Laster, L., Furst, L. & Korostoff, E. 1984 Biochemical mediators of the effects of mechanical forces and electric currents on mineralized tissues. *Calcif. Tissue int.* **36**, S86–S97.
- Dessau, W., Von der Mark, H., Von der Mark, K. & Fischer, S. 1980 Changes in the patterns of collagens and fibronectin during limb-bud chondrogenesis. *J. Embryol. exp. Morph.* **57**, 51–60.
- Duthie, R. B. & Barker, A. N. 1955 The histochemistry of the preosseus stage of bone repair studied by autoradiography. The effect of cortisone. *J. Bone Joint Surg.* **37B**, 691–710.
- Elliot-Smith, G. 1908 The most ancient splints. *Br. med. J.* **i**, 732–734.



- Enlow, D. H. 1975 *Hand book of facial growth* (423 pages.) Philadelphia, London and Toronto: W. B. Saunders.
- Feinberg, R. N. & Beebe, D. C. 1983 Hyaluronate in vasculogenesis. *Science, Wash.* **220**, 1177-1179.
- Friedenstein, A. J. 1980 Stromal mechanisms of bone marrow: cloning *in vitro* and retransplantation *in vivo*. In *Immunology of bone marrow transplantation* (ed. S. Thienfelde, H. Rodt & H. J. Kolb), pp. 19-29. Berlin, Heidelberg and New York: Springer-Verlag.
- Gautier, E., Cordey, J., Mathys, R., Rahn, B. A. & Perren, S. M. 1984 Porosity and remodelling of plated bone after internal fixation: result of stress shielding or vascular damage? In *Biomaterials and Biomechanics 1983* (ed. P. Ducheyne, G. Van der Perre & A. E. Aubert), pp. 195-200. Amsterdam: Elsevier.
- Greiff, J. 1978 Bone healing in rabbits after compression osteosynthesis: a comparative study between the radiological and histological findings. *Injury* **10**, 257-267.
- Gunst, M. A. 1980 Interference with blood supply through plating intact bone. In *Current concepts of internal fixation of fractures* (ed. H. K. Unthoff), pp. 268-276. Berlin, Heidelberg and New York: Springer-Verlag.
- Haines, J. F., Williams, E. A., Hargadon, E. J. & Davies, D. R. A. 1984 Is conservative treatment of displaced tibial shaft fractures justified? *J. Bone Joint Surg.* **66B**, 84-88.
- Hall, B. K. & Jacobson, H. N. 1975 The repair of fractured membrane bones in the newly hatched chick. *Anat. Rec.* **181**, 55-70.
- Ham, A. W. 1930 A histological study of the early phases of bone repair. *J. Bone Joint Surg.* **12**, 827-844.
- Ham, A. W. & Harris, W. R. 1971 Repair and transplantation of bone. In *The biochemistry and physiology of bone* (ed. G. H. Bourne), 2nd edn, vol. 3, pp. 337-399. New York and London: Academic Press.
- Hanaoka, H. 1979 The origin of the osteoclast. *Clin. Orthop.* **145**, 252-263.
- Hansmann 1886 Eine neue Methode der Fixirung der Fragmente bei complicirten Fracturen. *Verh. dt. Ges. Chir.* **15**, 134-137.
- Hunt, T. K., Knighton, D. R., Thakral, K. K., Goodson, W. H. & Andrews, W. S. 1984 Studies on inflammation and wound healing: angiogenesis and collagen synthesis stimulated *in vivo* by resident and activated wound macrophages. *Surgery* **96**, 48-54.
- Jaffe, L. F. 1981 Control of development by steady ionic currents. *Fedn Proc. Fedn Am. Socs exp. Biol.* **40**, 125-127.
- Jande, S. S. 1971 Fine structural study of osteocytes and their surrounding bone matrix with respect to their age in young chicks. *J. ultrastruct. Res.* **37**, 279-300.
- Jargiello, D. M. & Caplan, A. I. 1983 The establishment of vascular-derived microenvironments in the developing chick wing. *Dev. Biol.* **97**, 364-374.
- Jee, W. S. S. 1964 The influence of reduced local vascularity on the rate of internal reconstruction in adult long bone cortex. In *Bone biodynamics* (ed. H. M. Frost), pp. 259-277. London: J. & A. Churchill.
- Jotereau, F. V. & Le Douarin, N. M. 1978 The developmental relationships between osteocytes and osteoclasts: a study using the quail-chick nuclear marker in endochondral ossification. *Dev. Biol.* **63**, 253-265.
- Karlström, G. & Olerud, S. 1974 Fractures of the tibial shaft. A critical evaluation of treatment alternatives. *Clin. Orthop.* **105**, 82-115.
- Kato, Y., Watanabe, R., Nomura, Y., Tsuji, M., Suzuki, F., Raisz, L. G. & Canalis, E. 1982 Effect of bone-derived growth factor on DNA, RNA, and proteoglycan synthesis in cultures of rabbit costal chondrocytes. *Metabolism* **31**, 812-815.
- Kernek, C. B. & Wray, J. B. 1973 Cellular proliferation in the formation of fracture callus in the rat tibia. *Clin. Orthop.* **91**, 197-209.
- Ketenjian, A. Y., Jafri, A. M. & Arsenis, C. 1978 Studies on the mechanism of callus cartilage differentiation and calcification during fracture healing. *Orthop. Clinics* **9**, 43-65.
- Ko, J. S. & Bernard, G. W. 1981 Osteoclast formation *in vitro* from bone marrow mononuclear cells in osteoclast-free bone. *Am. J. Anat.* **161**, 415-425.
- Kuettner, K. E. & Pauli, B. U. 1983 Vascularity of cartilage. In *Cartilage* (ed. B. K. Hall), vol. 1 (*Structure, function and biochemistry*), pp. 281-312. New York: Academic Press.
- Lane, J. M., Boskey, A. L., Li, W. K. P., Eaton, B. & Posner, A. S. 1979 A temporal study of collagen, proteoglycan, lipid and mineral constituents in a model of endochondral osseous repair. *Metab. Bone Dis. rel. Res.* **1**, 319-324.
- Lane, J. M., Golembiewski, G., Boskey, A. L. & Posner, A. S. 1982 Comparative biochemical studies of the callus matrix in immobilized and non-immobilized fractures. *Metab. Bone Dis. rel. Res.* **4**, 61-68.
- Langer, R., Conn, H., Vacanti, J., Haudenschild, C. & Folkman, J. 1980 Control of tumor growth in animals by infusion of an angiogenesis inhibitor. *Proc. natn. Acad. Sci. USA.* **77**, 4331-4335.
- Leibovich, S. J. & Ross, R. 1975 The role of the macrophage in wound repair. *Am. J. Path.* **78**, 71-100.
- Leibovich, S. J. & Ross, R. 1976 A macrophage-dependent factor that stimulates the proliferation of fibroblasts *in vitro*. *Am. J. Path.* **84**, 501-514.
- Luk, S. C., Nopajaroonsri, C. & Simon, G. T. 1974 The ultrastructure of cortical bone in young adult rabbits. *J. ultrastruct. Res.* **46**, 184-205.
- Mathijssen, A. 1852 *Nieuwe wijze van aanwending van het gips-verband bij beenbreuken. Eene bijdrage tot de militaire chirurgie* (19 pages.) Haarlem: J. B. Van Loghem.
- McKibbin, B. 1978 The biology of fracture healing in long bones. *J. Bone Joint Surg.* **60B**, 150-162.

- Mindell, E. R., Rodbard, S. & Kwasman, B. G. 1971 Chondrogenesis in bone repair. A study of the healing fracture callus in the rat. *Clin. Orthop.* **79**, 187-196.
- Mohan, S., Linkhart, T., Farley, J. & Baylink, D. 1984 Bone-derived factors active on bone cells. *Calcif. Tissue int.* **36**, S139-S145.
- Müller, M. E., Allgöwer, M., Schneider, R. & Willenegger, H. 1969 *Manual of internal fixation: techniques recommended by the AO Group*, 2nd edn. (409 pages.) Berlin, Heidelberg and New York: Springer-Verlag.
- Olerud, S. & Danckwardt-Lillieström, G. 1971 Fracture healing in compression osteosynthesis. *Acta orthop. scand. Suppl.* **137**, 1-44.
- Perren, S. M. 1979 Physical and biological aspects of fracture healing with special reference to internal fixation. *Clin. orthop.* **138**, 175-196.
- Pritchard, J. J. 1964 Histology of fracture repair. In *Modern trends in orthopaedics* (ed. J. M. P. Clark), vol. 4. pp. 69-90. London: Butterworth.
- Rahn, B. A., Gallinaro, P., Baltensperger, A. & Perren, S. M. 1971 Primary bone healing. An experimental study in the rabbit. *J. Bone Joint Surg.* **53A**, 783-786.
- Reddi, A. H. 1983 Regulation of local differentiation of cartilage and bone by extracellular matrix: a cascade type mechanism. In *Limb development and regeneration* (ed R. O. Kelly, P. F. Goetinck & J. A. MacCabe), part B, pp. 261-268. New York: A. R. Liss.
- Rhineland, F. W. 1980 Vascular proliferation and blood supply during fracture healing. In *Current concepts of internal fixation of fractures* (ed. H. K. Uthoff), pp. 9-14. Berlin, Heidelberg and New York: Springer-Verlag.
- Rifas, L., Shen, V., Mitchell, K. & Peck, W. A. 1984 Macrophage-derived growth factor for osteoblast-like cells and chondrocytes. *Proc. natn. Acad. Sci. U.S.A.* **81**, 4558-4562.
- Schenk, R. 1978 *Histology of fracture repair and non-union*. Berne: AO Bulletin, Swiss Association for the Study of Internal Fixation. (40 pages.)
- Schenk, R. & Willenegger, H. 1967 Morphological findings in primary fracture healing. *Symp. biol. hung.* **7**, 75-86.
- Schweiberer, L. & Schenk, R. 1977 Histomorphologie und Vaskularisation der sekundären Knochenbruchheilung, unter besonderer Berücksichtigung der Tibiaschaftfraktur. *Unfallheilkunde* **80**, 275-286.
- Simmons, D. J. & Kahn, A. J. 1979 Cell lineage in fracture healing in chimeric bone grafts. *Calcif. Tiss. int.* **27**, 247-253.
- Sorgente, N., Kuettner, K. E., Soble, L. W. & Eisenstein, R. 1975 The resistance of certain tissues to invasion. II. Evidence for extractable factors in cartilage which inhibit invasion by vascularized mesenchyme. *Lab. Invest.* **32**, 217-222.
- Teitelbaum, S. L., Stewart, C. C. & Kahn, A. J. 1979 Rodent peritoneal macrophages as bone resorbing cells. *Calcif. Tiss. int.* **27**, 255-261.
- Toole, B. P. 1972 Hyaluronate turnover during chondrogenesis in the developing chick limb and axial skeleton. *Dev. Biol.* **29**, 321-329.
- Touw, J. J. A., Hemrika-Wagner, A. M. & Vermeiden, J. P. W. 1980 An electron microscopic, enzyme cytochemical study on the localization of lactate dehydrogenase (LDH) in osteoclasts and peritoneal macrophages of the rat and its implication for the process of bone resorption and the origin of osteoclasts. *Cell Tissue Res.* **209**, 111-116.
- Tran Van, P., Vignery, A. & Baron, R. 1982 An electron-microscopic study of the bone-remodelling sequence in the rat. *Cell Tissue Res.* **225**, 283-292.
- Volkman, A. & Gowans, J. L. 1965 The origin of macrophages from bone marrow in the rat. *Br. J. exp. Path.* **46**, 62-70.
- Warshawsky, H. & Moore, G. 1967 A technique for the fixation and decalcification of rat incisors for electron microscopy. *J. Histochem. Cytochem.* **15**, 542-549.
- Yeh, C.-K. & Rodan, G. A. 1984 Tensile forces enhance prostaglandin E synthesis in osteoblastic cells grown on collagen ribbons. *Calcif. Tissue int.* **36**, S67-S71.

## ABBREVIATIONS USED ON FIGURES

|     |                          |     |                           |     |                             |
|-----|--------------------------|-----|---------------------------|-----|-----------------------------|
| c   | collagen fibrils         | en  | endothelial cell          | mo  | monocyte                    |
| ca  | cartilage                | er  | erythrocyte               | nb  | new bone                    |
| cap | capillary                | f   | fibroblast                | ob  | osteoblast                  |
| cb  | cancellous bone          | fc  | fat cell                  | oc  | osteocyte                   |
| ch  | chondrocyte              | fs  | fractured surface         | ocl | osteoclast                  |
| chl | chondroclast             | ft  | fibrous tissue            | p   | periosteum                  |
| ctb | cortical bone            | g   | fracture gap              | pc  | periosteal callus           |
| d   | debris                   | gc  | Golgi complex             | pob | preosteoblast               |
| dch | degenerating chondrocyte | m   | mitochondrion             | rc  | remodelling cavity          |
| ec  | endosteal callus         | ma  | macrophage                | rer | rough endoplasmic reticulum |
| el  | elastic fibre            | mgc | multinucleated giant cell | tr  | trabecula                   |

The direction of the periosteum is towards the top of each figure unless otherwise indicated thus → P.

## DESCRIPTION OF PLATE 1

FIGURES 3–8. Radiographs of tibial fractures stabilized with a metal compression plate. Figures 3–7 are a series of radiographs of the tibia of a rabbit that was killed at 12 weeks. Figure 8 is a radiograph of the tibia of a different rabbit, killed at 26 weeks. Figure 3 is a radiograph taken immediately post-operation. The saw cut is seen in the cortex under the plate, and the fracture can be seen crossing both the proximal and distal cortices. Figure 4 is a 2-week radiograph; a thin layer of callus, of uniform thickness can be seen (arrow). Figure 5 is a 4-week radiograph; the callus is now more dense (arrow). Figure 6 is an 8-week radiograph; the fracture line is no longer visible, and a less dense area is present between the callus and cortex (arrow). Figure 7 is a 12-week radiograph. Figure 8 is a 26-week radiograph of a fully healed fracture. (Actual size.)

FIGURE 9. Photomicrograph of a mechanically stable fracture at 4 days. A thin layer of cancellous bone (cb) extends over the fracture on the periosteal surface. A new periosteum (p) is beginning to develop. The narrow fracture gap (g) contains some debris, but healthy cells are adjacent to it periosteally. (The numbers 11 and 12 denote the positions of figures 11 and 12.) (Magn. × 100.)

FIGURE 10. Photomicrograph of the endosteal callus of a 9-day fracture. The cancellous bone (cb) forms a cone over the fracture. The lamellae of the bone are thinner than those of the periosteal callus (see figures 9 and 13). The fracture gap (g) is filled by debris. (Magn. × 96.)

## DESCRIPTION OF PLATE 2

FIGURE 11. Electron micrograph of the developing periosteum at 4 days seen in figure 9 (= 11). Fibroblasts (f) are aligned parallel to the periosteal surface (p). They are separated by collagen fibrils (c) in differing orientations. Elastic fibres (el) are also present. (Magn. × 6300.)

FIGURE 12. Electron micrograph of the surface of a developing trabecula (tr) of the cancellous bone of the periosteal callus at 4 days seen in figure 9 (= 12). Its surface is covered by active osteoblasts (ob). (Magn. × 3700.)

## DESCRIPTION OF PLATE 3

FIGURE 13. Photomicrograph of a 9-day mechanically stable fracture. The narrow fracture gap (g) is filled by debris. A complete layer of cancellous bone (cb) with periosteum (p) covers the periosteal surface. The cortical bone is being invaded from the cancellous bone to form remodelling cavities (arrows). (The numbers 14 and 17 denote the positions of figures 14 and 17.) (Magn. × 26.)

FIGURE 14. Photomicrograph at higher magnification of the periosteal cancellous bone over the fracture gap seen in figure 13 (= 14). The large space over the gap is filled by cells. The cells are adjacent to, but do not penetrate, the gap (arrow). Osteoclastic resorption has occurred along the edge of the cortical bone (arrowheads). (Magn. × 96.)

FIGURE 15. Photomicrograph of a saw cut and endosteal callus at 12 days in a mechanically stable fracture. A small area of cartilage is present in the callus (arrowhead). The gap is between 110 and 150 μm wide. Cells have penetrated from the underlying cancellous bone (cb) and the straight sides indicate that there has been no resorption of the cortical bone. The contents of the gap become less organized away from the cancellous bone (arrow). (The number 16 denotes the position of figure 16.) (Magn. × 65.)

FIGURE 16. Photomicrograph at higher magnification of part of the gap seen in figure 15 (= 16). In the lower regions, the surface of the cortical bone is covered by spindle-shaped, fibroblast-like cells (f), while more rounded cells, macrophages, monocytes, and capillaries (cap) fill the central region. In the upper region there is less organization and debris (d) remains. (The number 18 denotes the position of figure 18.) (Magn.  $\times 240$ .)

FIGURE 17. Photomicrograph of part of the callus and periosteum seen in figure 13 (= 17). New lamellae of bone (arrows) are being laid down on the original trabeculae of cancellous bone (cb) and these are covered by the osteoblasts (ob). The cavities contain capillaries (cap) and other cells in a matrix. The new periosteum (p) has formed, but some of the connective tissue of the surrounding muscles is attached to it. (Magn.  $\times 108$ .)

#### DESCRIPTION OF PLATE 4

FIGURE 18. Electron micrograph of part of the gap seen in figures 15 and 16 (= 18). The surface of the cortical bone is covered by spindle-shaped, fibroblast-like cells (f). Some similar cells occur in the central region, together with monocytes (mo), a capillary (cap) and some red cells (er). These are surrounded by matrix containing many collagen fibrils (c). (Magn.  $\times 3460$ .)

FIGURE 19. Electron micrographs of a typical cavity in the cancellous bone of the periosteal callus at 9 days. The cavity is lined by osteoblasts (ob) with monocytes (mo) and a capillary (cap) in the centre. Osteocytes (oc) are trapped in the trabeculae (tr) of the bone. (Magn.  $\times 2500$ .)

#### DESCRIPTION OF PLATE 5

FIGURE 20. Photomicrograph of a 2-week mechanically stable fracture. The periosteal callus is more compact. The space in the cancellous bone over the narrow fracture gap (g) is filled by cells that have invaded the gap. (The number 21 denotes the position of figure 21.) (Magn.  $\times 39$ .)

FIGURE 21. Photomicrograph at higher magnification of the fracture gap and adjacent cancellous bone in figure 20 (= 21). The contours of the opposing fractured surfaces correspond approximately, which suggests that there has been little or no resorption; osteoclasts cannot be identified within the gap. The periosteal surface of the cortical bone has been eroded (arrows), and osteoclasts (ocl) are present in the depressions. (The number 22 denotes the position of figure 22.) (Magn.  $\times 161$ .)

FIGURE 22. Electron micrograph of part of the opening of the gap seen in figure 21 (= 22). Macrophages (ma) and monocytes (mo) are found adjacent to and entering the gap. There are no cells covering the fractured surface (fs). The cells are in a collagenous matrix. Osteoclasts (ocl) are found along the periosteal surface adjacent to the gap. (Magn.  $\times 1900$ .)

FIGURE 23. Photomicrographs of wide gap near the saw cut of the same fracture as in figure 21. A layer of new bone (nb) has been laid on the fractured surfaces, and a few osteocytes are trapped within it (arrows). This layer is covered by a layer of osteoblasts (ob). The central region contains a rich capillary network (cap). The remaining space is filled by a loose collagenous matrix in which macrophages, monocytes and fibroblasts are found. (The number 24 denotes the position of figure 24.) (Magn.  $\times 297$ .)

#### DESCRIPTION OF PLATE 6

FIGURE 24. Electron micrograph of an area of figure 23 (= 24). A row of osteoblasts (ob) covers the layer of new bone (nb) containing osteocytes (oc) that has been laid on the fractured surface (fs). Processes from the osteocytes (arrows) extend towards both the fracture surface and the layer of osteoblasts. The matrix between the osteoblasts and the capillary (cap) contains macrophages (ma), monocytes (mo) and occasional fibroblasts (f). (Magn.  $\times 2800$ .)

FIGURE 25. Electron micrograph of part of the layer of osteoblasts near that in figure 24. The cells are very close together, so that at this magnification it is impossible to distinguish the adjacent cell membranes. The cells are filled by irregular arrays of rough endoplasmic reticulum (rer) and large Golgi complexes (gc). A few mitochondria (m) are also present. The surface of the osteoblasts adjacent to the new bone (nb) is very irregular (arrow). A smaller cell (arrowheads), with more regular arrays of rough endoplasmic reticulum (rer) lies under the osteoblasts; it appears to be moving into the new bone to become an osteocyte. The fractured surface (fs) is very irregular. (Magn.  $\times 8200$ .)

FIGURE 26. Electron micrograph at higher magnification of the collagen fibrils (c) in the matrix of the fracture gap in figures 23 and 24. Part of an endothelial cell (en) and its basement membrane (arrow) are seen at the top of the micrograph. (Magn.  $\times 28200$ .)

## DESCRIPTION OF PLATE 7

- FIGURE 27. Photomicrograph of a mechanically stable fracture at 3 weeks. This shows the end of the saw cut and the beginning of the fracture (arrow). The gap is filled by new bone (nb). The periosteal callus (pc) is compact peripherally, but near the callus-cortex boundary there are very large cavities. The endosteal callus (ec) is conical in shape. Remodelling cavities are entering the cortical bone from the periosteal and endosteal calluses (arrowheads). (The number 30 denotes the position of figure 30.) (Magn.  $\times 32$ .)
- FIGURE 28. Photomicrograph of the saw cut shown in figure 27. The gap is filled by new bone (nb), except for a large remodelling cavity (rc) entering from the periosteal callus. Note that the limits of the saw cut are clearly defined by its straight sides (arrowheads). In some regions (arrows), the line is distorted by about 20–40  $\mu\text{m}$ ; this indicates a region where osteoclastic resorption has occurred. The fracture proper starts towards the endosteal surface, where the cortical bone is united. (Magn.  $\times 86$ .)
- FIGURE 29. Photomicrograph of the same saw cut as shown in figures 27 and 28, but of the region under the plate. The arrangement of the lamellae of new bone and cavities is more complex, but the gap is completely traversed by bone in several places (arrowheads). Some areas of resorption along the saw cut are seen (arrows). (Magn.  $\times 86$ .)
- FIGURE 30. Photomicrograph of a small area of the periosteal callus in figure 27 (= 30). The large cavity is the result of resorption and parts of its walls are lined by osteoclasts (arrowheads), whereas osteoblasts occur elsewhere. Capillaries (cap), macrophages and fibroblasts are found in the centre of the cavity. (Magn.  $\times 108$ .)
- FIGURE 31. Photomicrograph of the compressed region of a mechanically stable fracture at 3 weeks. The periosteal callus (pc) is very compact. A remodelling cavity is entering the cortex from the periosteal callus (arrowhead). The fracture is very accurately reduced and is seen as a dense line (arrows). (The number 32 denotes the position of figure 32. (Magn.  $\times 37$ .)
- FIGURE 32. Photomicrograph of part of the fracture seen in figure 31 (= 32). The accurate reduction of the fracture is obvious, but a narrow gap, about 6  $\mu\text{m}$  wide, is filled by densely stained material. Remodelling cavities (rc) are seen near the fracture, and one has crossed it (arrow). (Magn.  $\times 157$ .)

## DESCRIPTION OF PLATE 8

- FIGURE 33. Photomicrograph of a 3-week mechanically stable fracture in which the reduction is not accurate; there has been a slight downward displacement of the fragment on the left. This has resulted in the formation of two gaps (g) about 60  $\mu\text{m}$  wide separated by an area in which the fracture surfaces are in contact (arrow). The upper gap is open to the cavities in the periosteal callus, but the lower gap is closed by bone from the endosteal callus (ec). The contents of these two gaps differ; in the region in the figure, the upper gap still contains debris, whereas the lower gap is filled by cartilage (arrowheads). (The number 35 denotes the position of figure 35.) (Magn.  $\times 113$ .)
- FIGURE 34. Electron micrograph to show the contents of the upper region of the gap shown in figure 33. The cells (arrows) appear undifferentiated and lie in a matrix of collagen fibrils with some remaining debris. (Magn.  $\times 1900$ .)
- FIGURE 35. Electron micrograph to show the contents of the lower gap in figure 33 (= 35). The cells are hypertrophied chondrocytes (ch) in large lacunae in a cartilage-type matrix. (Magn.  $\times 2400$ .)

## DESCRIPTION OF PLATE 9

- FIGURE 36. Photomicrograph of a 4-week mechanically stable fracture. A gap (g) is present in the central region, but large remodelling cavities (rc) and regions of transverse lamellae of new bone (nb) are seen both periosteally and endosteally. (Magn.  $\times 86$ .)
- FIGURE 37. Photomicrograph at higher magnification of the fracture in figure 36. New bone (nb) is being laid down around part of each remodelling cavity (rc), but osteoclasts (ocl) are present elsewhere. (Magn.  $\times 163$ .)
- FIGURE 38. Photomicrograph of the same 4-week fracture seen in figure 36, but at about 1 mm distant. Large remodelling cavities (rc) are orientated across the cortex and only a few short regions of the fracture gap remain (arrow). (Magn.  $\times 86$ .)
- FIGURE 39. Photomicrograph at higher magnification of the fracture in figure 38. The cavities have well organized contents, but only a little new bone (nb) has been laid down. They are linked by narrow gaps (arrow). (Magn.  $\times 163$ .)

FIGURE 40. Photomicrograph of a compressed region of a 4-week mechanically stable fracture; the fracture takes a zig-zag course across the cortex (arrowheads). The gap is obscured both periosteally and endosteally by areas of remodelling (arrows), and only a few remodelling cavities (rc) have penetrated to the central region. (Magn.  $\times 24$ .)

FIGURE 41. Photomicrograph at higher magnification of the fracture in figure 40. The gap is less than  $9\ \mu\text{m}$  wide. Part of it is obscured by the large cavity with osteoclasts (ocl), which are widening the gap. (Magn.  $\times 157$ .)

FIGURE 42. Photomicrograph of the region opposite the plate of the same 4-week fracture shown in figures 40 and 41. Here the fracture is compressed (arrows) and the remodelling cavities cross the fracture perpendicularly. (Magn.  $\times 108$ .)

#### DESCRIPTION OF PLATE 11

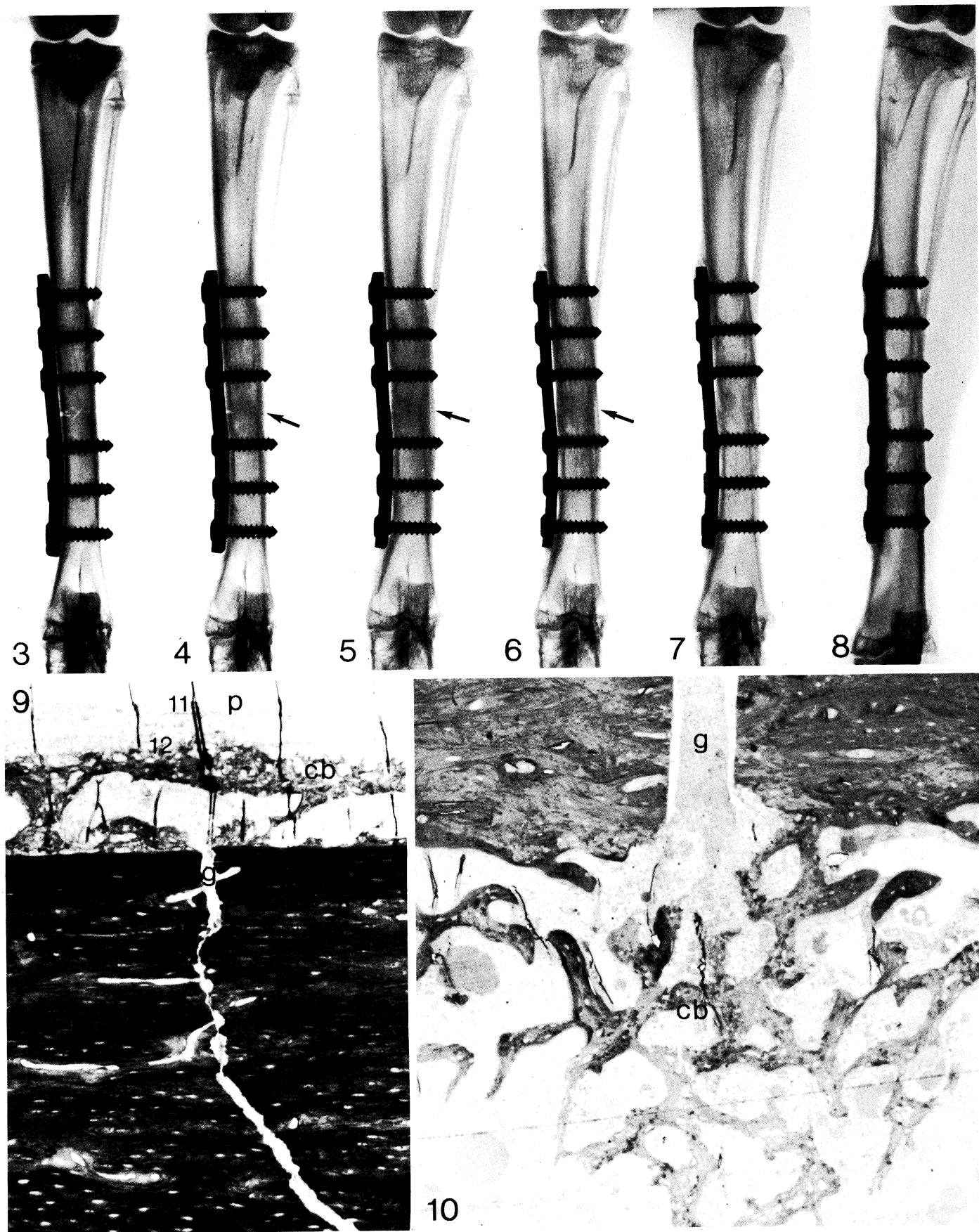
FIGURE 45. Photomicrograph of an 8-week mechanically stable fracture in a region opposite the plate. The periosteal callus is eroded along the cortex and large cavities, filled by fat cells (fc), are present. At both the periosteal and endosteal ends of the fracture, areas of remodelled new bone (nb) are present, which suggests that a narrow gap has been enlarged before healing. (Magn.  $\times 24$ .)

FIGURE 46. Photomicrograph at higher magnification of the fracture in figure 45. In the central region, there are still narrow gaps (arrows) that are being enlarged and crossed by remodelling cavities (rc). (Magn.  $\times 86$ .)

FIGURE 47. Photomicrograph of the end of the saw cut region of a 6-week mechanically stable fracture. The saw cut, which may still be identified by its straight sides (arrowheads), is filled by transverse lamellae of new bone, and longitudinally orientated remodelling cavities (rc) are encroaching on it. (Magn.  $\times 173$ .)

FIGURE 48. Photomicrograph of a 6-week mechanically stable fracture. Both the periosteal and endosteal ends are united by transverse lamellae of new bone (nb). These are linked by a narrow gap (g), which is traversed by a remodelling cavity (rc). The gap contains some cells. (The number 49 denotes the position of figure 49.) (Magn.  $\times 113$ .)

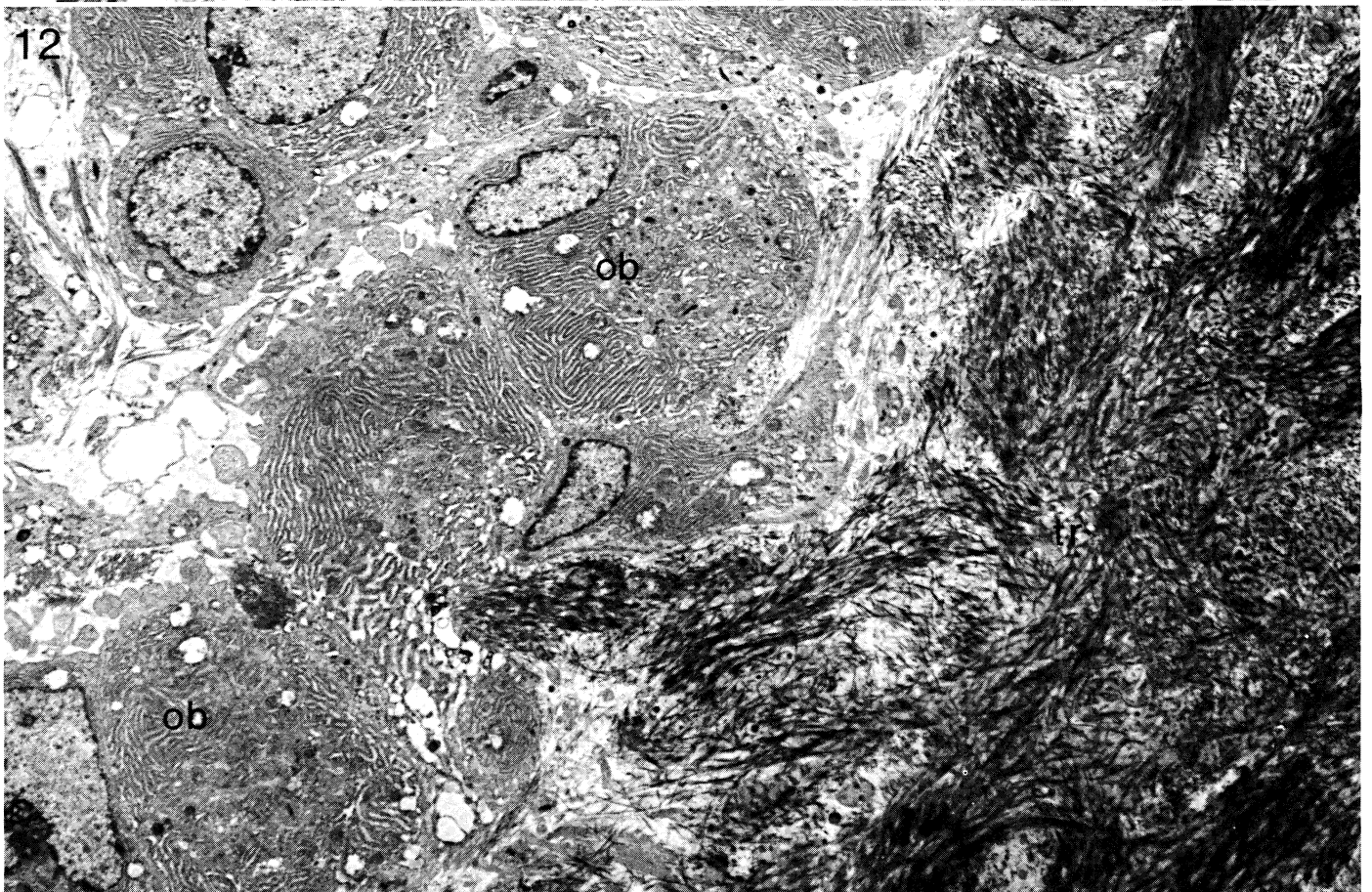
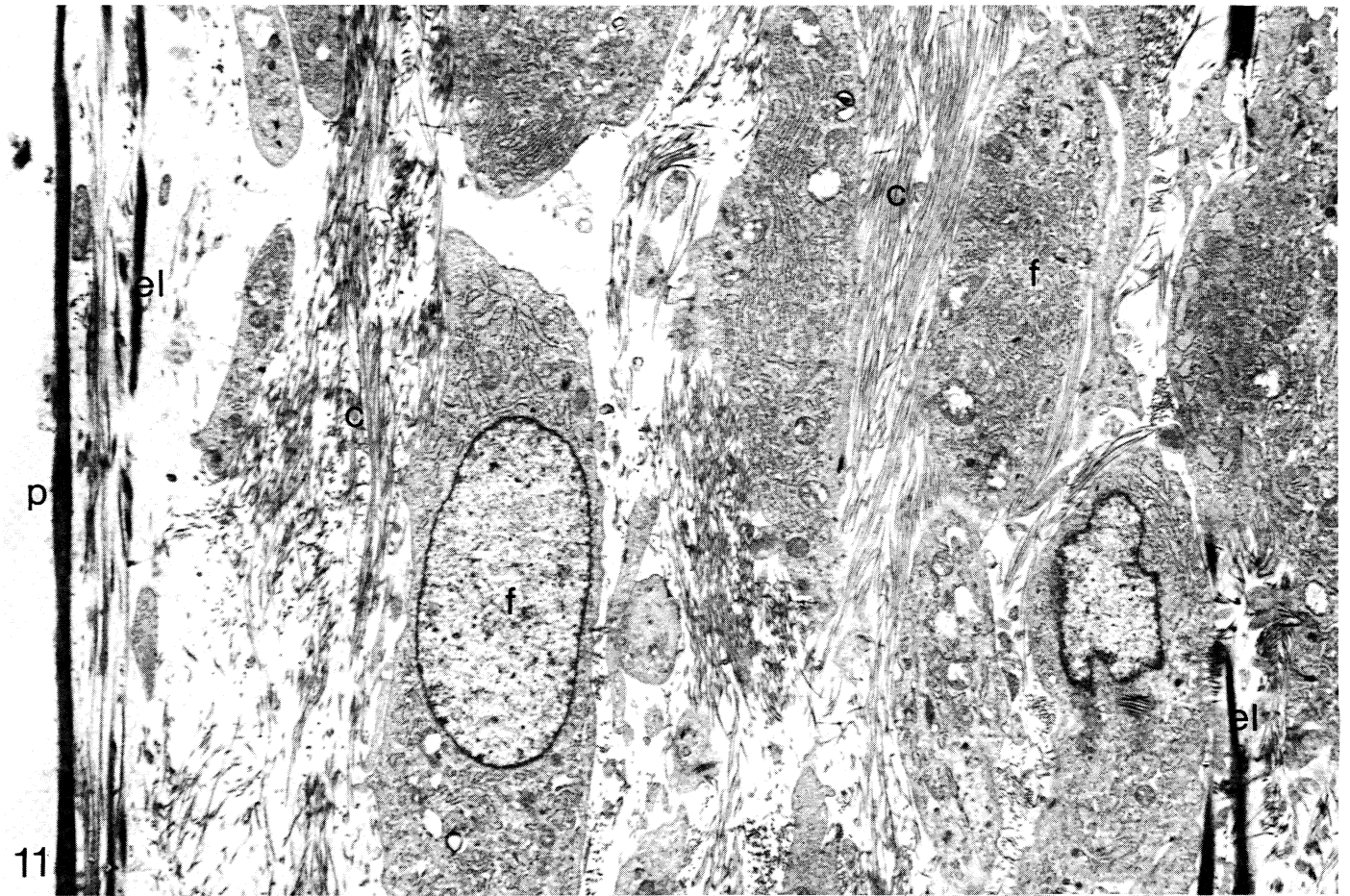
FIGURE 49. Electron micrograph of a small part of the gap in figure 48 (= 49). A cell, which has processes (arrows) radiating from it, and which has much rough endoplasmic reticulum (rer) and many mitochondria (m), is present in a disorganized matrix of large-diameter collagen fibrils (c). The fractured surface (fs) can be seen. (Magn.  $\times 14400$ .)



FIGURES 3-10. For description see page 299.

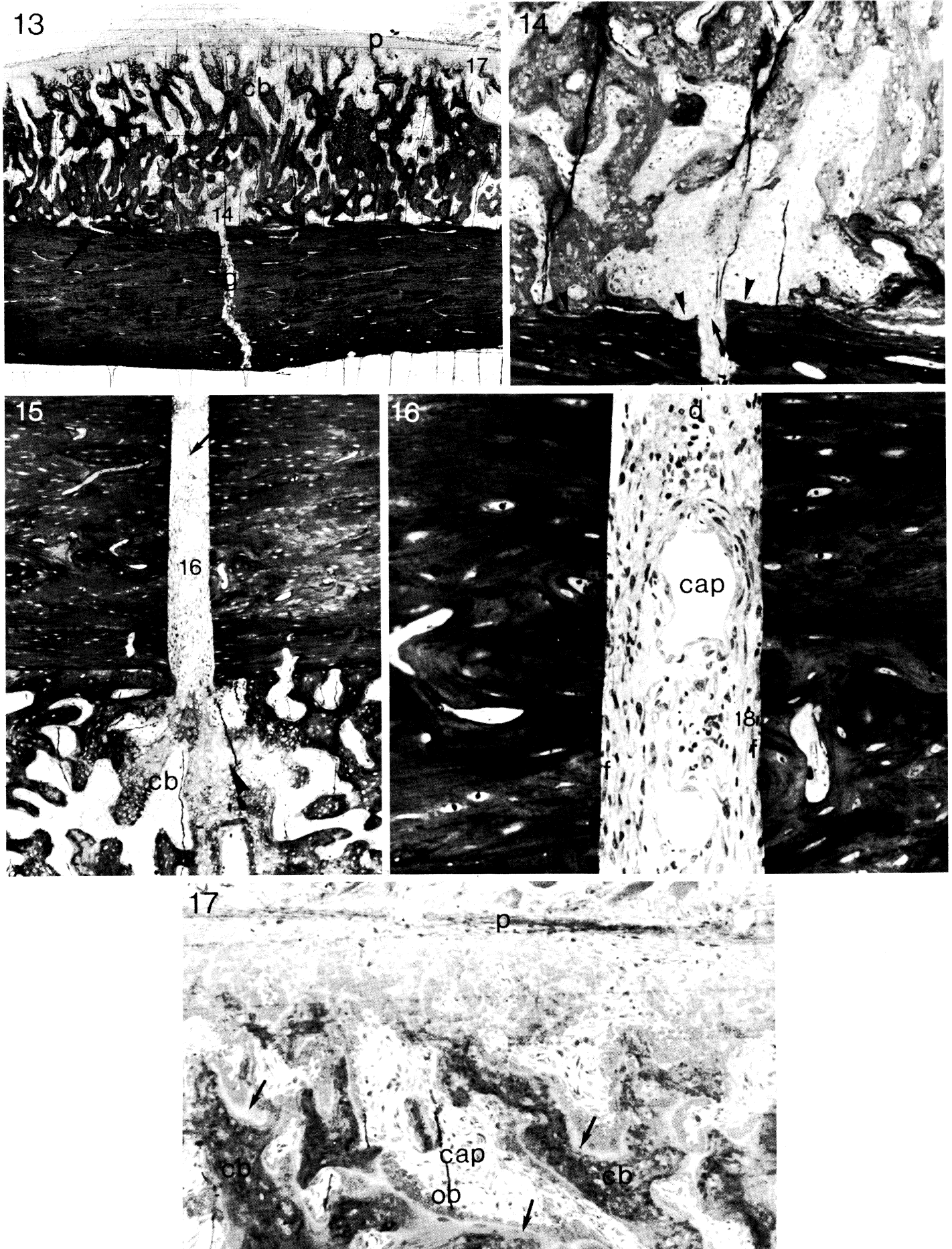
(Facing p. 302)



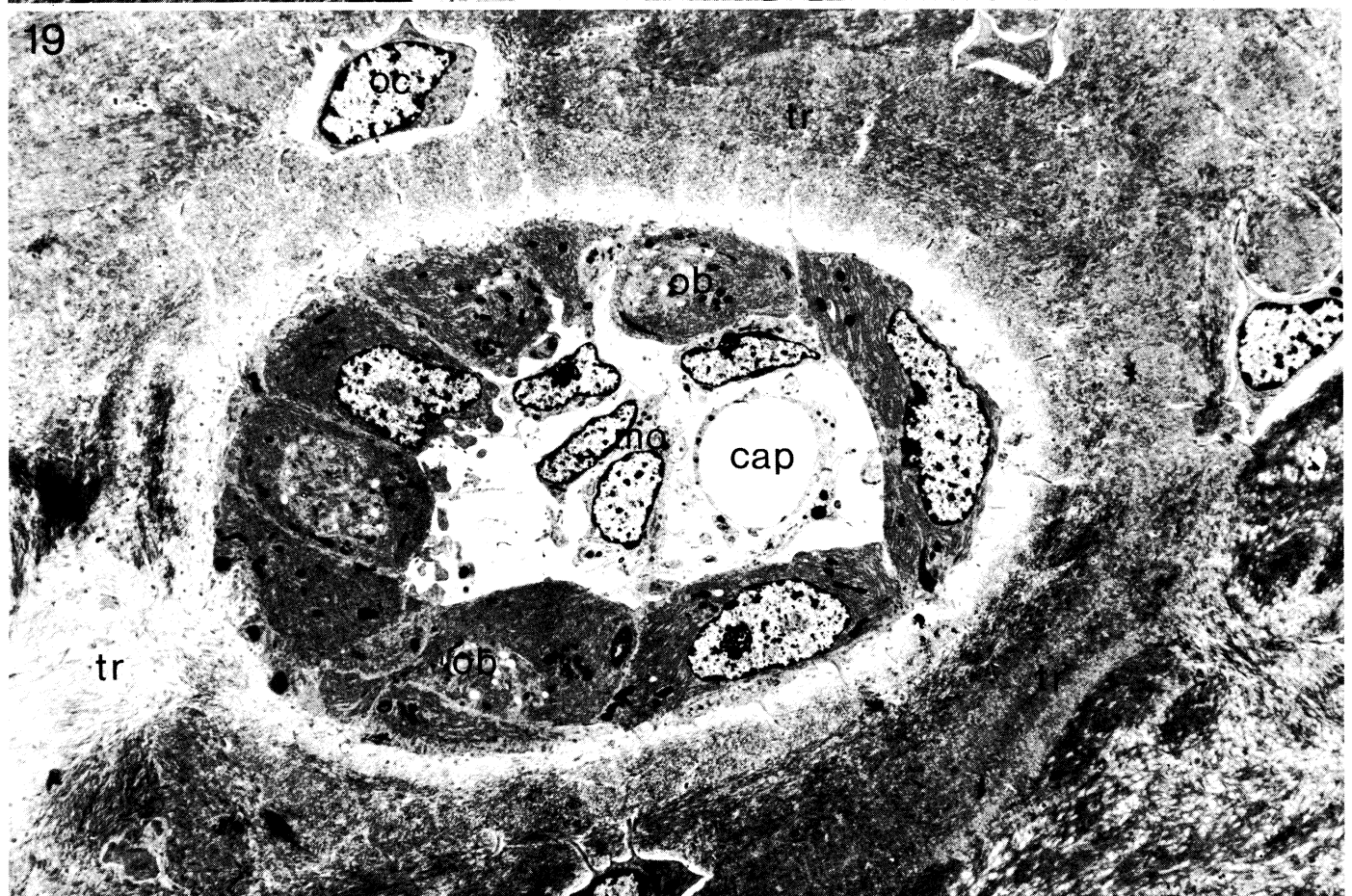
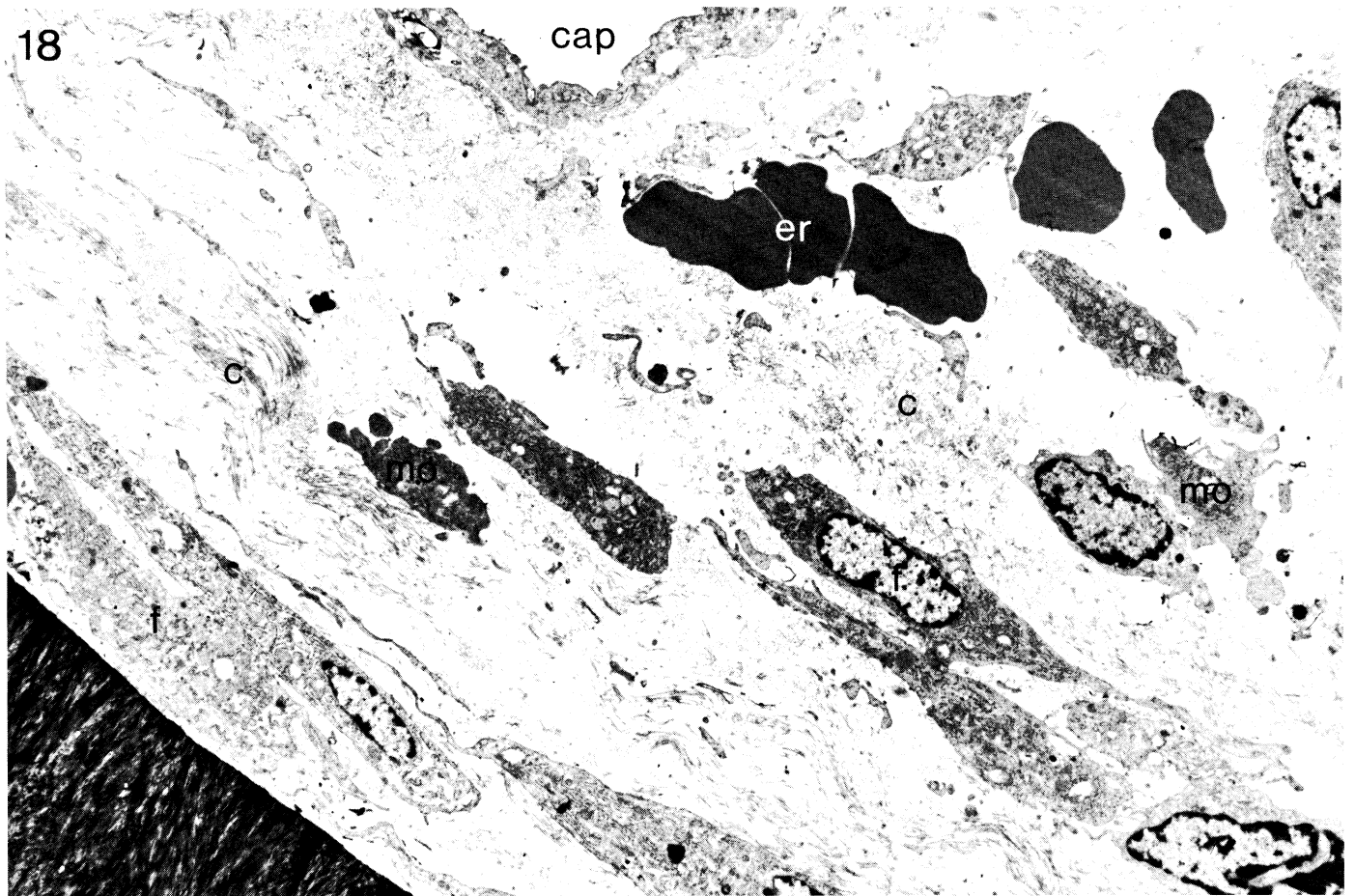


FIGURES 11 AND 12. For description see page 299.



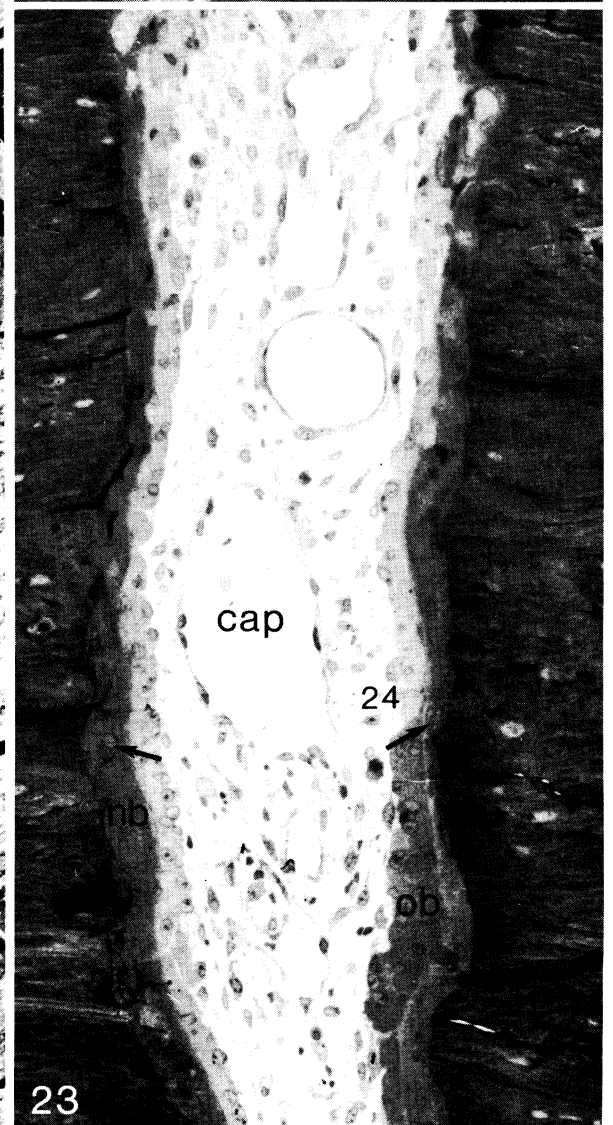
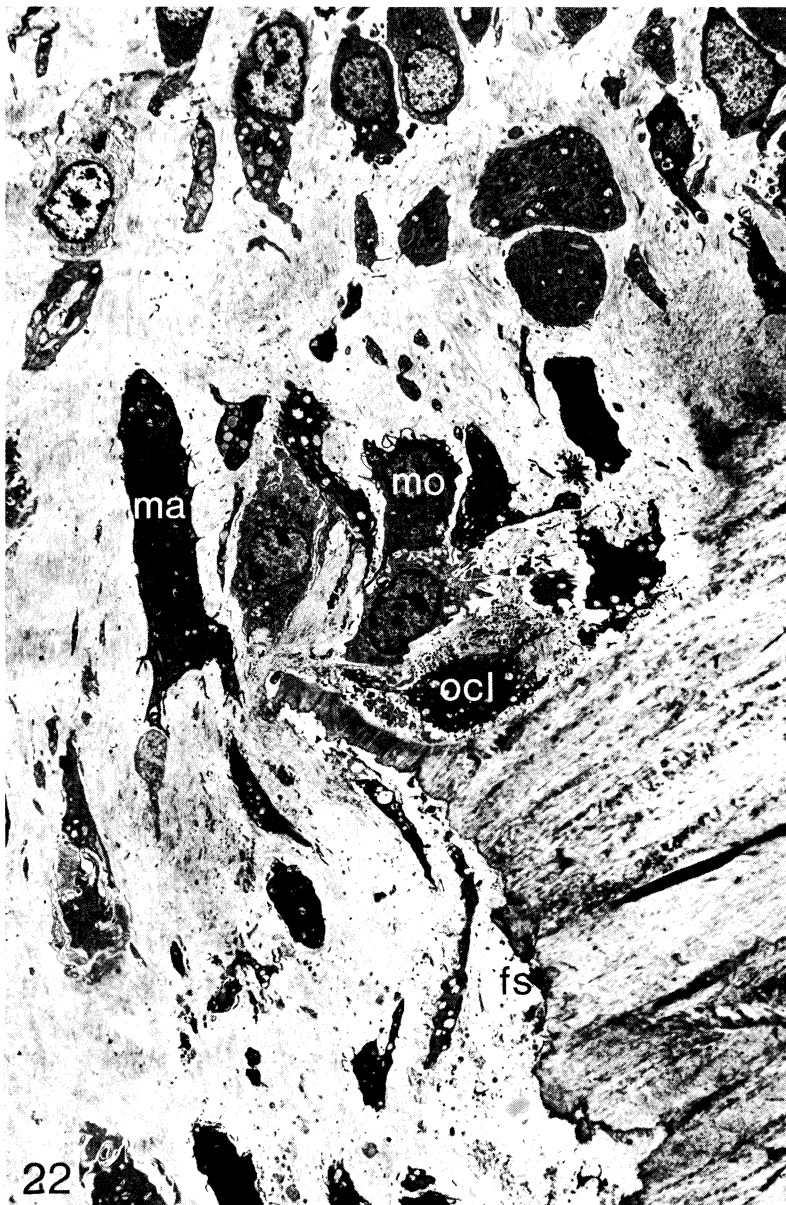
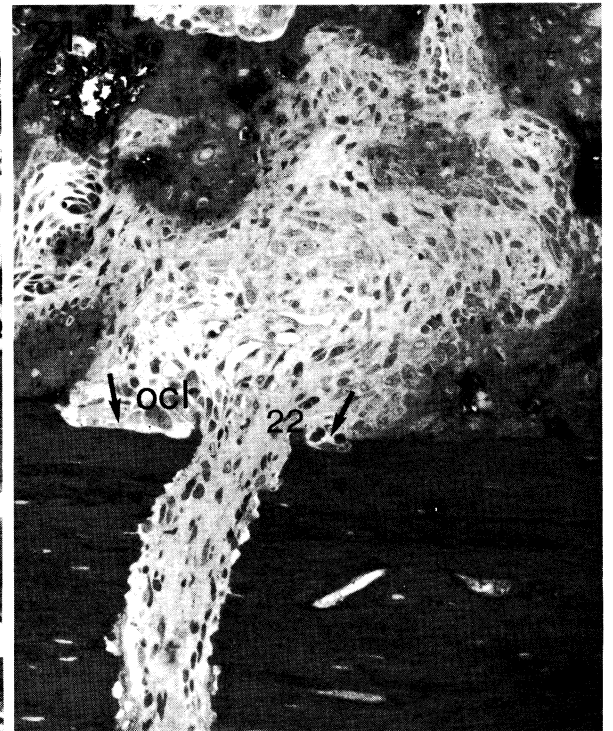
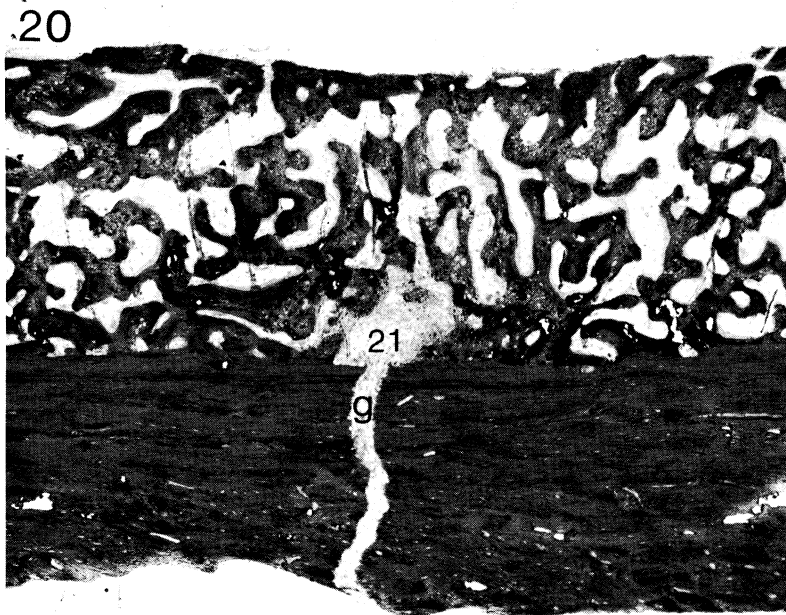


FIGURES 13–17. For description see pages 299 and 300.



FIGURES 18 AND 19. For description see page 300.



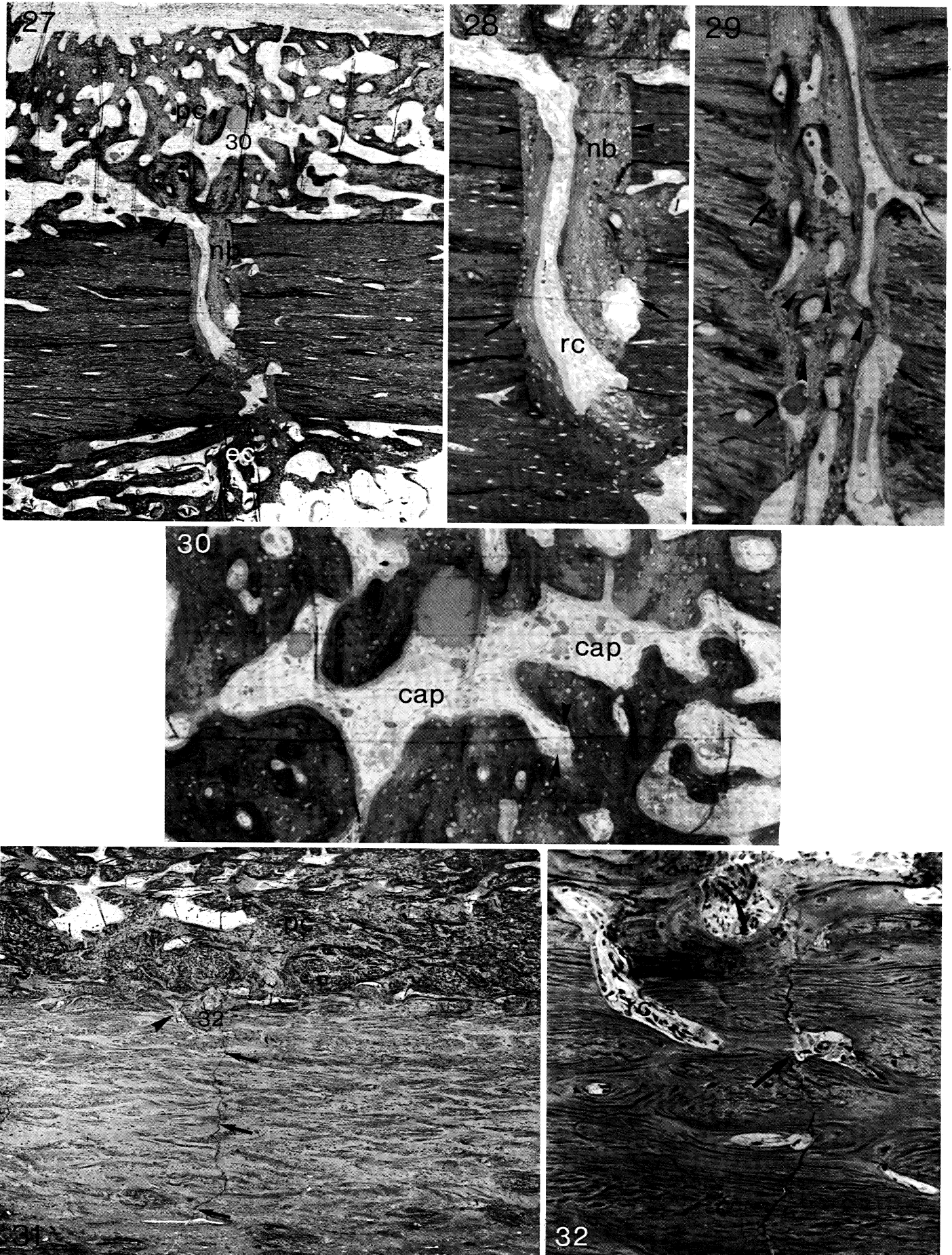


FIGURES 20-23. For description see page 300.



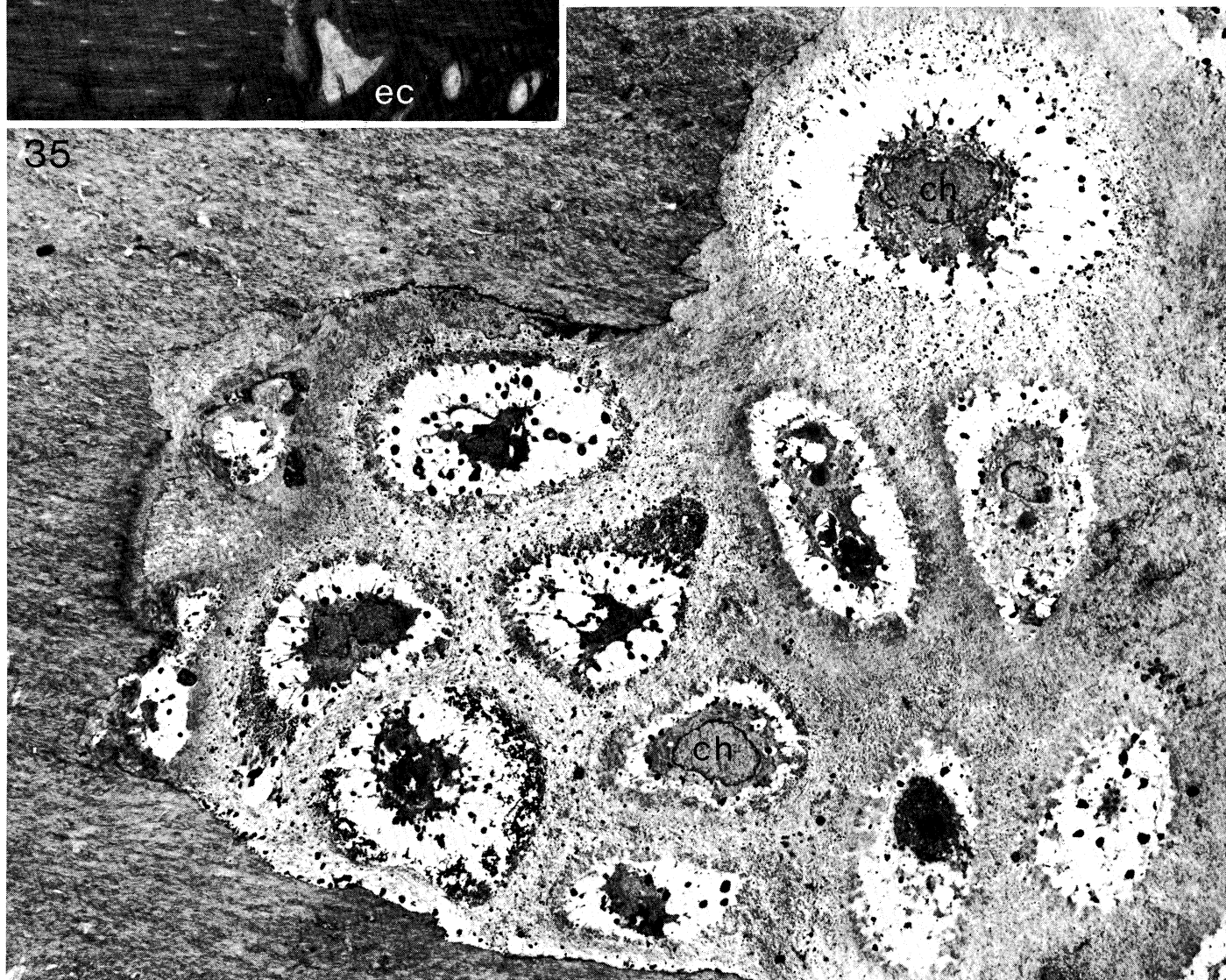
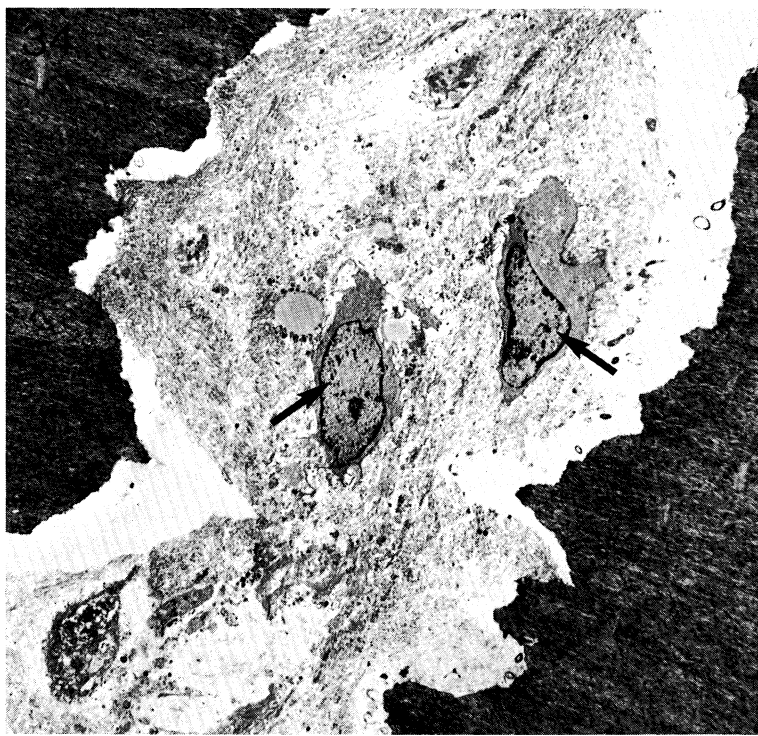
FIGURES 24-26. For description see page 300.





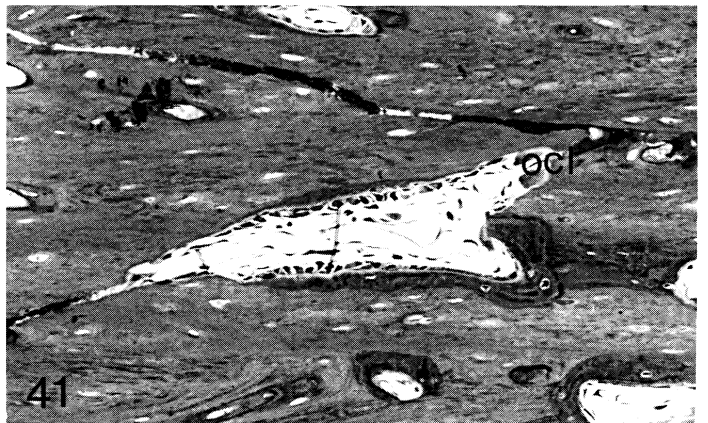
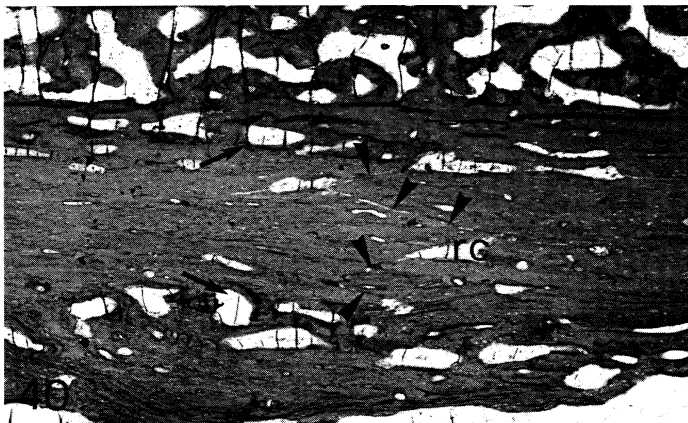
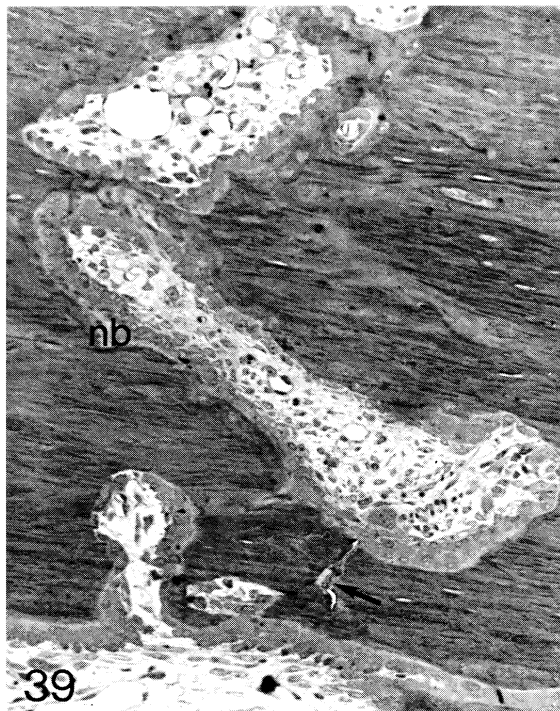
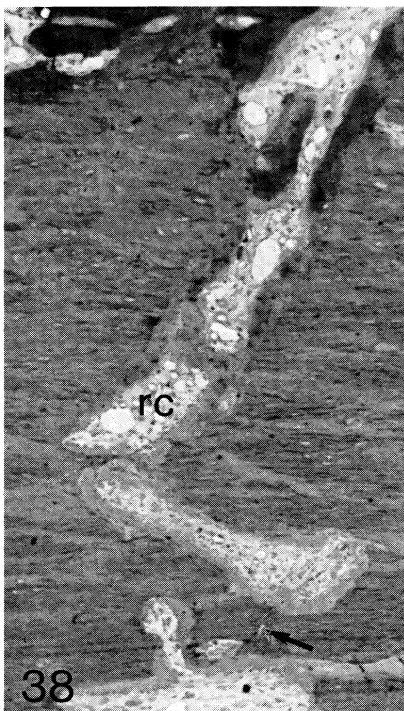
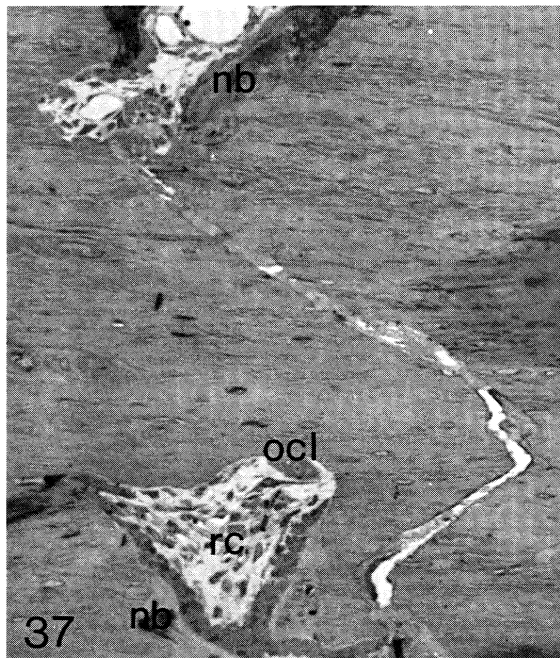
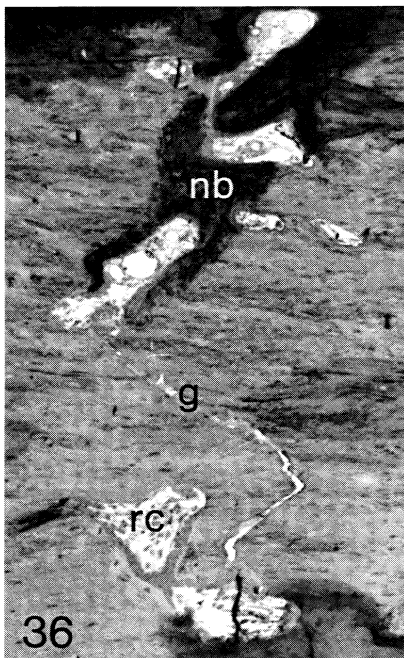
FIGURES 27-32. For description see page 301.





FIGURES 33–35. For description see page 301.





FIGURES 36-42. For description see pages 301 and 302.

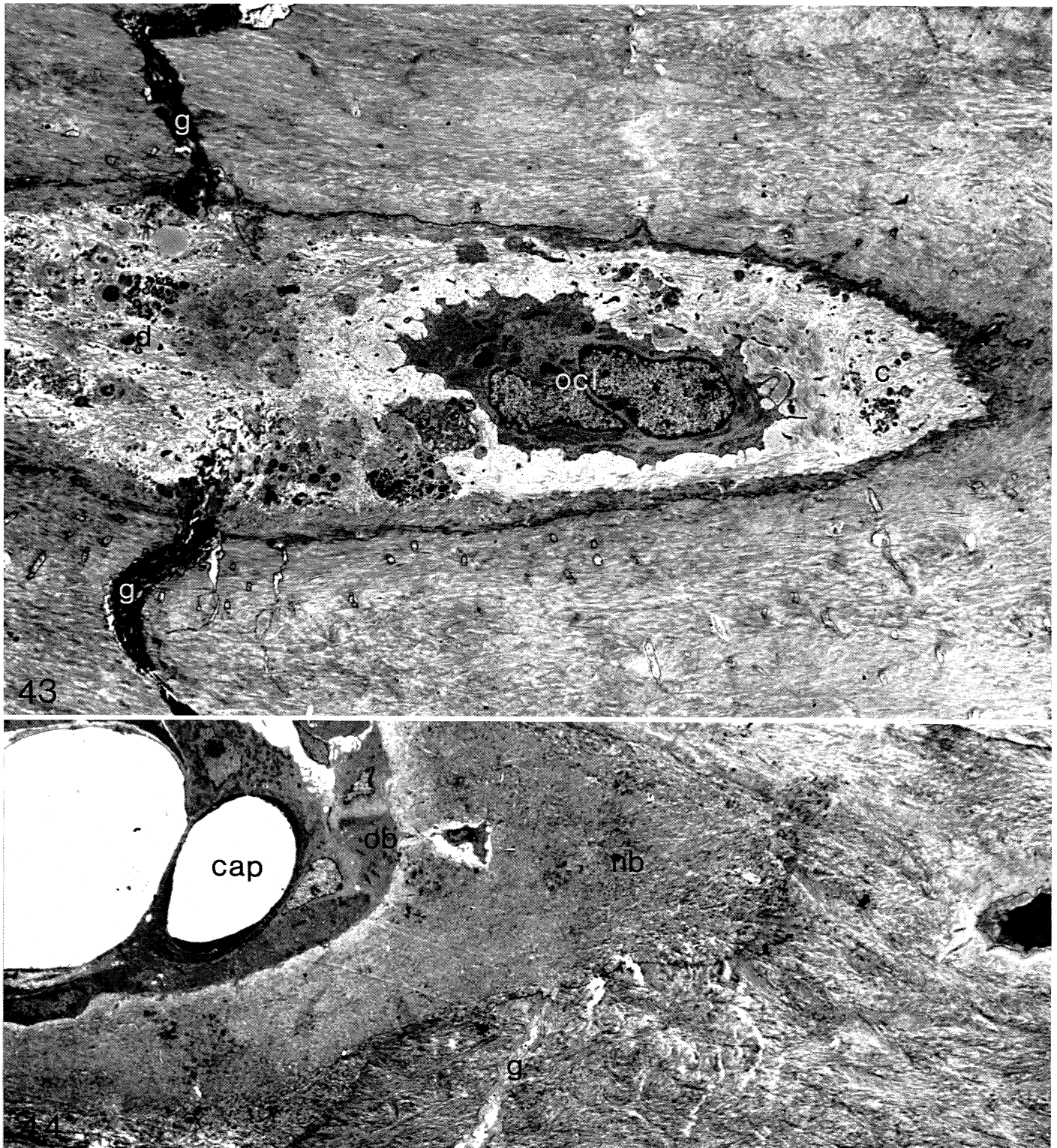
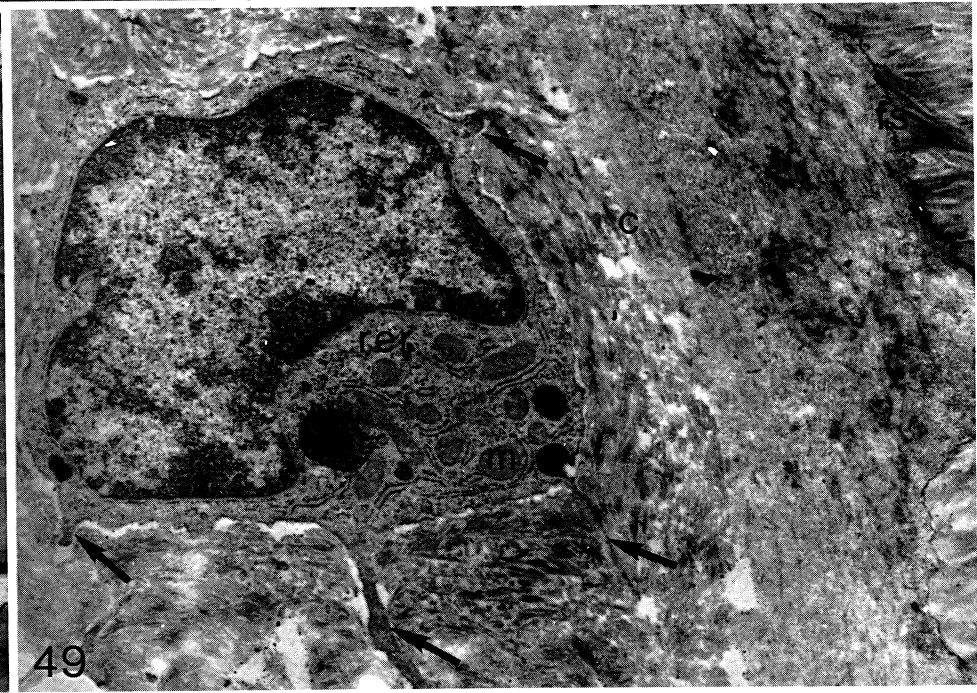
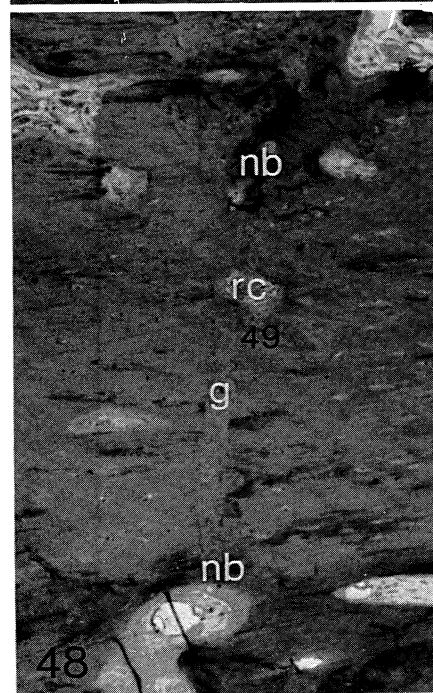
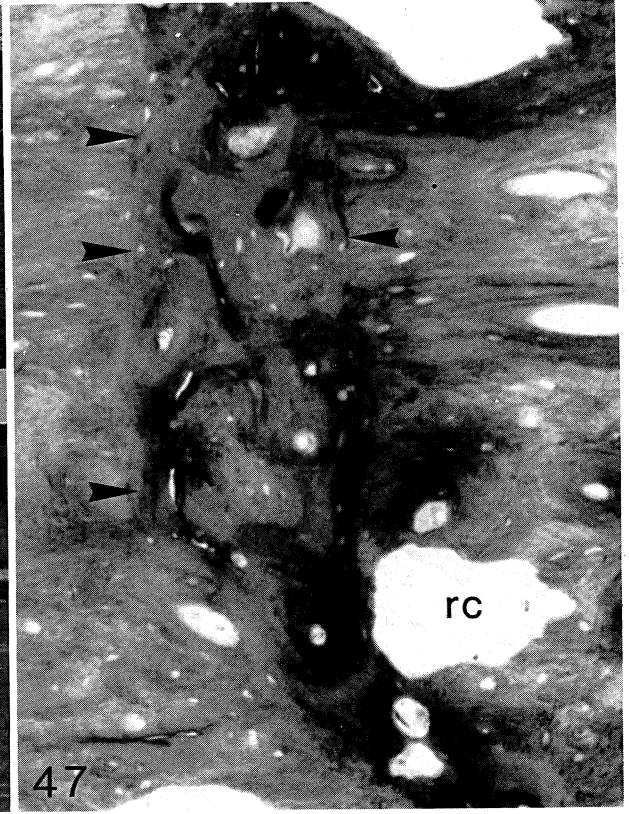


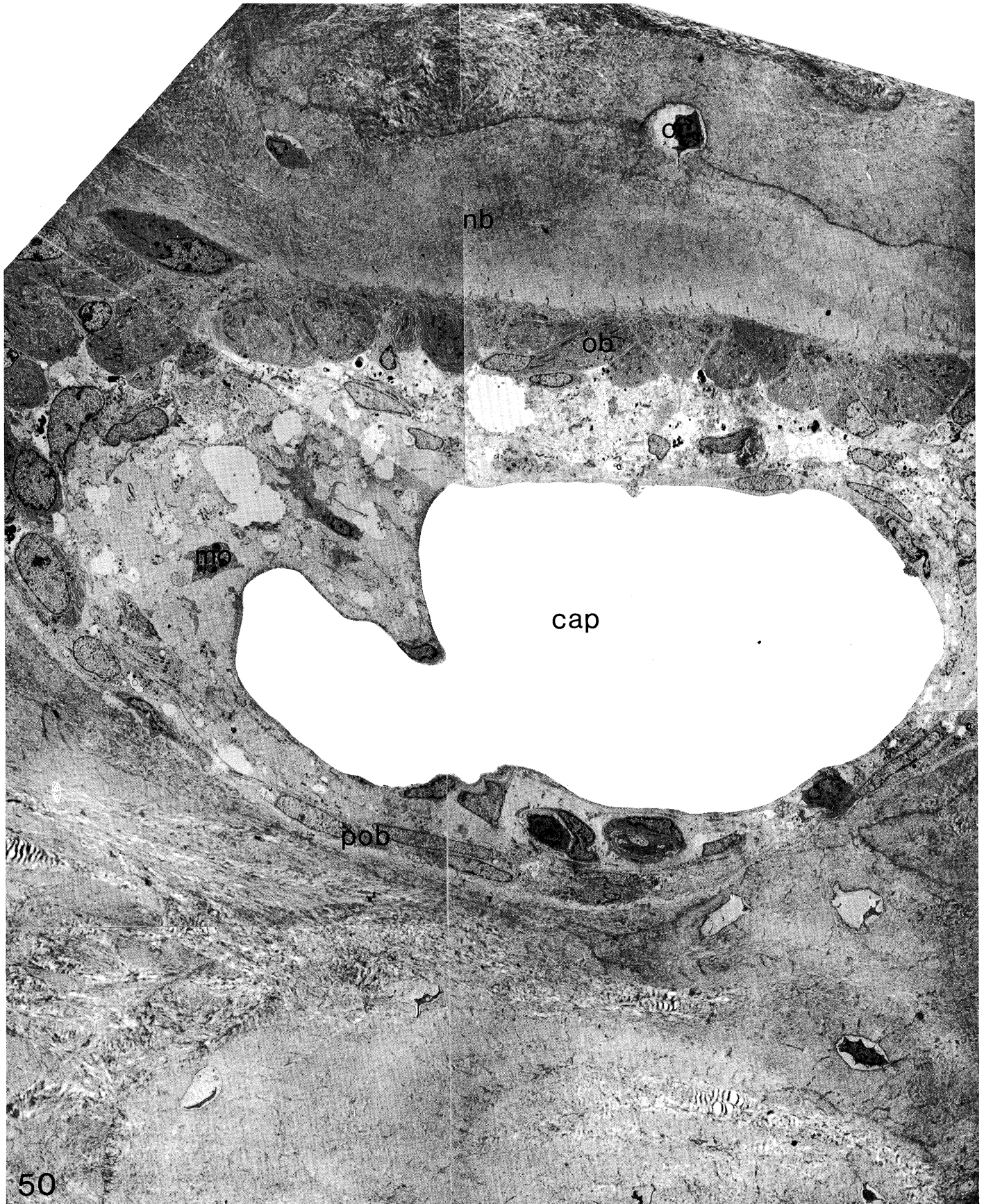
FIGURE 43. Electron micrograph of the leading end of a remodelling cavity crossing the fracture shown in figure 42. An osteoclast (ocl) and a few small collagen fibrils (c) are seen at the leading end, and most of the rest of the cavity is filled by debris (d). The narrow fracture gap (g), about  $1\ \mu\text{m}$  wide, is filled by electron dense, amorphous material. (Magn.  $\times 4300$ .)

FIGURE 44. Electron micrograph of the posterior end of a remodelling cavity in the same 4-week fracture. Here the fracture is partly bridged by new bone (nb), but the gap (g) still remains elsewhere. The capillaries (cap) and osteoblasts (ob) of the remodelling cavity are seen to the left of the micrograph. (Magn.  $\times 1800$ .)





FIGURES 45-49. For description see page 302.



50

FIGURE 50. A montage of electron micrographs to show a cavity and its associated new bone in the fracture shown in figure 47. The cavity is lined partly by osteoblasts (ob), which have laid down new bone (nb) in which osteocytes (oc) are trapped. On the other side the cavity is lined by spindle-shaped cells, which may be pre-osteoblasts (pob). The cavity is partly filled by a large capillary (cap). A collagenous matrix surrounds the capillary. Various cells, including monocytes (mo) and fibroblasts, are in this matrix. (Magn.  $\times 1400$ .)



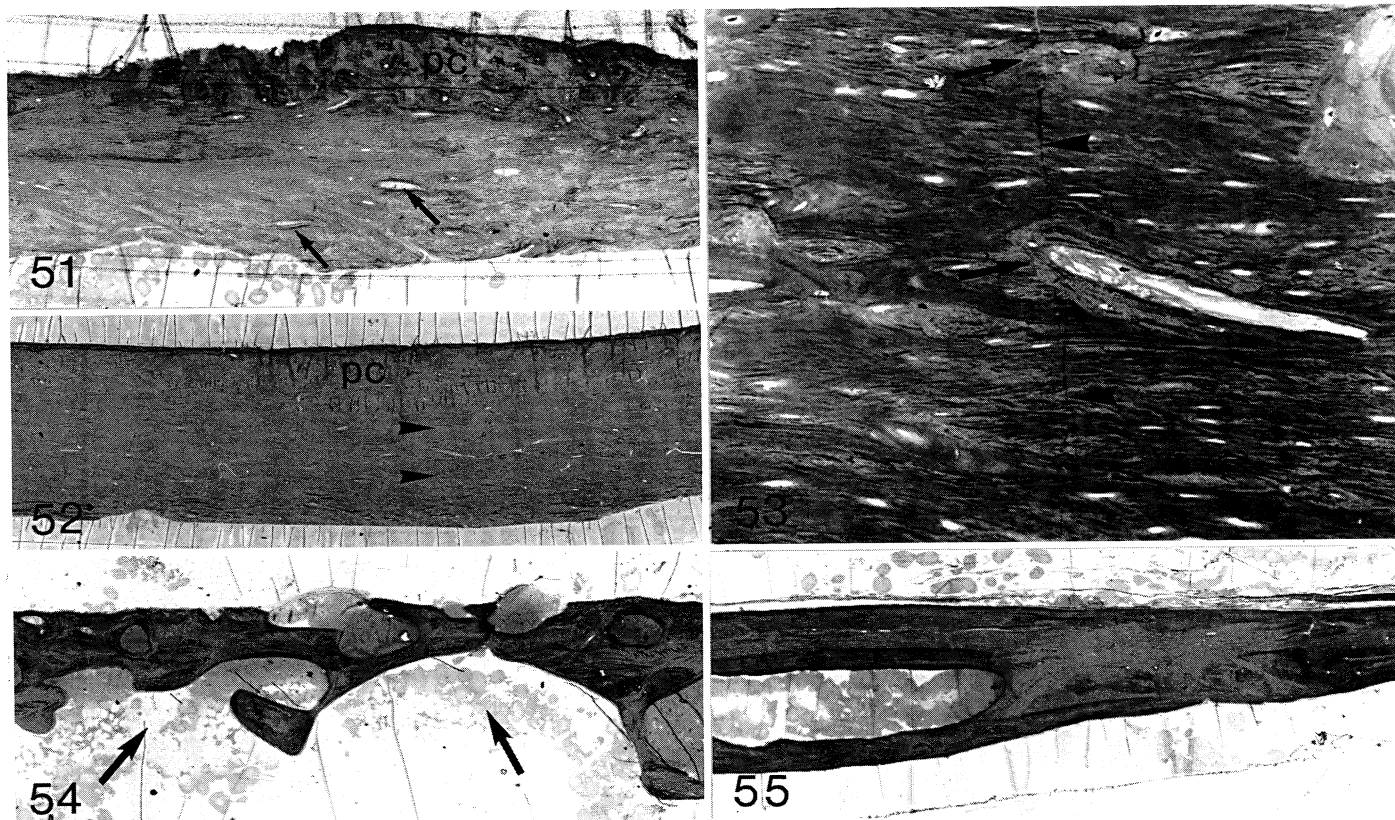
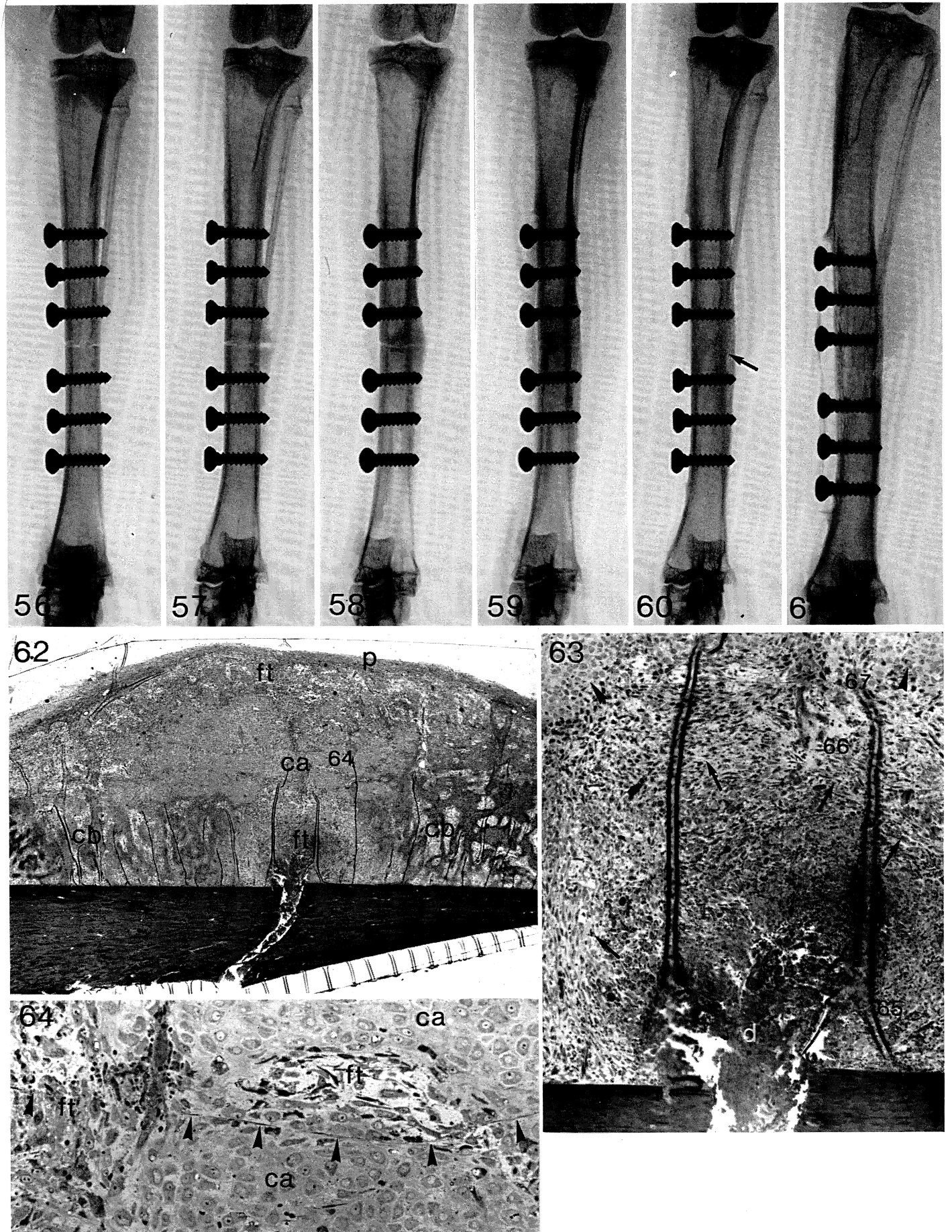


FIGURE 51. Photomicrograph of a 12-week mechanically stable fracture. The fracture site cannot be seen. The periosteal callus (pc) is thin. The original cortical bone shows signs of remodelling activity (arrows). (Magn.  $\times 26$ ).

FIGURE 52. Photomicrograph of an 18-week mechanically stable fracture. The remains of the periosteal callus (pc) can be distinguished by the irregularly orientated bone. The fracture here is compressed (arrowheads). (Magn.  $\times 26$ .)

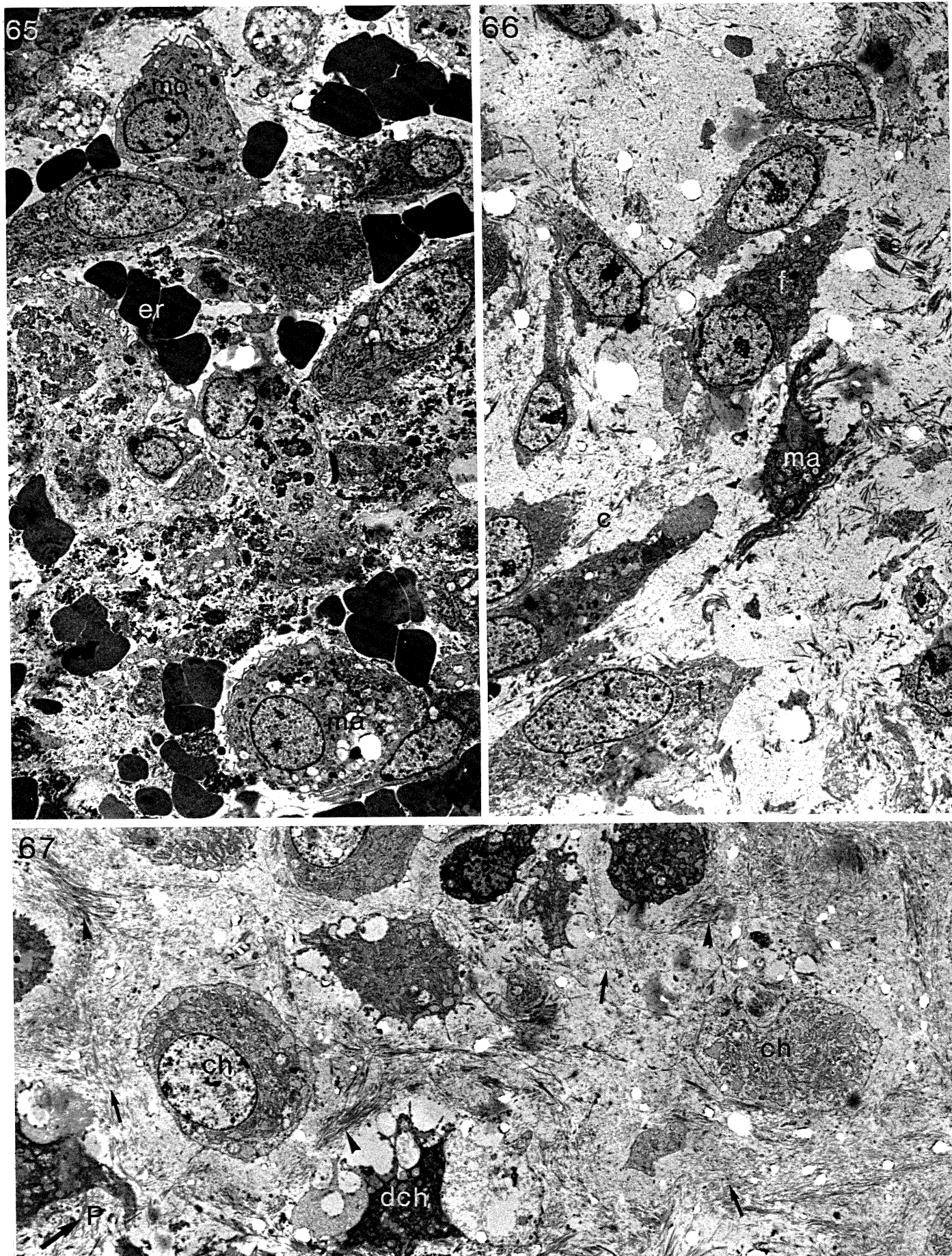
FIGURE 53. Photomicrograph at higher magnification of the fracture in figure 52. The fracture (arrowheads) can be traced across the cortex, except for two regions where remodelling cavities have crossed it (arrows). (Magn.  $\times 197$ .)

FIGURES 54 AND 55. Photomicrographs of different regions of a mechanically stable fracture at 1 year. The fracture site cannot be distinguished. Figure 54 shows the cortex under the plate, which is thin with very large cavities, filled with fat cells, which are open endosteally (arrows). Figure 55 is from the side of the bone; the cortex is thin and large cavities filled with fat cells are present. (Magn.  $\times 26$ .)



FIGURES 56-64. For description see facing plate 16.





FIGURES 65-67. For description see facing plate 16.

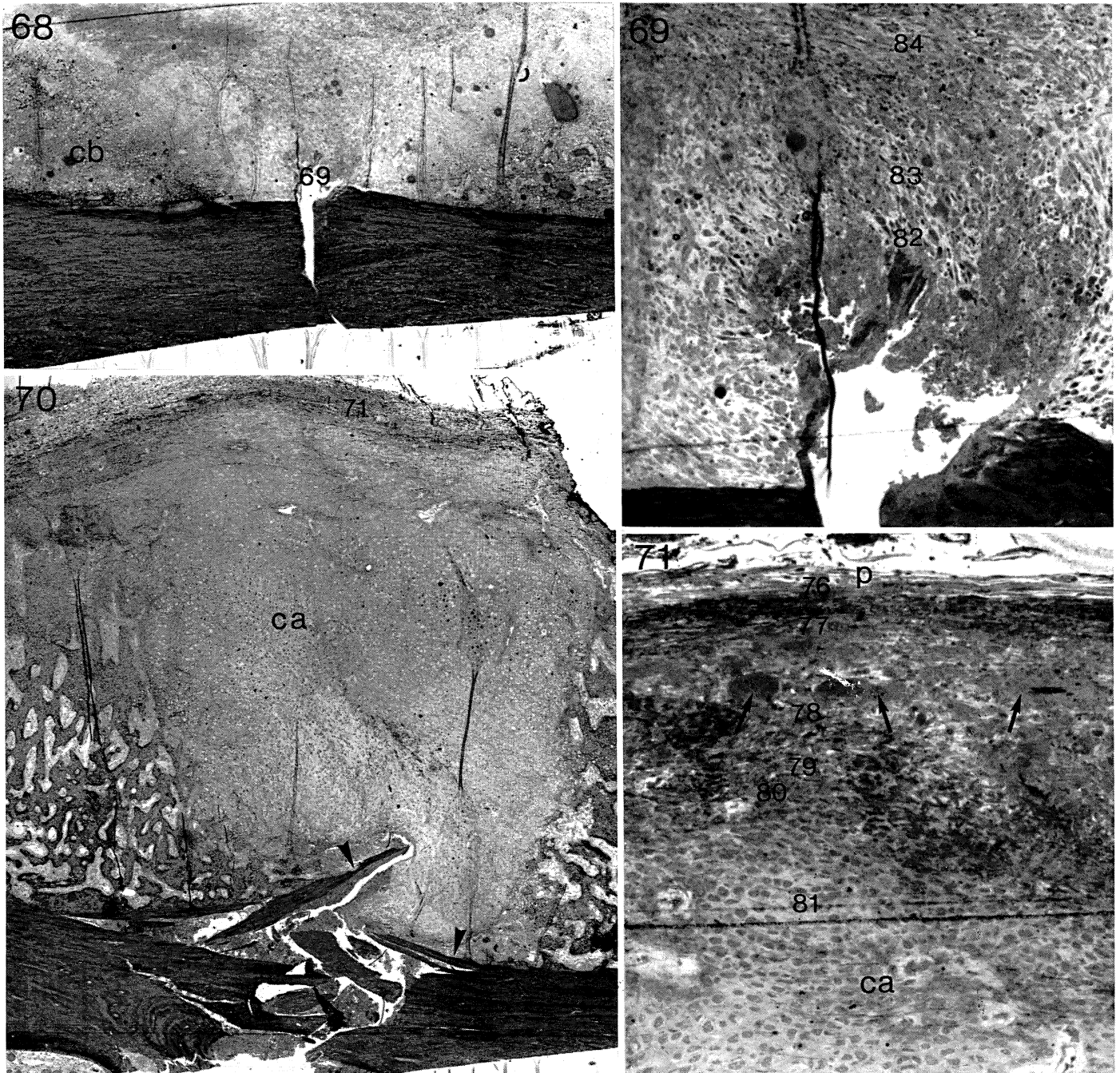


FIGURE 68. Photomicrograph of an 8-day mechanically unstable fracture. The cancellous bone (cb) of the periosteal callus is approaching the fracture gap from both sides. Most of the debris near the gap has been removed and the area is populated by mesenchymal cells. (The number 69 denotes the position of figure 69.) (Magn.  $\times 29$ .)

FIGURE 69. Photomicrograph of the area over the fracture gap in figure 68 (= 69). The mesenchymal cells surround the remaining debris protruding from the gap. No capillaries are present. (The numbers 82, 83 and 84 denote the positions of figures 82, 83 and 84.) (Magn.  $\times 108$ .)

FIGURE 70. Photomicrograph of a 9-day mechanically unstable fracture. This is the cortex opposite the plate and the fracture is comminuted. The callus is now a thick layer and the region over the gap is filled by cartilage (ca). There are signs of osteoclastic activity on the spicules of cortical bone (arrowheads). (The number 71 denotes the position of figure 71.) (Magn.  $\times 24$ .)

FIGURE 71. Photomicrograph of the periosteal region of the fracture in figure 70 (= 71). The longitudinal orientation of the fibres in the periosteum (p) can be seen. Beneath the periosteum there are layers of developing bone (arrows) and fibrous tissue (ft). These overlie the cartilage (ca). (The numbers 76-81 denote the positions of figures 76-81.) (Magn.  $\times 130$ .)



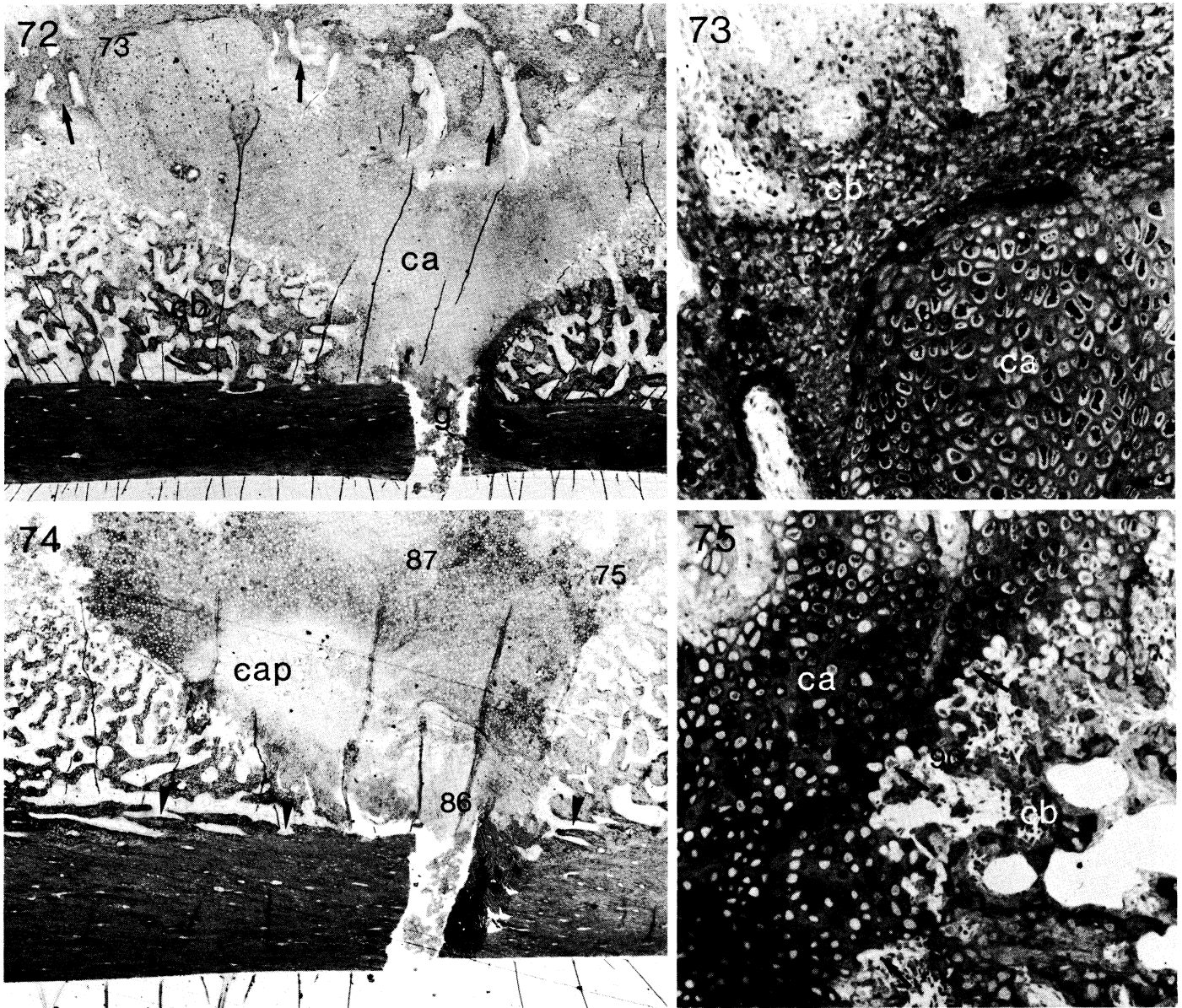
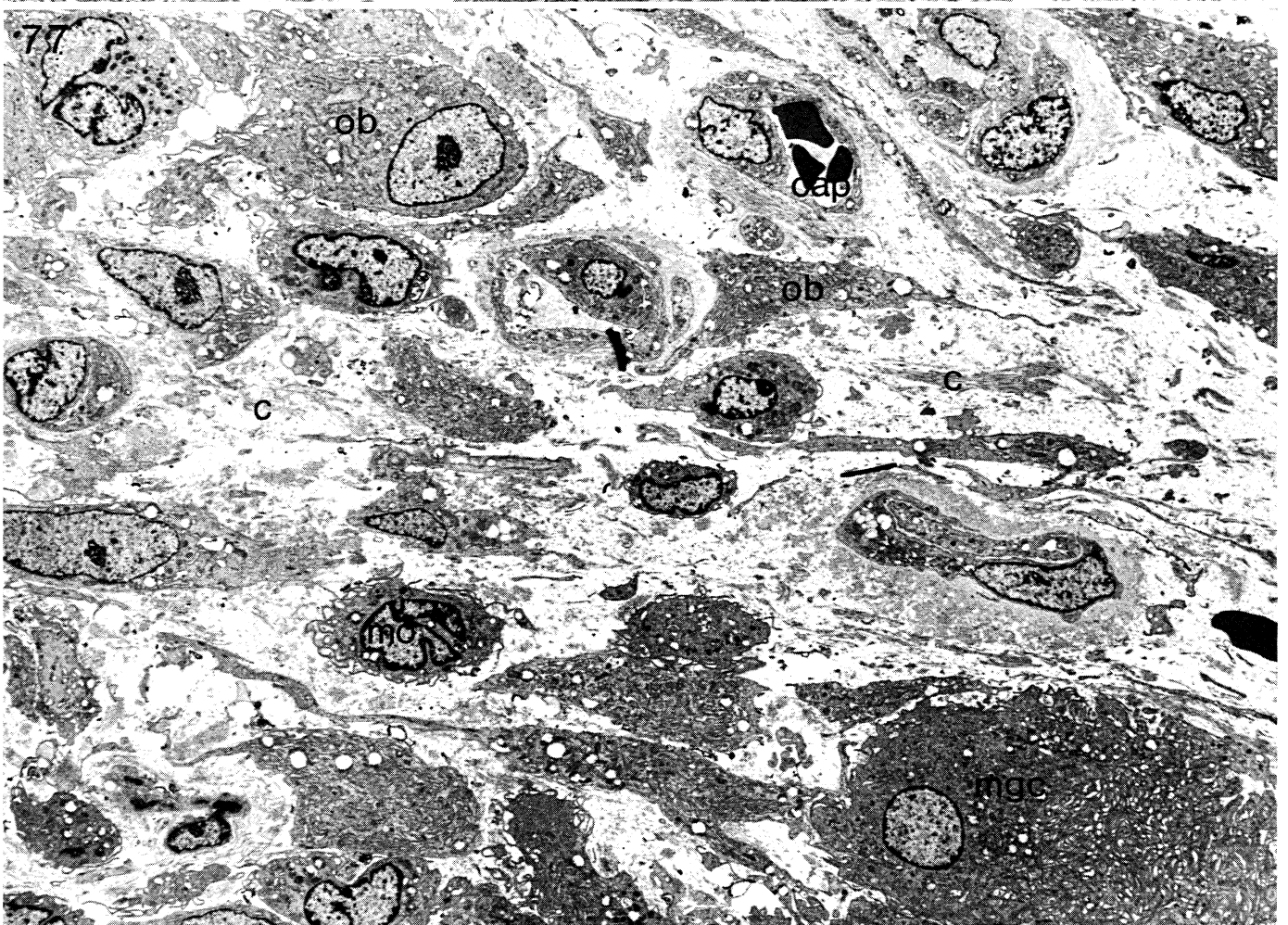
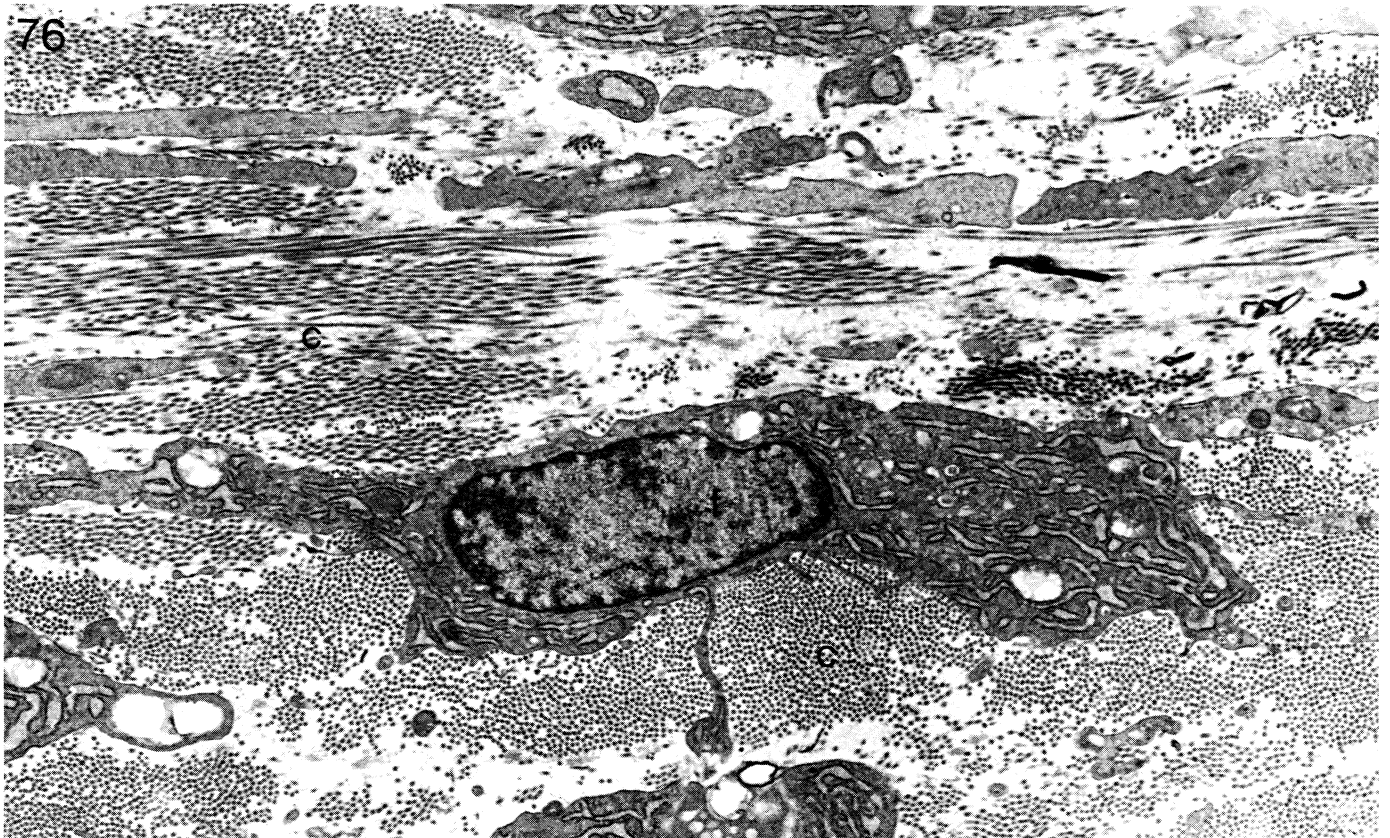


FIGURE 72. Photomicrograph of a 12-day mechanically unstable fracture. The fracture gap (g) is filled by debris that meets the cartilage (ca), which is in turn surrounded by the cancellous bone (cb) of the callus; an external layer of bone now covers the cartilage (arrows). (The number 73 denotes the position of figure 73.) (Magn.  $\times 24$ .)

FIGURE 73. Photomicrograph of a small area of the callus in figure 72 (= 73). The close juxtaposition of the cancellous bone (cb) and cartilage (ca) is seen. (The numbers 88 and 89 denote the positions of figures 88 and 89.) (Magn.  $\times 130$ .)

FIGURE 74. Photomicrograph of the same 12-day fracture shown in figure 73, but in a region opposite the plate. The callus is similar to that in figure 73, but there is a small region of large, sinusoid-like capillaries (cap) in the cartilage. Osteoclastic activity is apparent along the cortical bone (arrowheads). (The numbers 75, 86 and 87 denote the positions of figures 75, 86 and 87.) (Magn.  $\times 24$ .)

FIGURE 75. Photomicrograph of a small region of figure 74 (= 75). The cancellous bone (cb) is encroaching onto the cartilage (ca) and endochondral ossification is taking place (arrows). (The number 90 denotes the position of figure 90.) (Magn.  $\times 130$ .)



FIGURES 76 AND 77. For description see facing plate 17.



#### DESCRIPTION OF PLATE 14

FIGURES 56–61. Radiographs of tibial fractures stabilized with a plastic plate; the plastic is lucent to X-rays and hence cannot be seen. Figures 56–60 are a series of radiographs of the tibia of a rabbit killed at 12 weeks. Figure 61 is a radiograph of the tibia of a different rabbit, killed at 39 weeks. Figure 56 is a radiograph taken immediately post-operation. The fracture gap is clearly visible. Figure 57 is a 2-week radiograph. A layer of callus is developing along the cortex opposite the plate; it widens as it approaches the fracture, but a lucent area exists over the fracture gap. Figure 58 is a 4-week radiograph. The callus is thicker and although there is still a lucent line over the fracture, it is narrower. Figure 59 is a 6-week radiograph. The callus is now thinner, and it forms a complete layer over the fracture. The fracture gap is less distinct. Figure 60 is an 8-week radiograph. The callus is thinner, and it is less dense near the cortex (arrow). Figure 61 is a 39-week radiograph from another rabbit. The fracture is not visible. A thin layer of callus is still present and the variable density of the bone suggests that remodelling is taking place in the cortex. (Actual size.)

FIGURE 62. Photomicrograph of a 6-day mechanically unstable fracture. The periosteal callus is developing. Cancellous bone (cb) is forming on either side of the fracture, but over the fracture there is an area of fibrous tissue (ft). Peripherally some areas of cartilage (ca) are developing. The whole is covered by a layer of fibrous tissue (ft) and new periosteum (p). (The number 64 denotes the position of figure 64.) (Magn.  $\times 19$ .)

FIGURE 63. Photomicrograph of the area adjacent to the fracture gap in figure 62. Debris (d) protrudes from the gap. An area of irregularly arranged mesenchymal cells covers the debris, and is surrounded by a layer of spindle-shaped cells with a preferred orientation encircling the gap (arrows). Farther away some areas of cartilage (arrowheads) are forming. (The numbers 65, 66 and 67 denote the positions of figures 65, 66 and 67.) (Magn.  $\times 77$ .)

FIGURE 64. Photomicrograph of part of the developing cartilage in figure 62 (= 64). An elastic fibre (arrowheads) extends from the fibrous tissue (ft) into the cartilage (ca). (Magn.  $\times 209$ .)

#### DESCRIPTION OF PLATE 15

FIGURE 65. Electron micrograph of the area adjacent to the debris protruding from the fracture gap at 6 days in figure 63 (= 65). The cells are either phagocytic macrophages (ma) and monocytes (mo), or fibroblasts (f). In some areas a collagenous matrix (c) has been secreted, in other areas debris is present. Red cells (er) are scattered throughout this region. (Magn.  $\times 2200$ .)

FIGURE 66. Electron micrograph of the region in figure 63 (= 66) in which the cells show a preferred orientation. Most of the cells are fibroblasts (f), but some macrophages (ma) are present. The matrix contains bundles of collagen fibrils (c). (Magn.  $\times 2300$ .)

FIGURE 67. Electron micrograph of the area at the edge of the developing cartilage in figure 63 (= 67). The cells are diverse; some appear to be degenerating chondrocytes (dch), others appear to be active chondrocytes (ch). The matrix contains both thin, cartilage-type collagen fibrils (arrows) and bundles of thicker collagen fibrils (arrowheads). (Magn.  $\times 2300$ .)

## DESCRIPTION OF PLATE 18

FIGURE 76. Electron micrograph of the developing periosteum of the 9-day fracture in figures 70 and 71 (= 76). The fibroblasts (f) lie parallel to the surface. The collagen fibrils (c) are in layers orientated at right angles. (Magn.  $\times 10300$ .)

FIGURE 77. Electron micrograph of an area just under the periosteum of the fracture in figure 71 (= 77). The cells in the upper part of the micrograph are rounded, and have much rough endoplasmic reticulum, which suggests that they are differentiating into osteoblasts (ob). Capillaries (cap) are also present. Under this layer there are some monocytes (mo) and a large cell, which might be a multinucleated giant cell (mgc). The matrix contains irregular bundles of collagen fibrils (c). (Magn.  $\times 2300$ .)

## DESCRIPTION OF PLATE 19

FIGURE 78. Electron micrograph of a region below that in figure 88 (see figure 71 = 78). An area of developing trabeculae (tr) of cancellous bone with osteoblasts (ob) and an occasional monocyte (mo) merges into a region of flattened cells, most of which are fibroblasts (f). A few monocytes (mo) are present. (Magn.  $\times 2300$ .)

FIGURE 79. Electron micrograph of a deeper layer (see figure 71 = 79) in which the cells are spindle-shaped and longitudinally orientated. They all appear to be fibroblasts (f). (Magn.  $\times 2300$ .)

## DESCRIPTION OF PLATE 20

FIGURE 80. Electron micrograph at higher magnification of a region near to that of figure 79 (see figure 71 = 80) showing fibroblasts (f), bundles of collagen fibrils (c) and elastic fibres (el) in the matrix. (Magn.  $\times 8600$ .)

FIGURE 81. Electron micrograph of the upper region of the cartilage in figure 71 (= 81). The chondrocytes (ch) appear healthy with cytoplasm full of rough endoplasmic reticulum. The matrix is heterogeneous; the collagen fibrils are mostly thin, but there are also bundles of thick collagen fibrils (c) and long elastic fibres (arrows). (Magn.  $\times 2300$ .)

## DESCRIPTION OF PLATE 21

FIGURE 82. Electron micrograph of the region near the fracture gap of the 8-day fracture in figure 69 (= 82). There are macrophages (ma) and monocytes (mo) among the debris (d); a fragment of bone is present at the bottom. An occasional fibroblast (f) is seen near to a matrix with a few collagen fibrils (c). Occasional red cells (er) remain. (Magn.  $\times 2200$ .)

FIGURE 83. Electron micrograph of an area farther from the gap than that in figure 82 (see figure 69 = 83). Here there are more fibroblasts (f) and the collagenous matrix is more-developed. Macrophages (ma) and monocytes (mo) are present, and also a few red cells (er) and lipid droplets (l), some of which have been phagocytosed (arrows). (Magn.  $\times 2200$ .)

## DESCRIPTION OF PLATE 22

FIGURE 84. Electron micrograph of the area of figure 69 (= 84) in which fibroblasts (f) are arranged in a semicircle around the fracture gap. The matrix is well developed with bundles of collagen fibrils (c) and there are some elastic fibres (el). A small capillary (cap) is present. (The number 85 denotes the position of figure 85.) (Magn.  $\times 2900$ .)

FIGURE 85. Electron micrograph at higher magnification of an area of figure 84 (= 85) to show the structure of the matrix. The collagen fibrils are banded (arrows) and are grouped to form fibres. The elastic fibre (el) consists of an electron-lucent core surrounded by microfibrils. (Magn.  $\times 14200$ .)

## DESCRIPTION OF PLATE 23

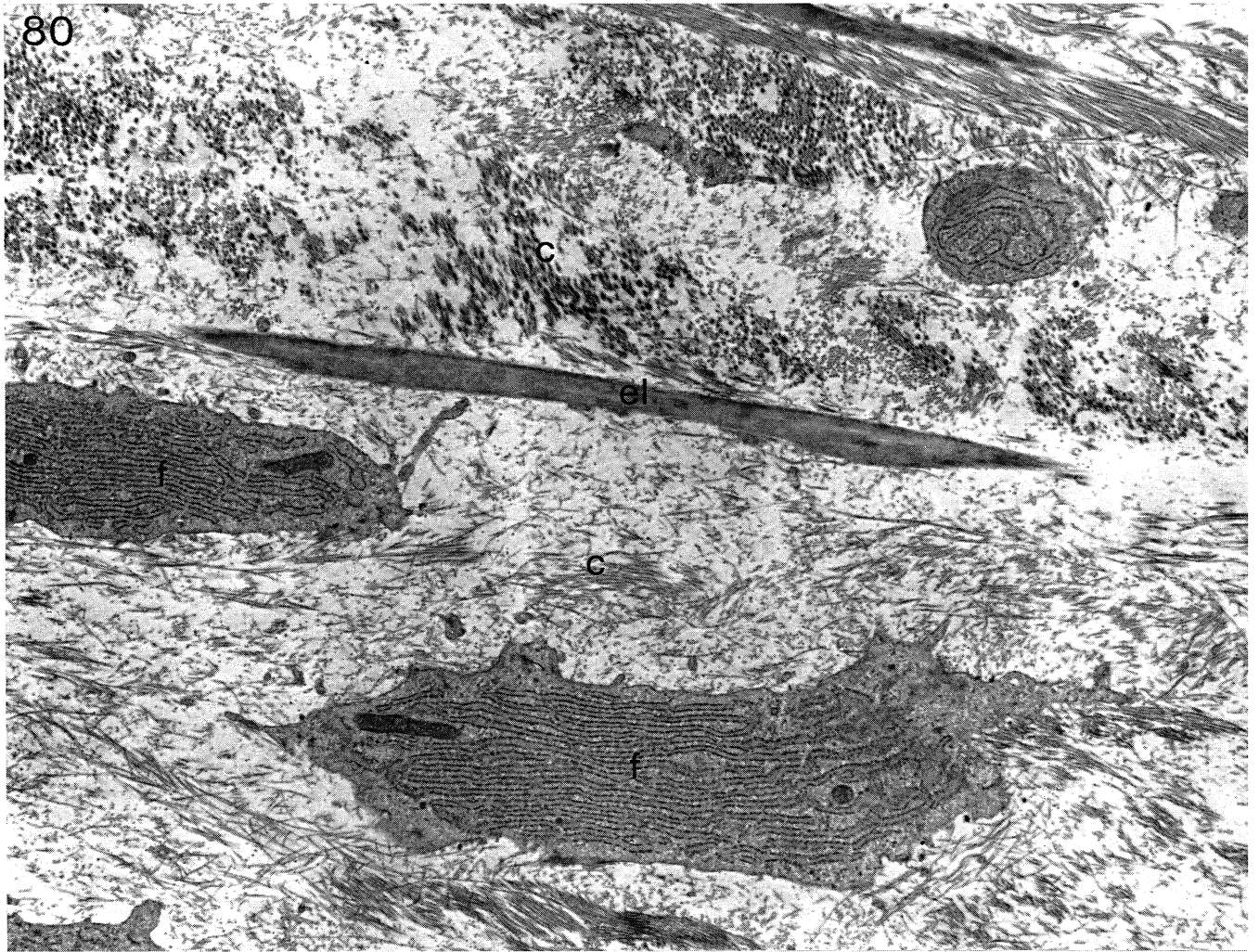
FIGURE 86. Electron micrograph of the area adjacent to the gap in figure 74 (= 86). Cartilaginous matrix abuts directly onto the debris, and incorporates some into the matrix (arrows). The matrix contains thin collagen fibrils. The chondrocytes (ch) are healthy and have much rough endoplasmic reticulum. (Magn.  $\times 2400$ .)

FIGURE 87. Electron micrograph of an area of cartilage in the middle of the callus in figure 74 (= 87). The matrix is very heterogeneous; there are bundles of thick collagen fibrils (arrows) among the thin, cartilage-type fibrils. The chondrocytes (ch) are degenerating and some appear to be in lacunae (arrowheads). (Magn.  $\times 2400$ .)



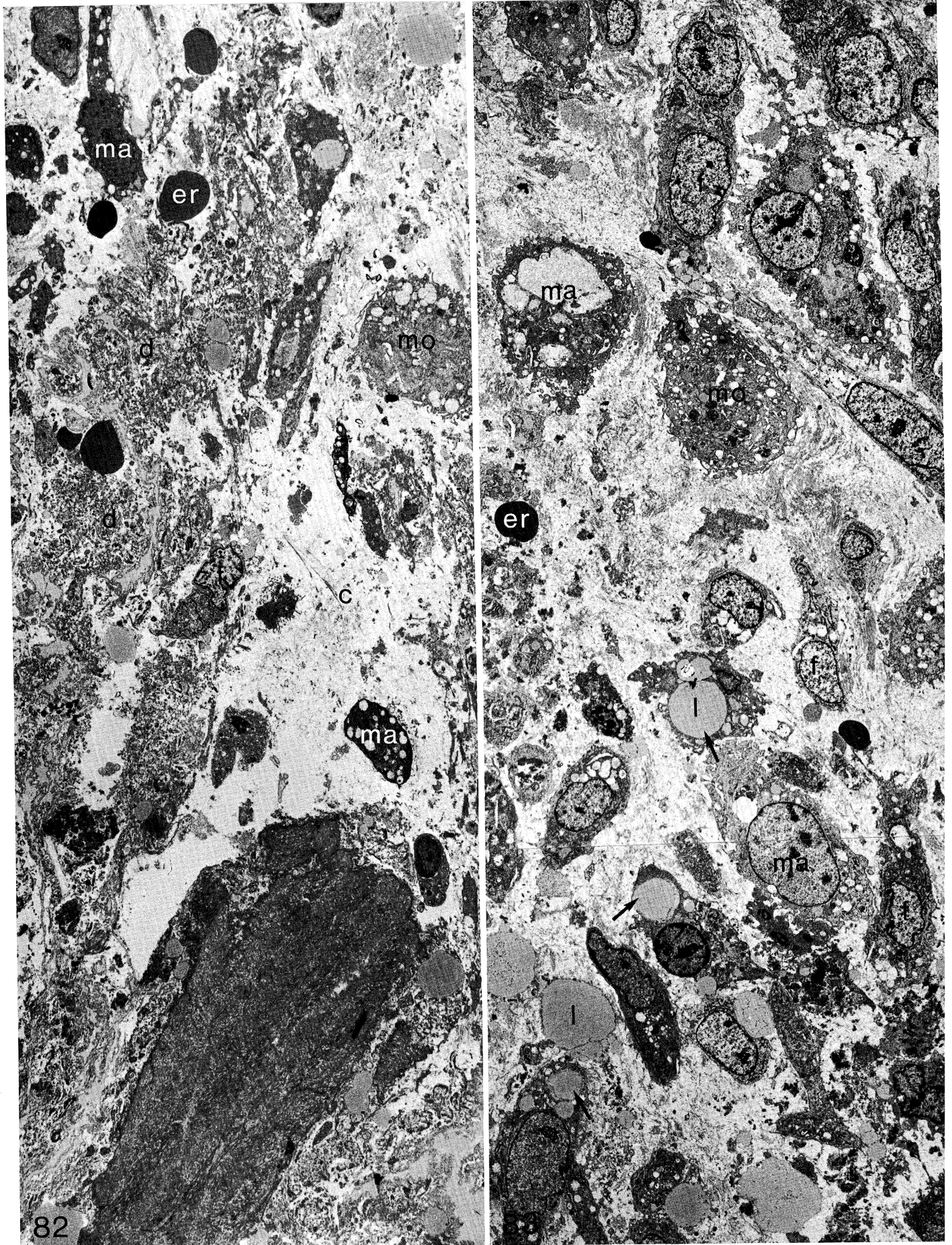
FIGURES 78 AND 79. For description see facing plate 17.





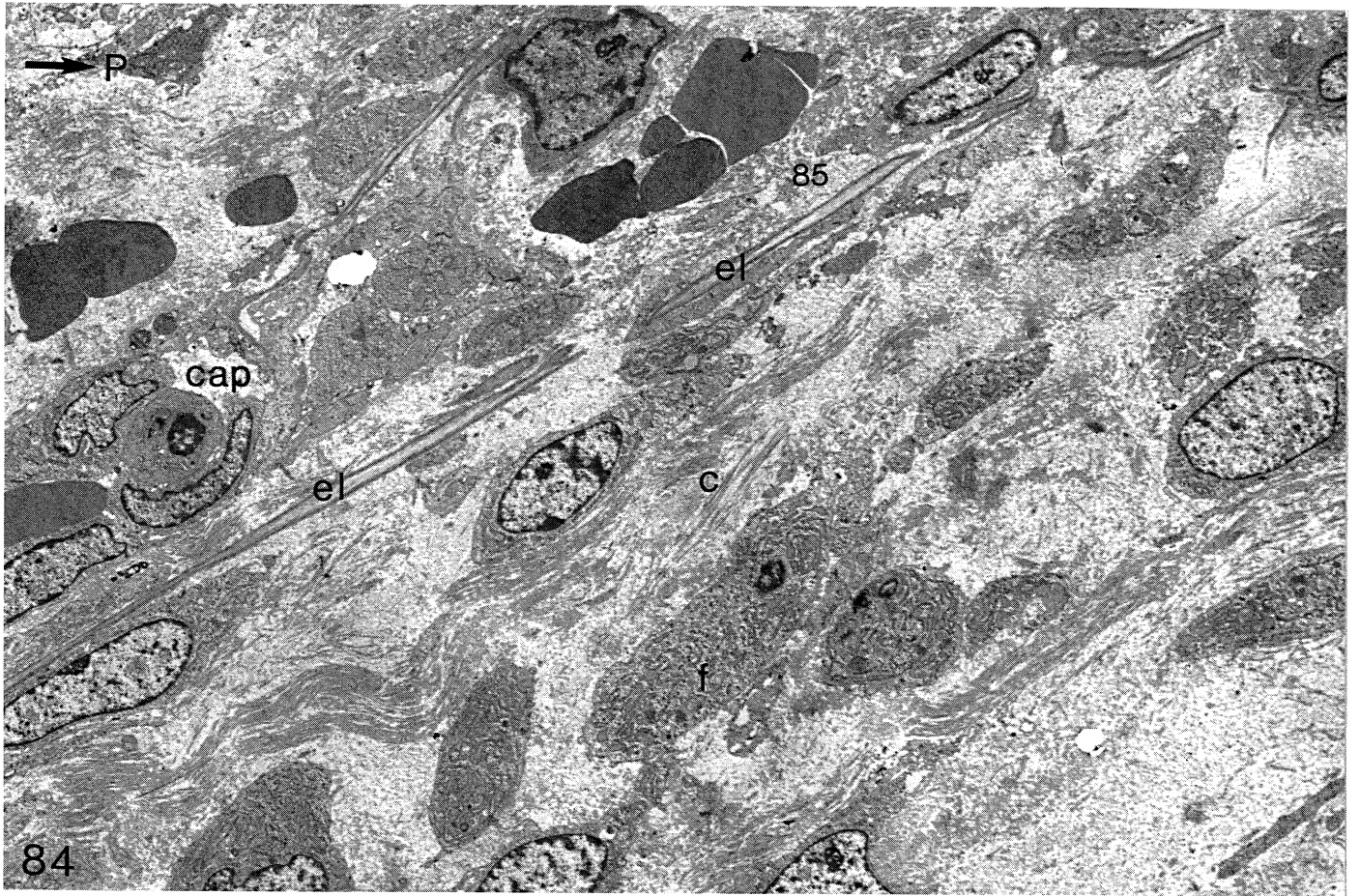
FIGURES 80 AND 81. For description see facing plate 17.





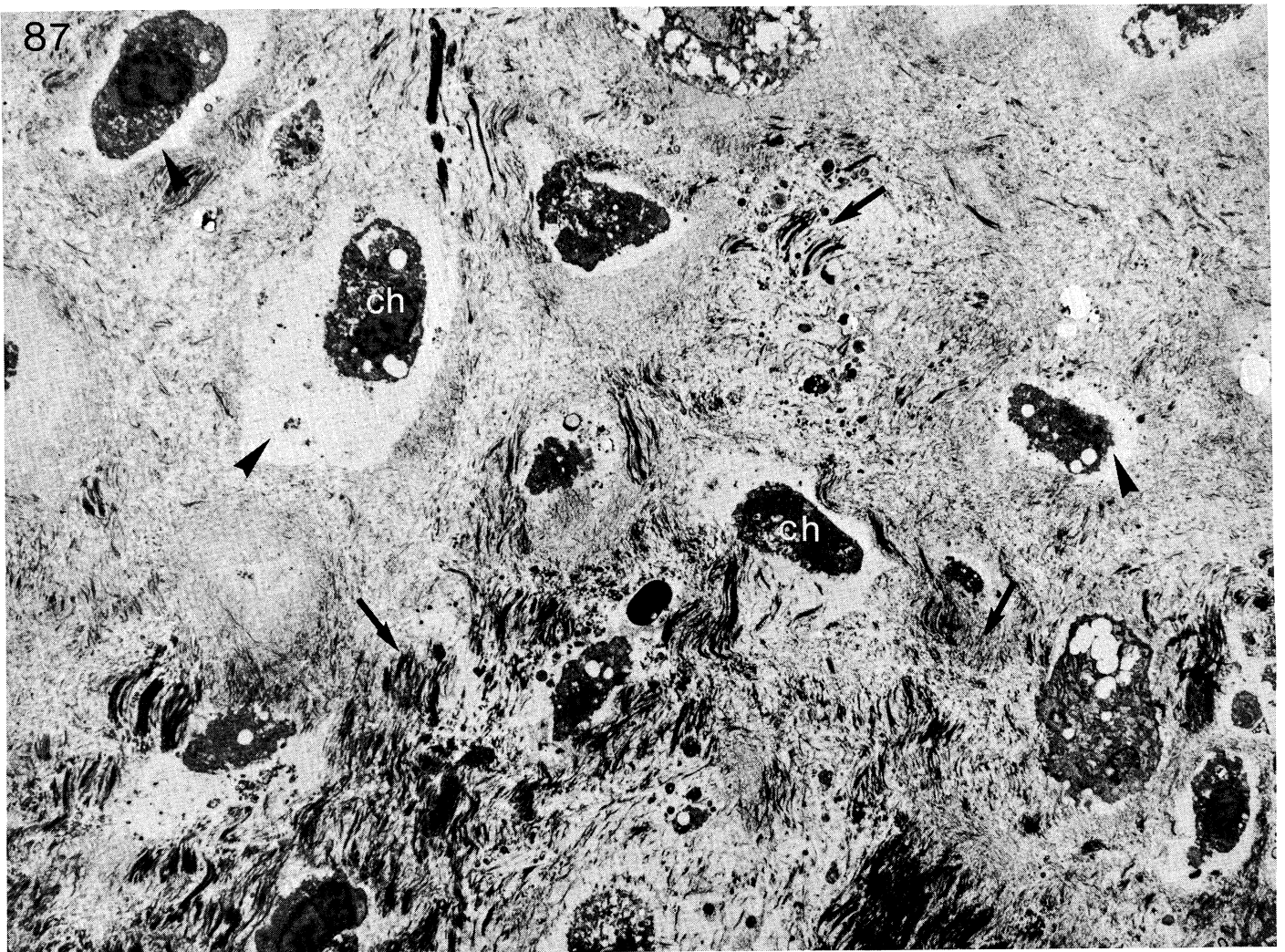
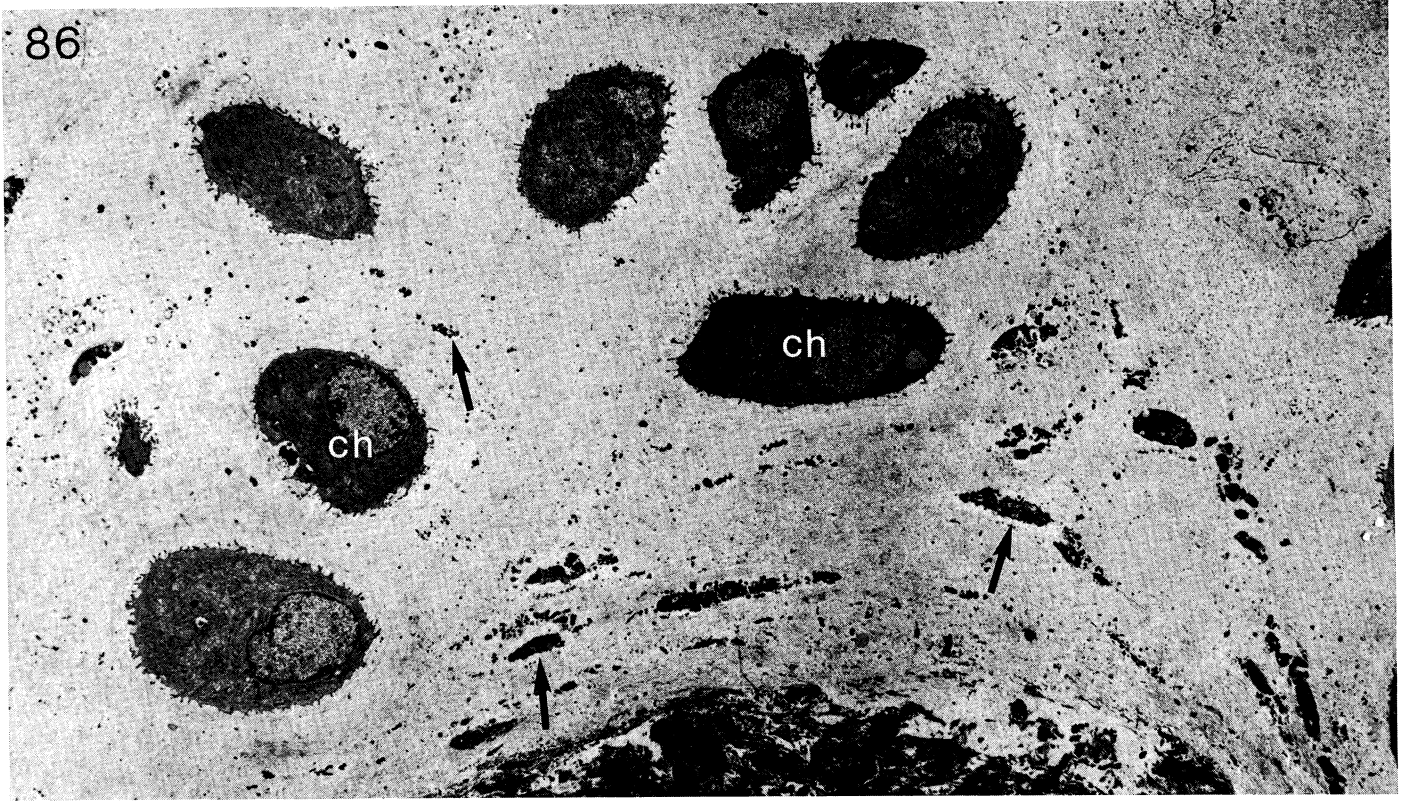
FIGURES 82 AND 83. For description see facing plate 17.





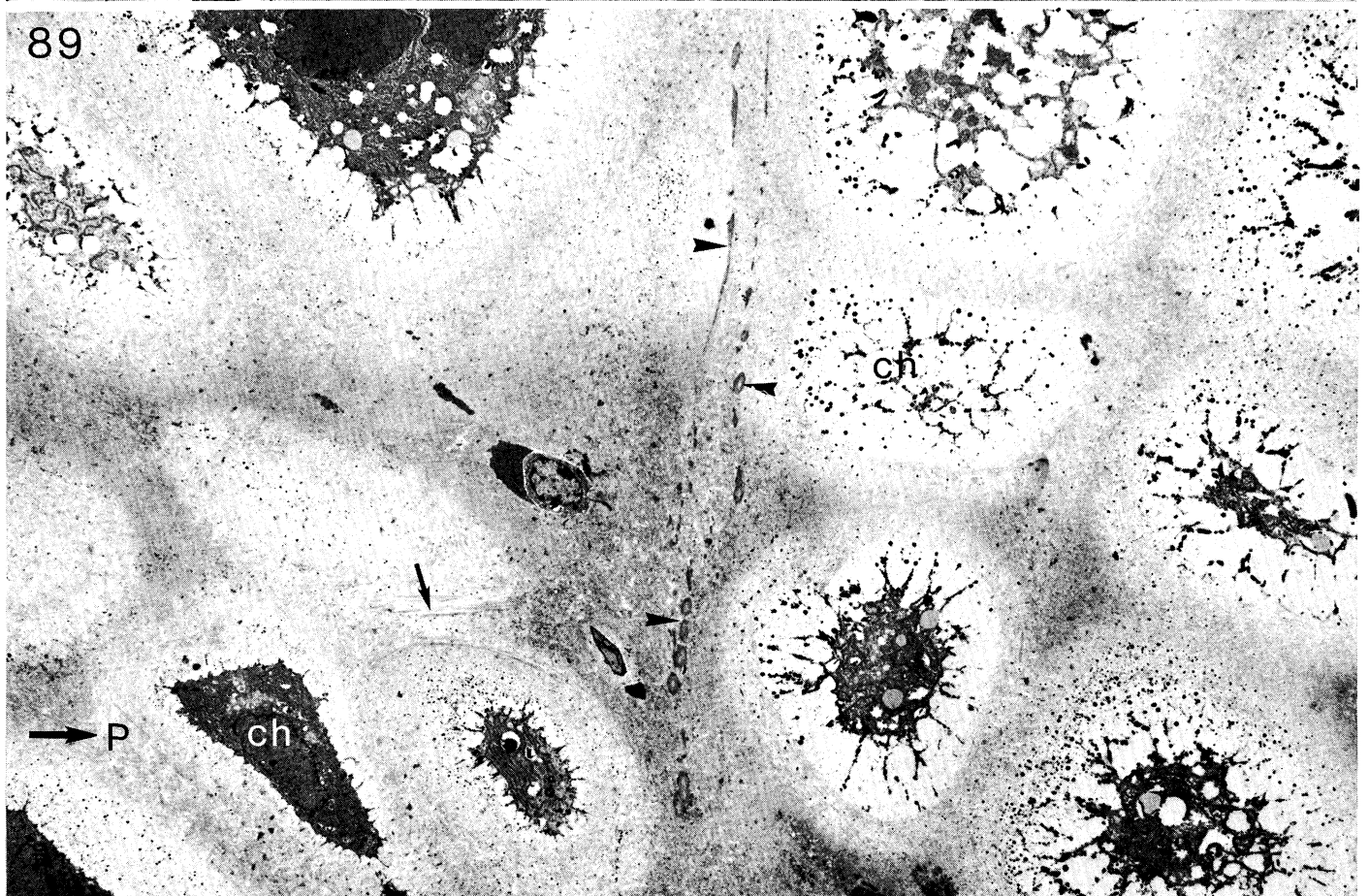
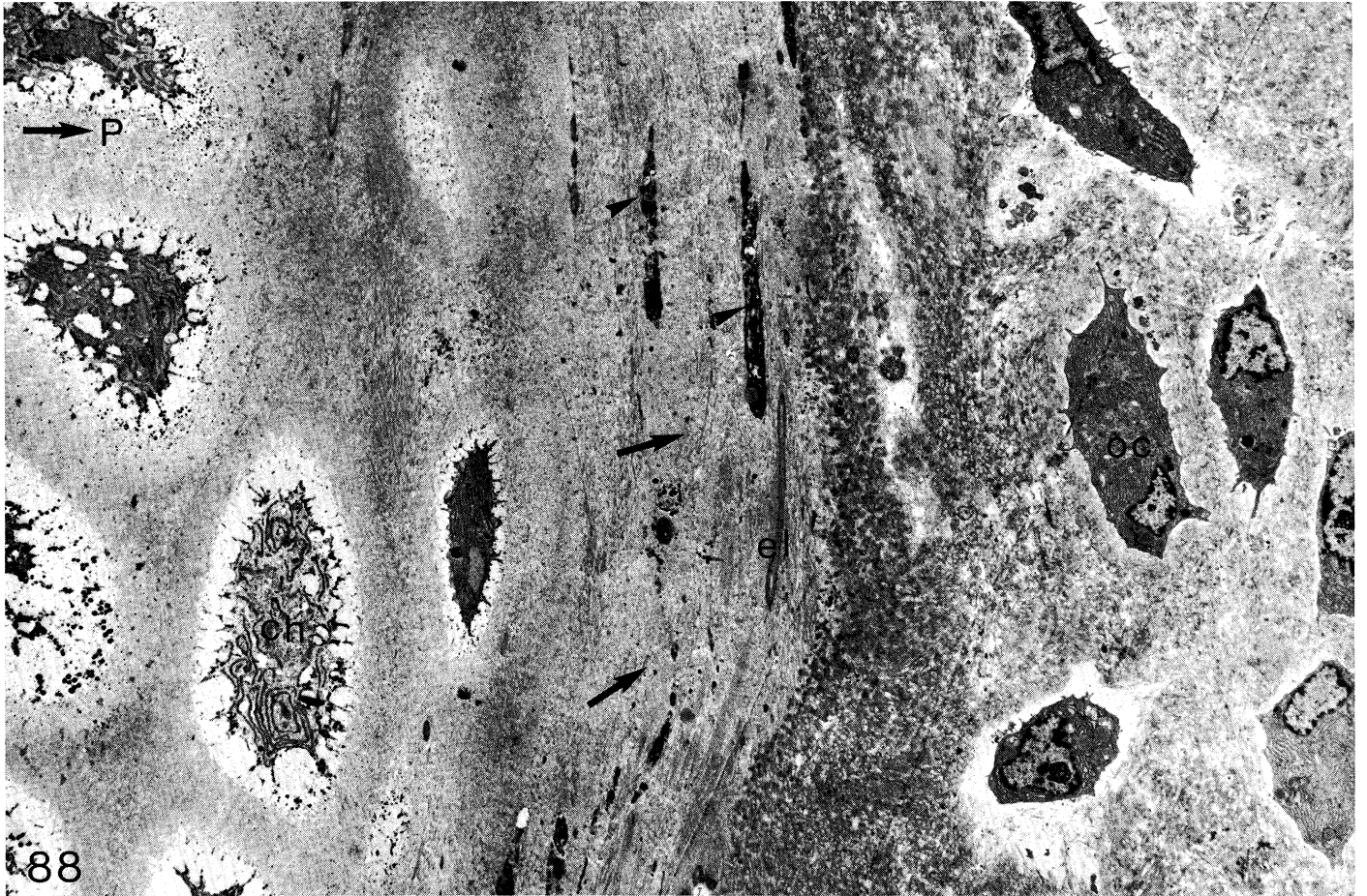
FIGURES 84 AND 85. For description see facing plate 17.





FIGURES 86 AND 87. For description see facing plate 17.





FIGURES 88 AND 89. For description see opposite.



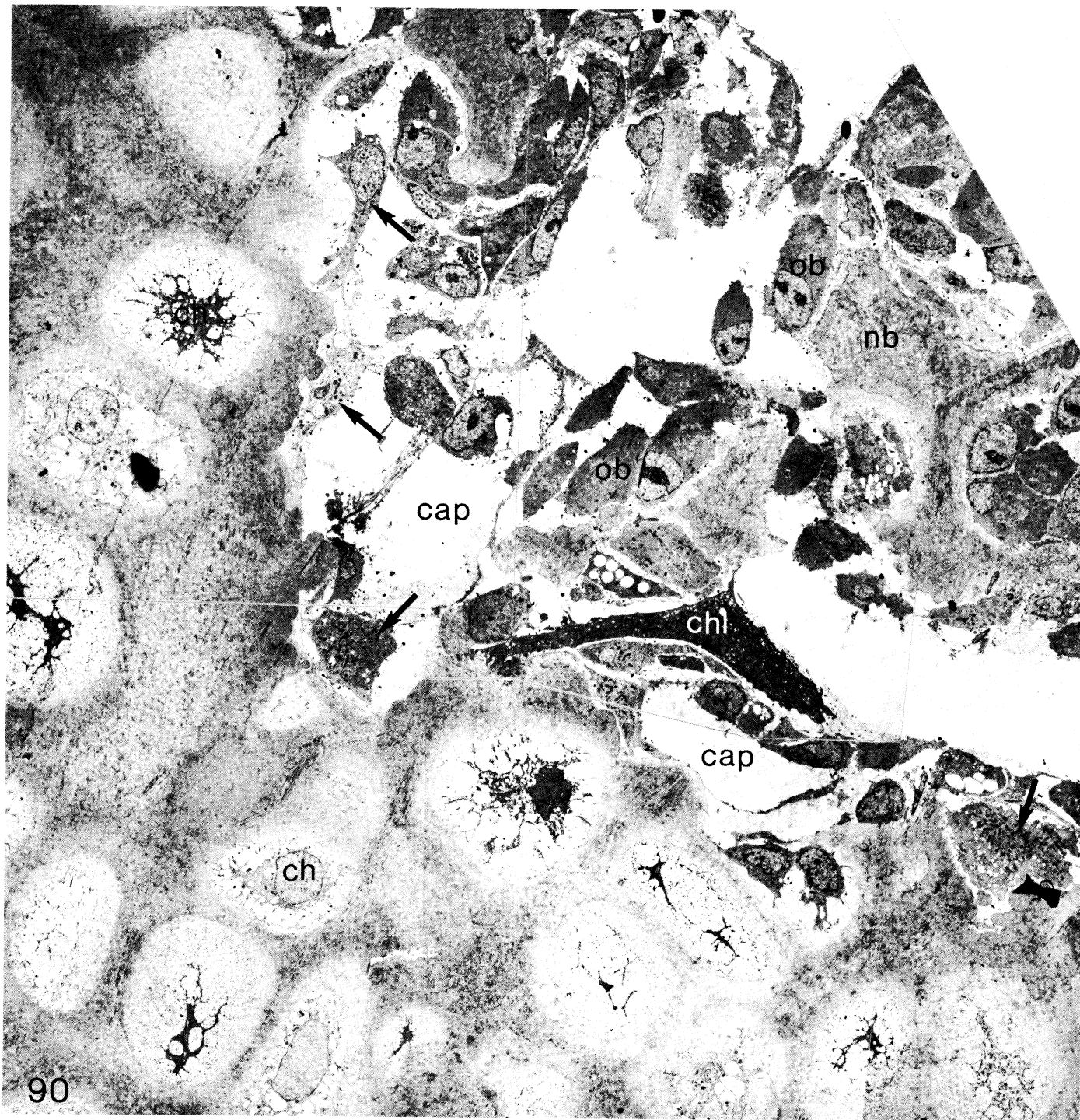
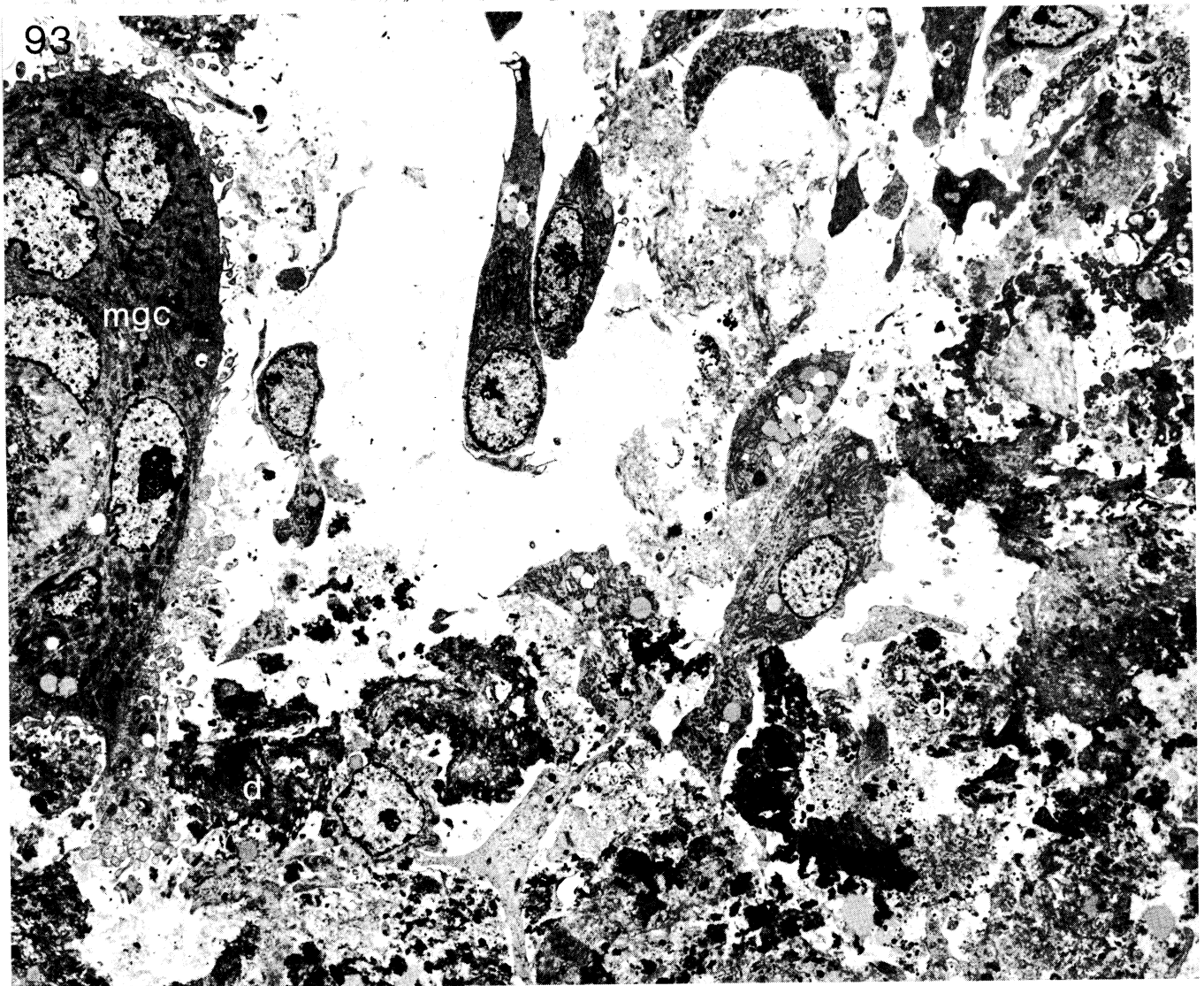
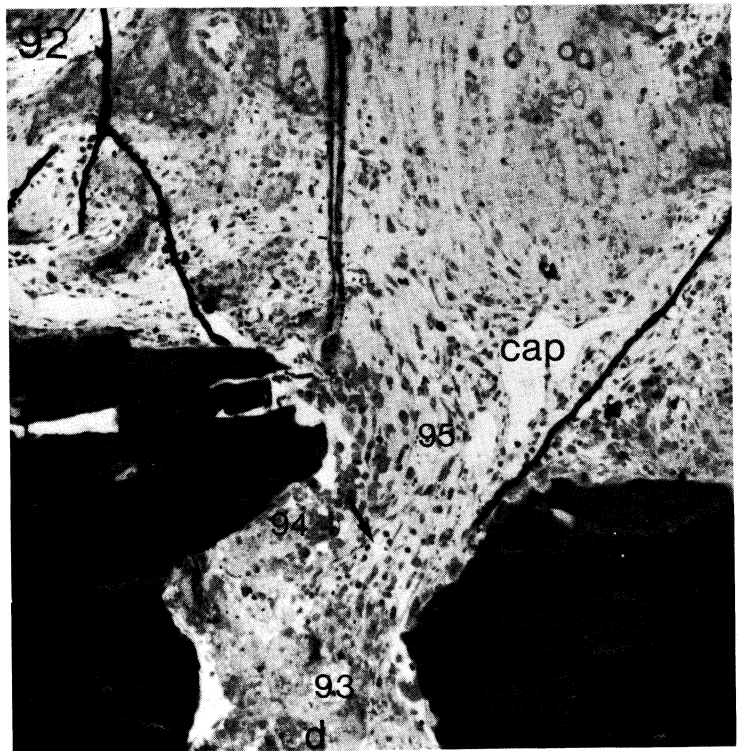
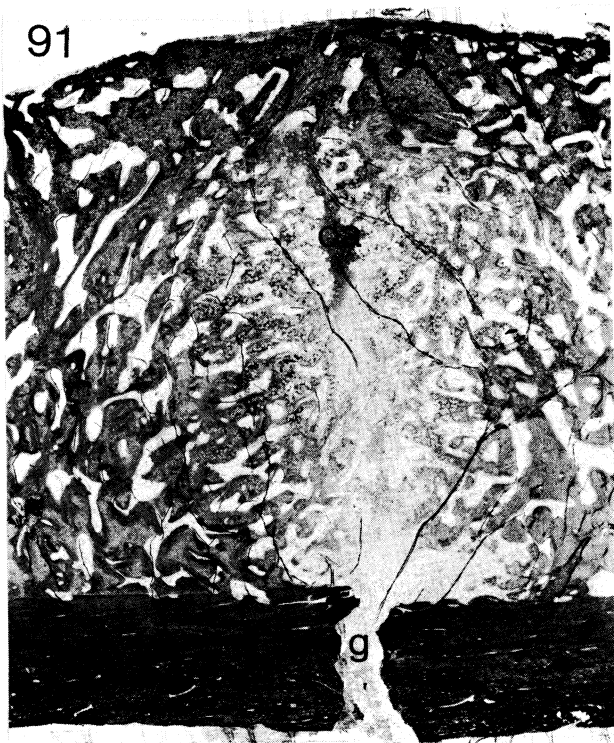


FIGURE 90. This montage of electron micrographs shows a region of endochondral ossification in the callus in figure 75 (= 90). The cartilage matrix, with hypertrophied chondrocytes (ch), is being resorbed by a series of cells, chondroclasts (chl) and mononuclear cells (arrows). Capillaries (cap) are invading the eroded areas, followed by osteoblasts (ob) laying down new bone (nb). (Magn.  $\times 1400$ .)

#### DESCRIPTION OF PLATE 24

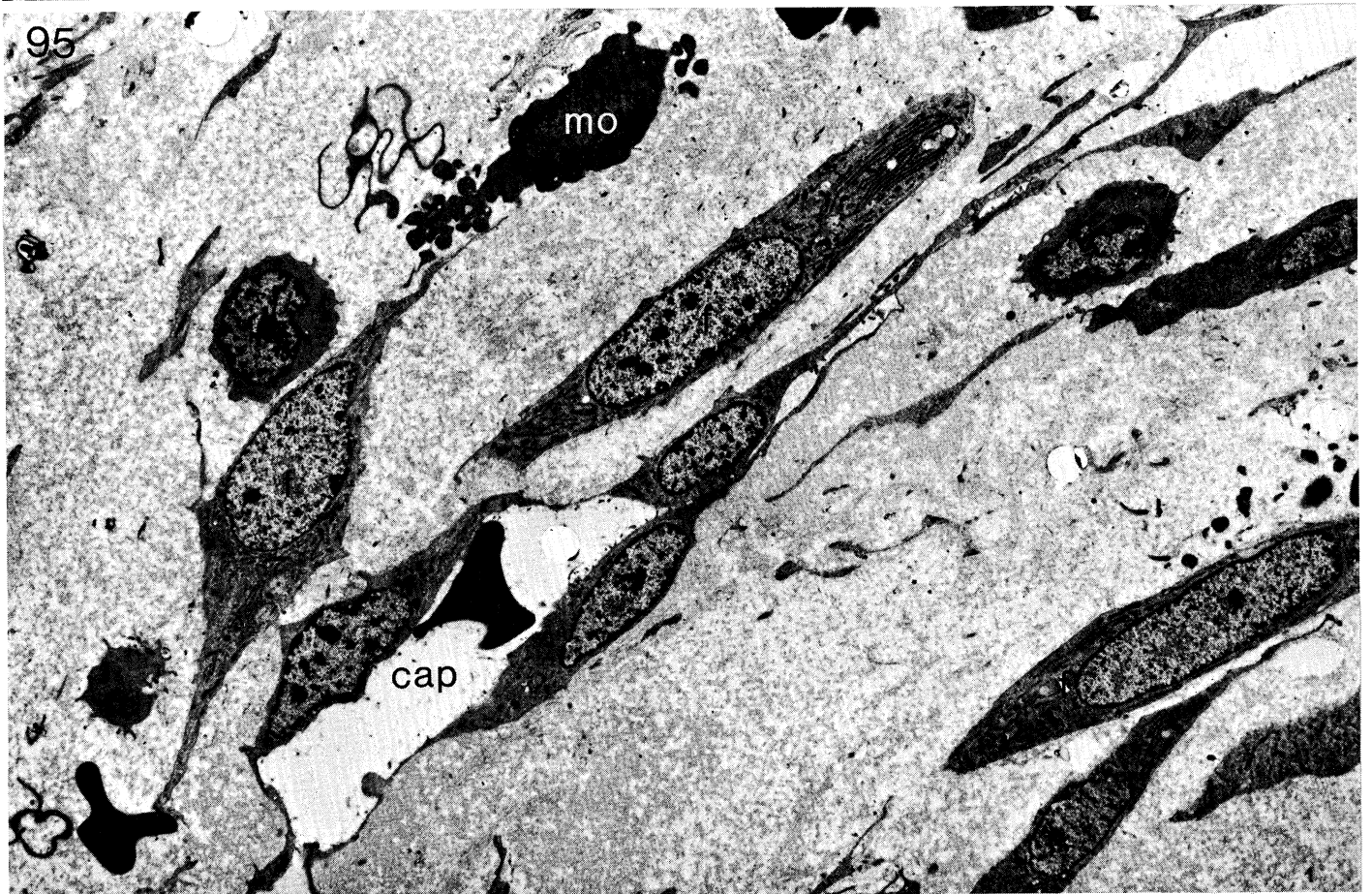
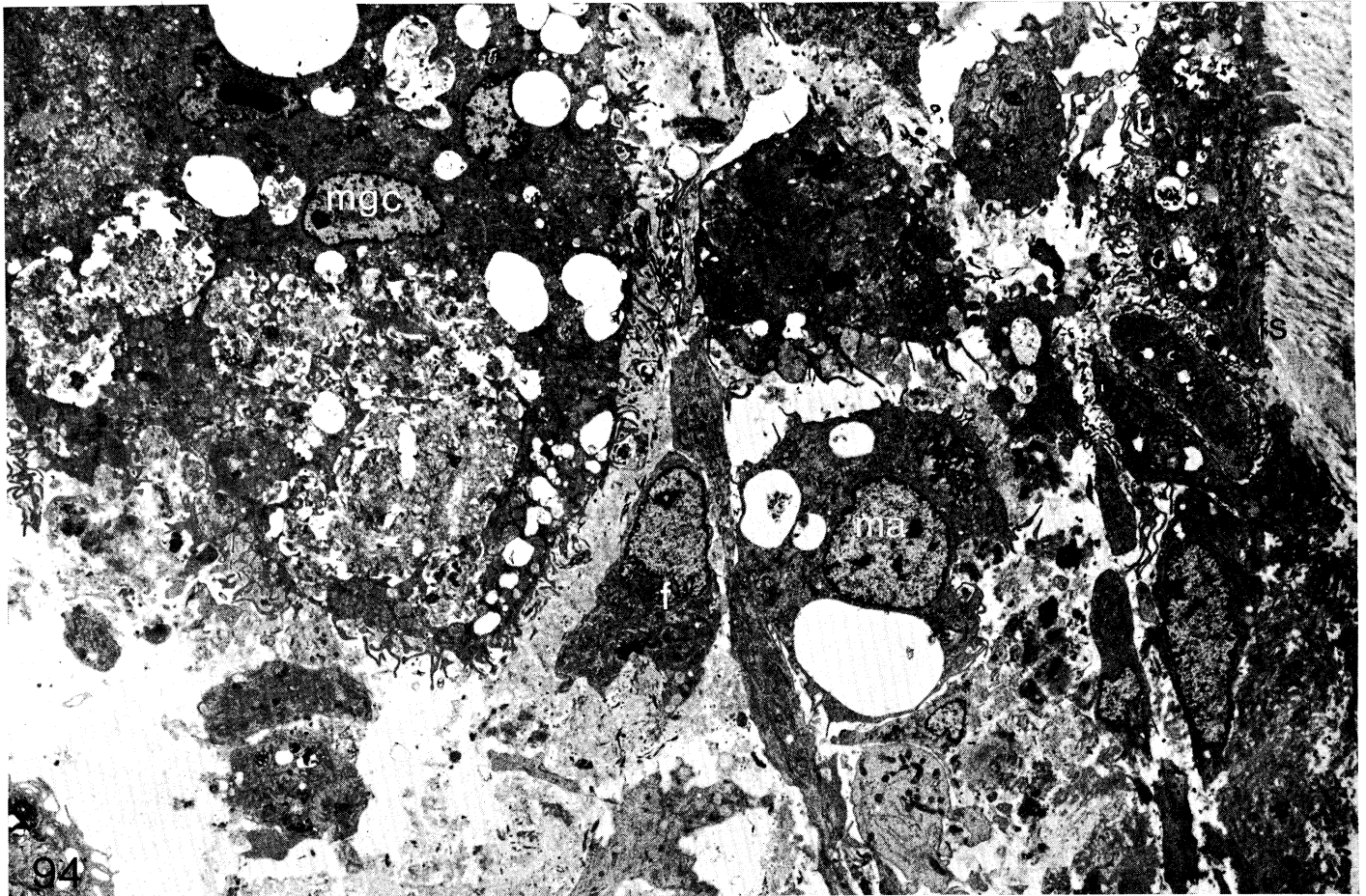
FIGURE 88. Electron micrograph of the junction between cartilage and bone in the peripheral regions of the callus in figure 73 (= 88). The bone matrix on the right, which contains healthy osteocytes (oc), is separated from the cartilage matrix on the left, which contains hypertrophied chondrocytes (ch) in lacunae, by a layer of dense matrix (arrows). This layer contains collagen fibrils of differing diameters, elastic fibres (el) and flattened degenerating cells (arrowheads). (Magn.  $\times 2400$ .)

FIGURE 89. Electron micrograph of the cartilage in the peripheral regions of the callus in figure 73 (= 89). The chondrocytes (ch) are hypertrophied and in lacunae. The matrix contains mainly thin fibrils, but some thicker collagen fibrils (arrow) and elastic fibres (arrowheads) are also present. (Magn.  $\times 2400$ .)

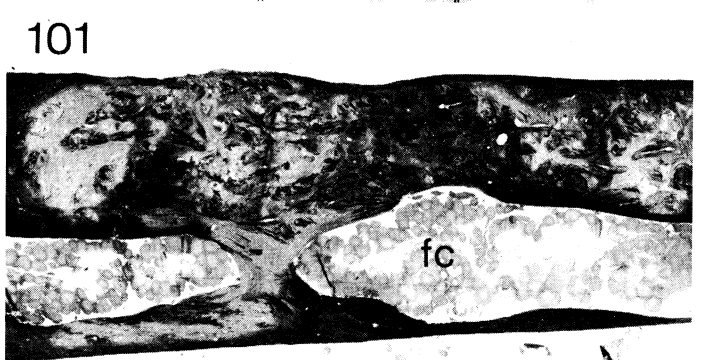
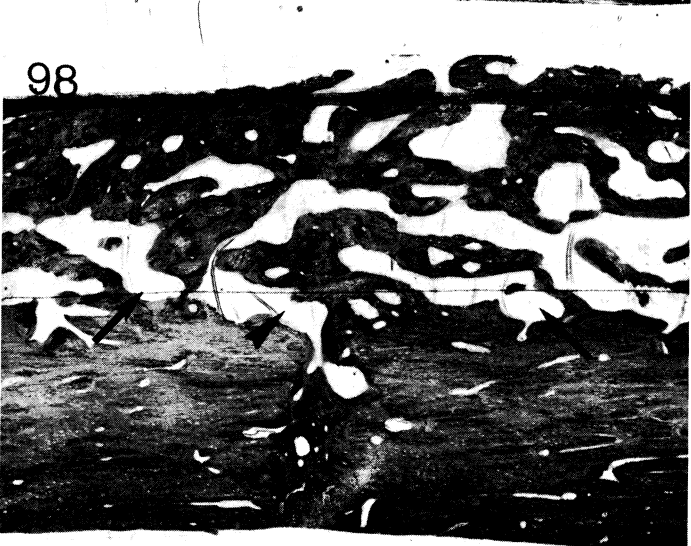
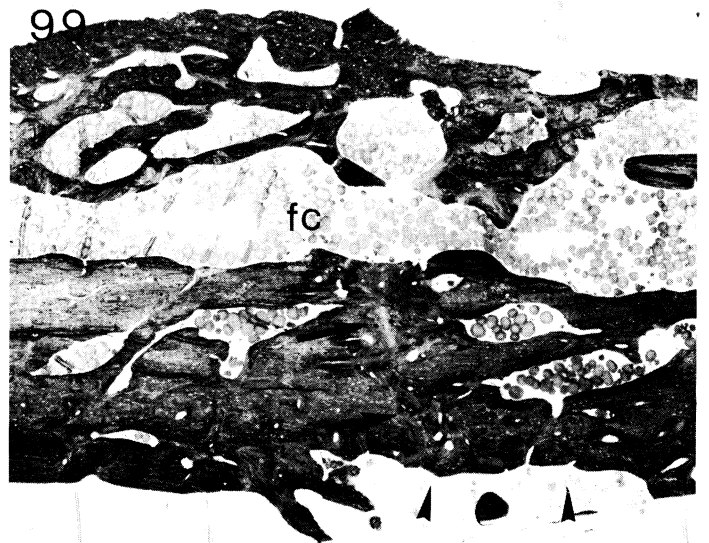
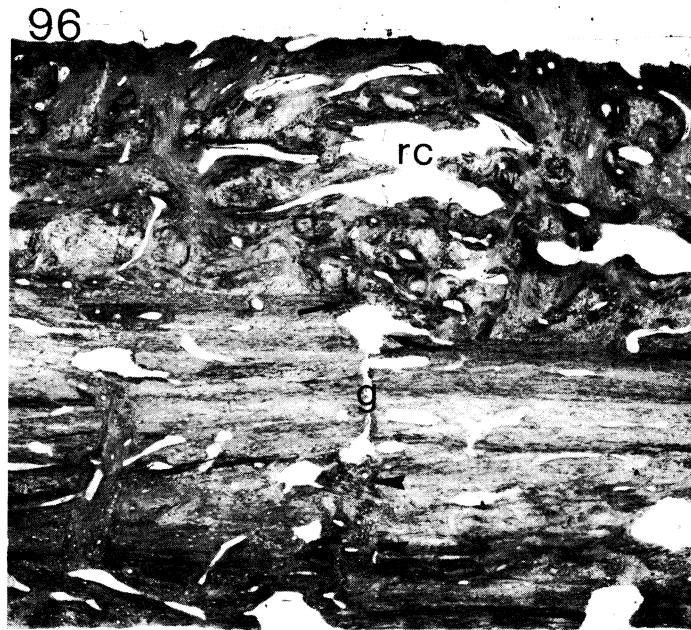


FIGURES 91-93. For description see facing plate 28.





FIGURES 94 AND 95. For description see facing plate 28.



FIGURES 96-102. For description see opposite.

## DESCRIPTION OF PLATE 26

- FIGURE 91. Photomicrograph of a 4-week mechanically unstable fracture. Only remnants of cartilage (ca) remain in the periosteal callus. More bone has been laid down on the trabeculae of cancellous bone, so that it appears more compact. A well vascularized area of fibrous tissue surrounds, and is beginning to penetrate, the fracture gap (g). (Magn.  $\times 19$ .)
- FIGURE 92. Photomicrograph of the periosteal end of the fracture gap in figure 91. Large capillaries (cap) lie in the fibrous tissue which is invading the gap. Debris (d) is still present deep in the gap, but it is being removed by phagocytic cells. Behind these, the cells are more ordered (arrow). (The numbers 93, 94 and 95 denote the positions of figures 93, 94 and 95.) (Magn.  $\times 130$ .)
- FIGURE 93. Electron micrograph of an area deep in the gap shown in figure 92 (= 93). The debris (d) is being removed in this area by a multinucleated giant cell (mgc). Some fibroblasts (f) are also present. Magn.  $\times 2800$ .)

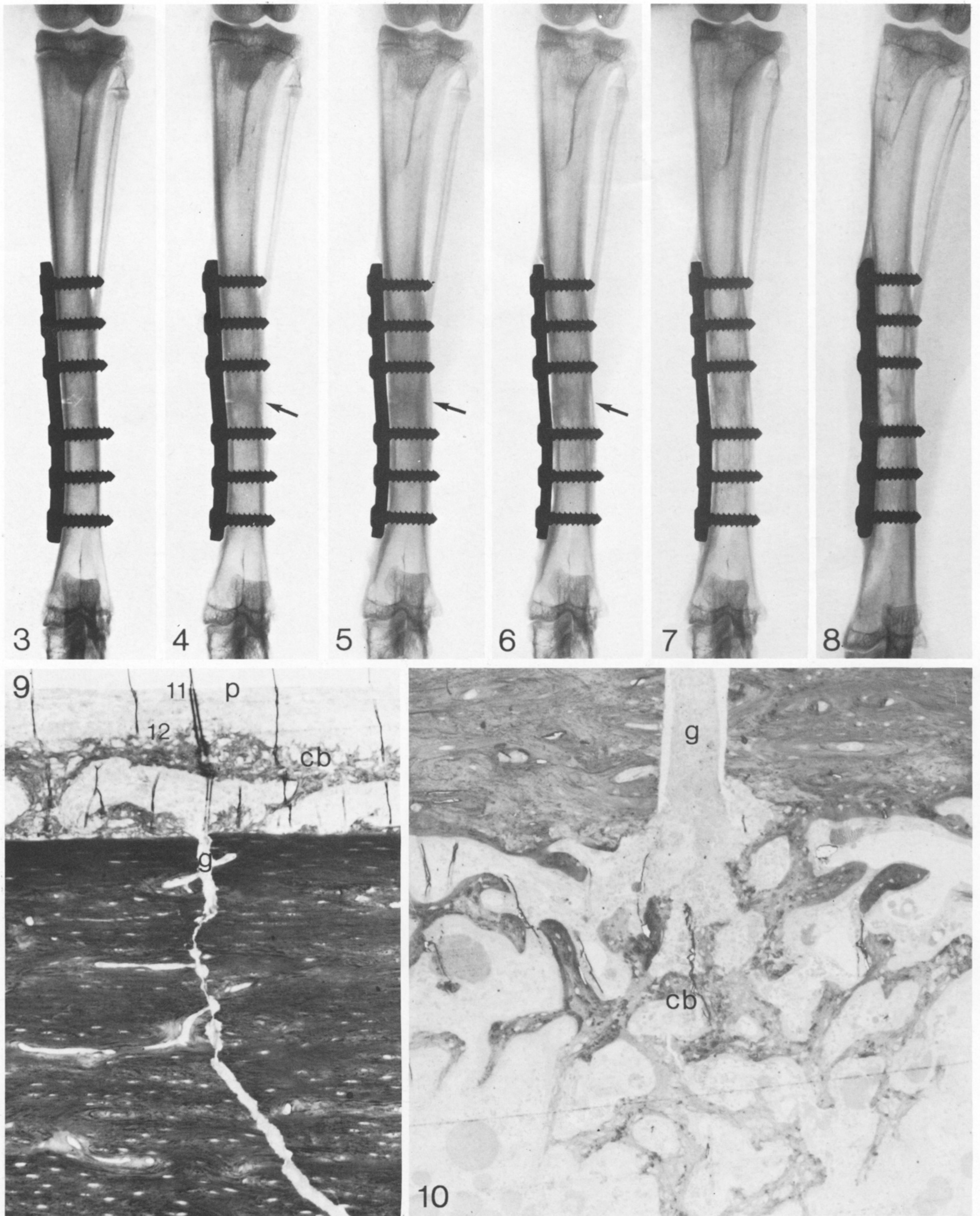
## DESCRIPTION OF PLATE 27

- FIGURE 94. Electron micrograph of an area of figure 92 (= 94) along the edge of the gap. The fractured surface (fs) is covered by osteoclasts (ocl) that are resorbing it. Within the gap there is still some debris, which is being removed by macrophages (ma) and a multinucleated giant cell (mgc). Fibroblasts (f) are also present. (Magn.  $\times 2800$ .)
- FIGURE 95. Electron micrograph of an area of figure 92 (= 95) in the middle of the gap. A capillary (cap), fibroblasts (f) and monocytes (mo) lie in a collagenous matrix. (Magn.  $\times 2800$ .)

## DESCRIPTION OF PLATE 28

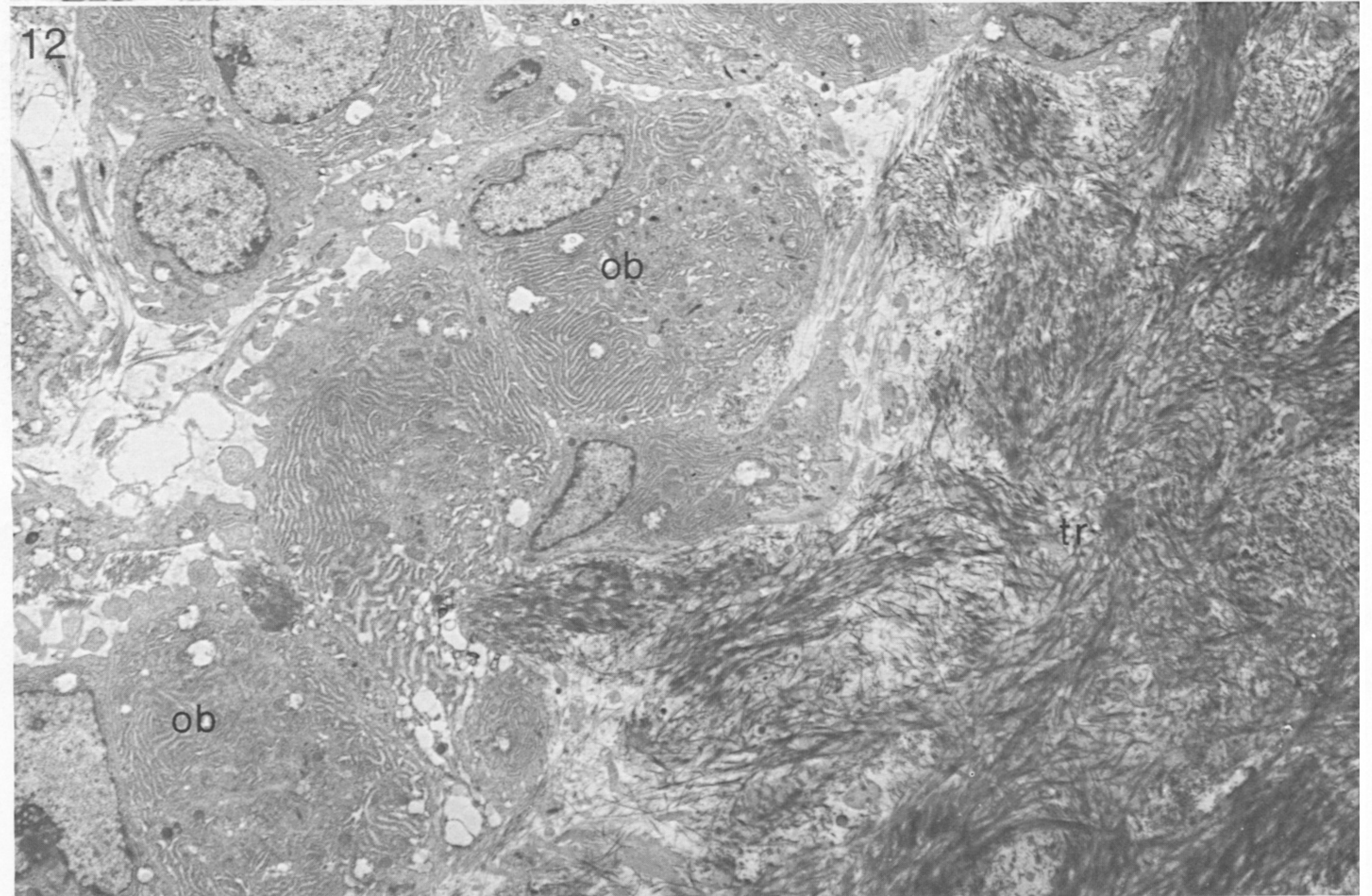
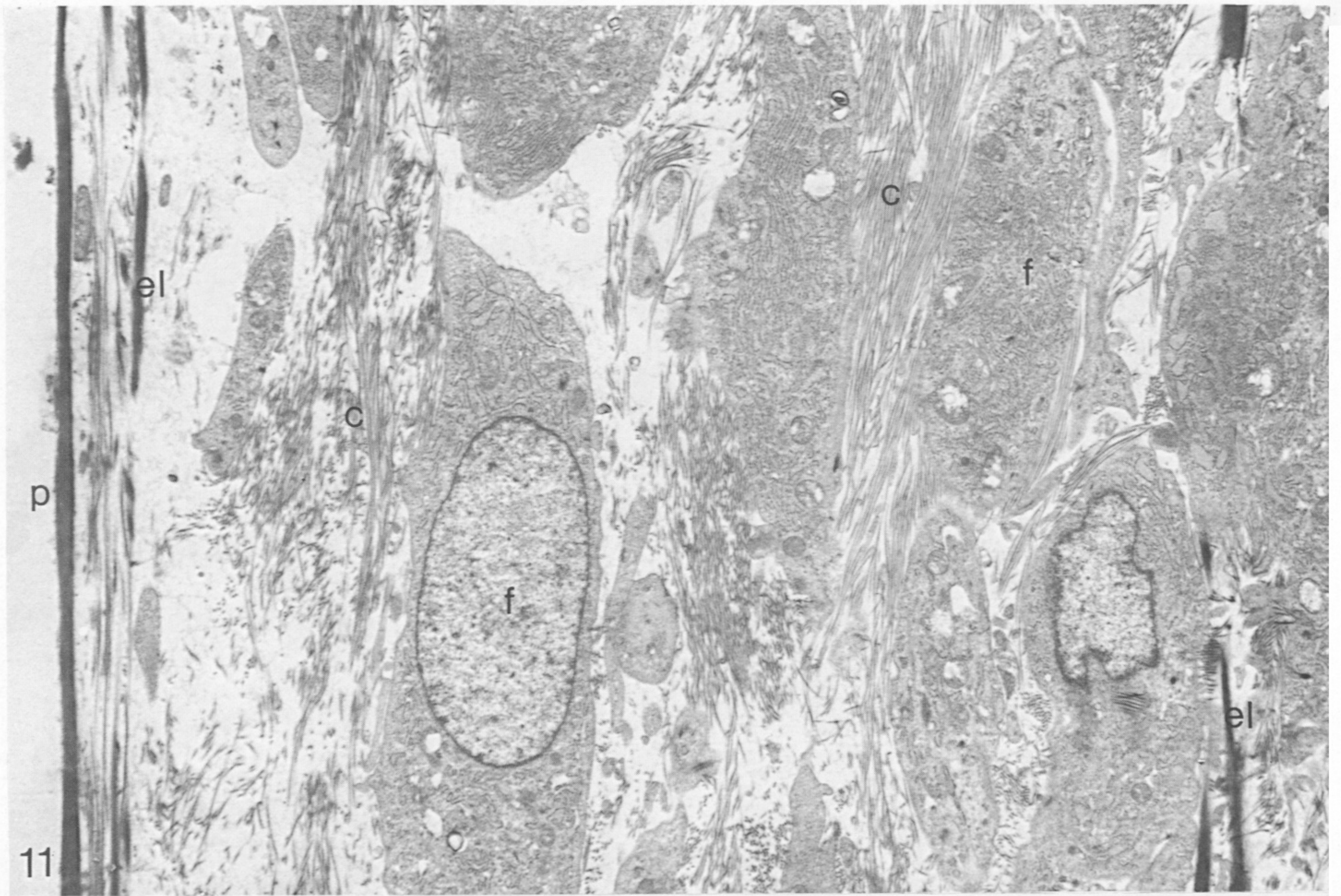
- FIGURE 96. Photomicrograph of a 5-week mechanically unstable fracture. The periosteal callus is for the most part compact, but some large resorption cavities (rc) are present. The fractured cortex is slightly misaligned (arrows) and a narrow gap (g), filled by debris, is present. There are remodelling cavities at each end. Towards the endosteal surface, there is a wide region of transverse lamellae of new bone (arrowheads). (Magn.  $\times 31$ .)
- FIGURE 97. Photomicrograph of the saw cut region of a 6-week fracture that was initially mechanically unstable. There is no periosteal callus as this part of the saw cut was under the plate. The saw cut is filled by transverse lamellae of new bone, and its overall width is between 0.6 and 0.9 mm. In some places the edge of the saw cut is visible (arrowheads). Longitudinal remodelling cavities (arrows) are invading the transverse lamellae. (Magn.  $\times 32$ .)
- FIGURE 98. Photomicrograph of the fracture region of the 6-week fracture in figure 97. The periosteal callus has large remodelling cavities, especially along the cortex-callus junction (arrows). The fracture gap is filled by transverse lamellae, which are being invaded by longitudinal remodelling cavities; one is entering the cortical bone from the periosteal callus (arrowhead). (Magn.  $\times 25$ .)
- FIGURE 99. Photomicrograph of a 12-week fracture that was initially mechanically unstable. The periosteal callus is eroded and the large cavities are filled by fat cells (fc). The position of the fracture is indicated by the transverse lamellae of bone in the cortex (arrows). There are also resorption cavities, filled with fat cells, in the cortical bone. There is some resorption from the endosteal surface (arrowheads). (Magn.  $\times 23$ .)
- FIGURE 100. Photomicrograph of an initially mechanically unstable fracture region at 18 weeks. The site of the fracture cannot be identified. The bone is compact, but the osteons and lamellae are orientated in varying directions. (Magn.  $\times 26$ .)
- FIGURE 101. Photomicrograph of an initially mechanically unstable fracture region at 26 weeks. The bone towards the periosteal surface consists of irregularly orientated osteons, whereas that towards the endosteal surface contains large resorption cavities filled by fat cells (fc). (Magn.  $\times 26$ .)
- FIGURE 102. Photomicrograph of an initially mechanically unstable fracture region at 1 year. Large resorption cavities, filled by fat cells, are open to both the endosteal and periosteal surfaces. The bone in this region is thin, but it is from the side of the tibia and not from under the plate. (Magn.  $\times 23$ .)





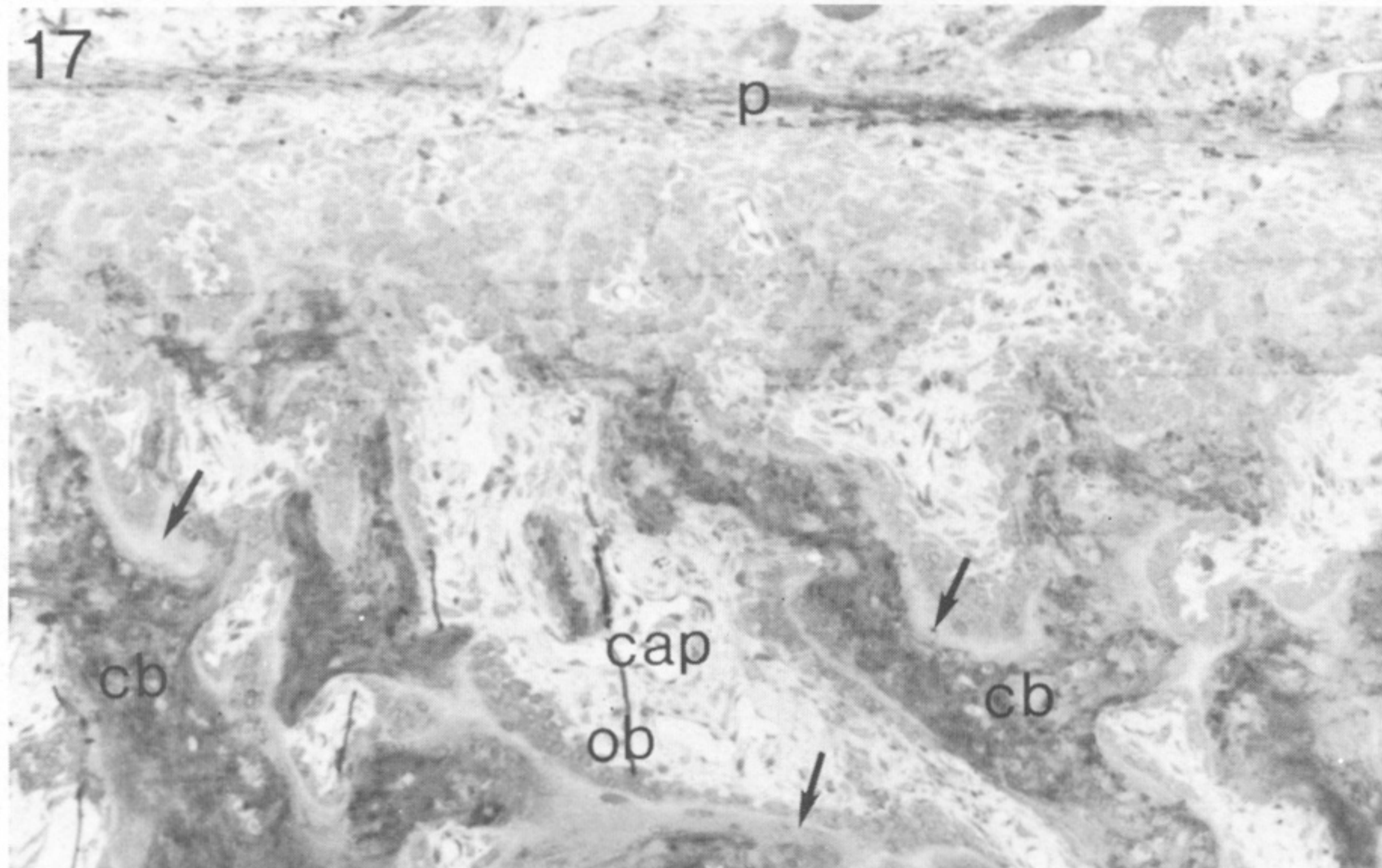
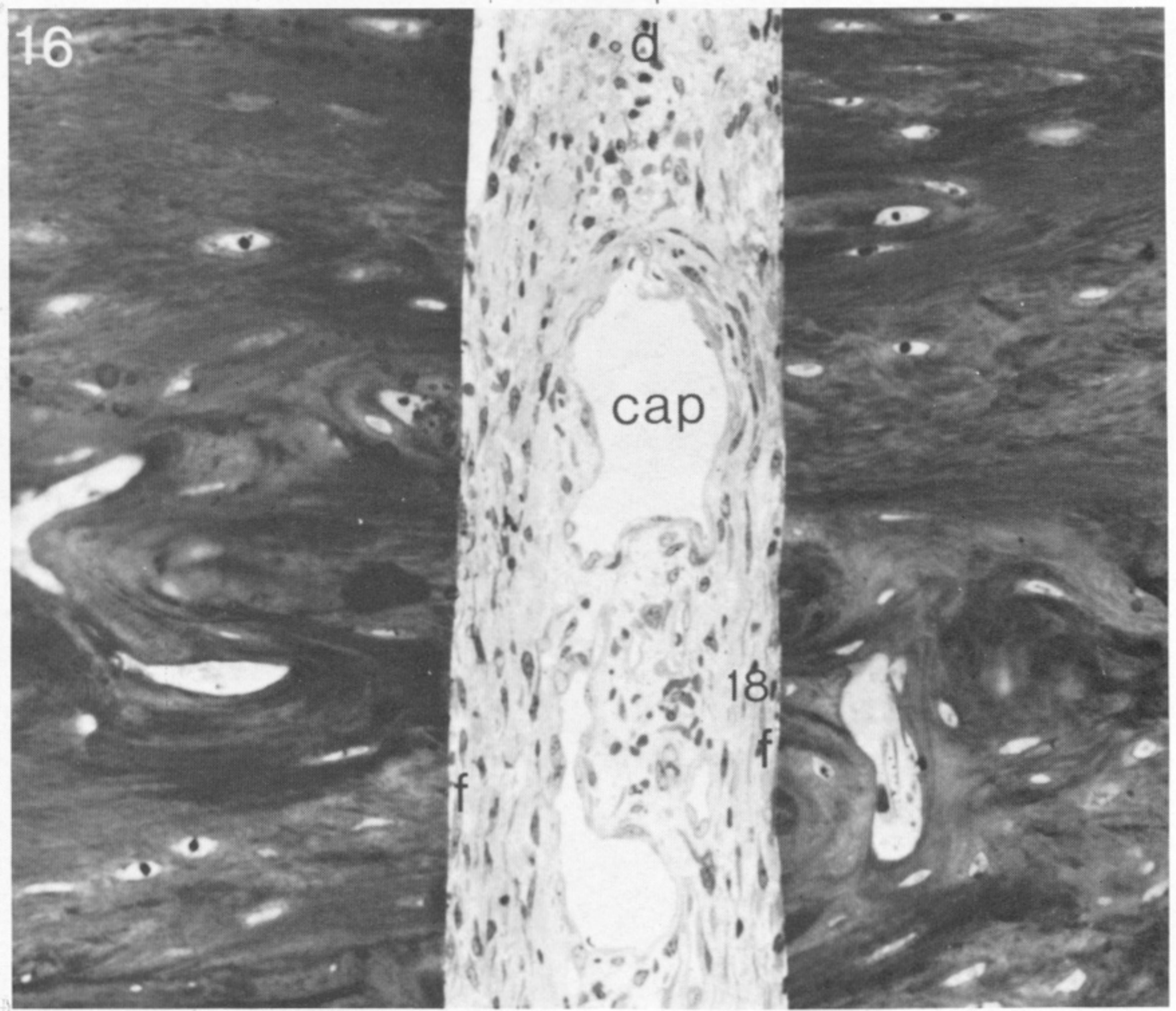
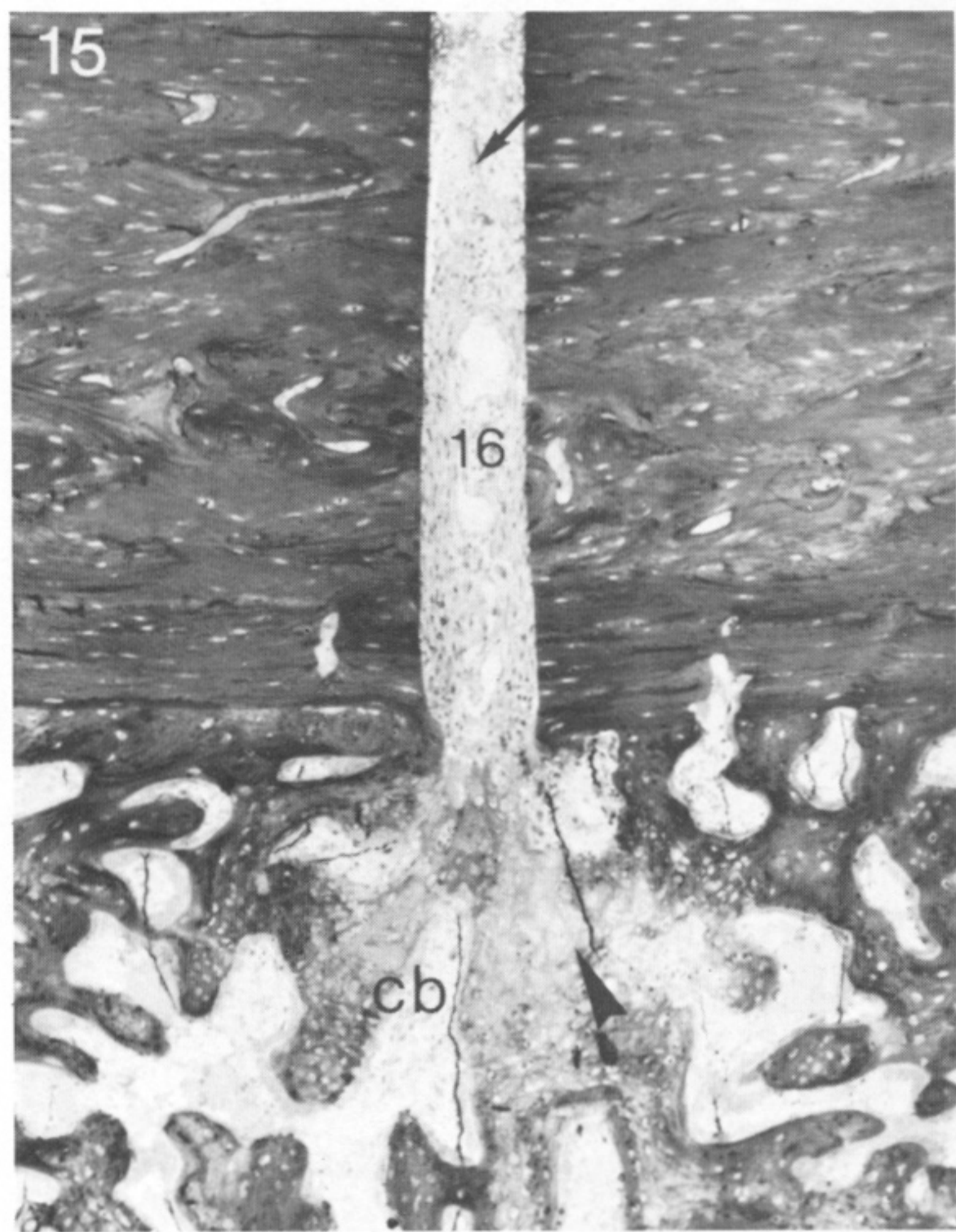
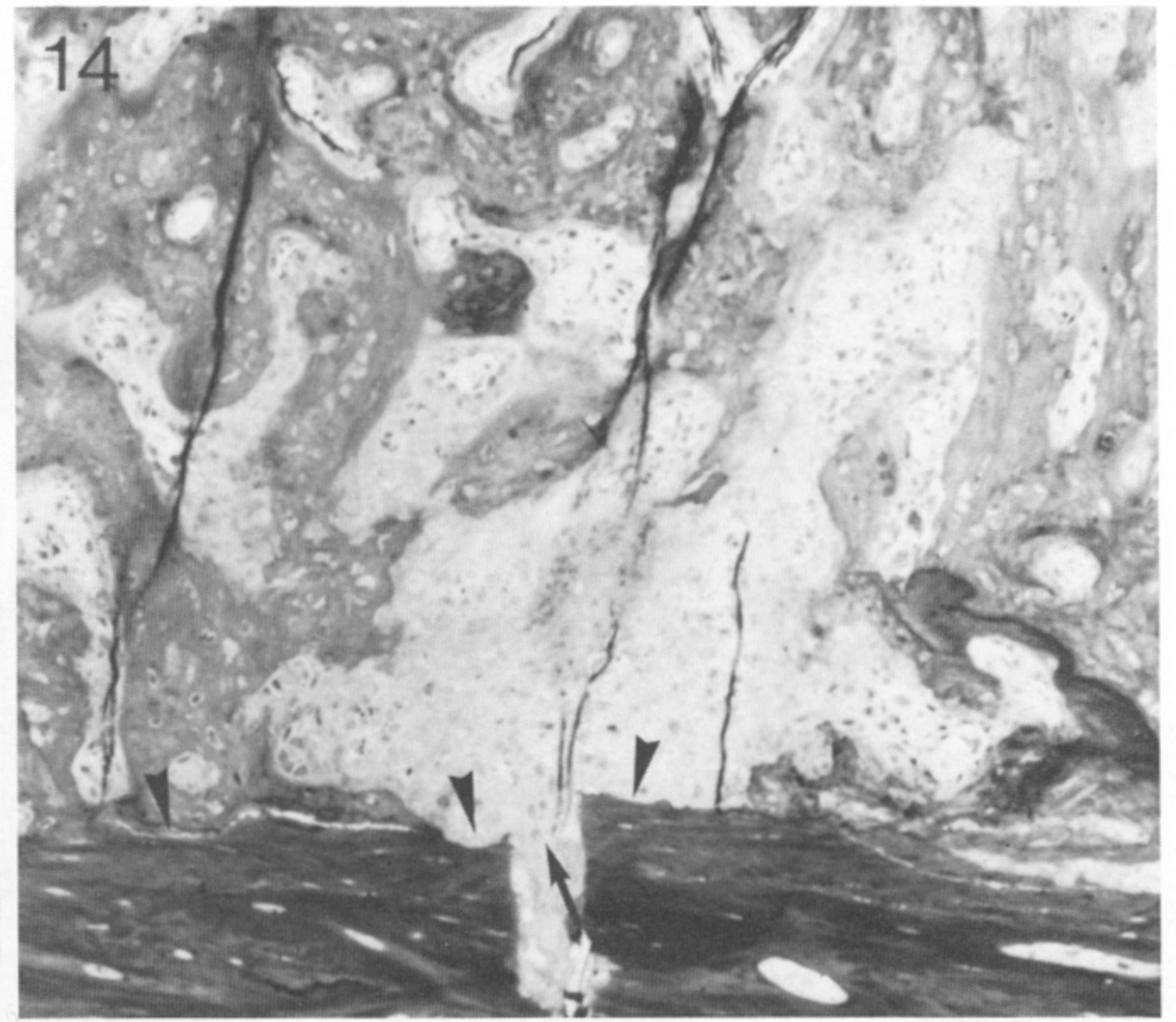
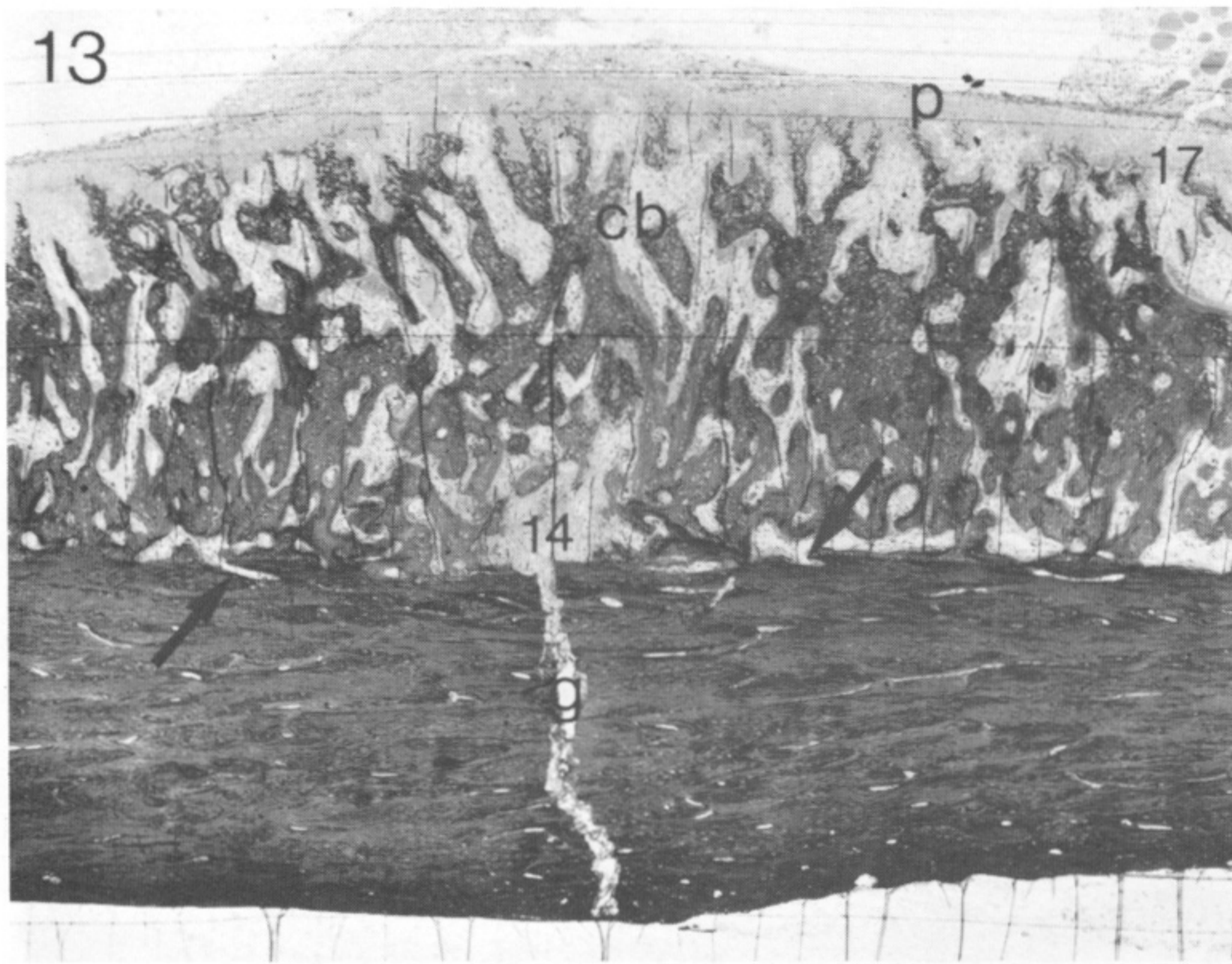
FIGURES 3-10. For description see page 299.





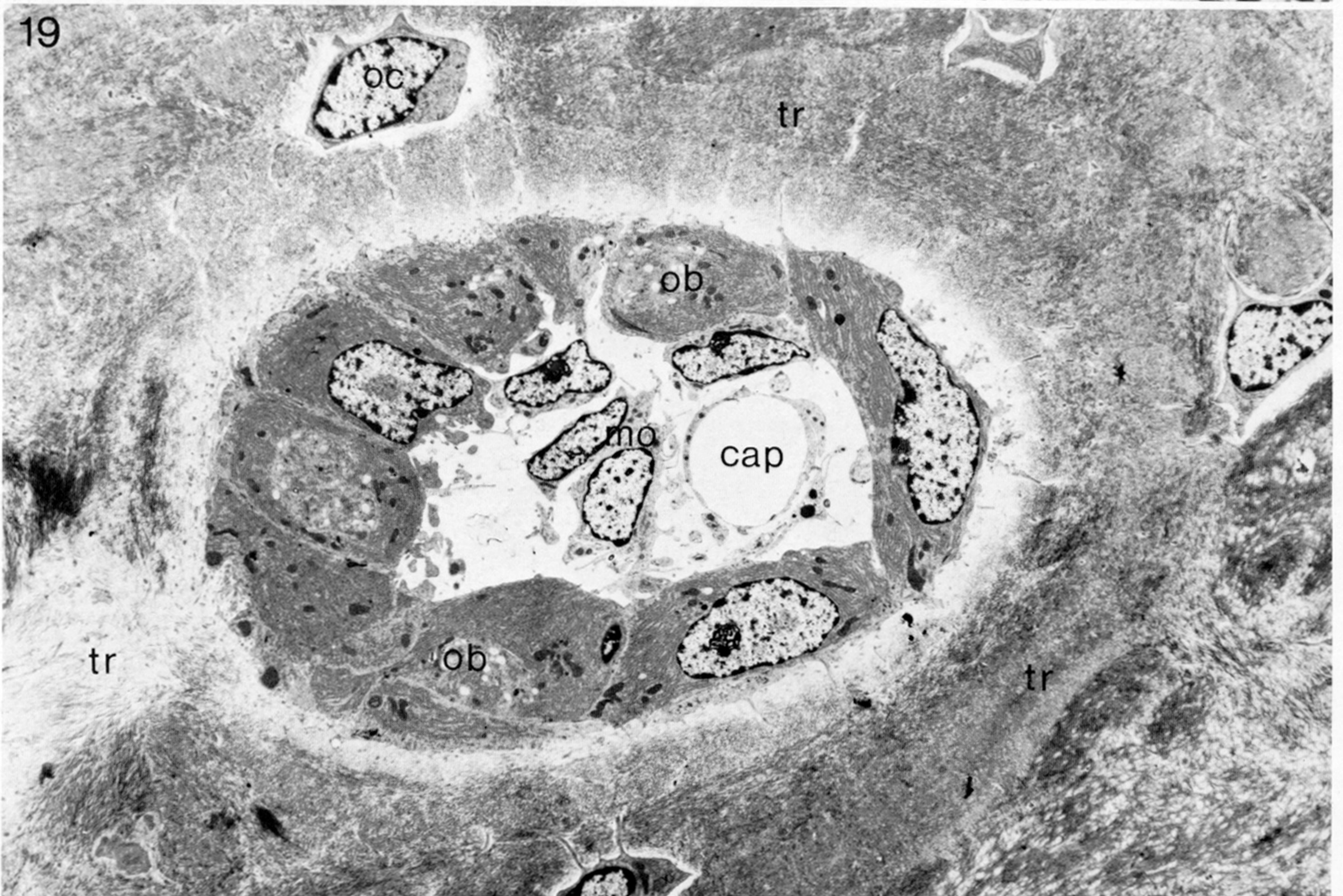
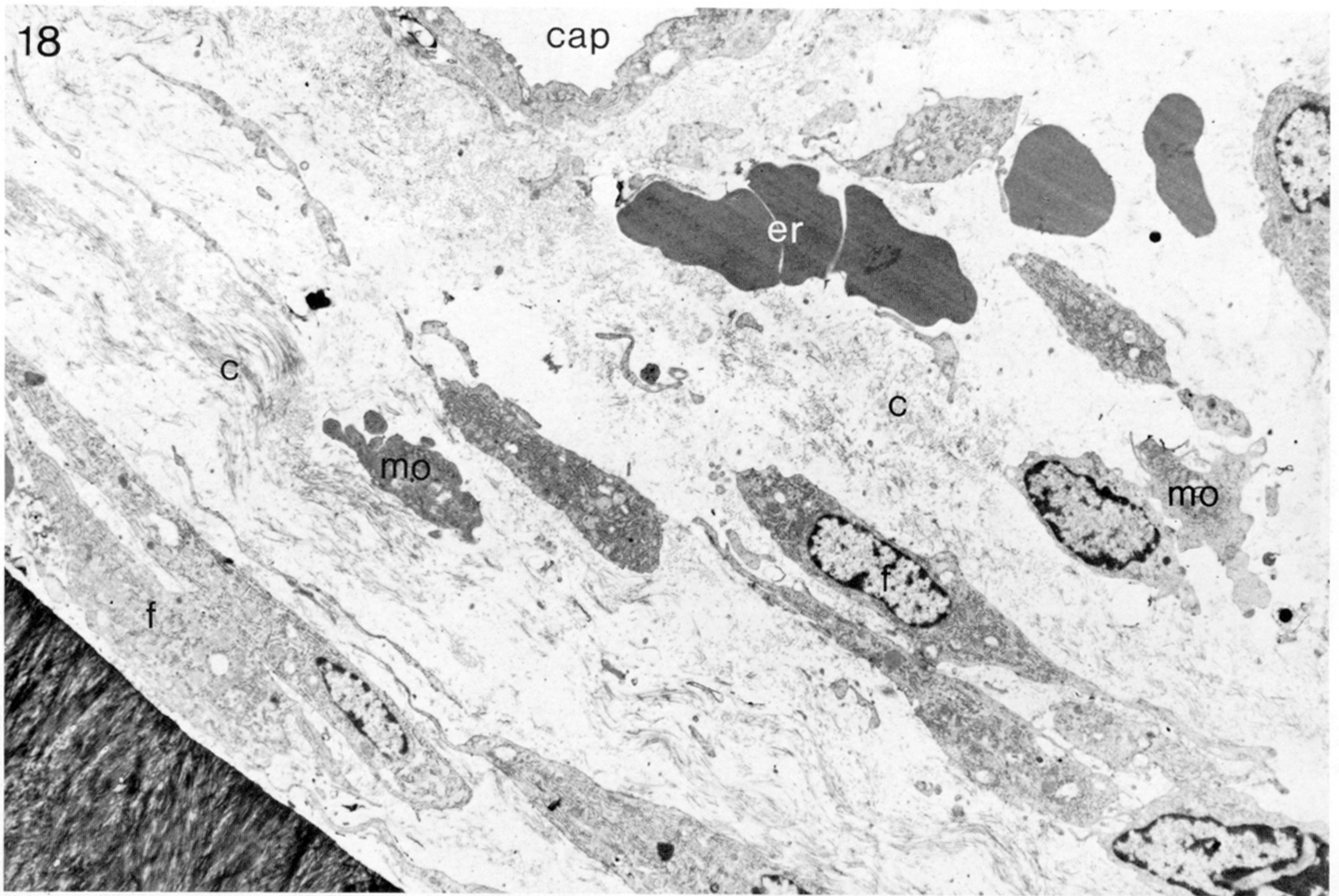
FIGURES 11 AND 12. For description see page 299.





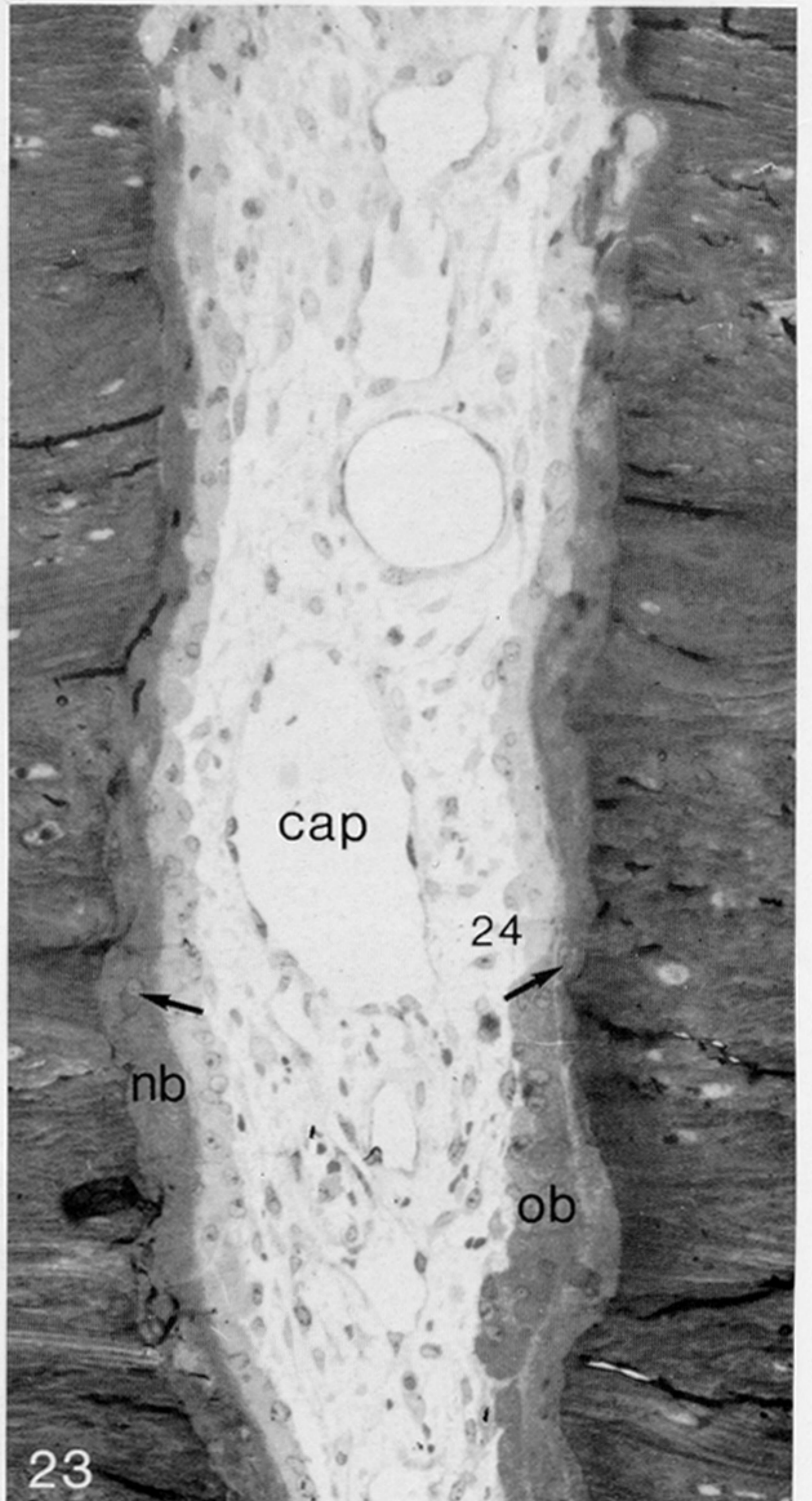
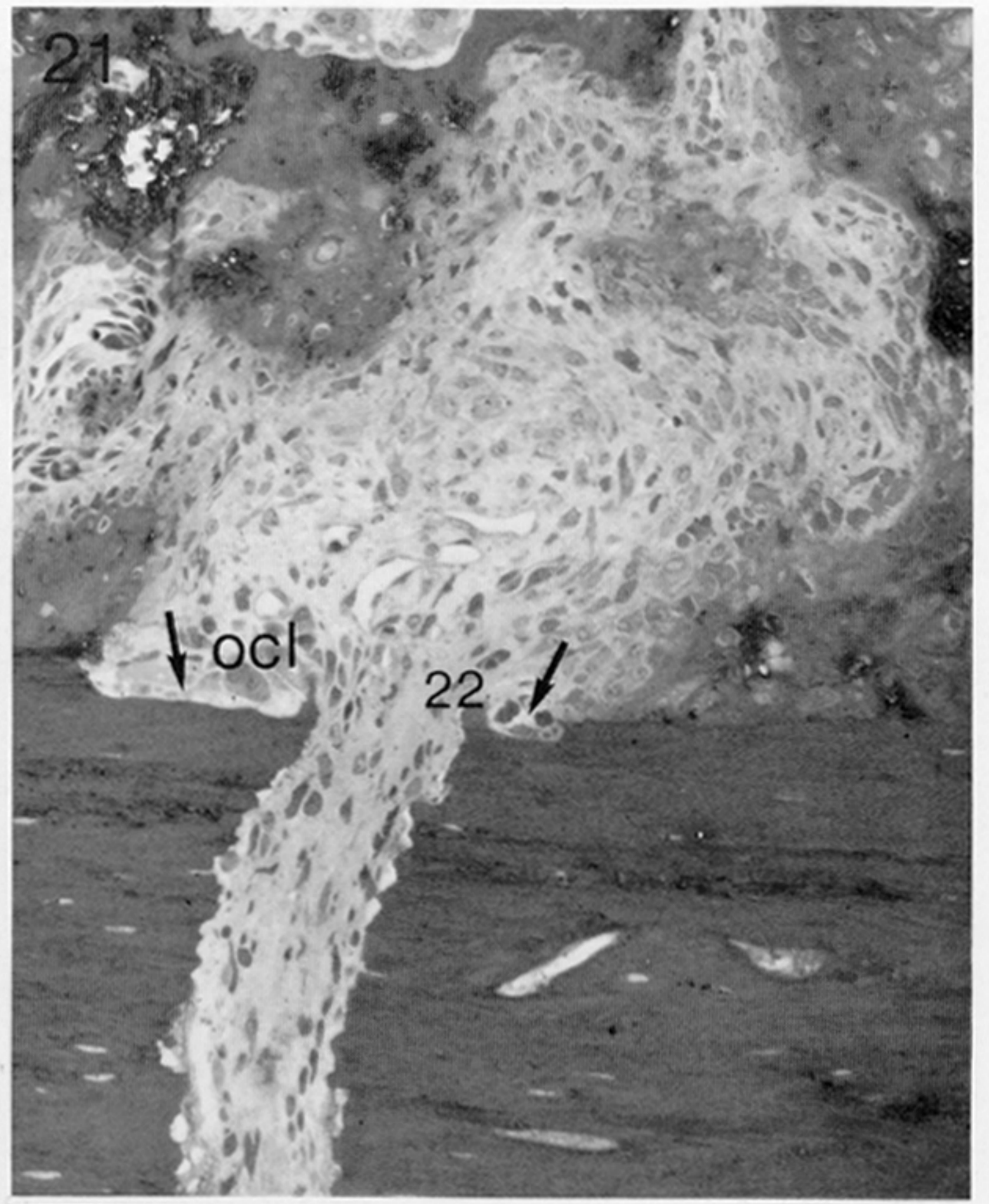
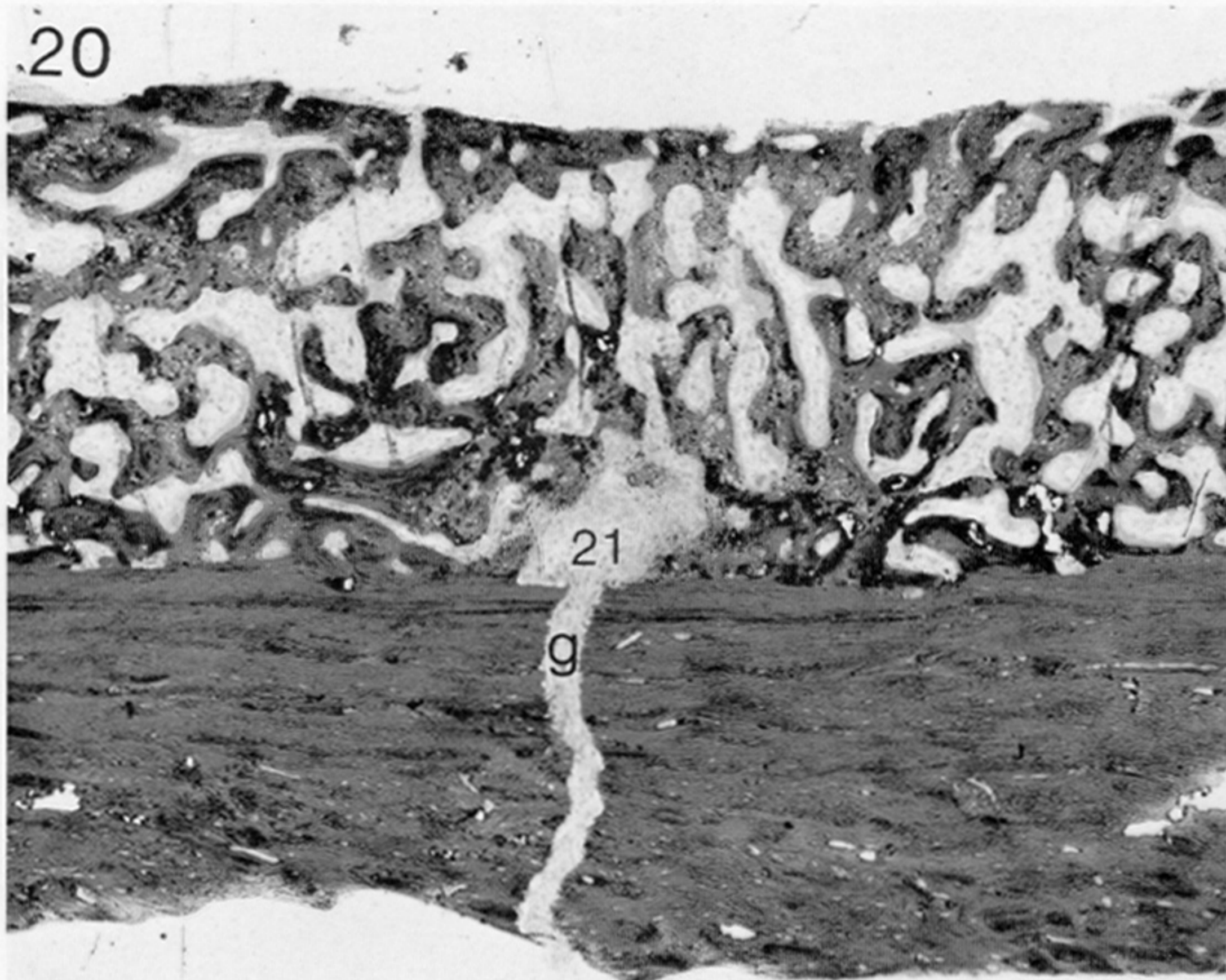
FIGURES 13-17. For description see pages 299 and 300.





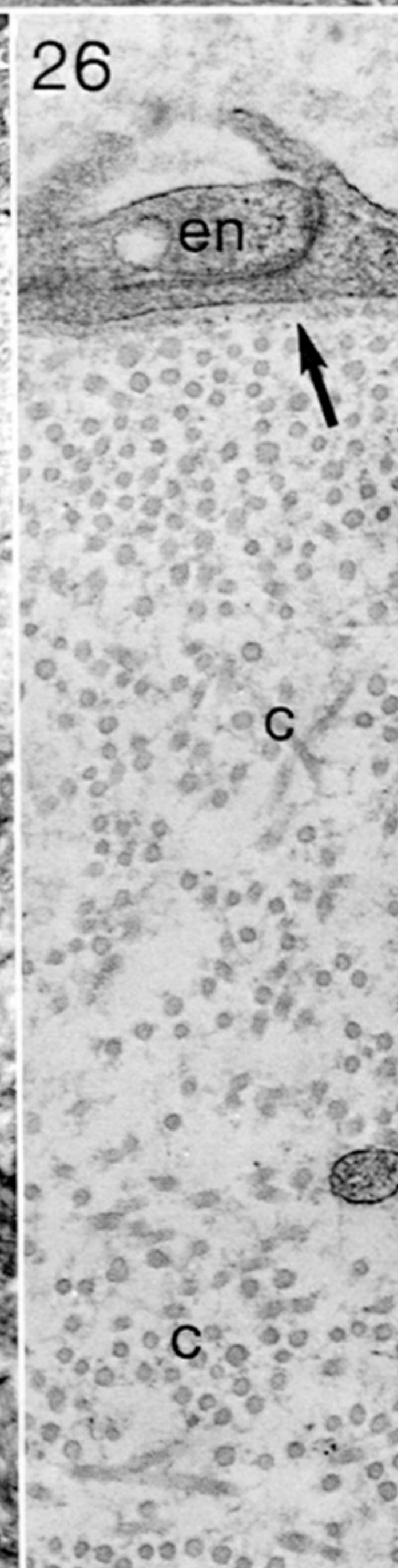
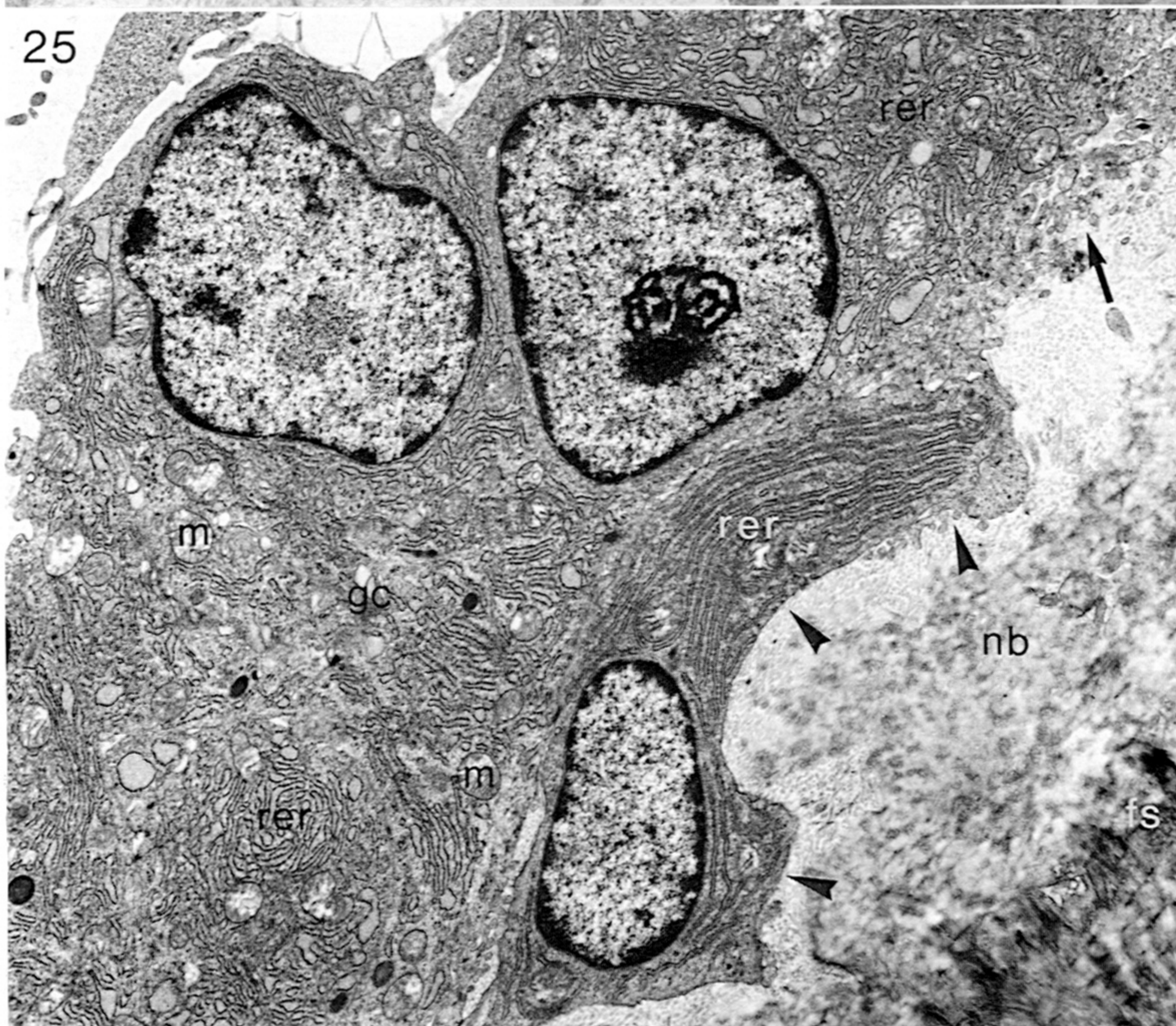
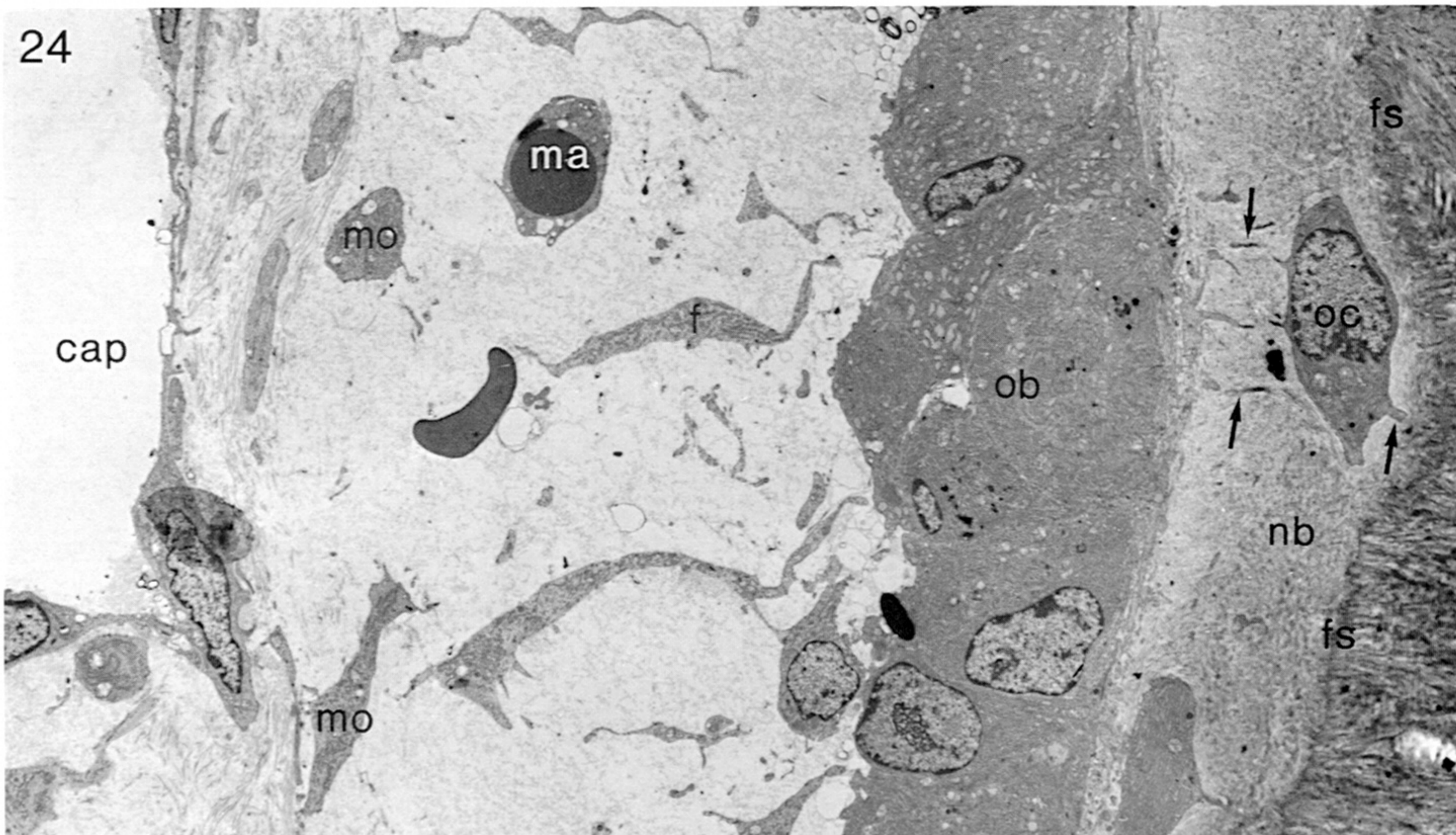
FIGURES 18 AND 19. For description see page 300.





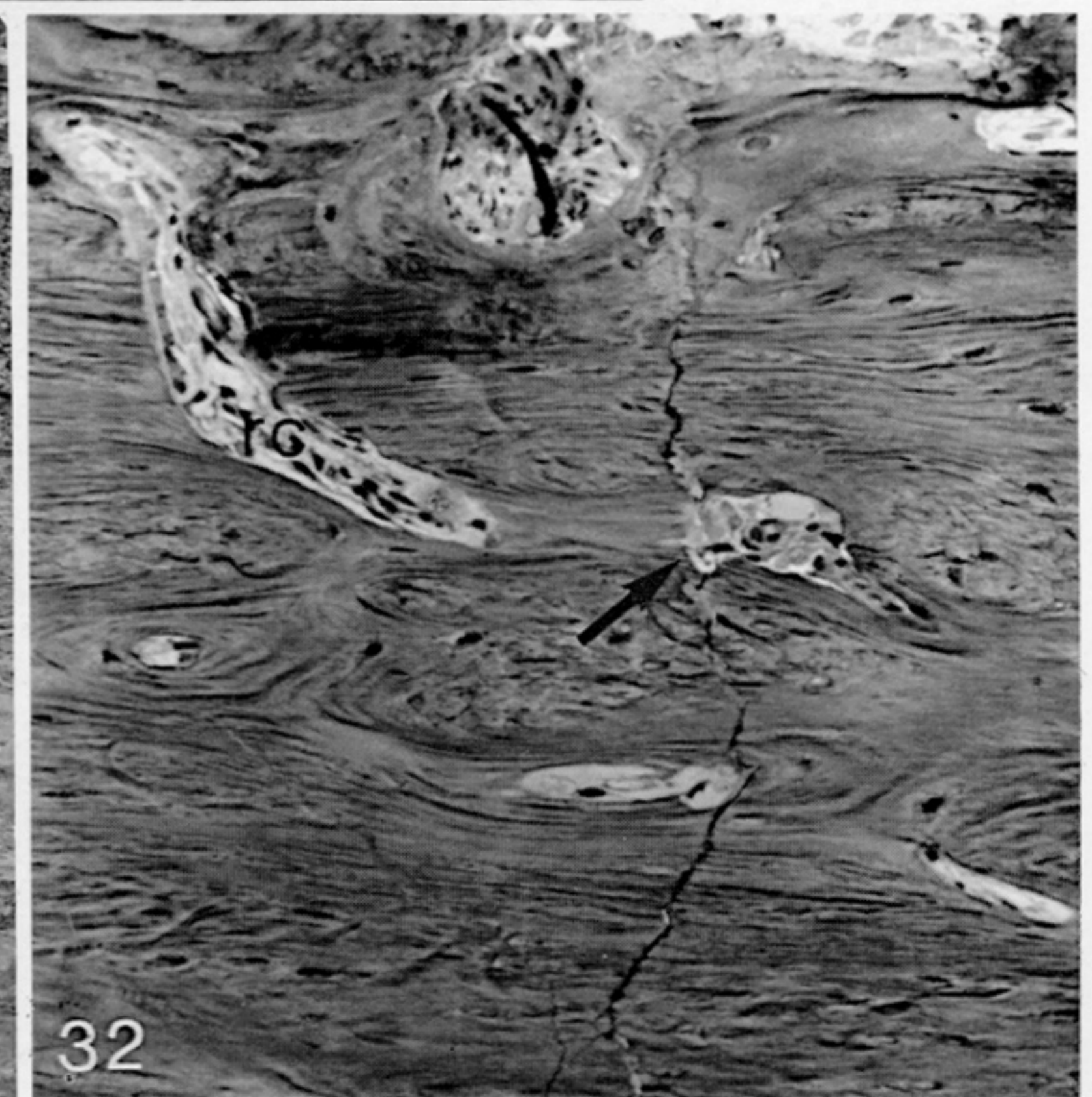
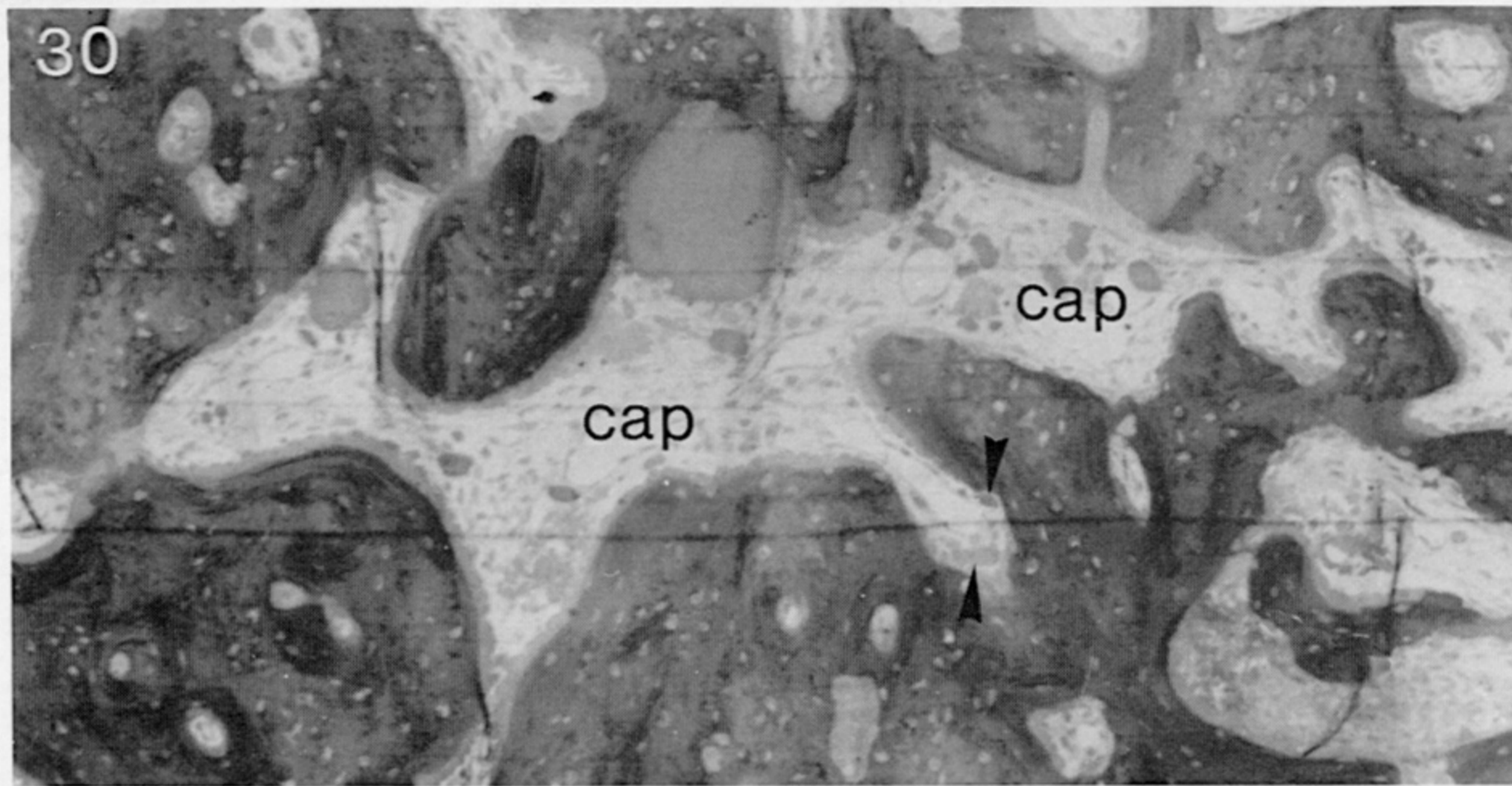
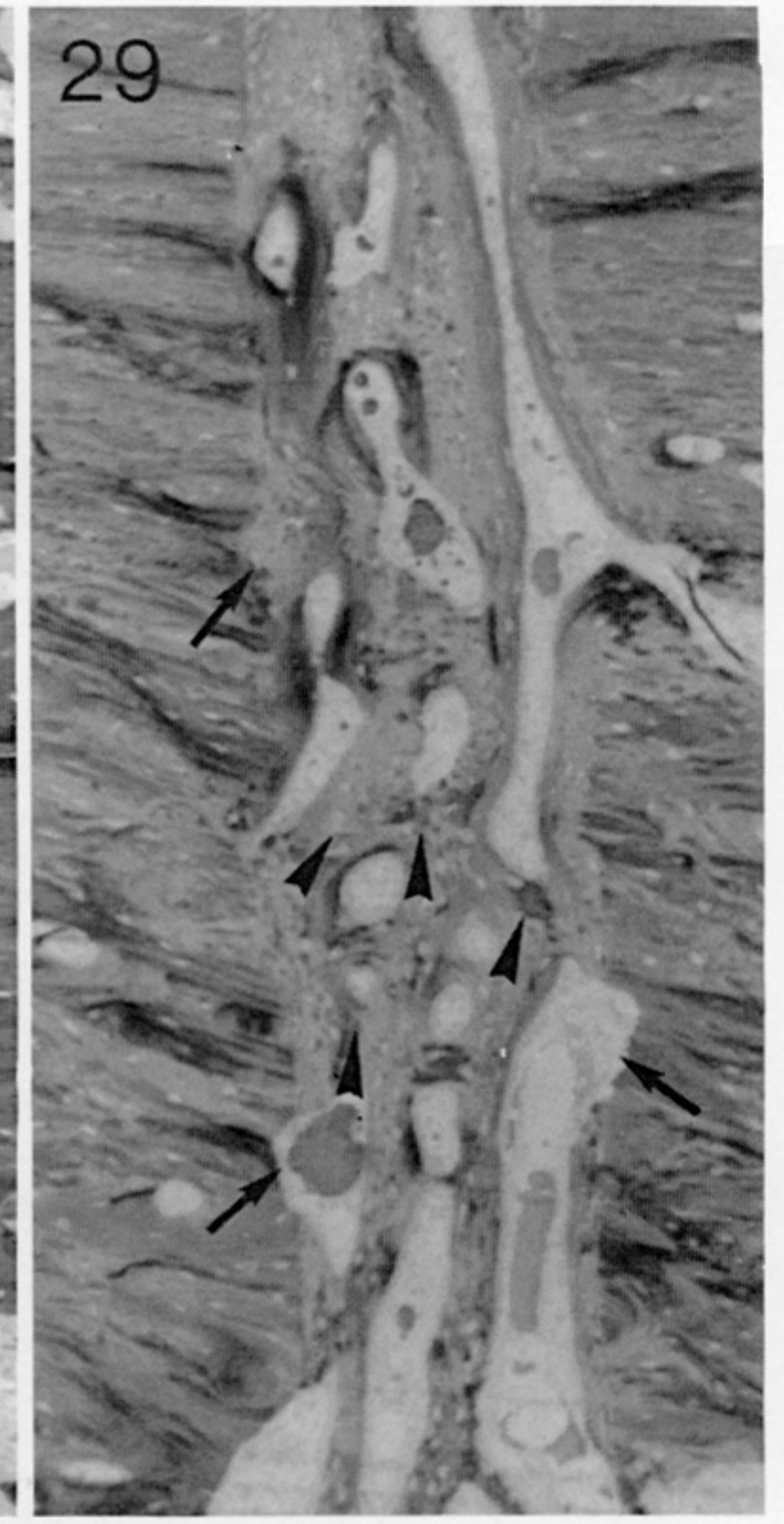
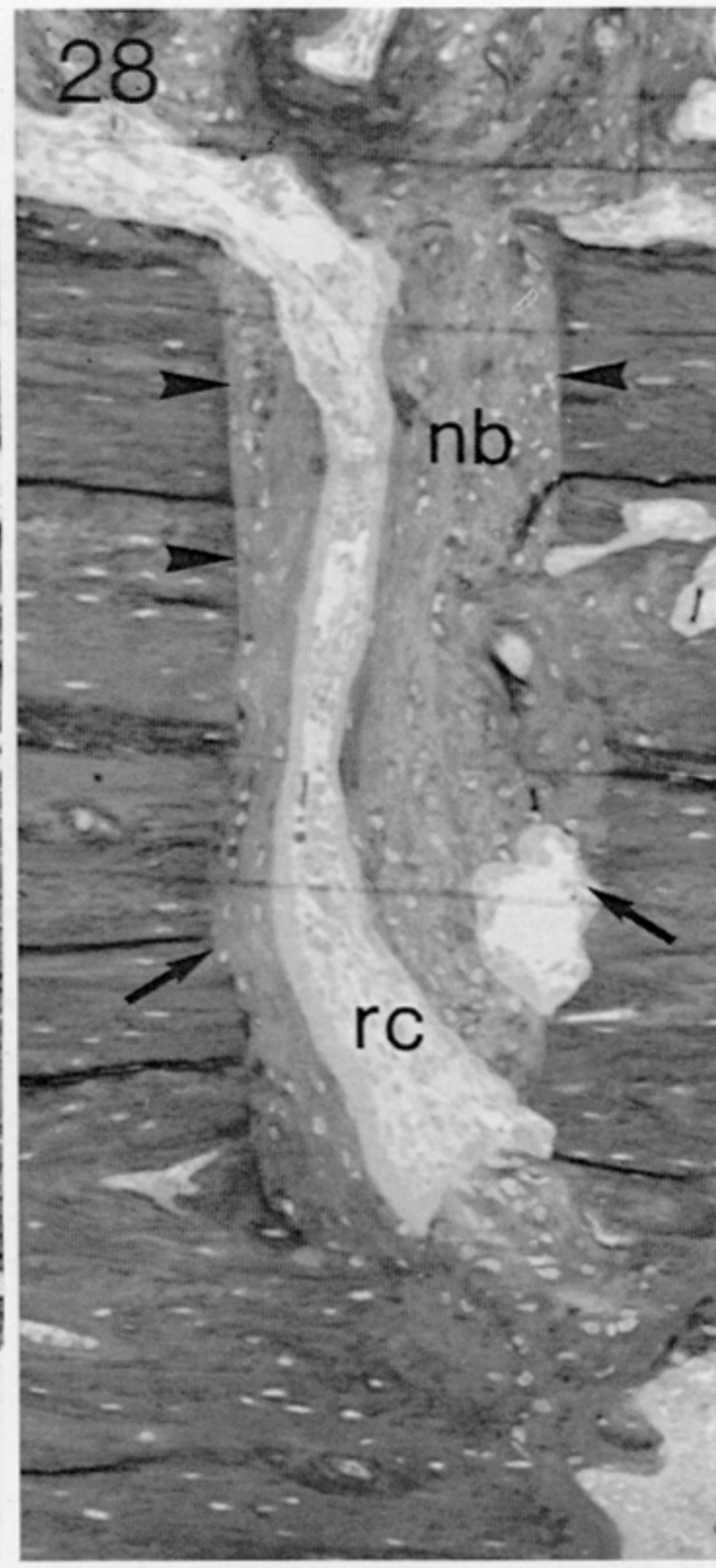
FIGURES 20-23. For description see page 300.





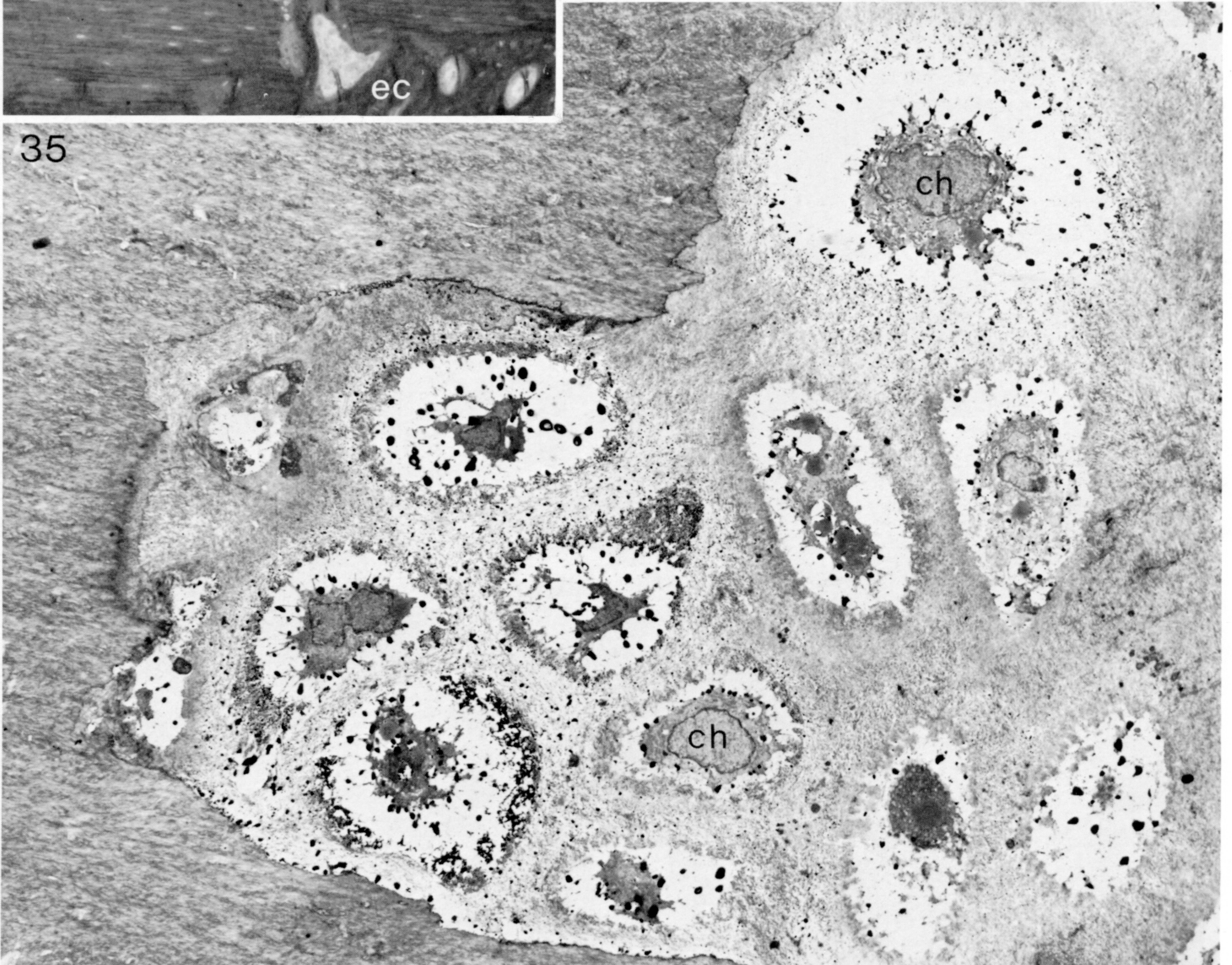
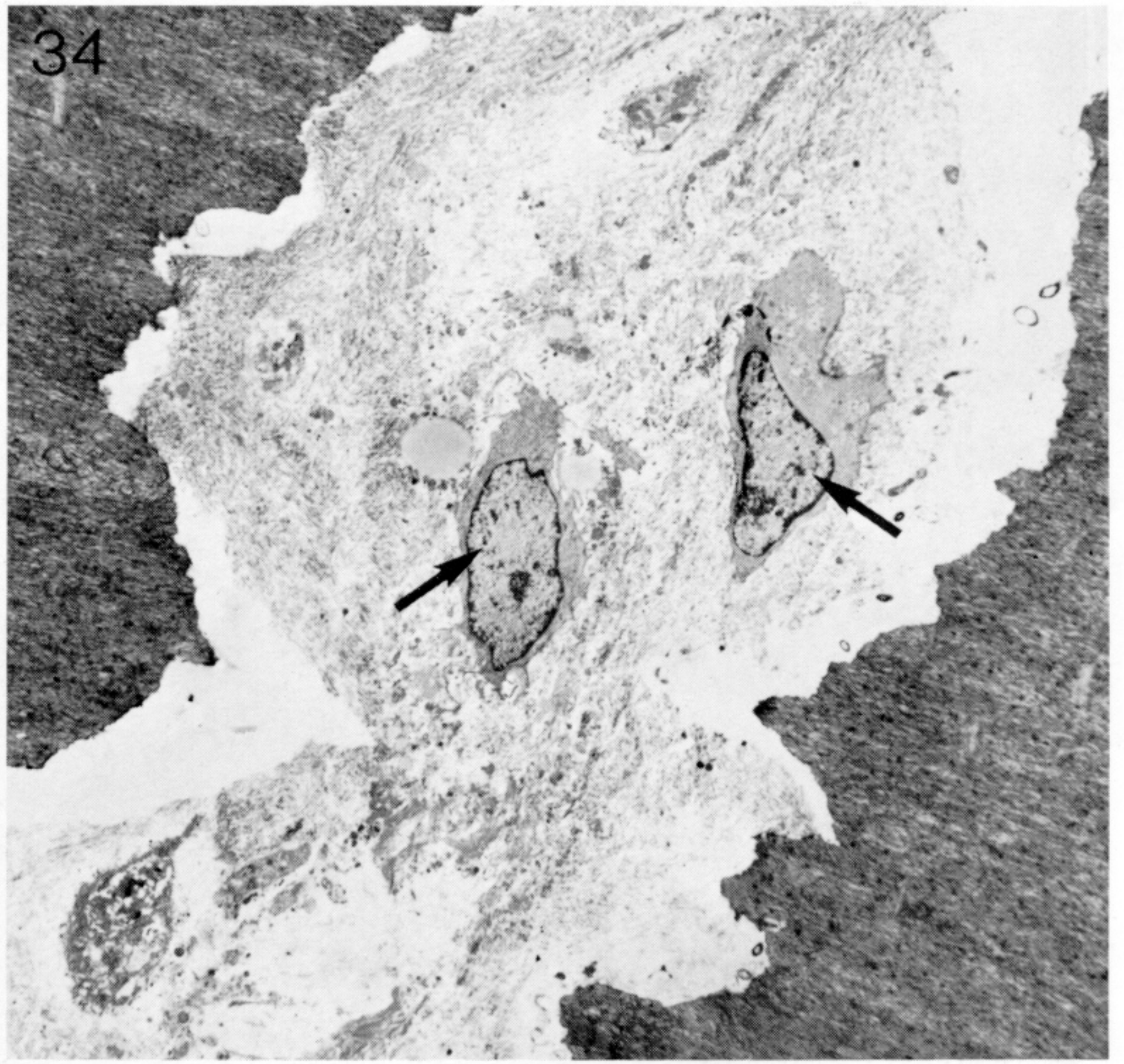
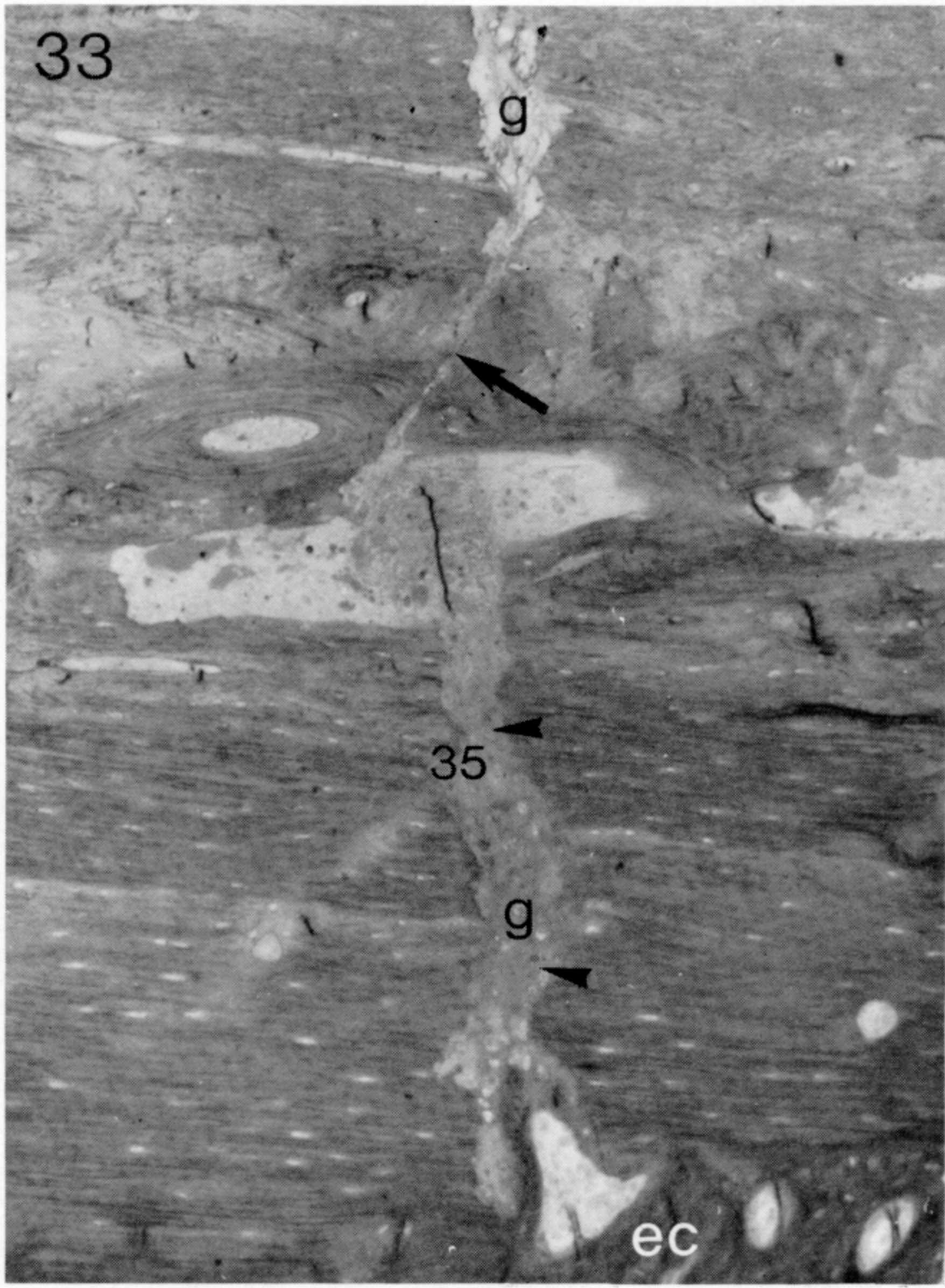
FIGURES 24-26. For description see page 300.





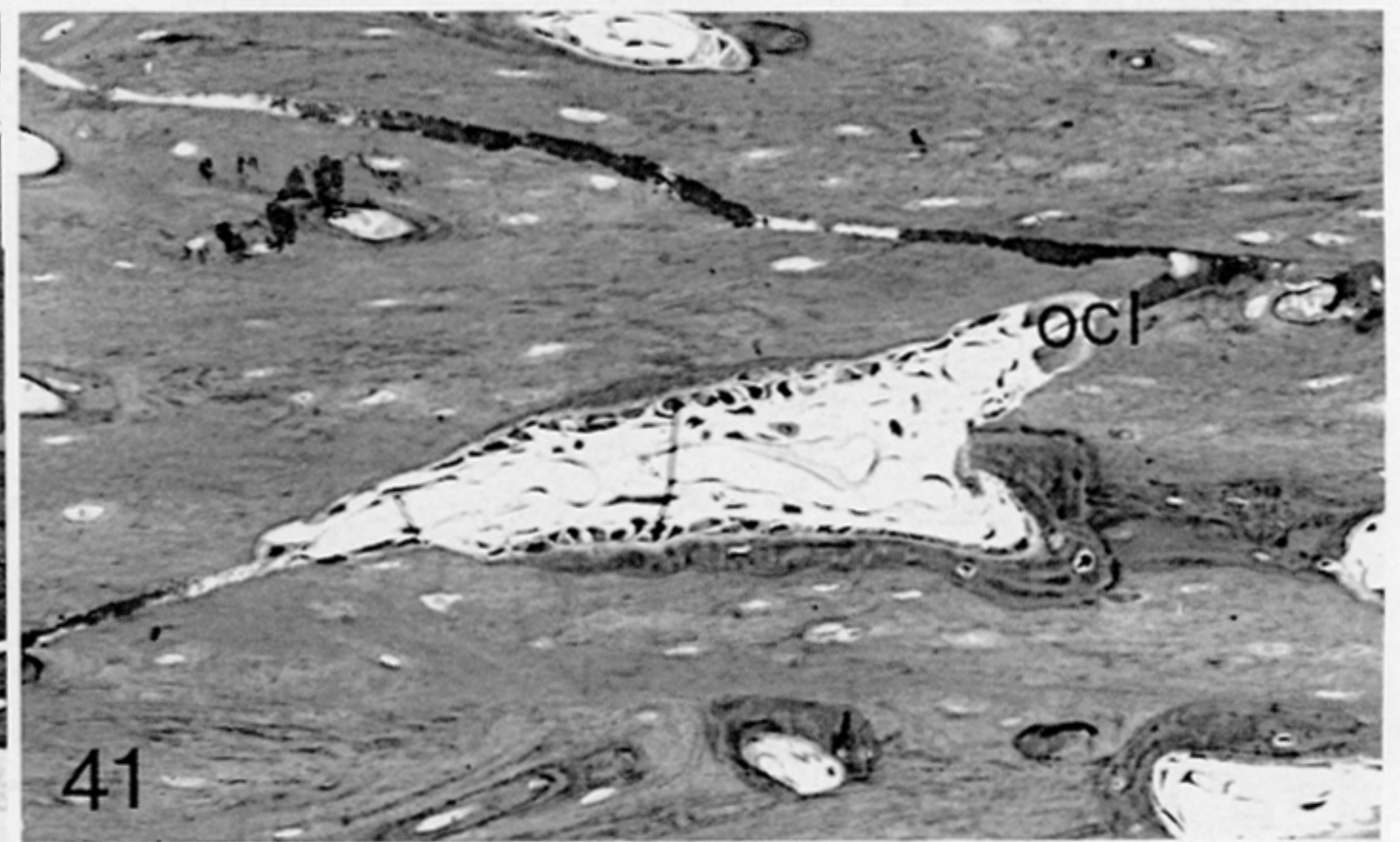
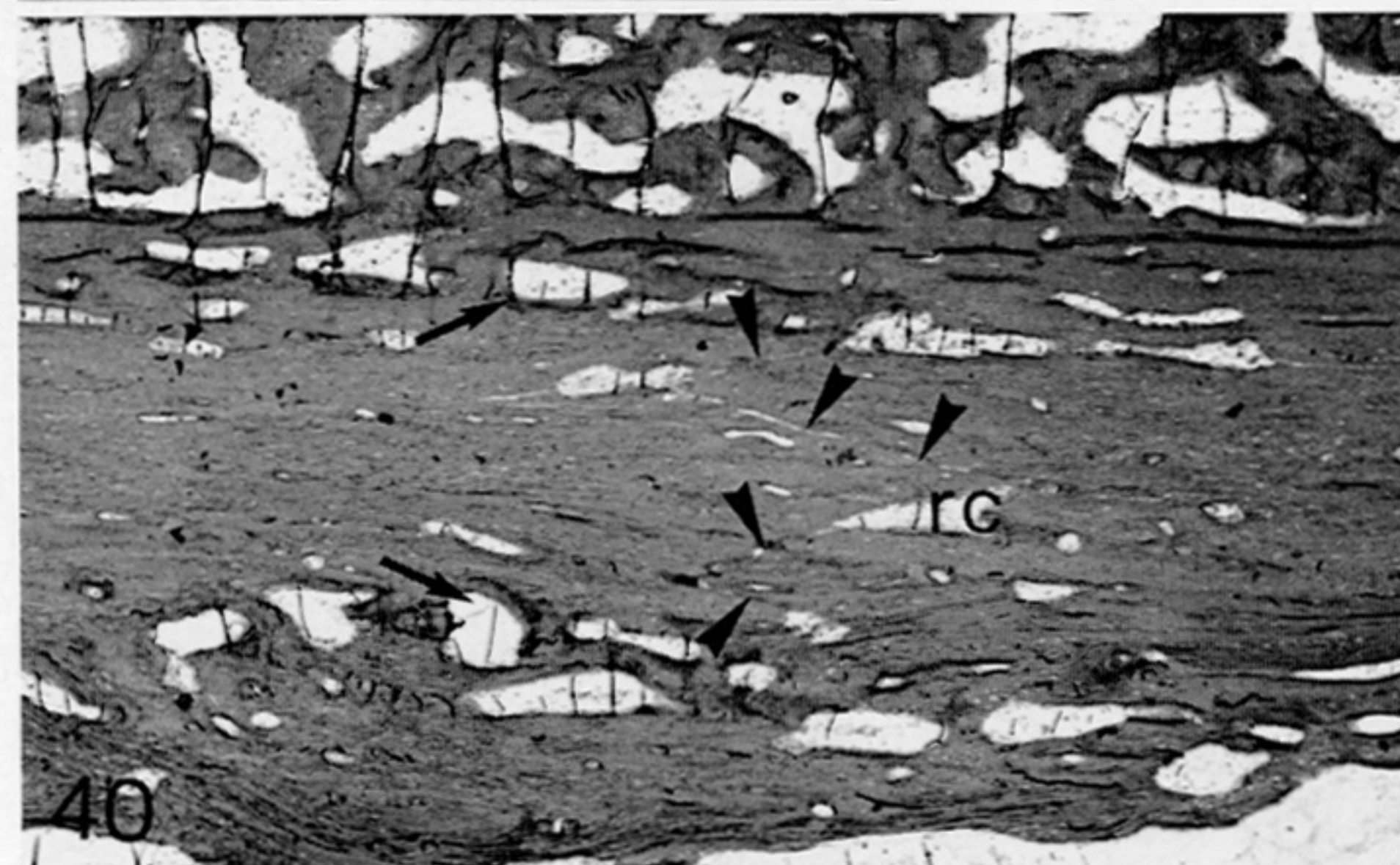
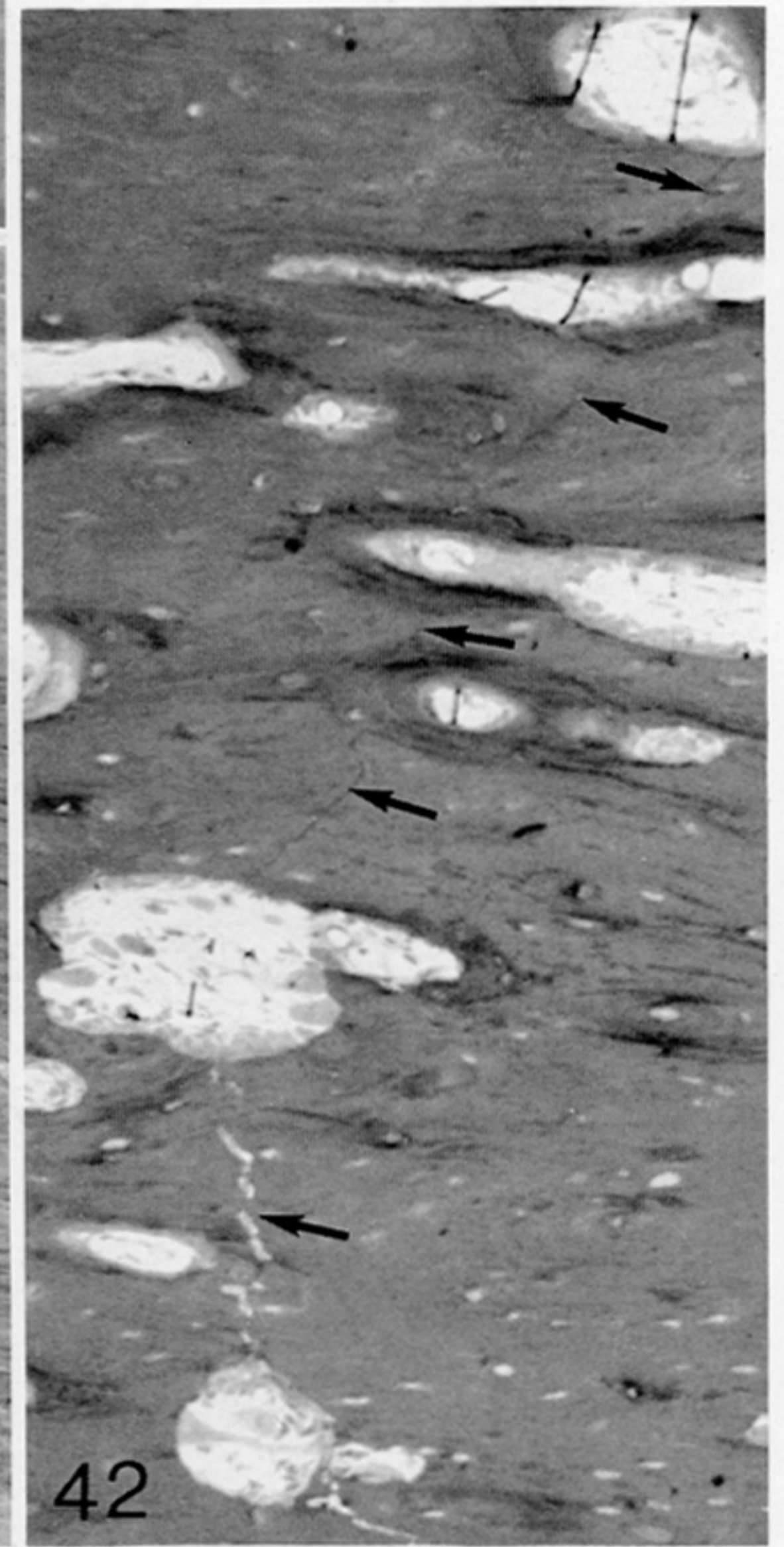
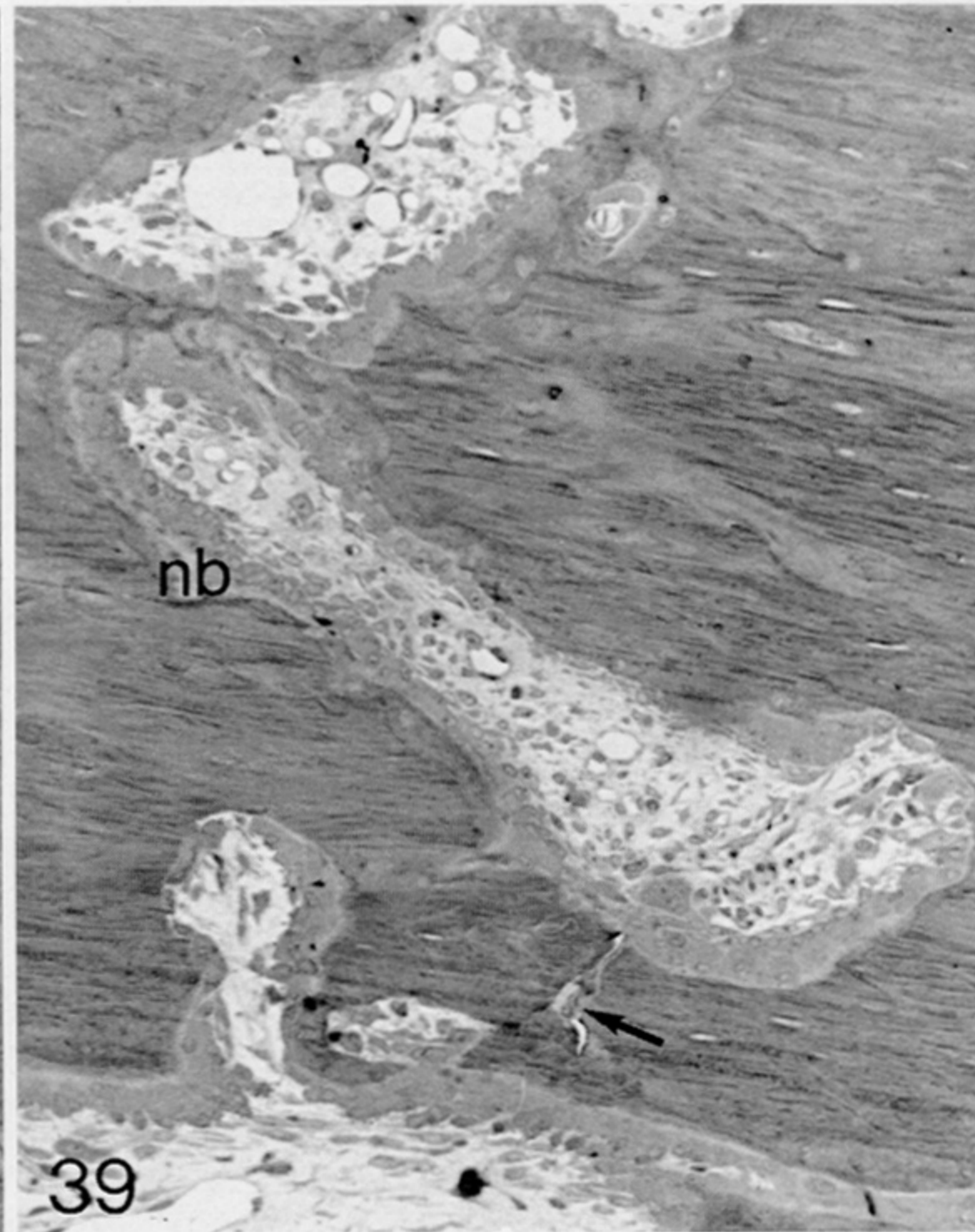
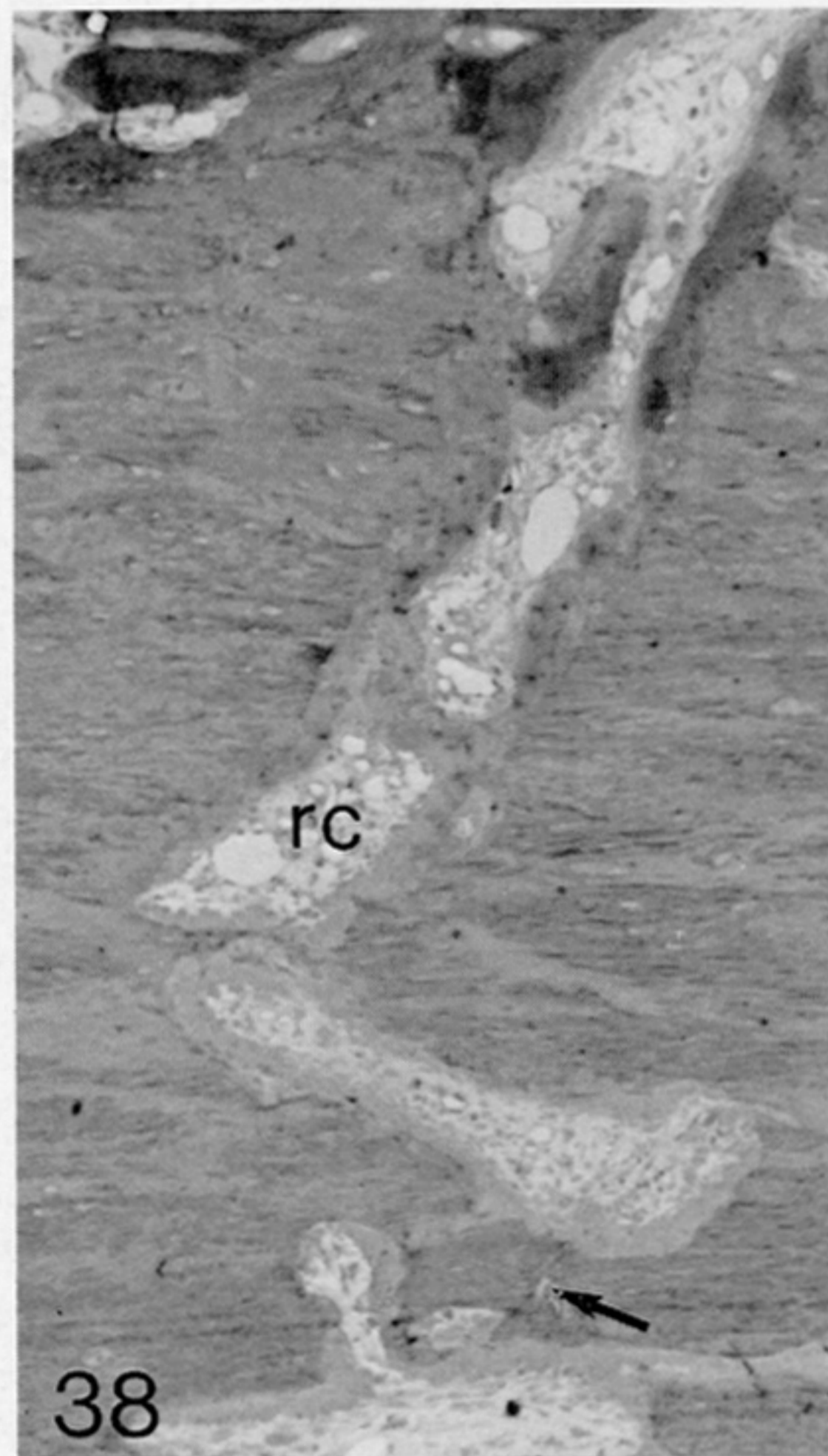
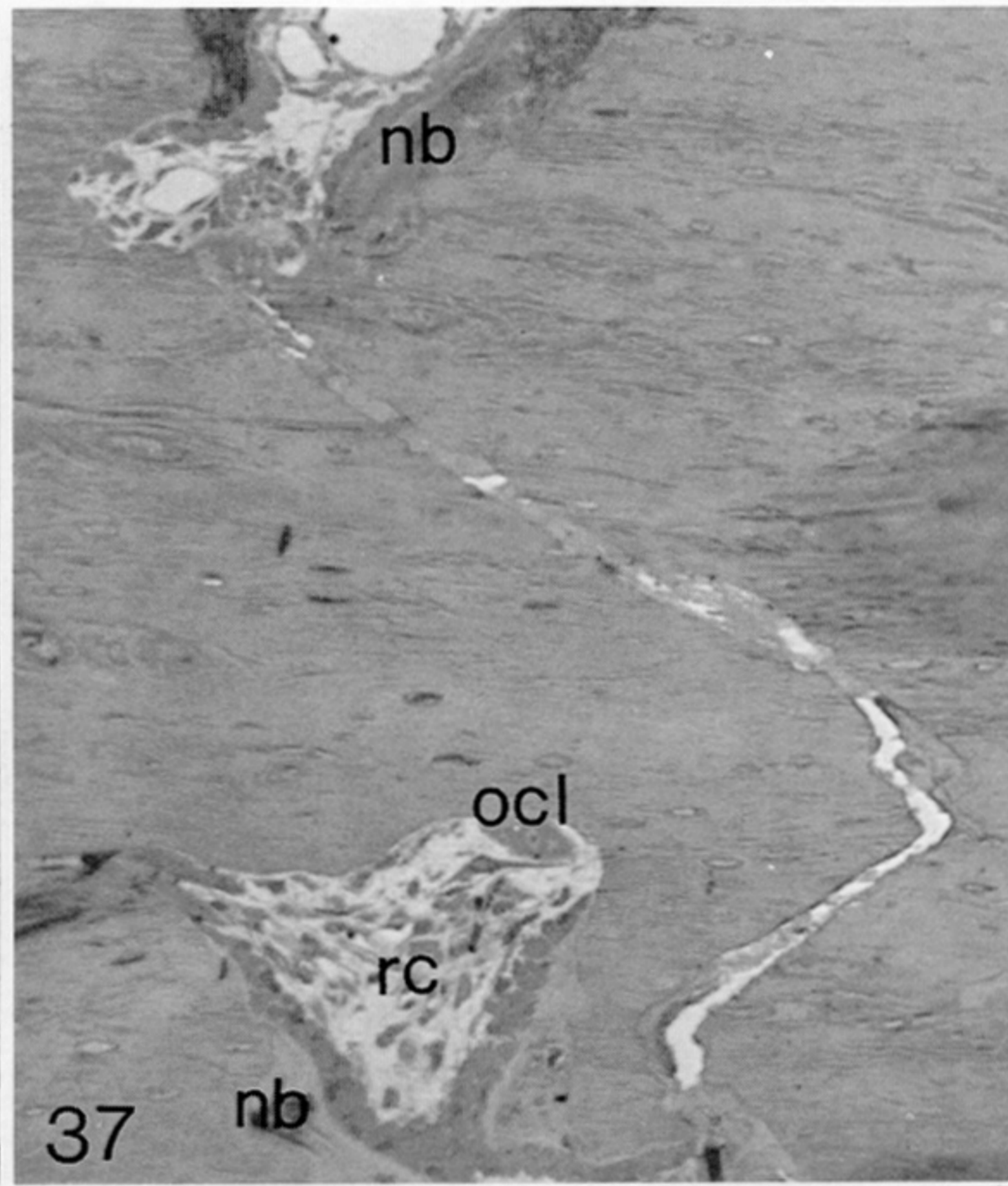
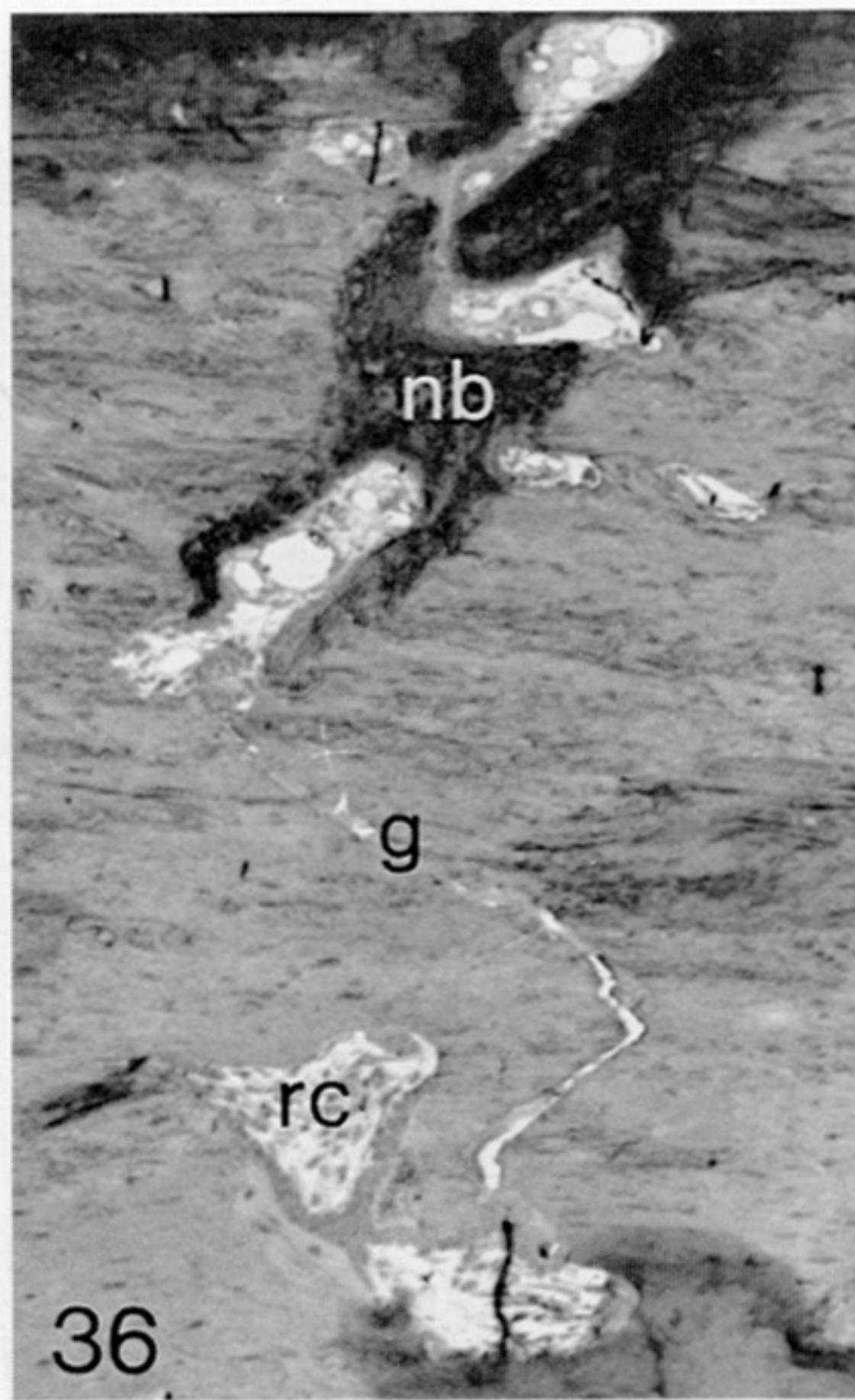
FIGURES 27-32. For description see page 301.





FIGURES 33-35. For description see page 301.





FIGURES 36-42. For description see pages 301 and 302.



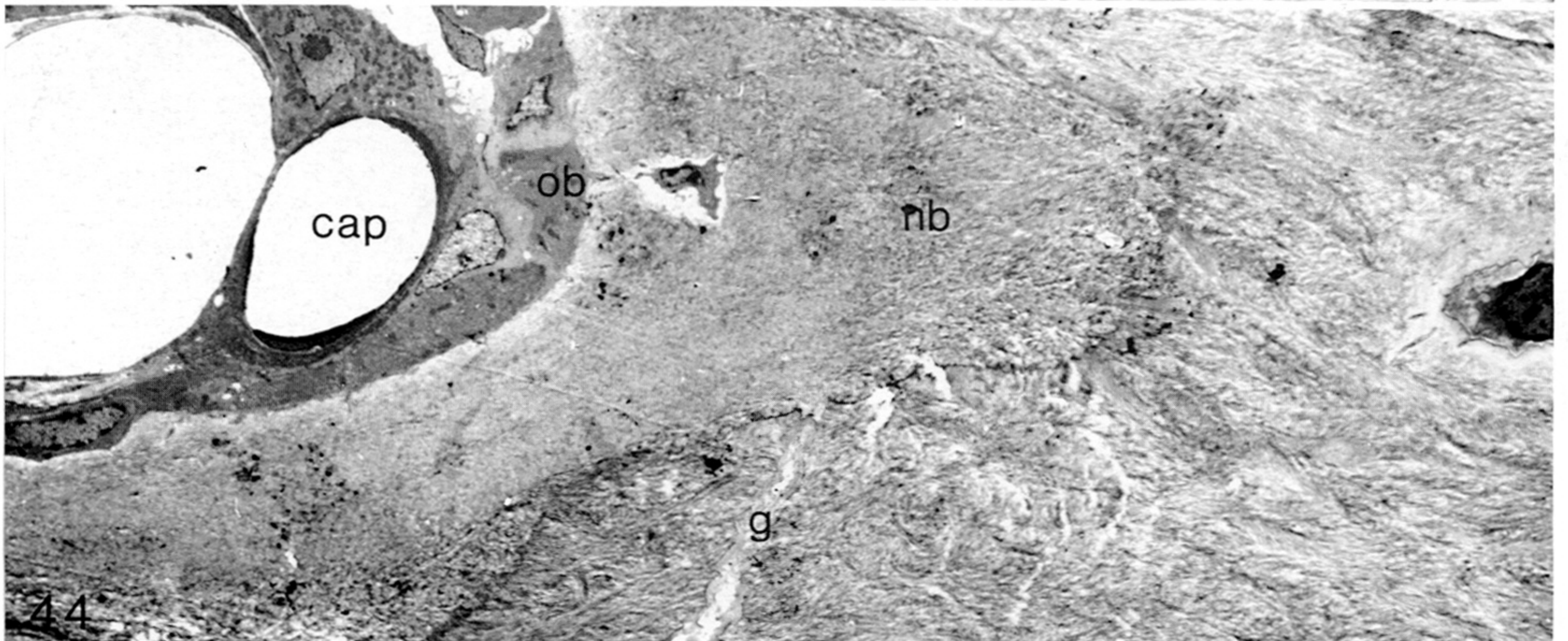
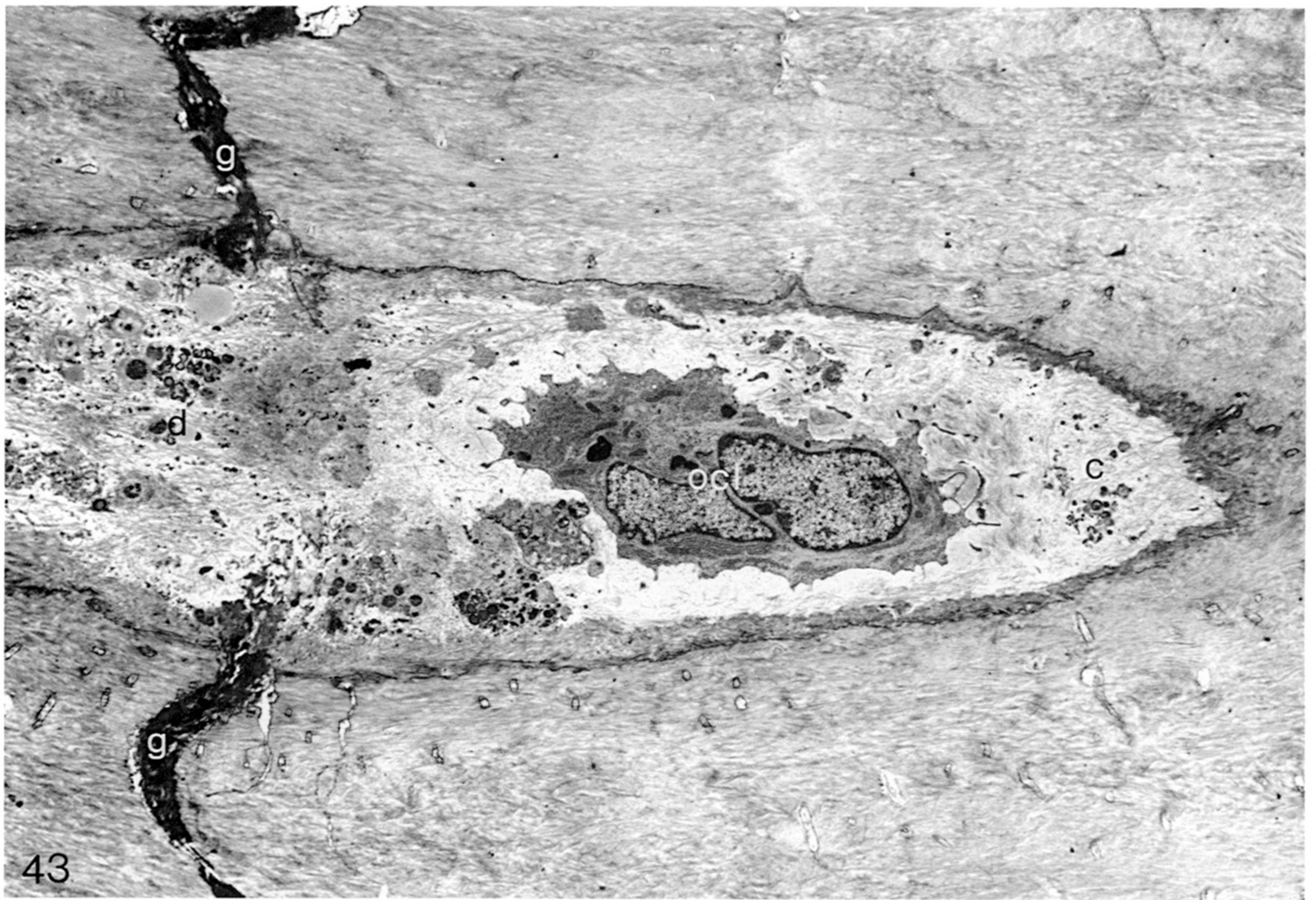
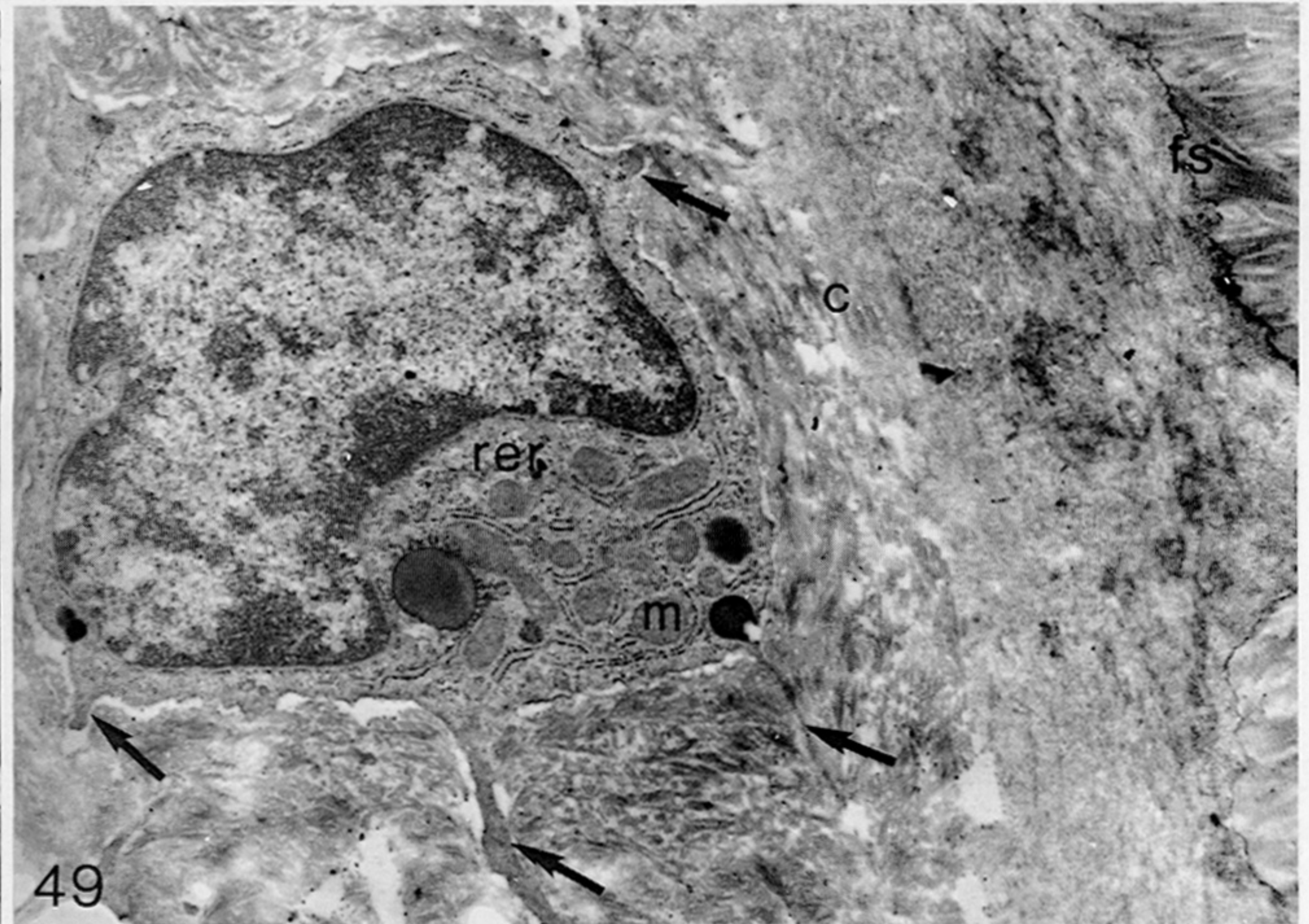
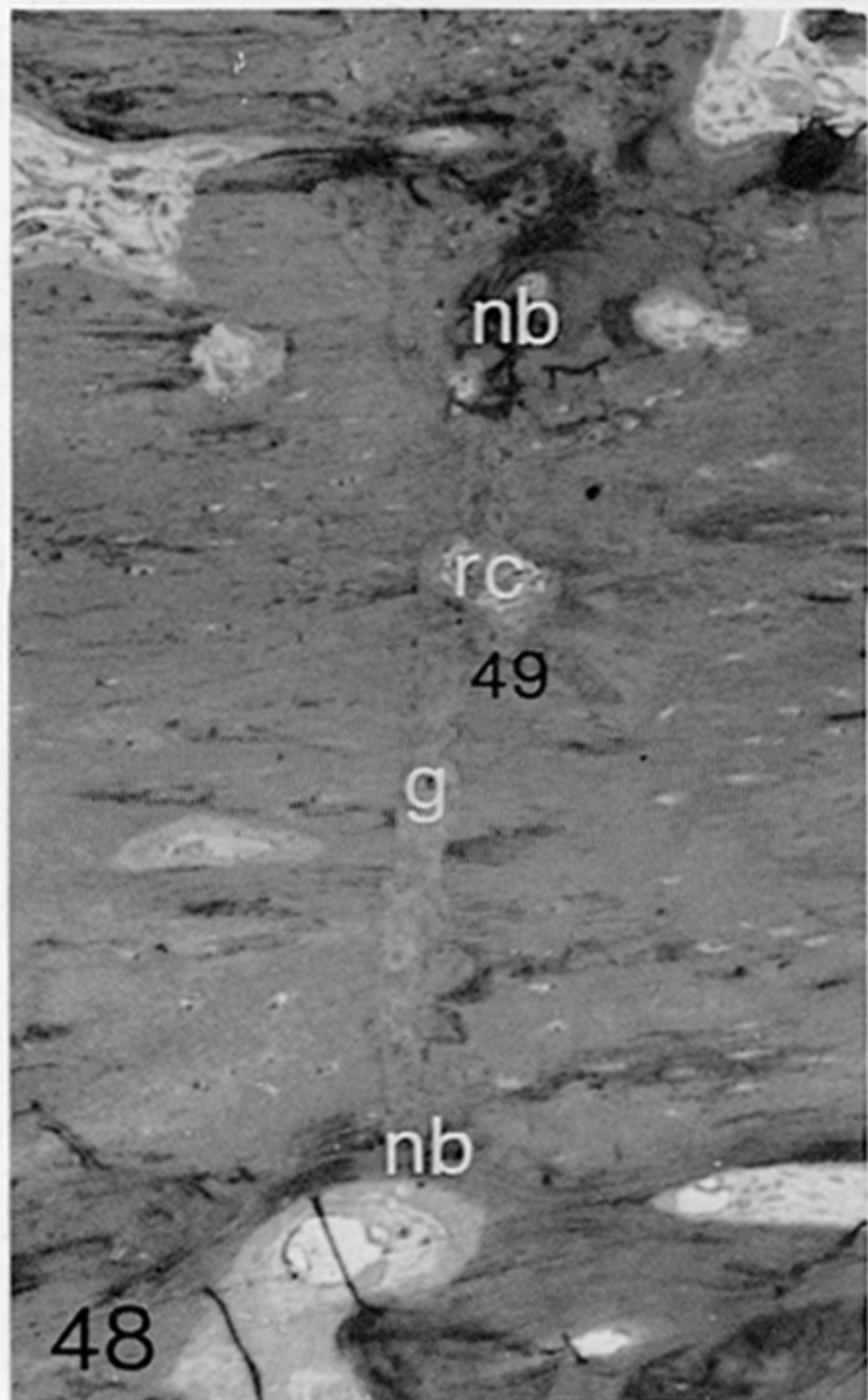
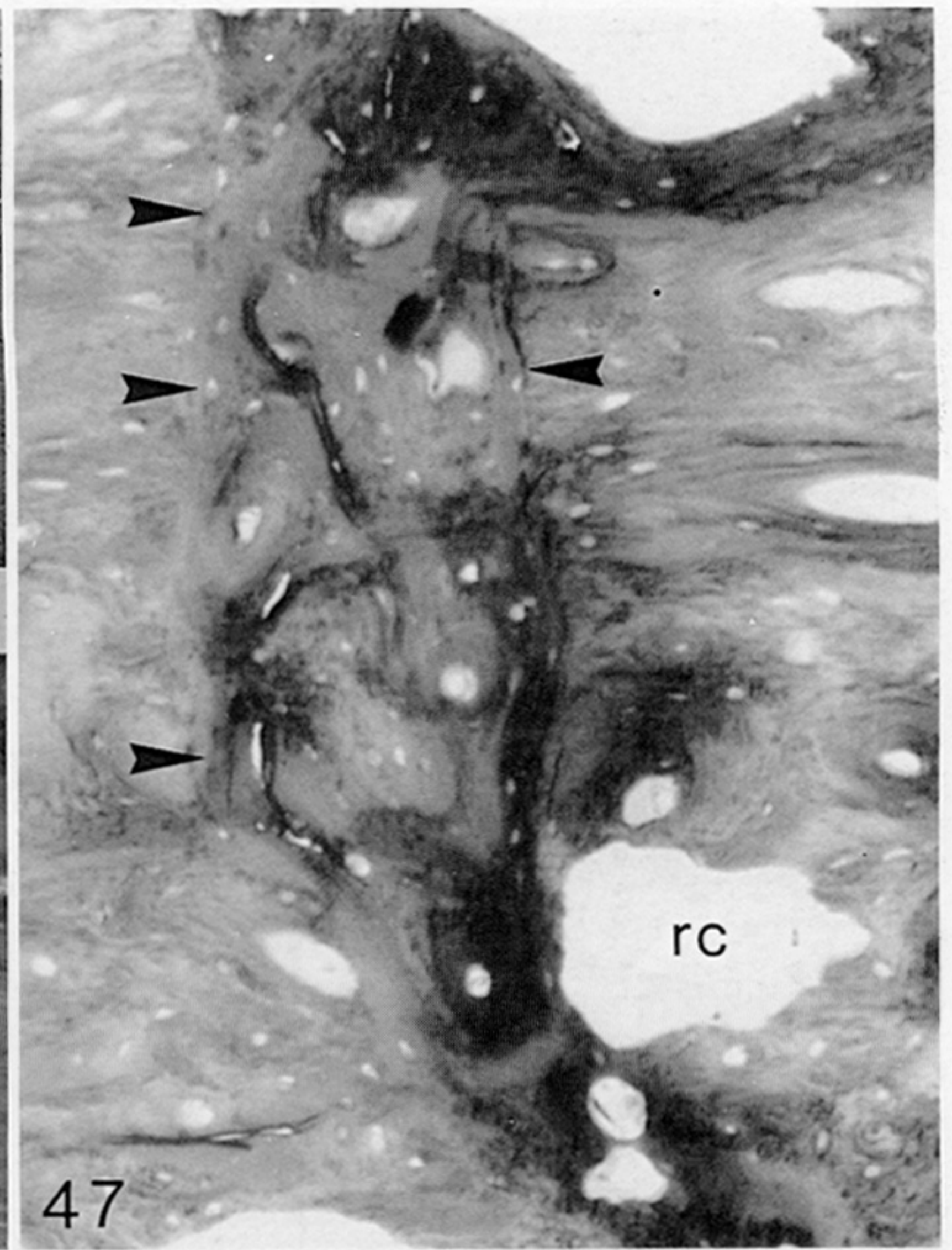
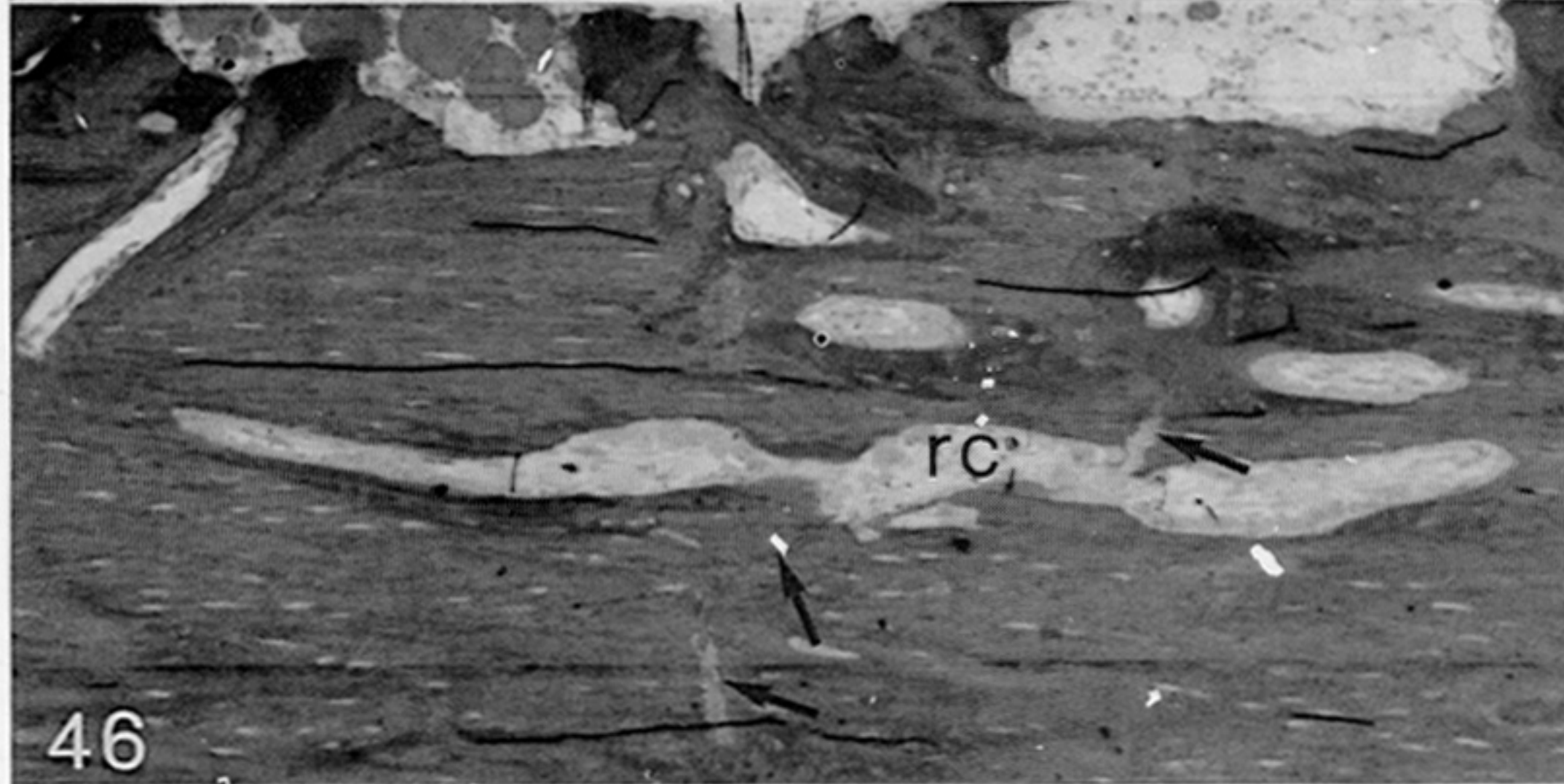


FIGURE 43. Electron micrograph of the leading end of a remodelling cavity crossing the fracture shown in figure 42. An osteoclast (ocl) and a few small collagen fibrils (c) are seen at the leading end, and most of the rest of the cavity is filled by debris (d). The narrow fracture gap (g), about 1  $\mu\text{m}$  wide, is filled by electron dense, amorphous material. (Magn.  $\times 4300$ .)

FIGURE 44. Electron micrograph of the posterior end of a remodelling cavity in the same 4-week fracture. Here the fracture is partly bridged by new bone (nb), but the gap (g) still remains elsewhere. The capillaries (cap) and osteoblasts (ob) of the remodelling cavity are seen to the left of the micrograph. (Magn.  $\times 1800$ .)





FIGURES 45-49. For description see page 302.



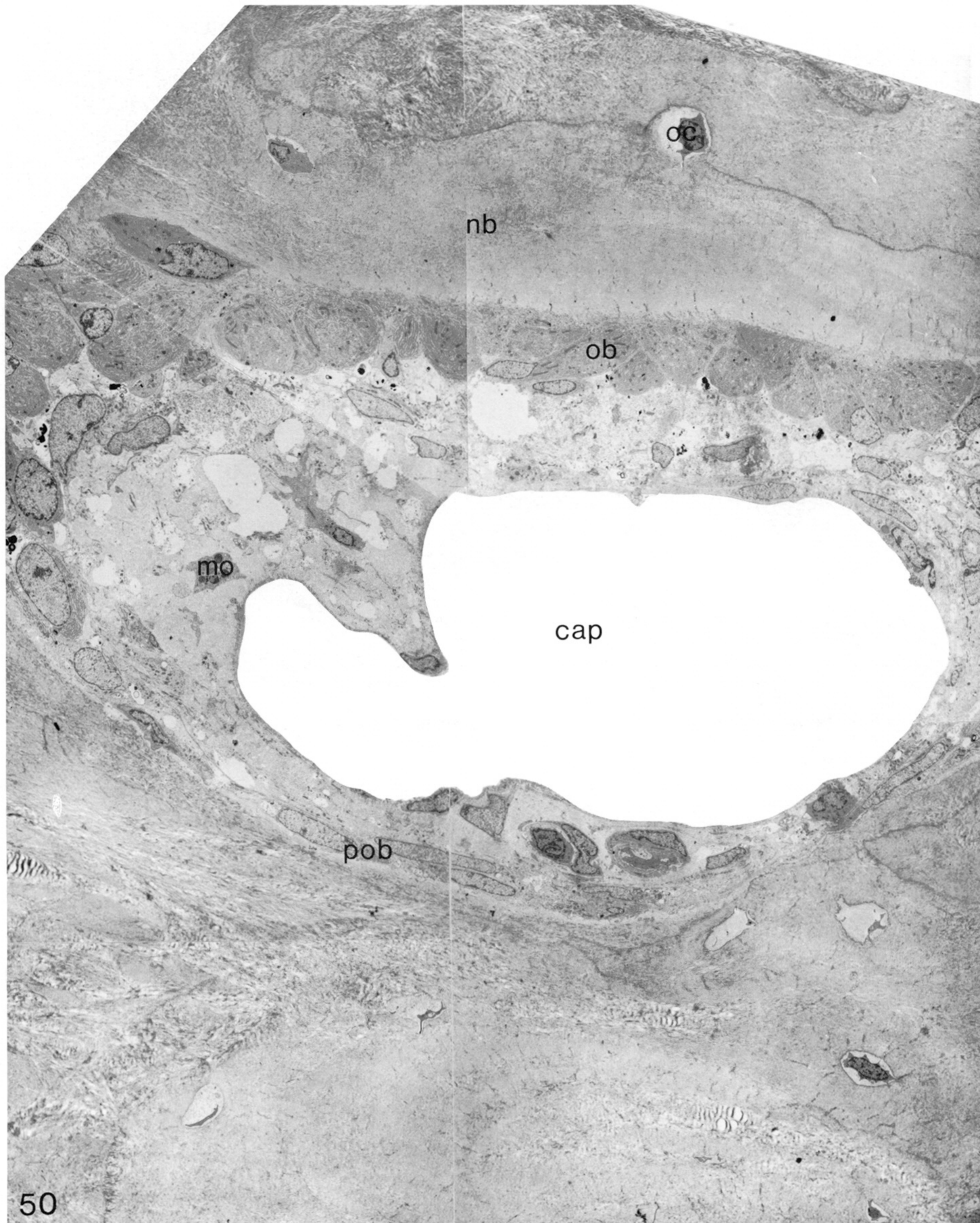


FIGURE 50. A montage of electron micrographs to show a cavity and its associated new bone in the fracture shown in figure 47. The cavity is lined partly by osteoblasts (ob), which have laid down new bone (nb) in which osteocytes (oc) are trapped. On the other side the cavity is lined by spindle-shaped cells, which may be pre-osteoblasts (pob). The cavity is partly filled by a large capillary (cap). A collagenous matrix surrounds the capillary. Various cells, including monocytes (mo) and fibroblasts, are in this matrix. (Magn.  $\times 1400$ .)



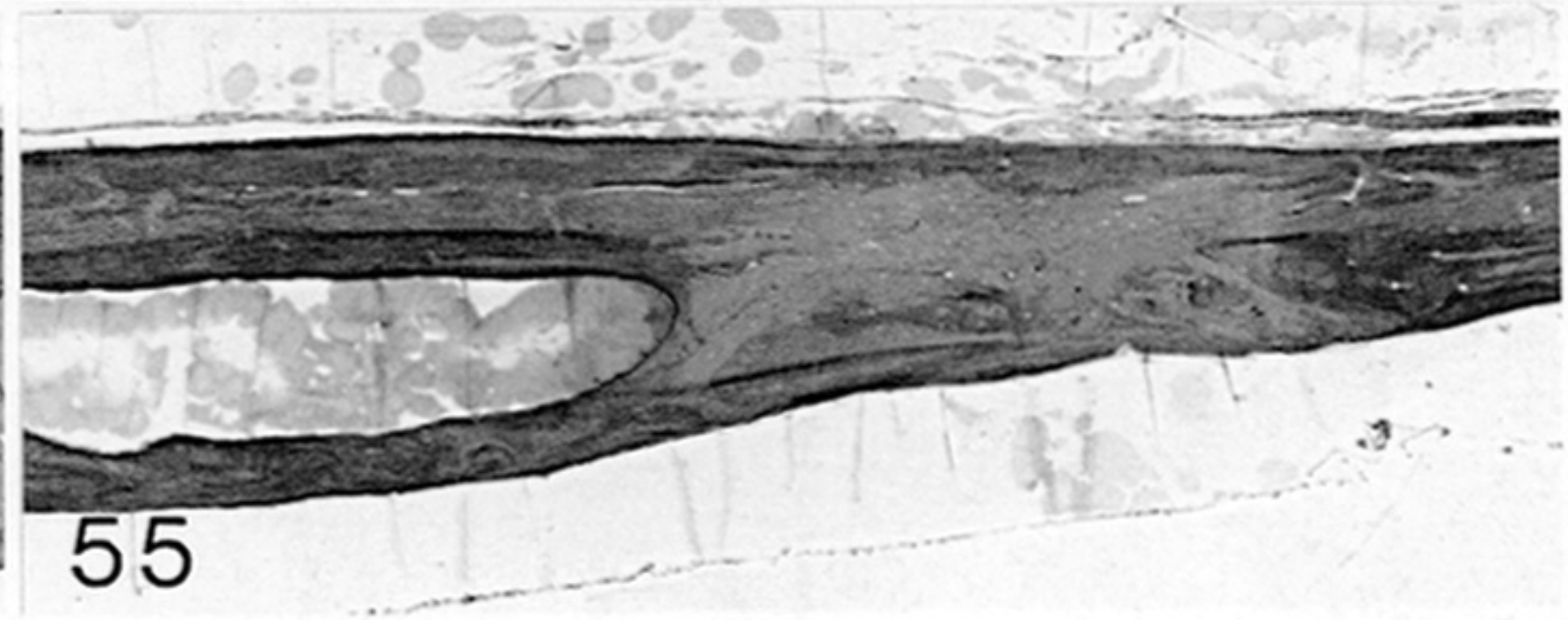
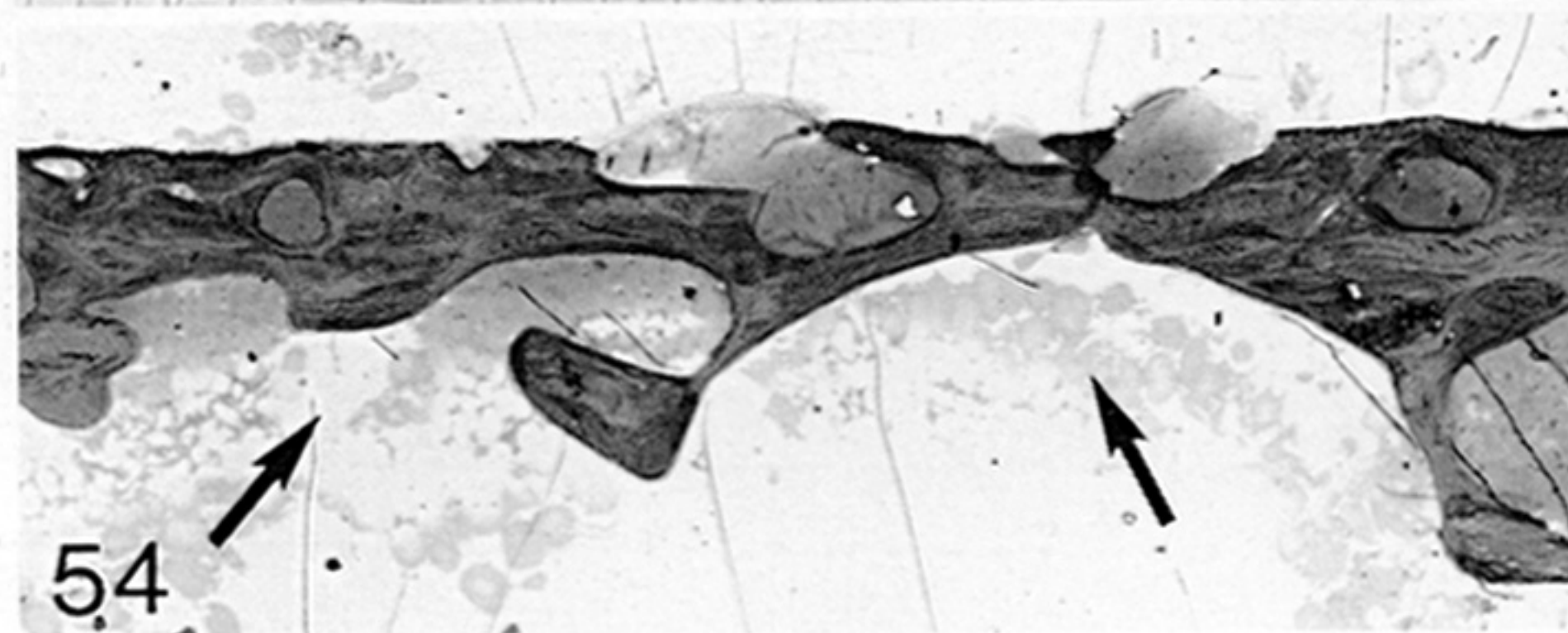
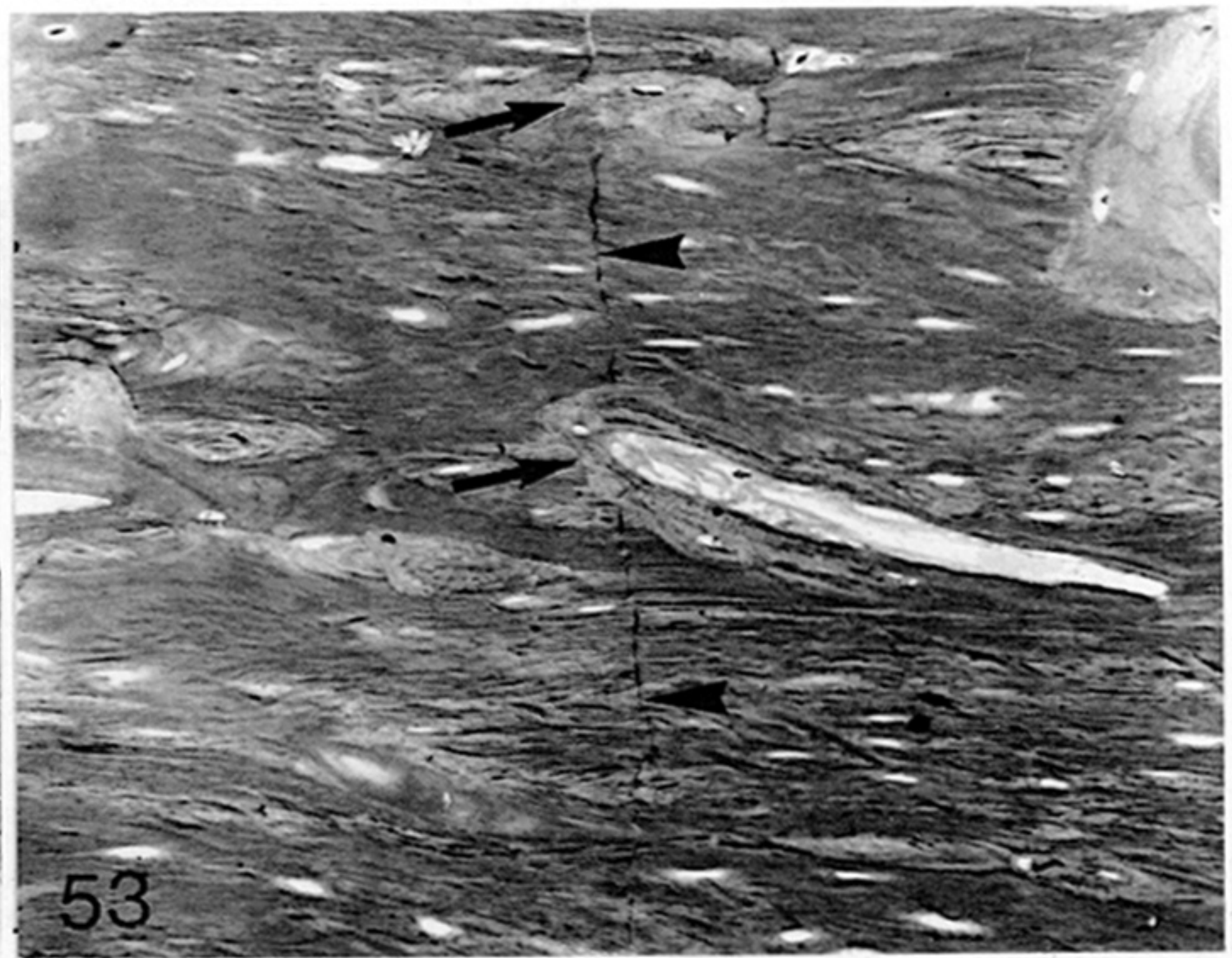
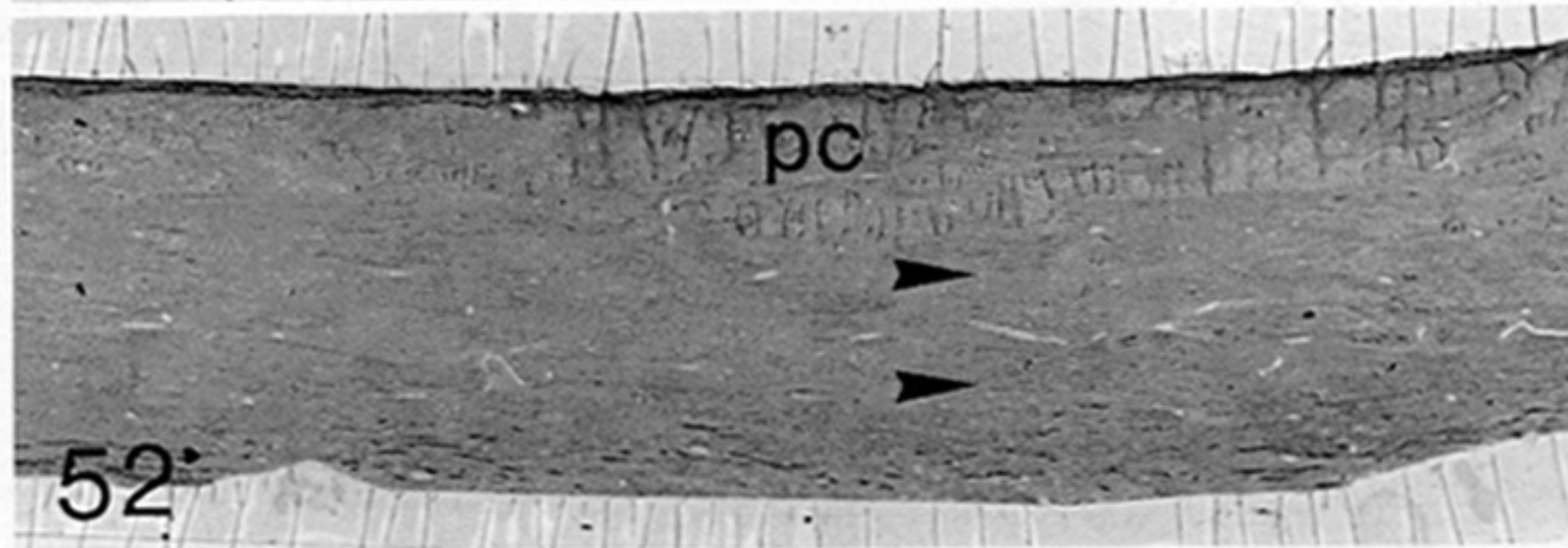
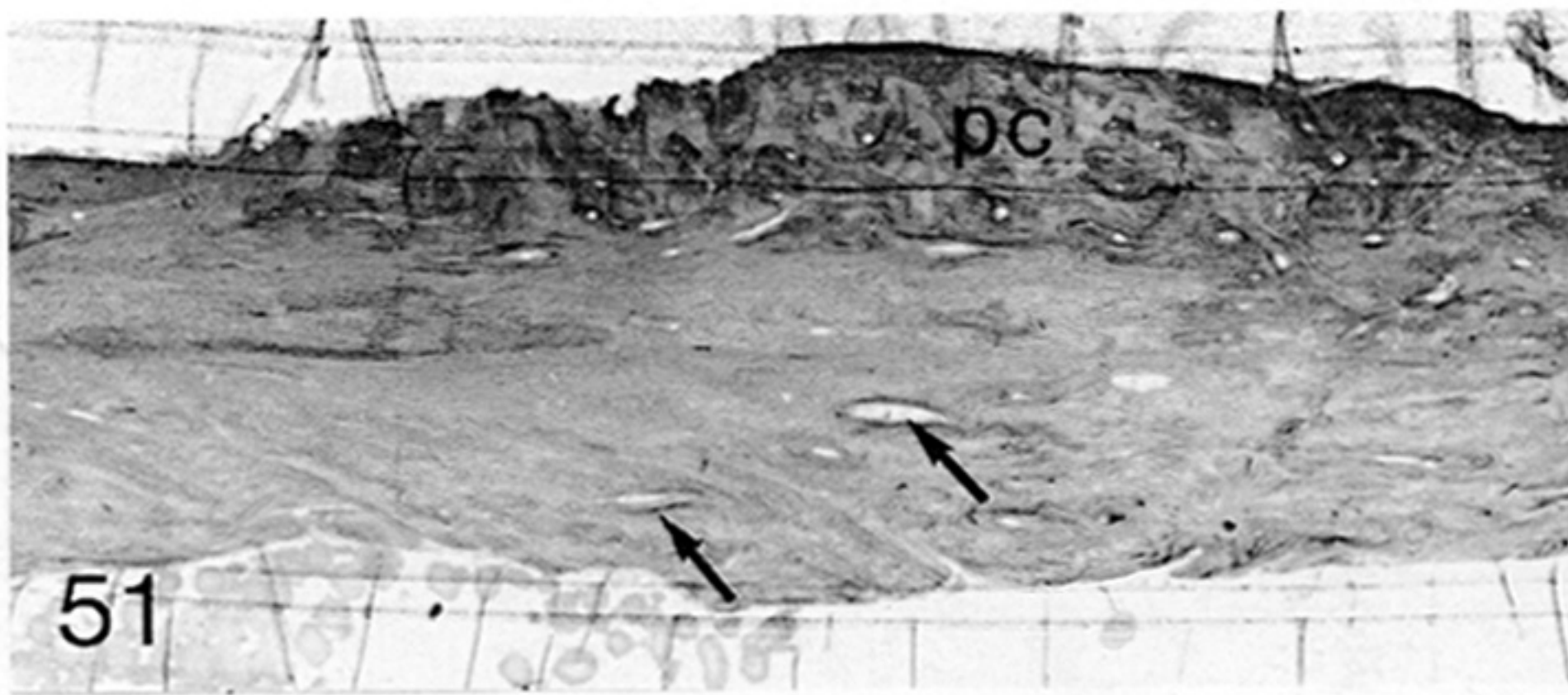


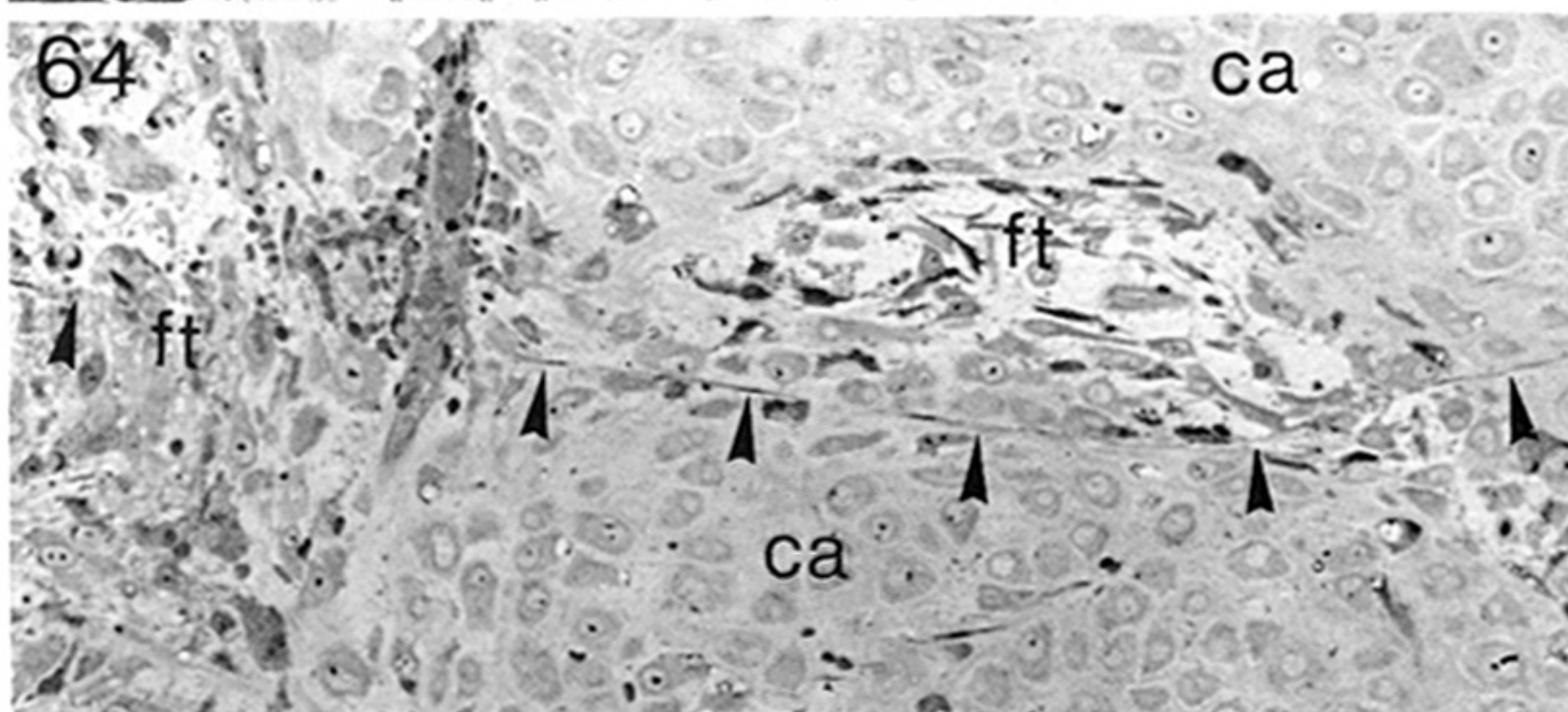
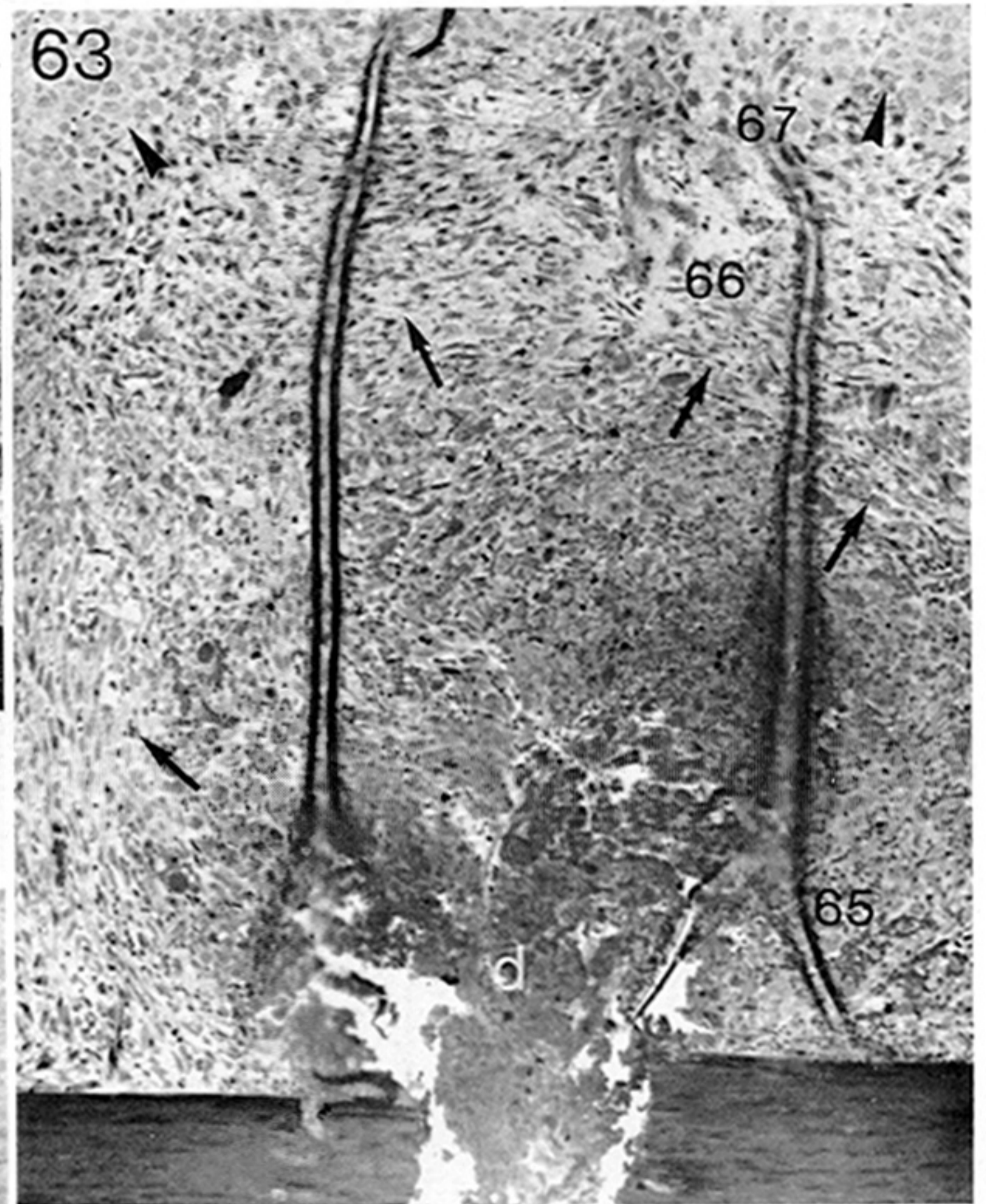
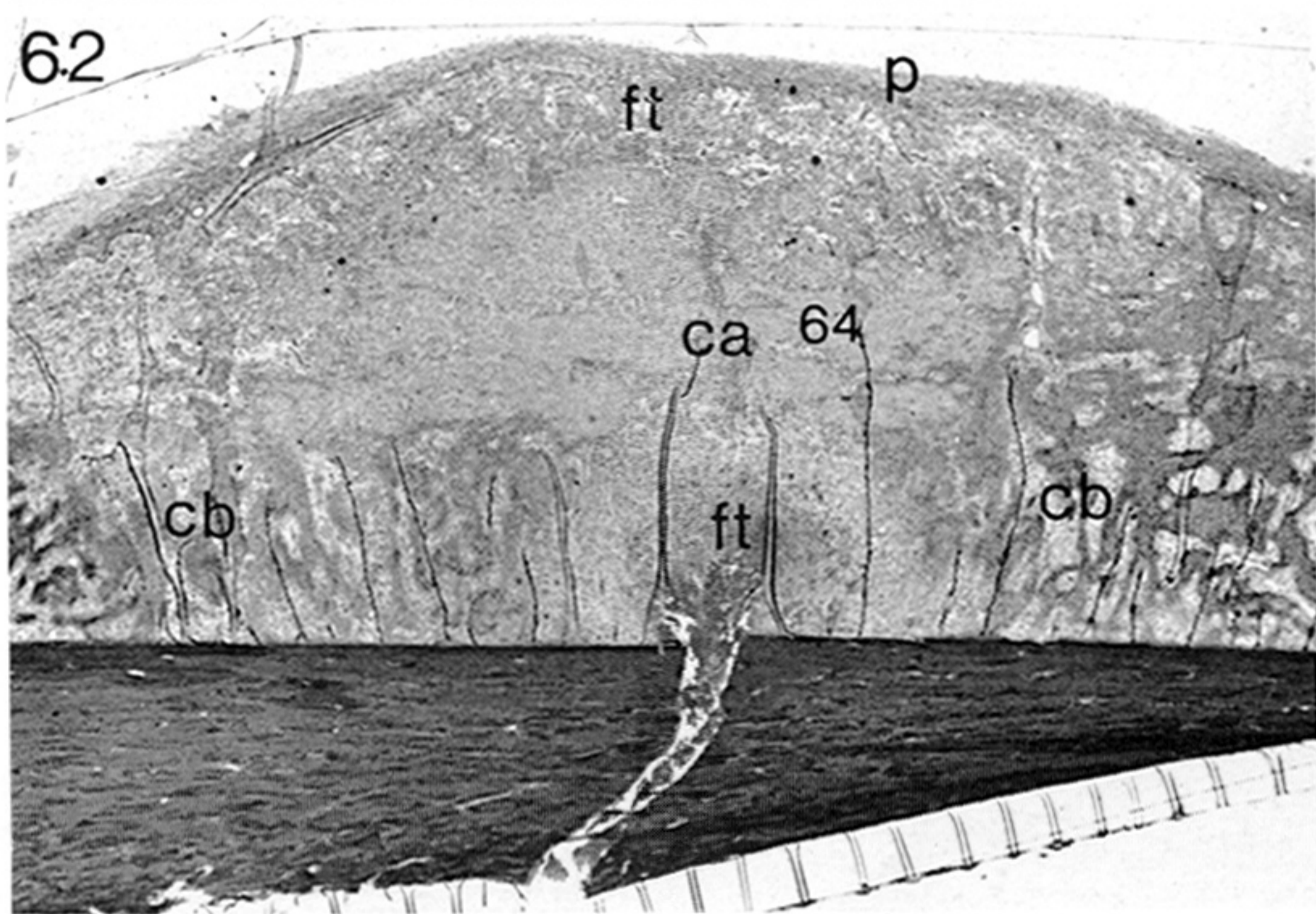
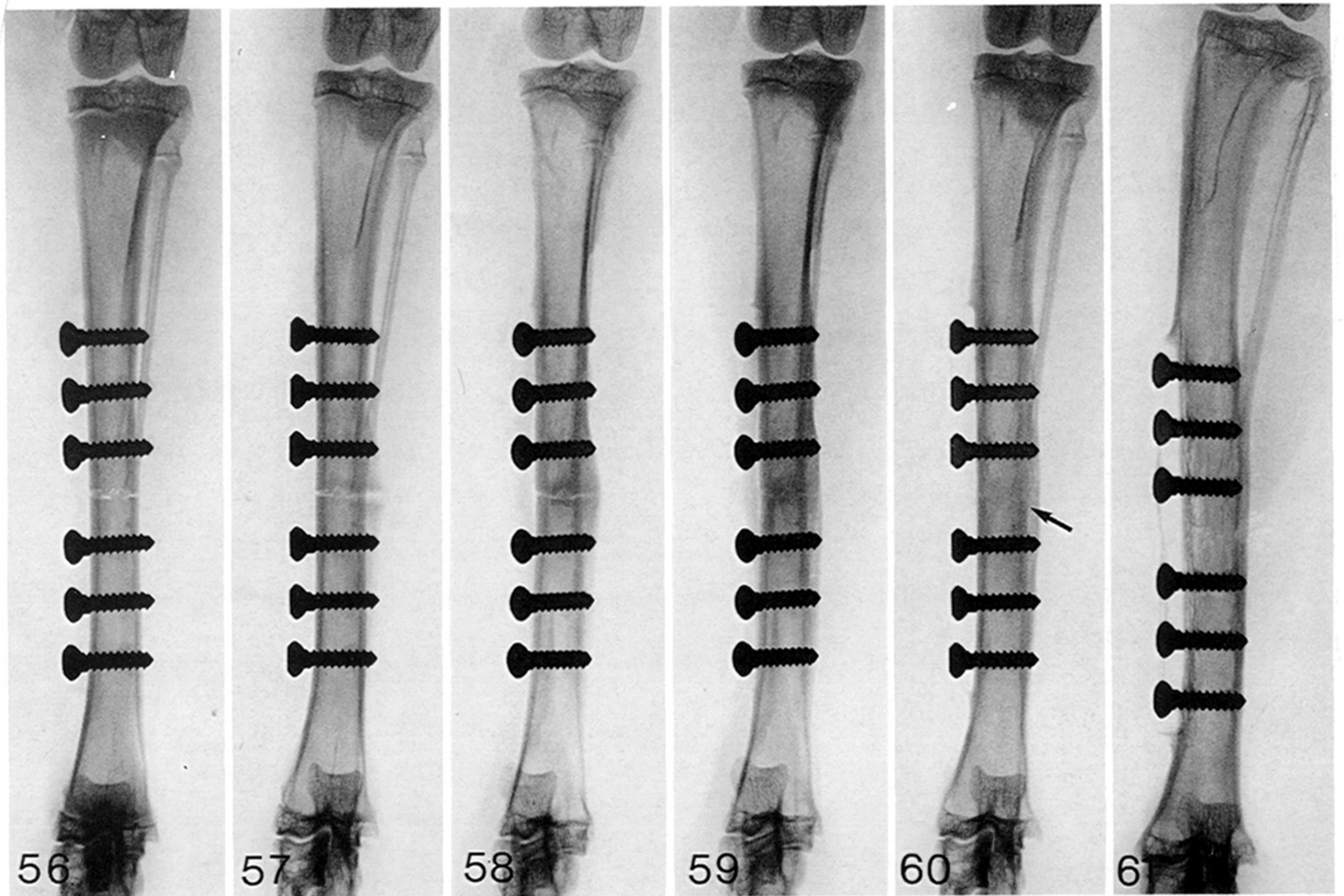
FIGURE 51. Photomicrograph of a 12-week mechanically stable fracture. The fracture site cannot be seen. The periosteal callus (pc) is thin. The original cortical bone shows signs of remodelling activity (arrows). (Magn.  $\times 26$ ).

FIGURE 52. Photomicrograph of an 18-week mechanically stable fracture. The remains of the periosteal callus (pc) can be distinguished by the irregularly orientated bone. The fracture here is compressed (arrowheads). (Magn.  $\times 26$ .)

FIGURE 53. Photomicrograph at higher magnification of the fracture in figure 52. The fracture (arrowheads) can be traced across the cortex, except for two regions where remodelling cavities have crossed it (arrows). (Magn.  $\times 197$ .)

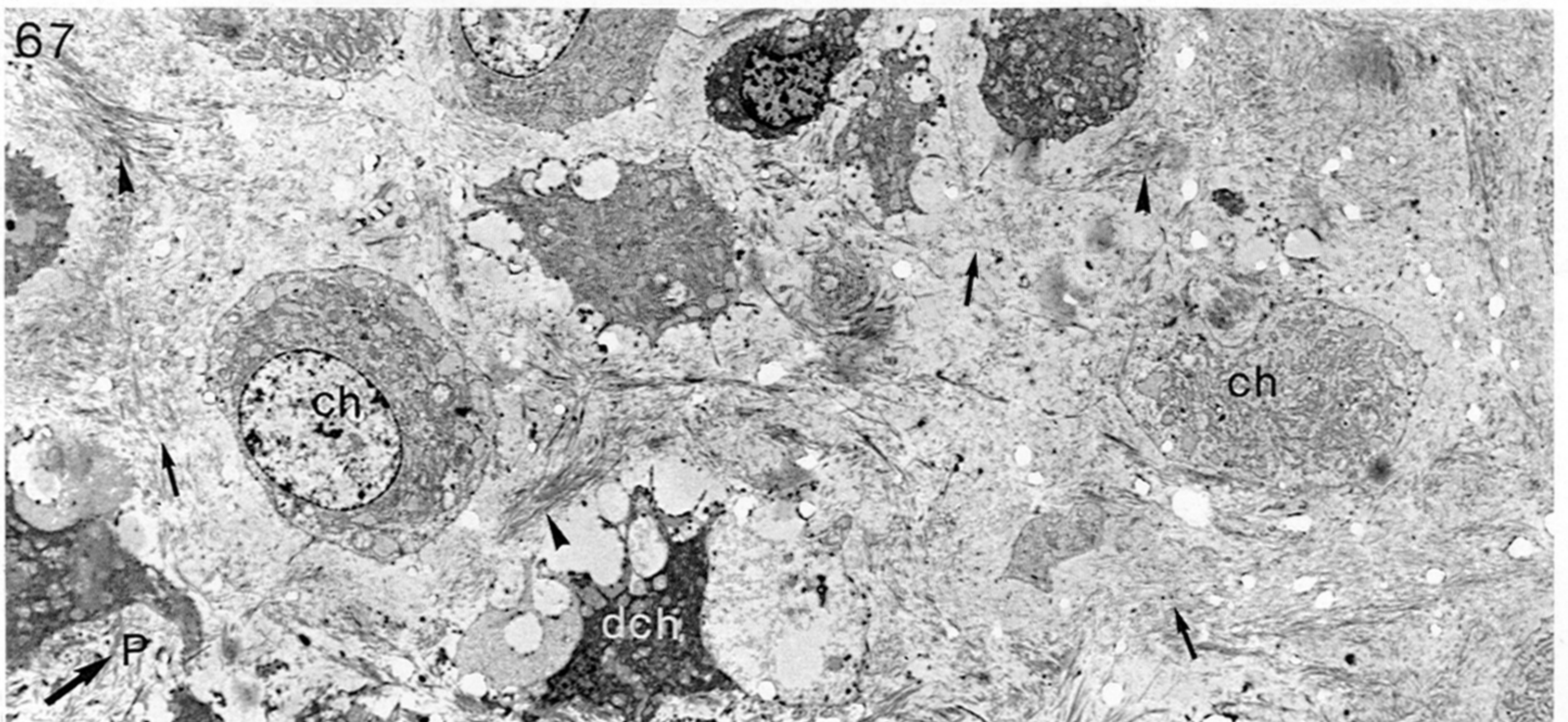
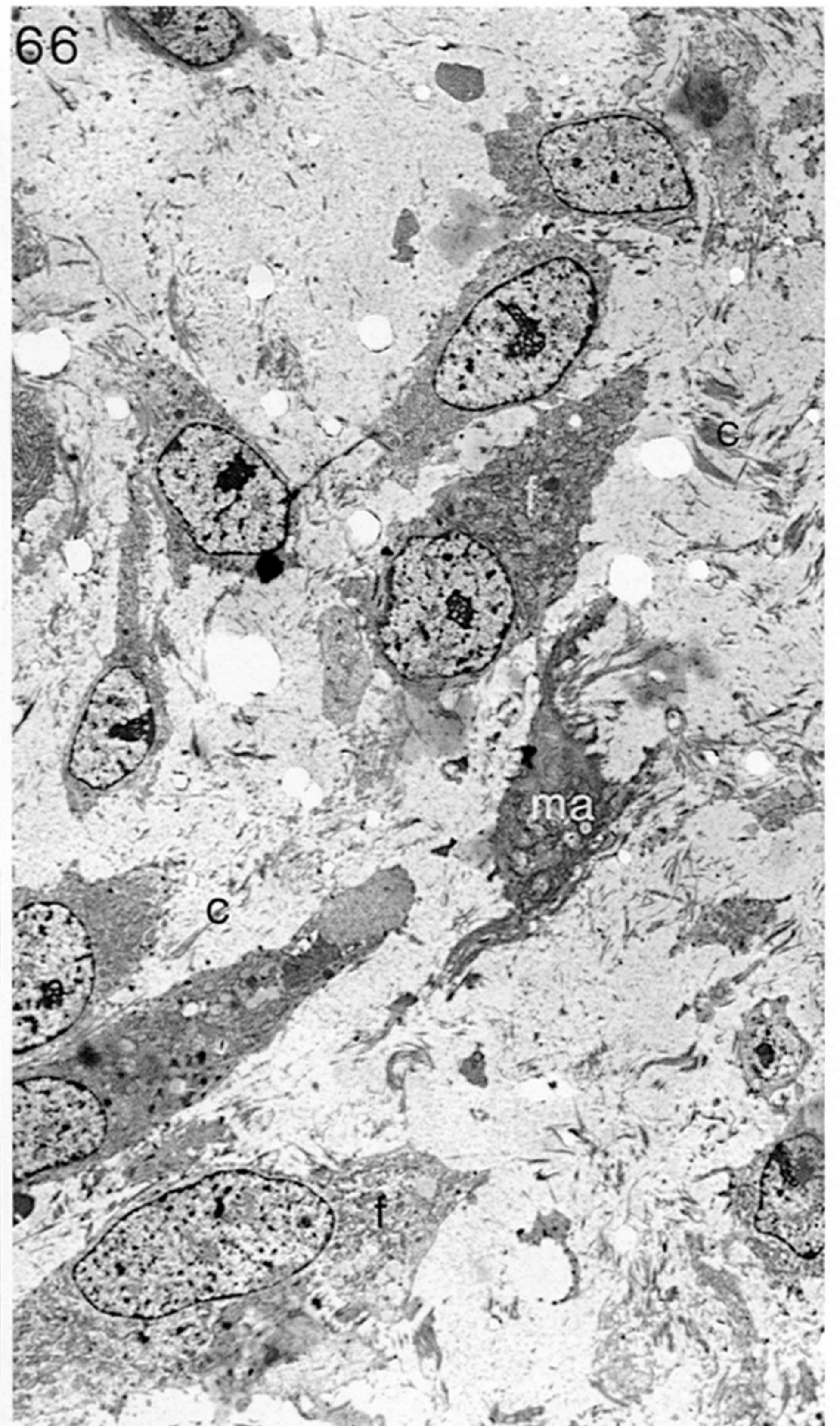
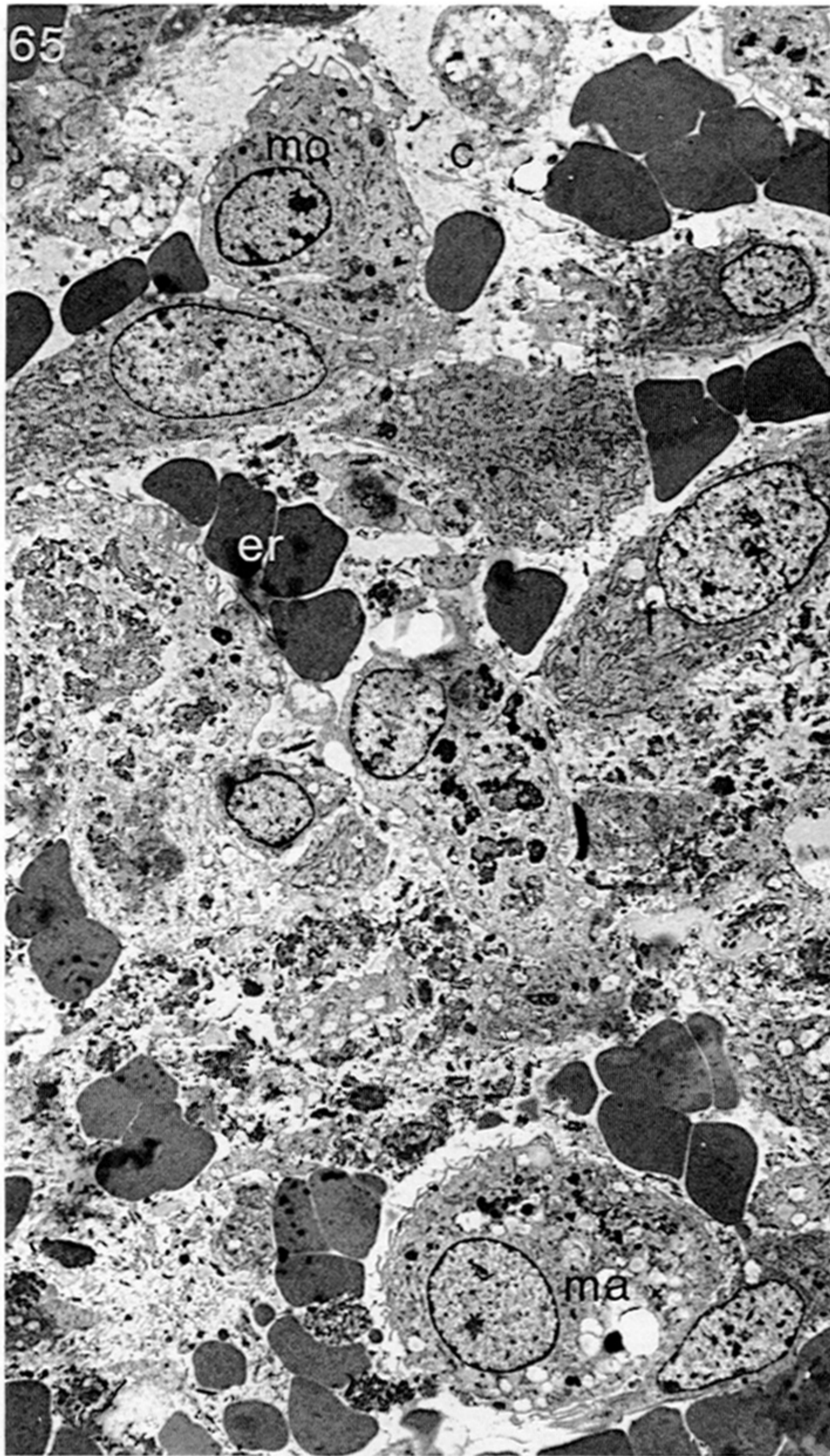
FIGURES 54 AND 55. Photomicrographs of different regions of a mechanically stable fracture at 1 year. The fracture site cannot be distinguished. Figure 54 shows the cortex under the plate, which is thin with very large cavities, filled with fat cells, which are open endosteally (arrows). Figure 55 is from the side of the bone; the cortex is thin and large cavities filled with fat cells are present. (Magn.  $\times 26$ .)





FIGURES 56-64. For description see facing plate 16.





FIGURES 65-67. For description see facing plate 16.



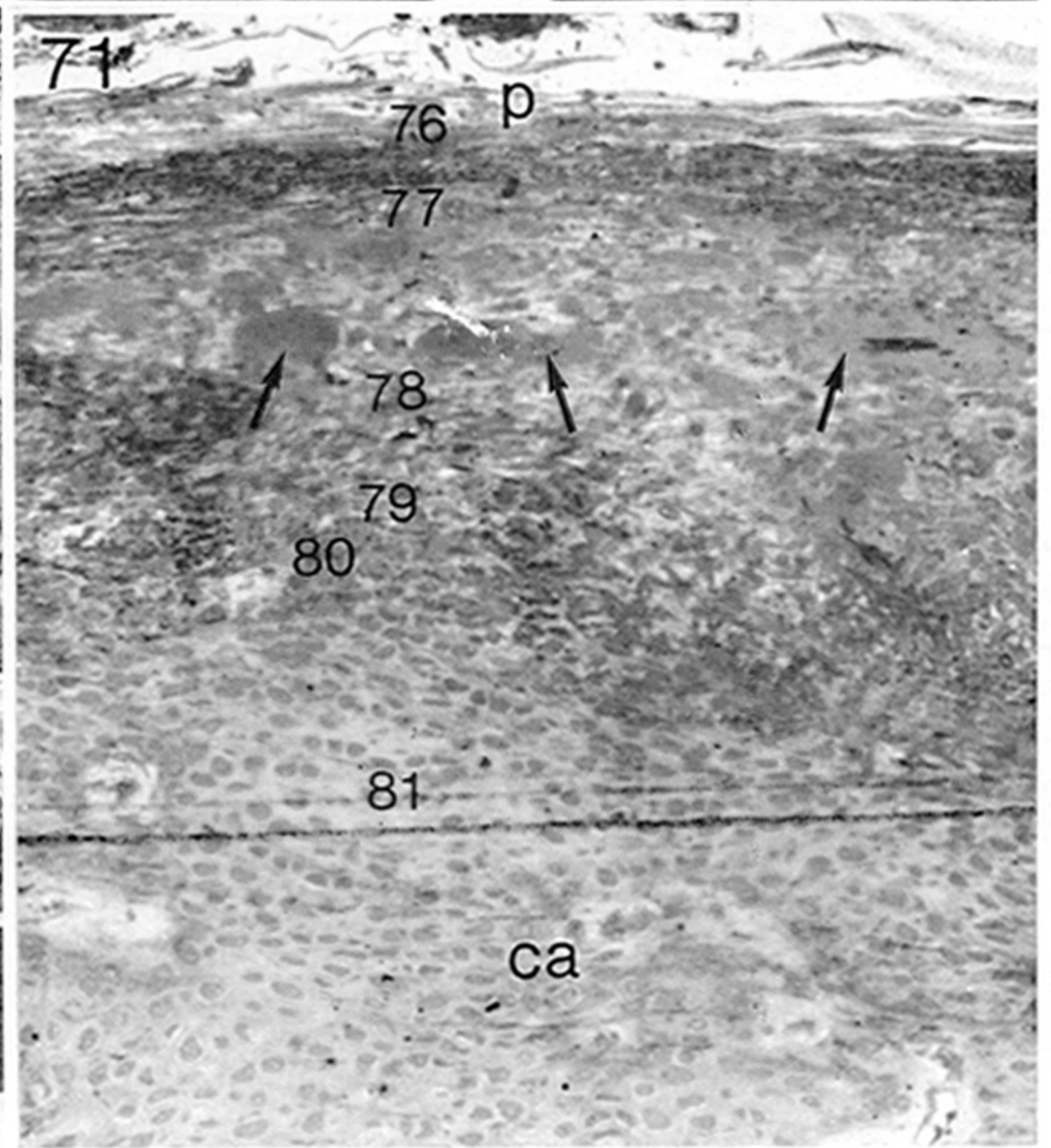
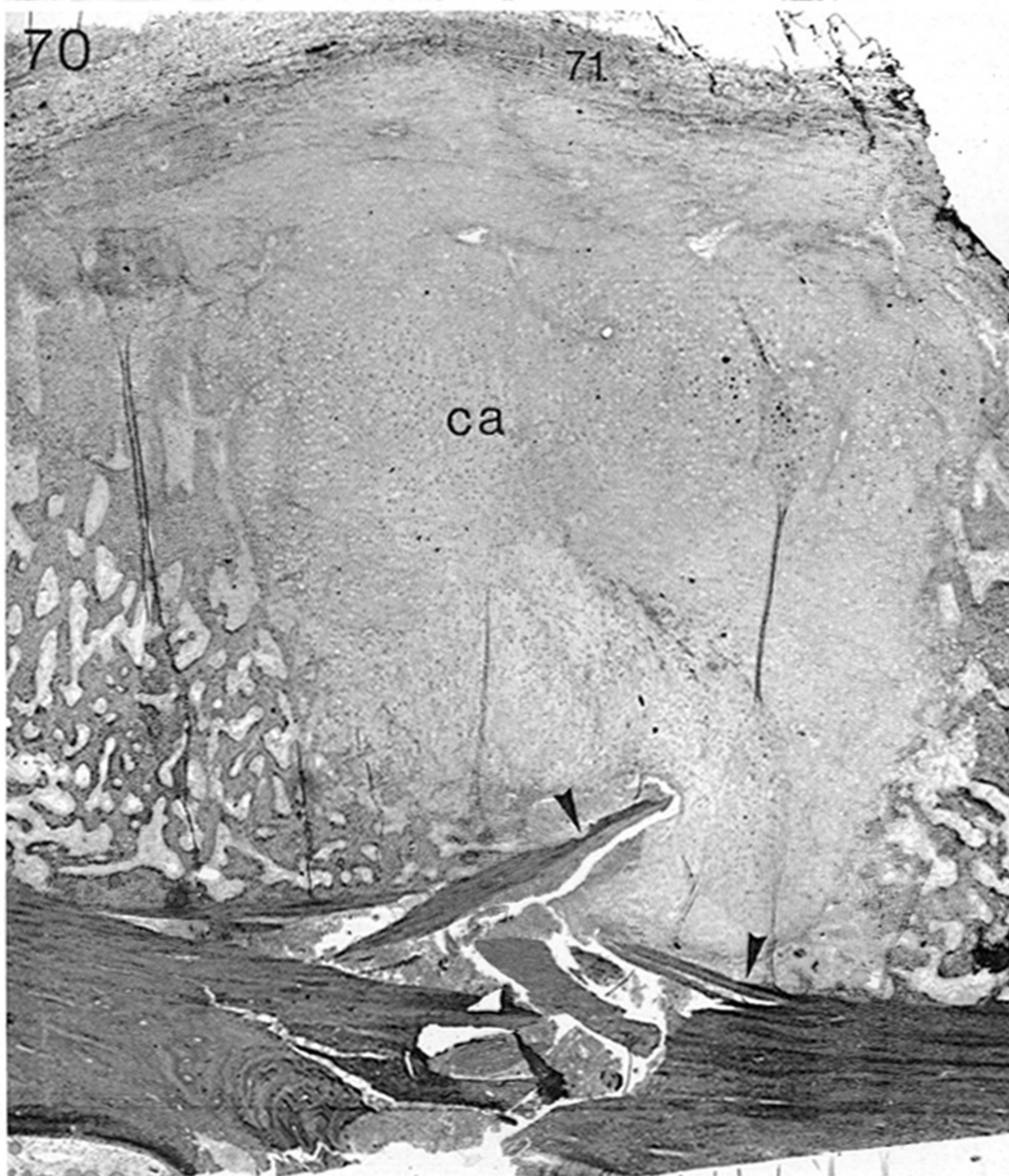
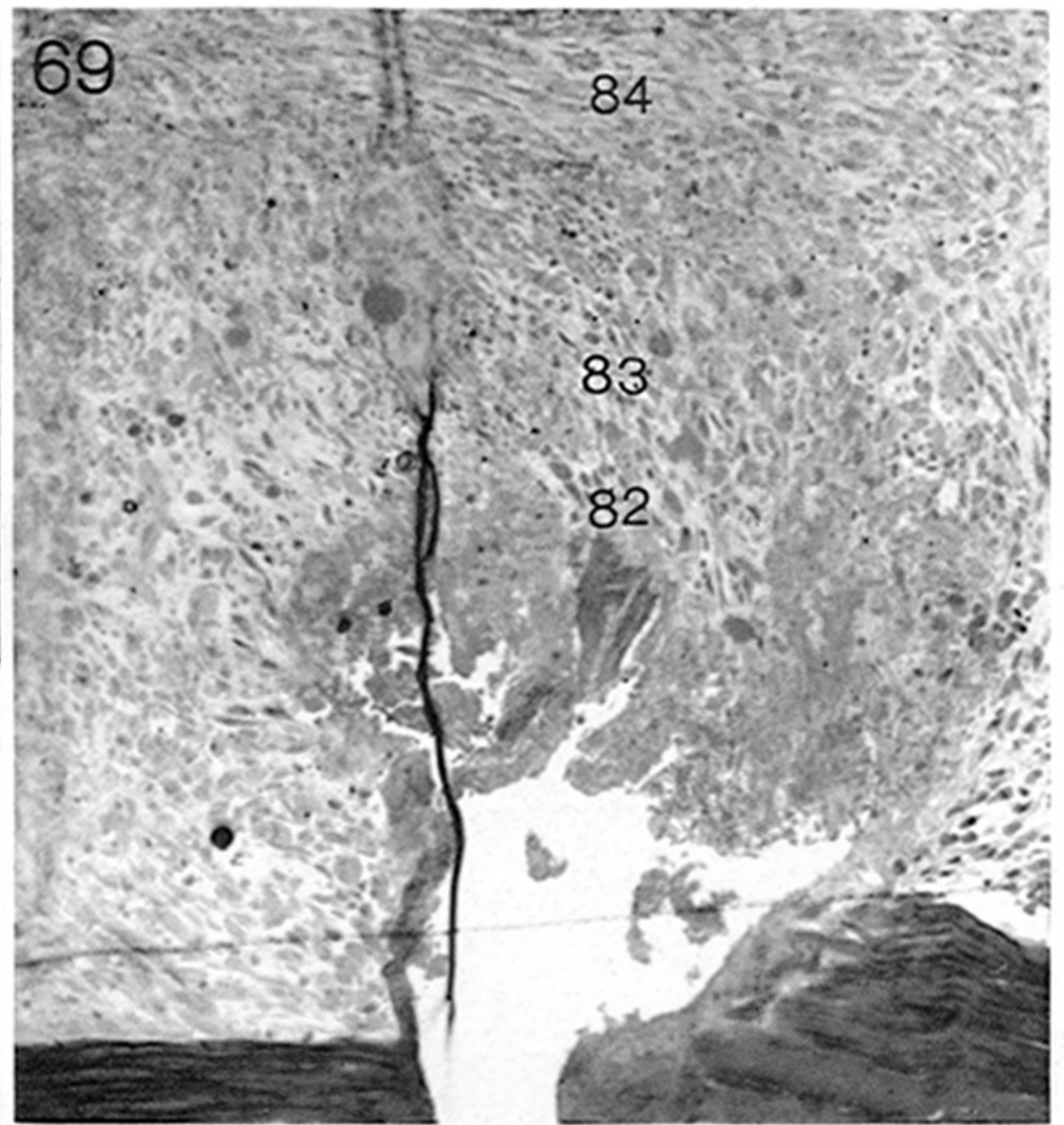
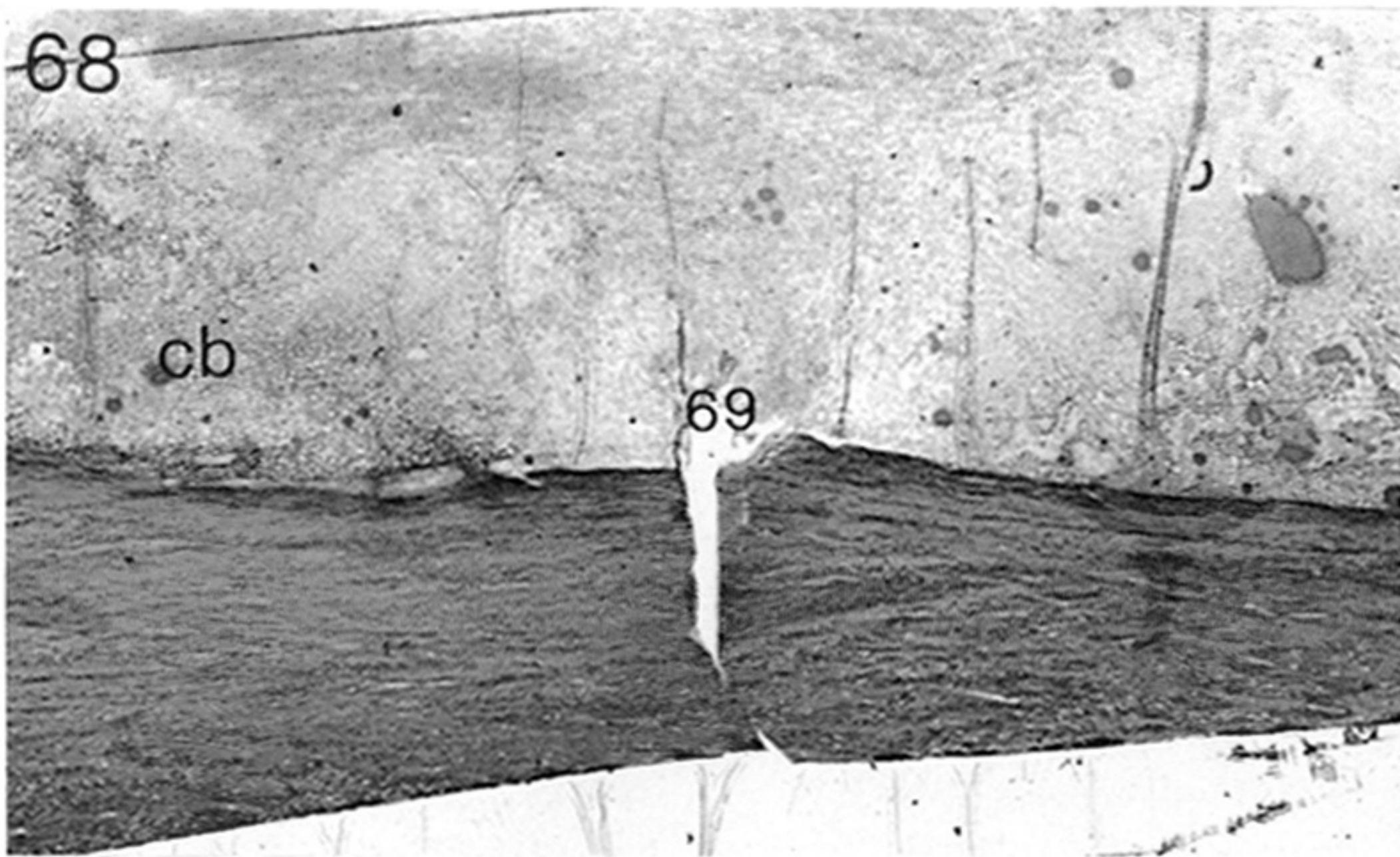


FIGURE 68. Photomicrograph of an 8-day mechanically unstable fracture. The cancellous bone (cb) of the periosteal callus is approaching the fracture gap from both sides. Most of the debris near the gap has been removed and the area is populated by mesenchymal cells. (The number 69 denotes the position of figure 69.) (Magn.  $\times 29$ .)

FIGURE 69. Photomicrograph of the area over the fracture gap in figure 68 (= 69). The mesenchymal cells surround the remaining debris protruding from the gap. No capillaries are present. (The numbers 82, 83 and 84 denote the positions of figures 82, 83 and 84.) (Magn.  $\times 108$ .)

FIGURE 70. Photomicrograph of a 9-day mechanically unstable fracture. This is the cortex opposite the plate and the fracture is comminuted. The callus is now a thick layer and the region over the gap is filled by cartilage (ca). There are signs of osteoclastic activity on the spicules of cortical bone (arrowheads). (The number 71 denotes the position of figure 71.) (Magn.  $\times 24$ .)

FIGURE 71. Photomicrograph of the periosteal region of the fracture in figure 70 (= 71). The longitudinal orientation of the fibres in the periosteum (p) can be seen. Beneath the periosteum there are layers of developing bone (arrows) and fibrous tissue (ft). These overlie the cartilage (ca). (The numbers 76-81 denote the positions of figures 76-81.) (Magn.  $\times 130$ .)



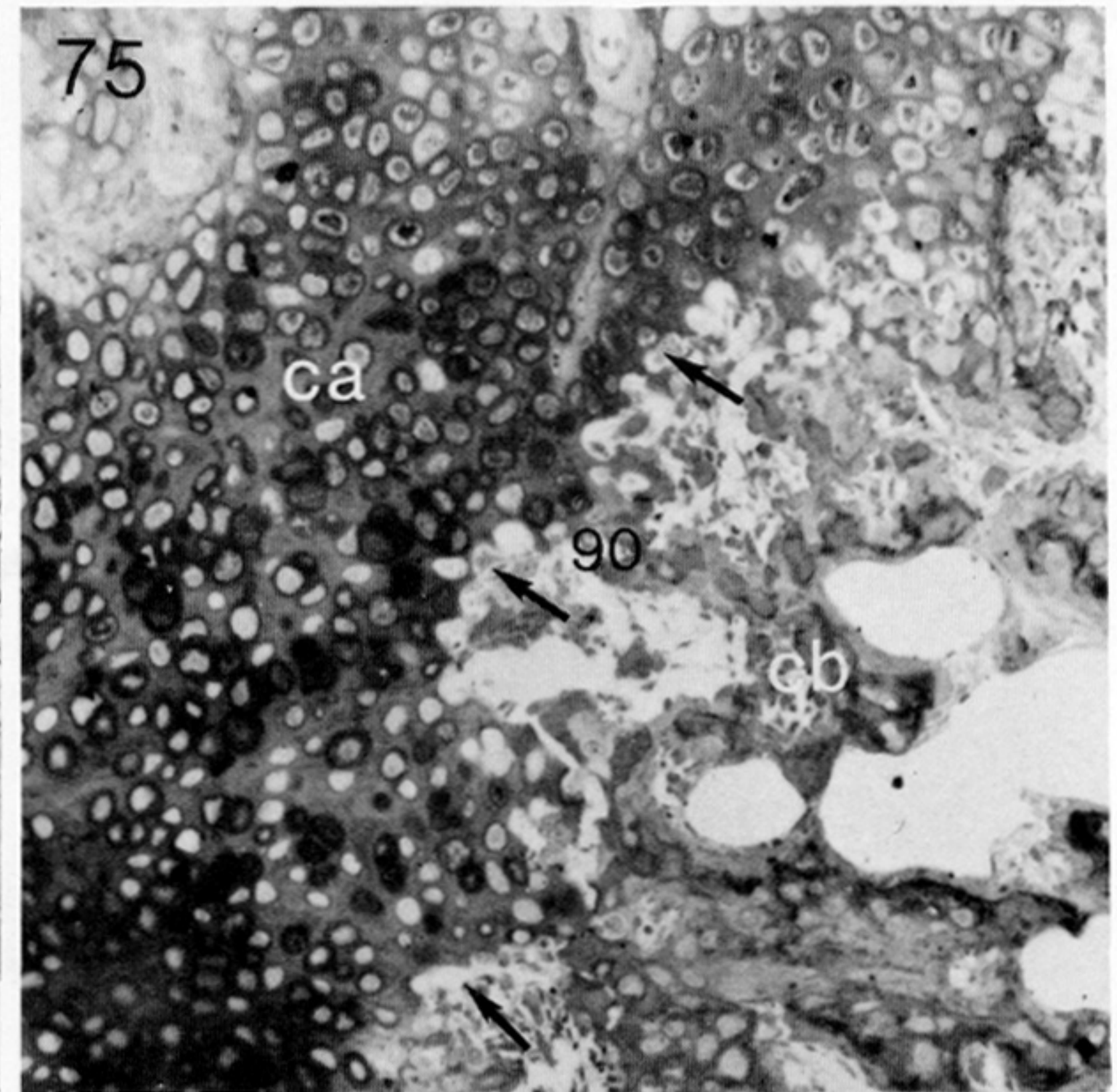
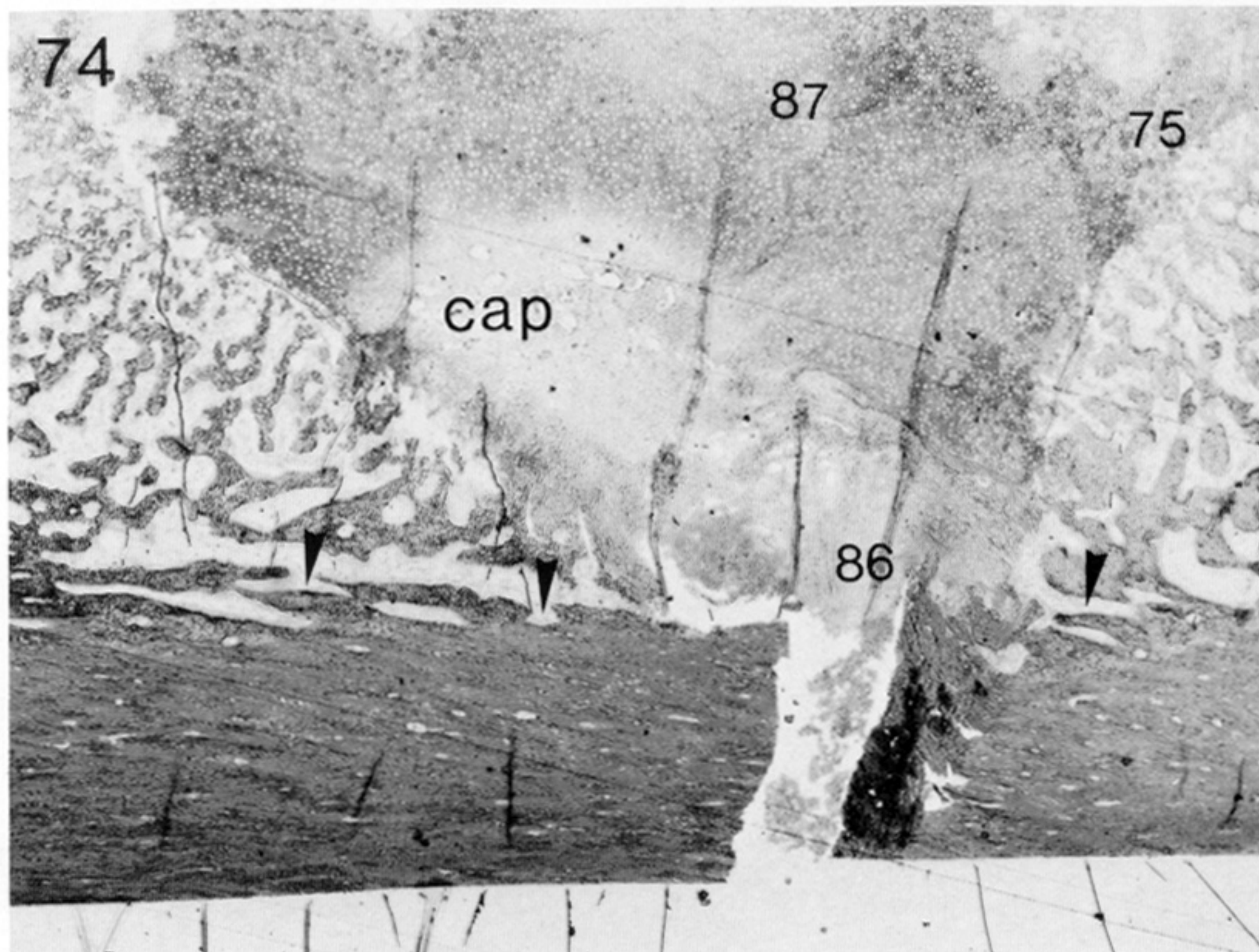
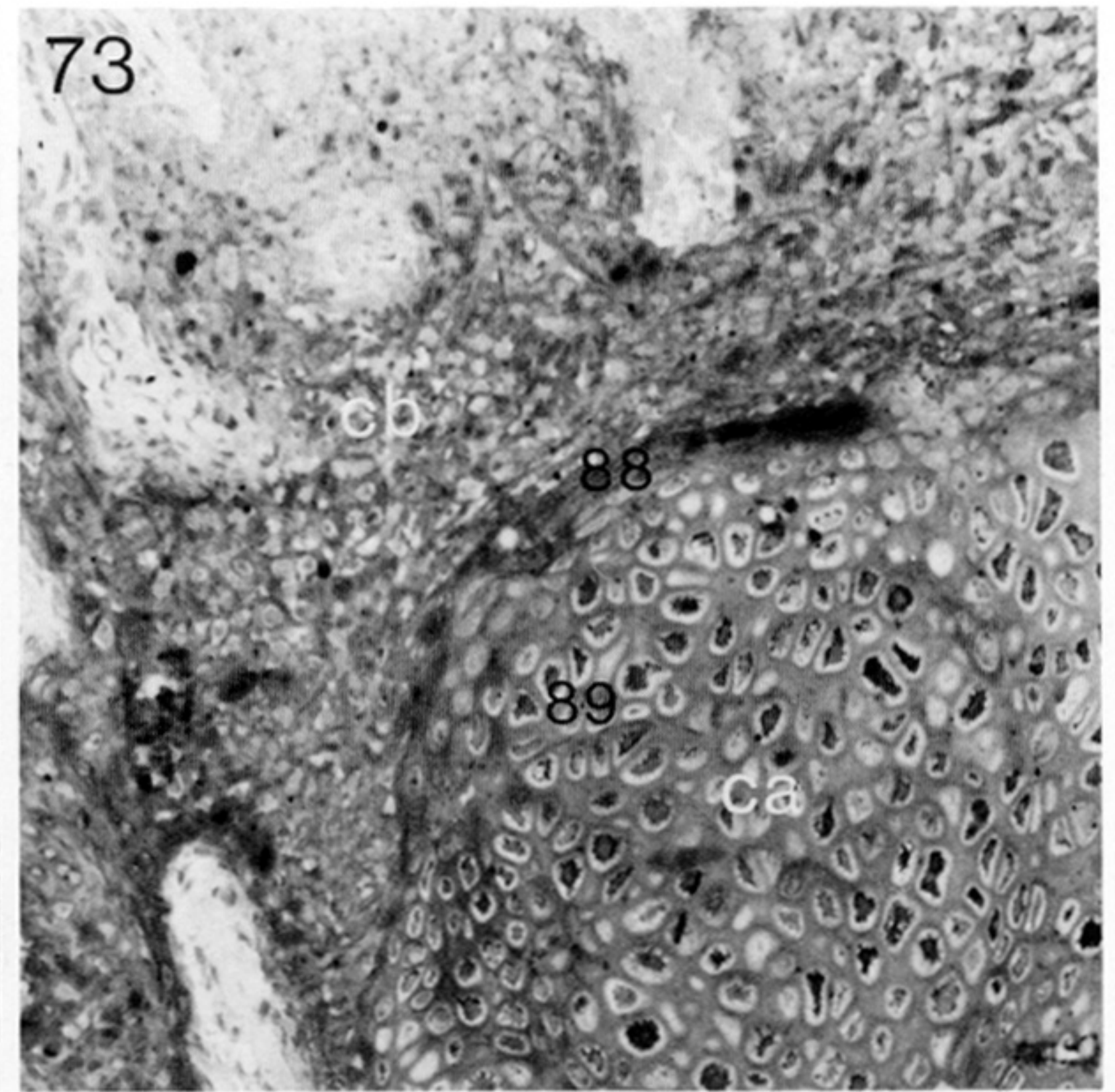
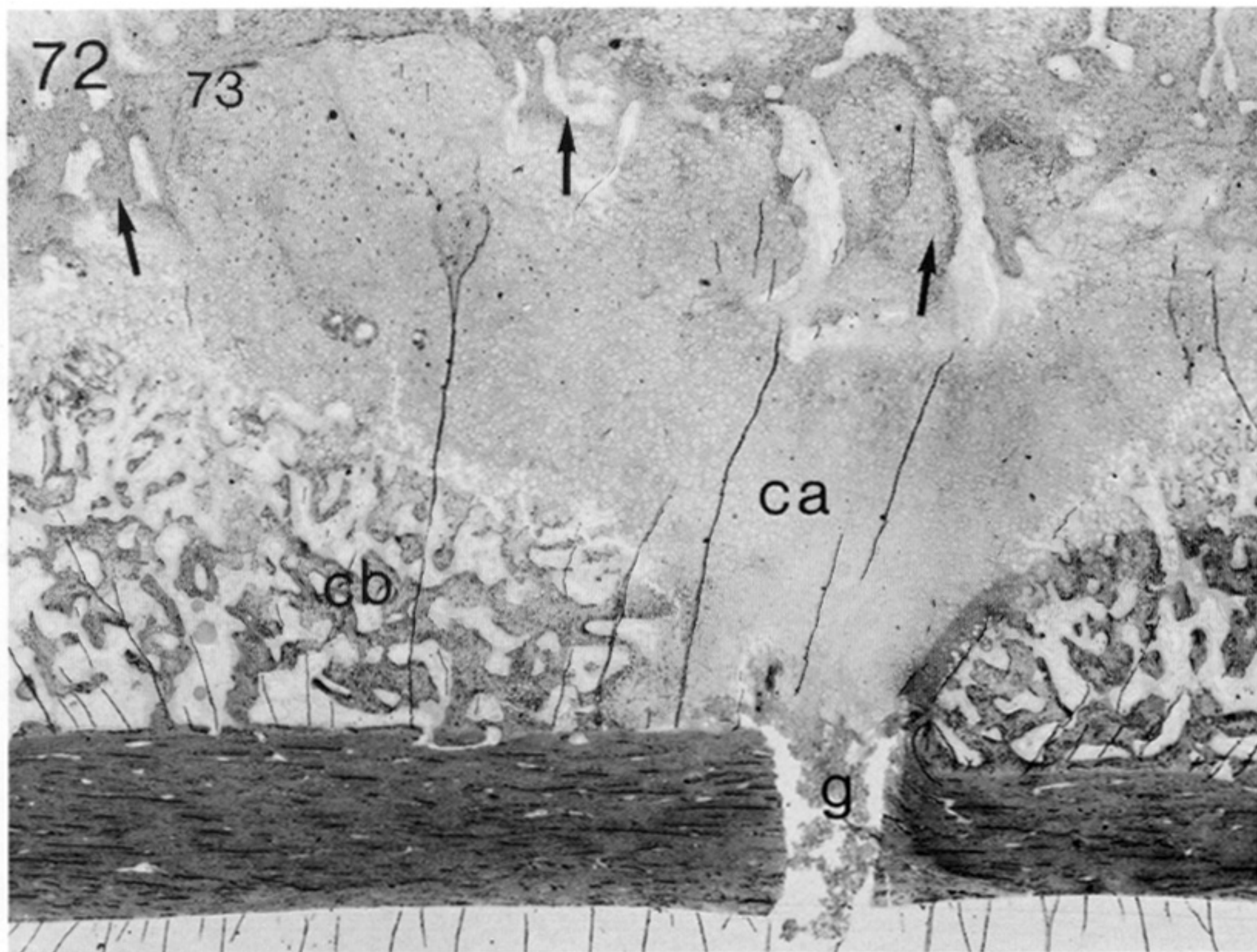


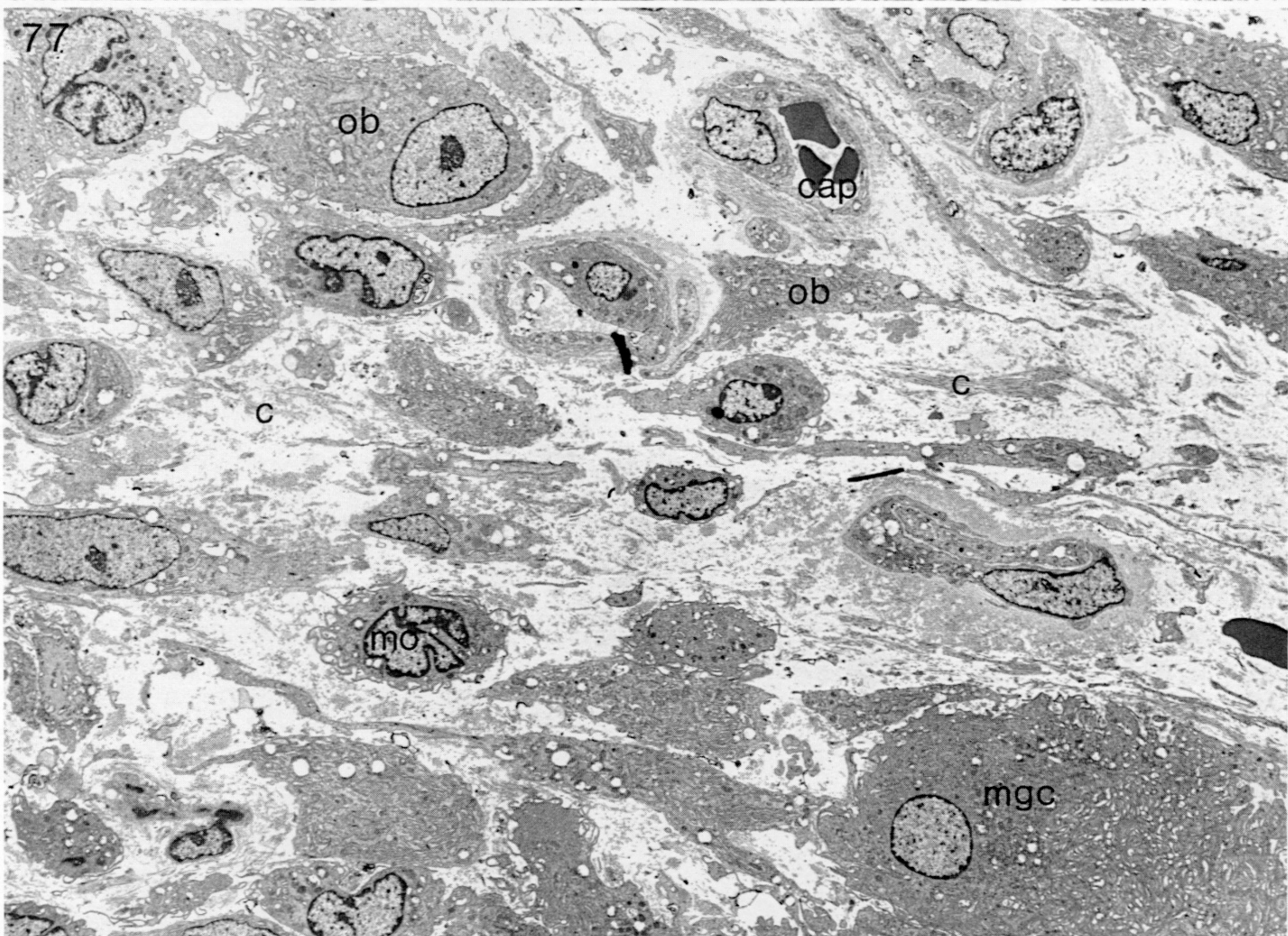
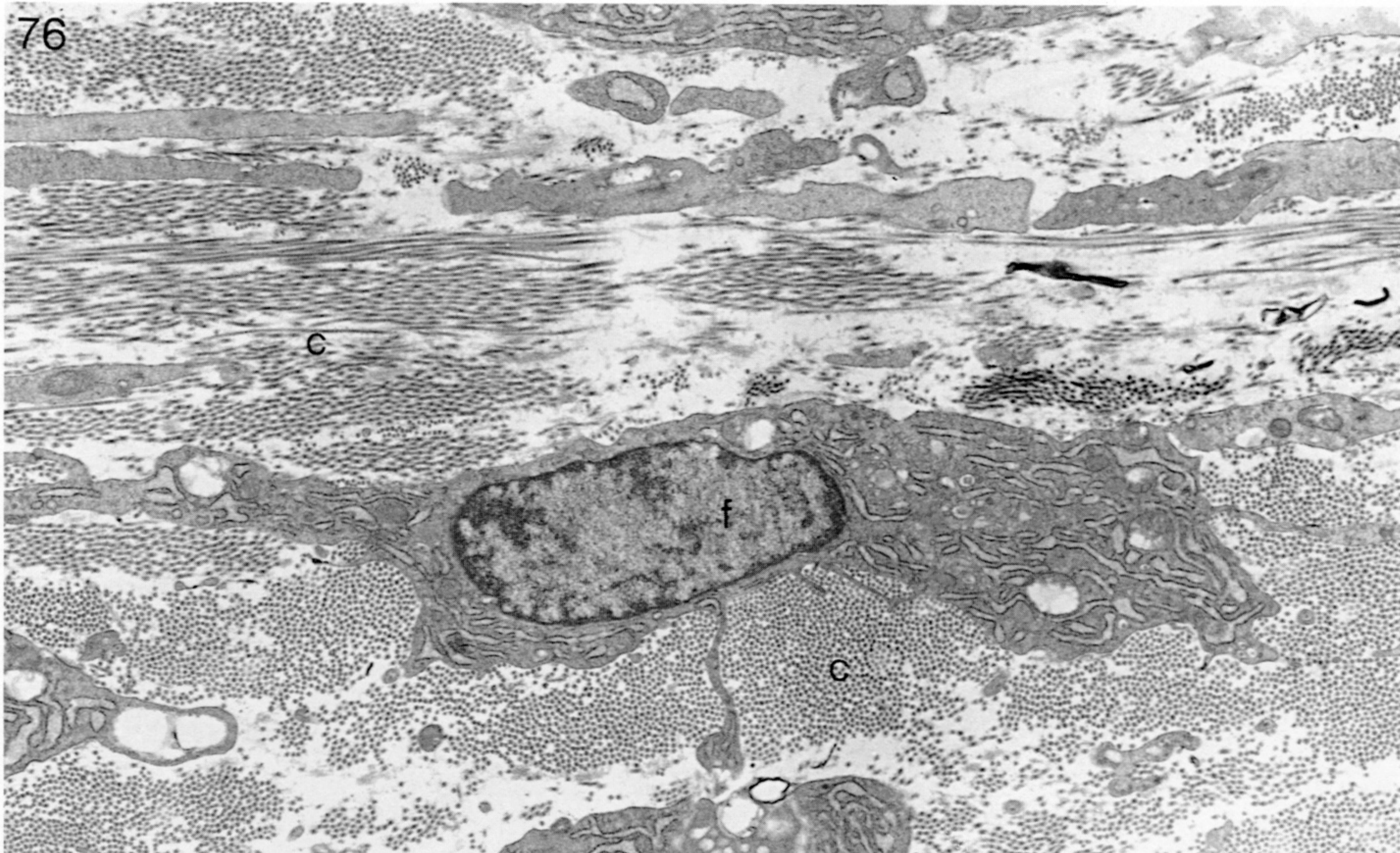
FIGURE 72. Photomicrograph of a 12-day mechanically unstable fracture. The fracture gap (g) is filled by debris that meets the cartilage (ca), which is in turn surrounded by the cancellous bone (cb) of the callus; an external layer of bone now covers the cartilage (arrows). (The number 73 denotes the position of figure 73.) (Magn.  $\times 24$ .)

FIGURE 73. Photomicrograph of a small area of the callus in figure 72 (= 73). The close juxtaposition of the cancellous bone (cb) and cartilage (ca) is seen. (The numbers 88 and 89 denote the positions of figures 88 and 89.) (Magn.  $\times 130$ .)

FIGURE 74. Photomicrograph of the same 12-day fracture shown in figure 73, but in a region opposite the plate. The callus is similar to that in figure 73, but there is a small region of large, sinusoid-like capillaries (cap) in the cartilage. Osteoclastic activity is apparent along the cortical bone (arrowheads). (The numbers 75, 86 and 87 denote the positions of figures 75, 86 and 87.) (Magn.  $\times 24$ .)

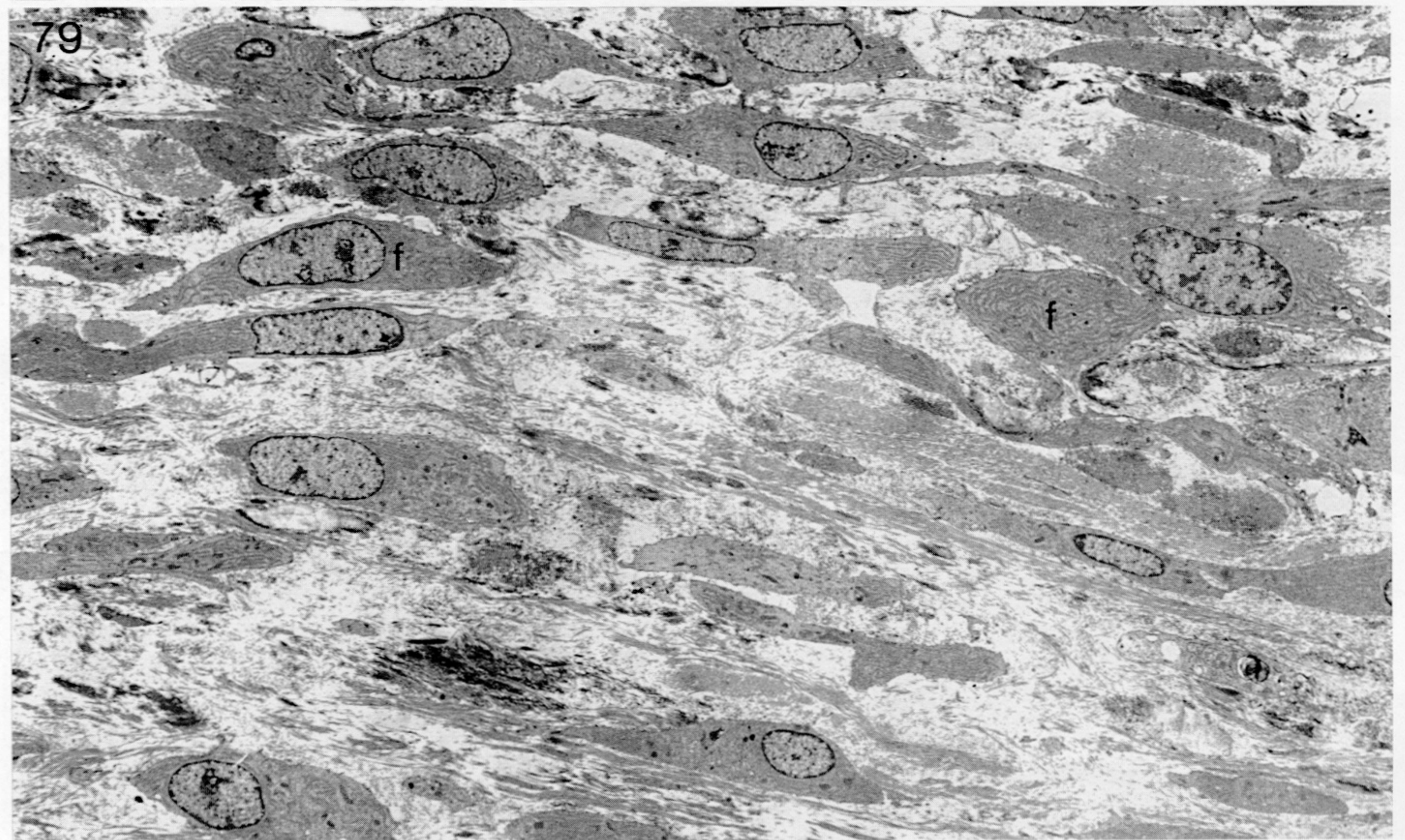
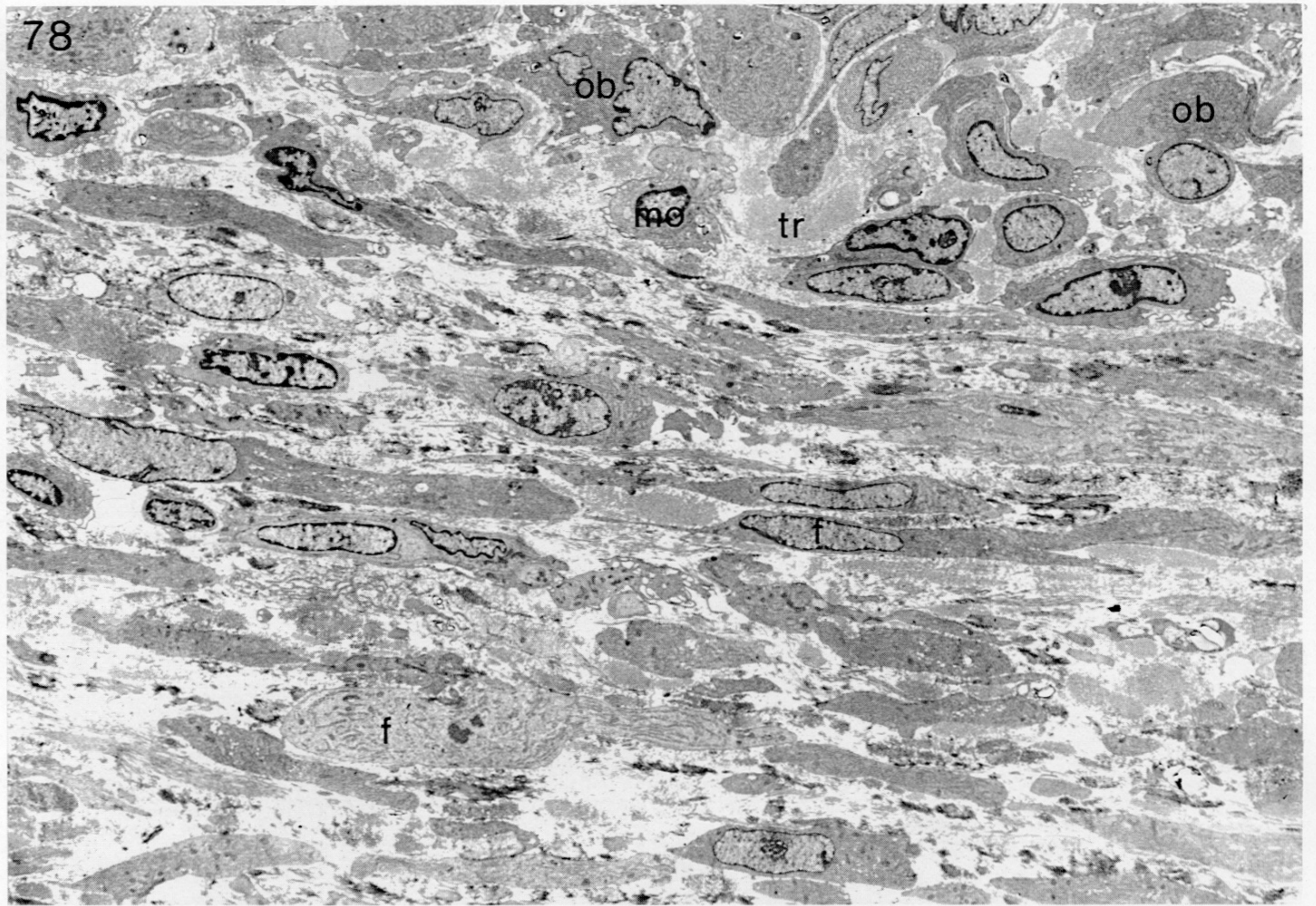
FIGURE 75. Photomicrograph of a small region of figure 74 (= 75). The cancellous bone (cb) is encroaching onto the cartilage (ca) and endochondral ossification is taking place (arrows). (The number 90 denotes the position of figure 90.) (Magn.  $\times 130$ .)





FIGURES 76 AND 77. For description see facing plate 17.





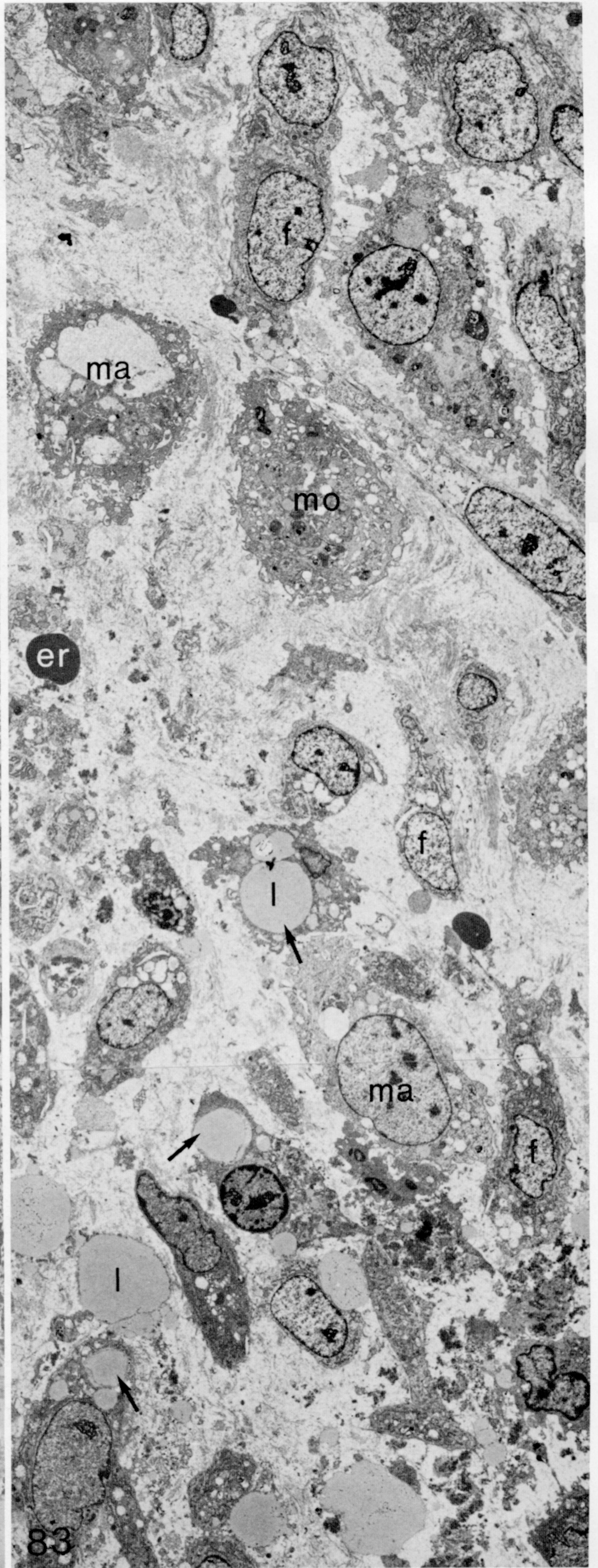
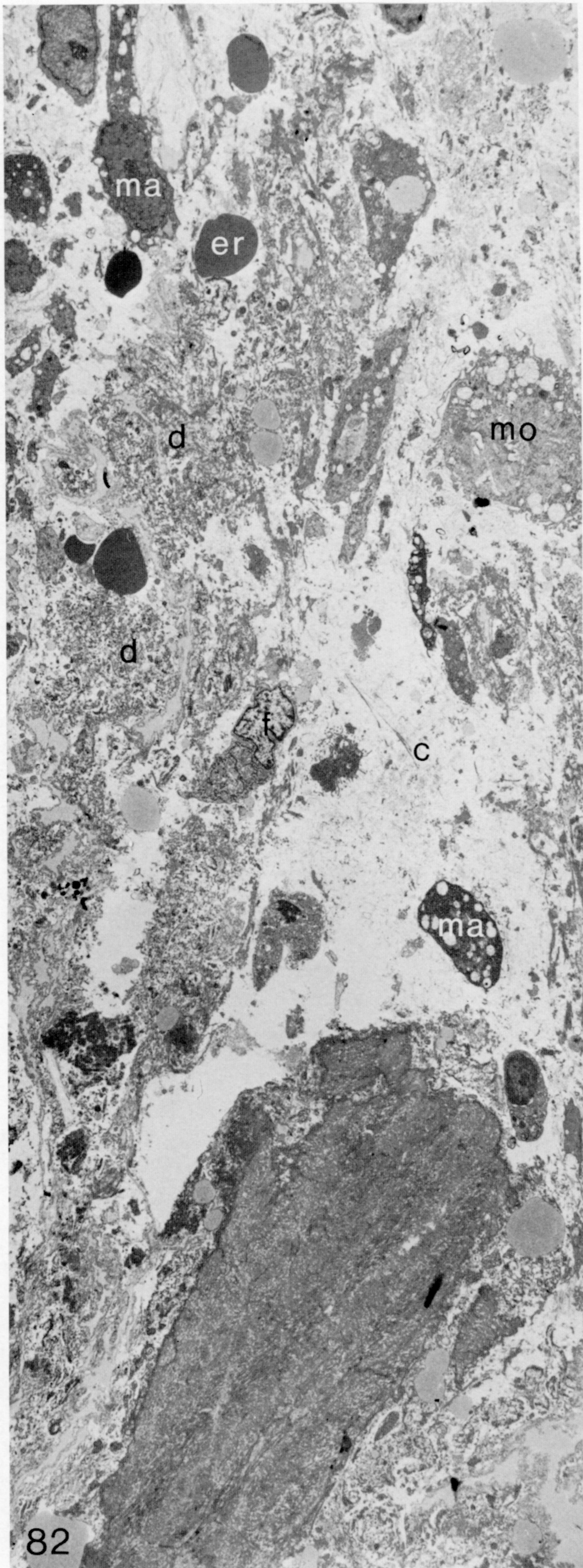
FIGURES 78 AND 79. For description see facing plate 17.





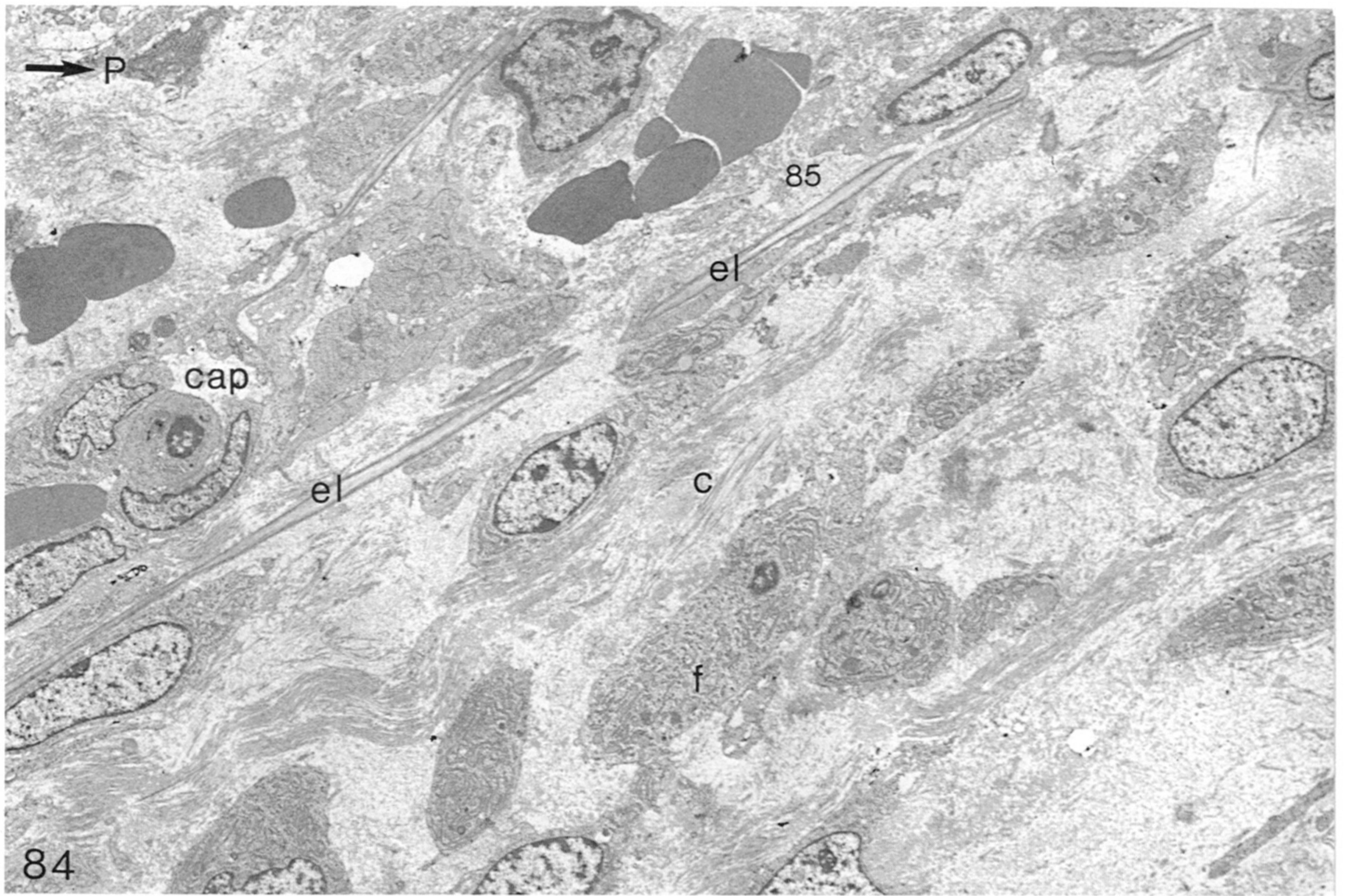
FIGURES 80 AND 81. For description see facing plate 17.





FIGURES 82 AND 83. For description see facing plate 17.





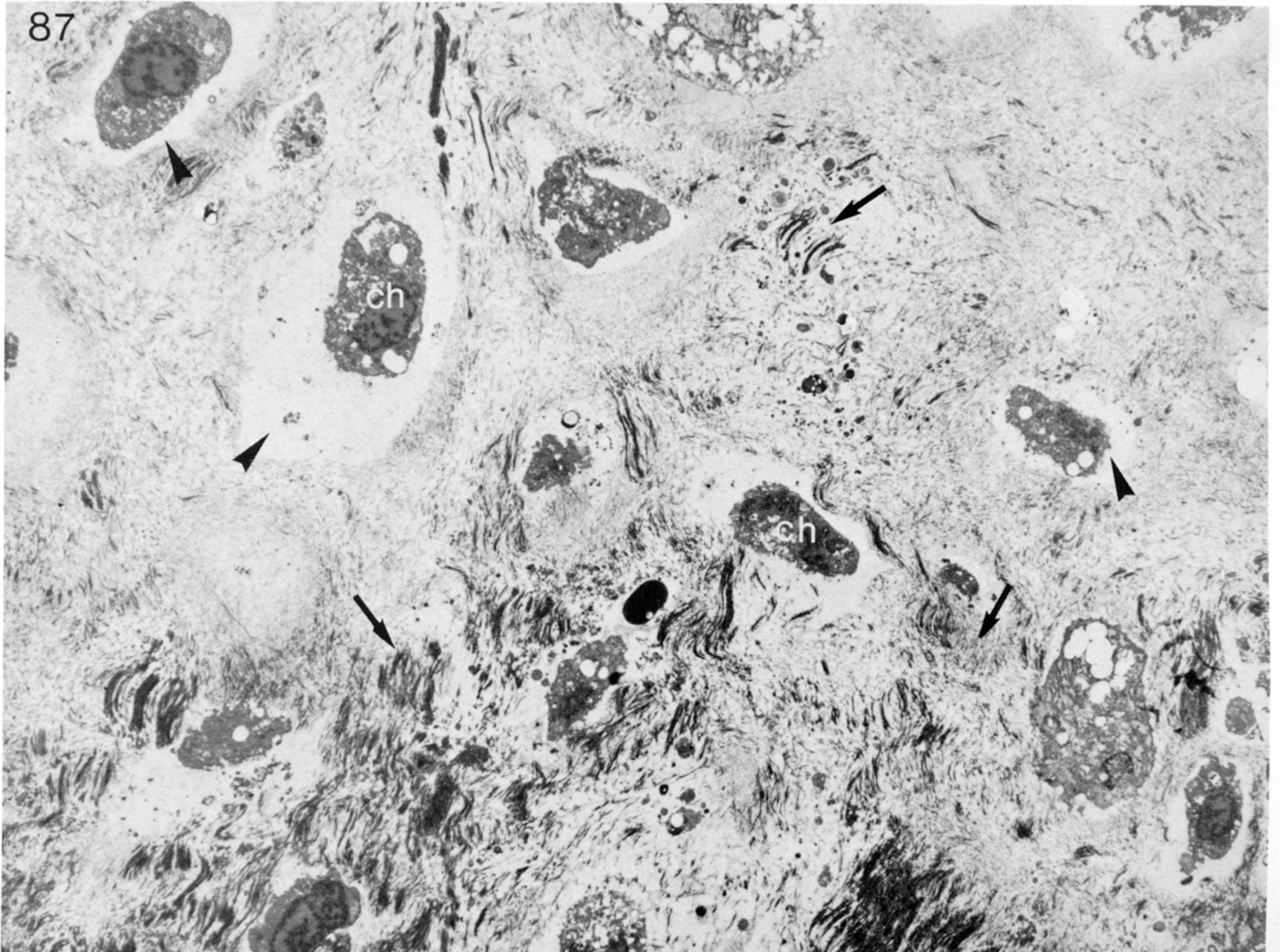
FIGURES 84 AND 85. For description see facing plate 17.



86

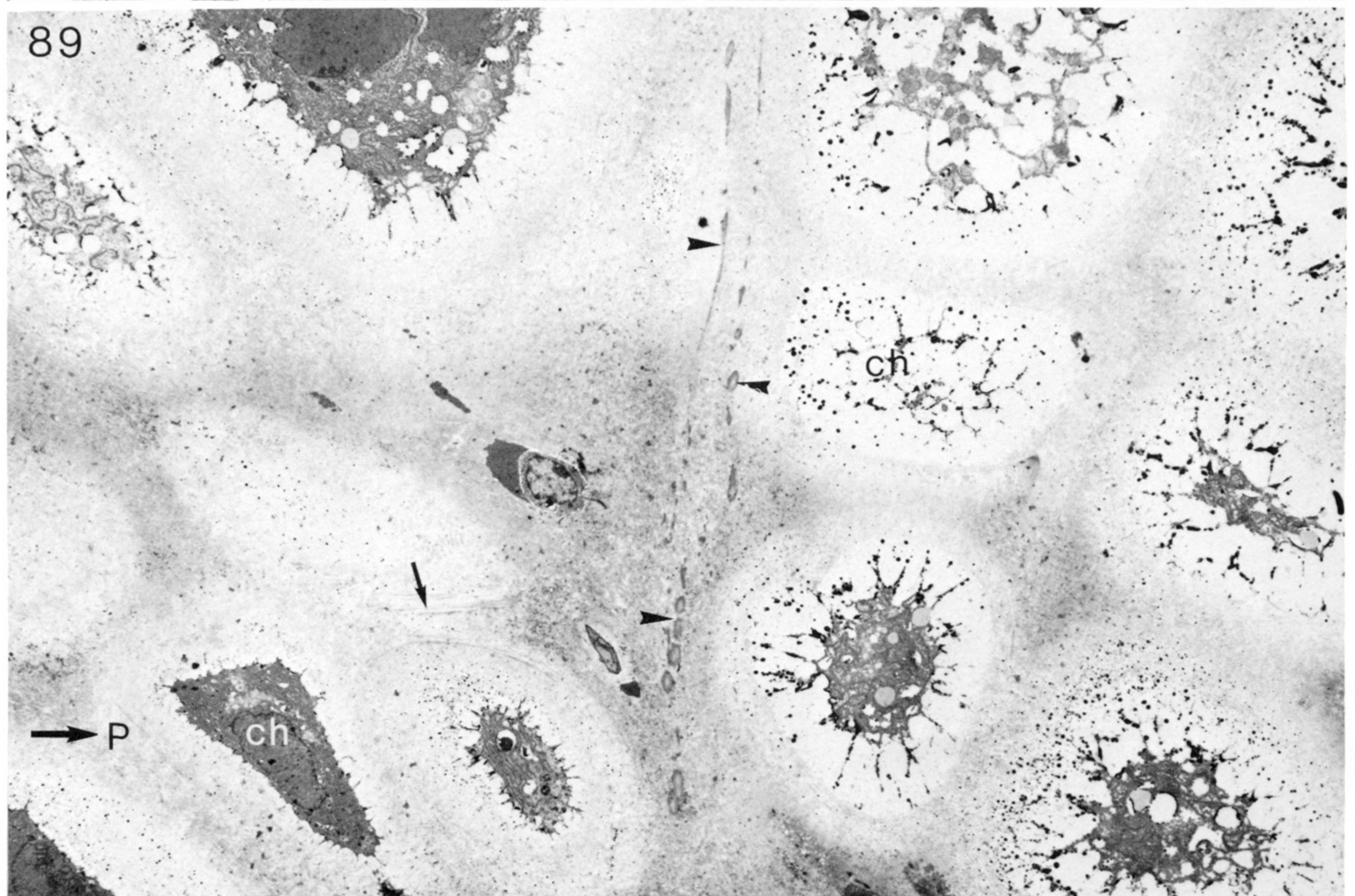
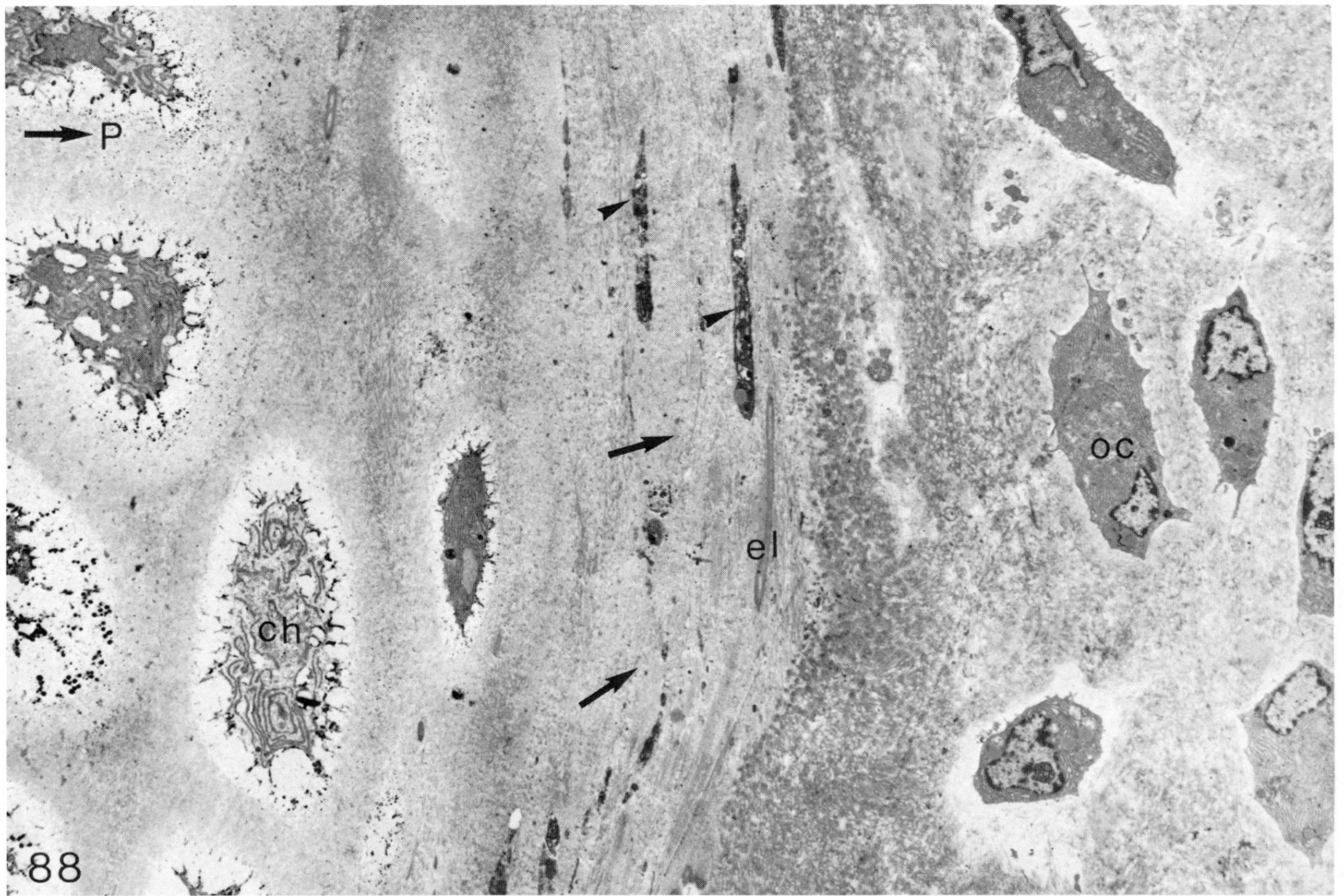


87



FIGURES 86 AND 87. For description see facing plate 17.





FIGURES 88 AND 89. For description see opposite.



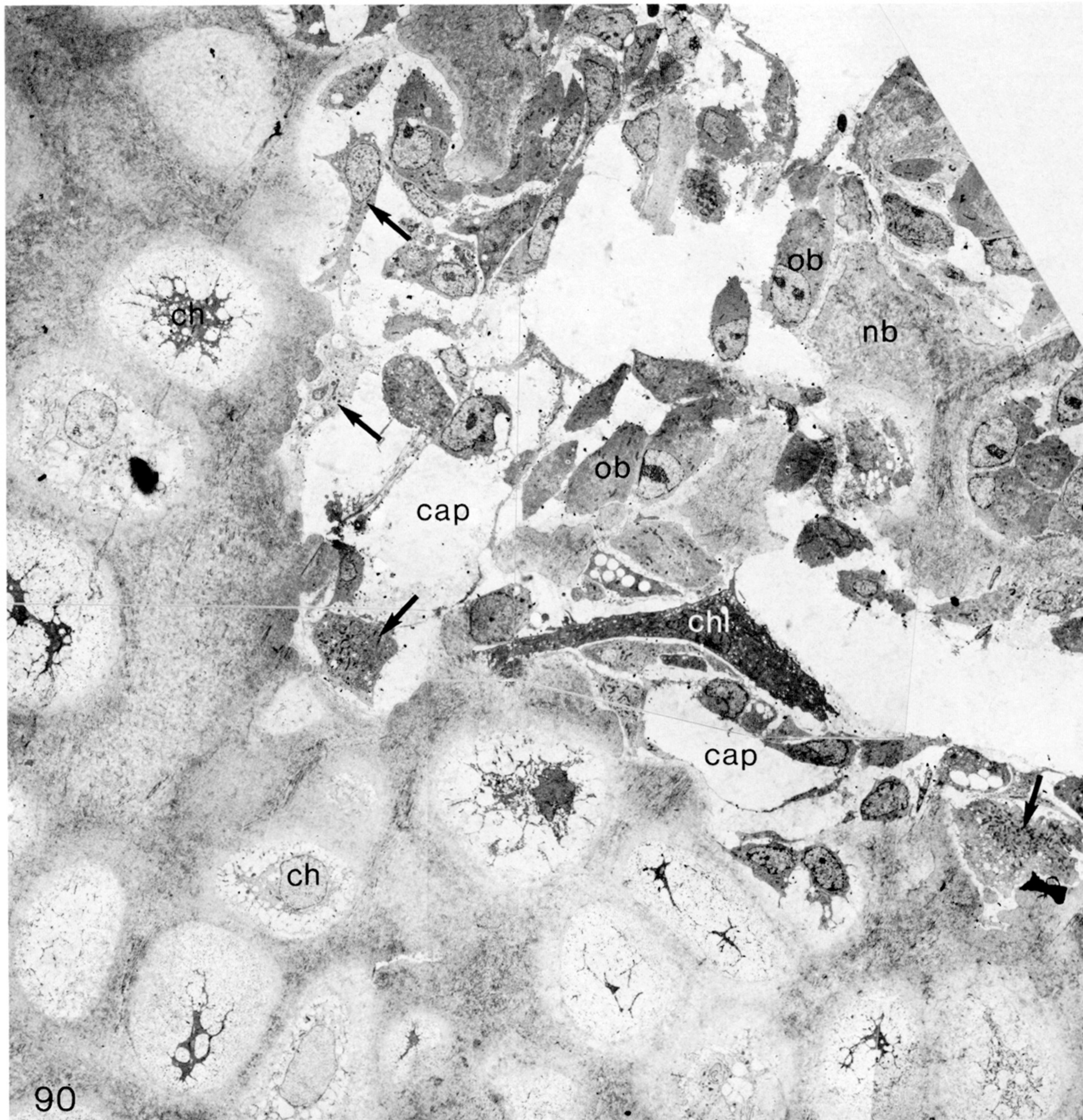
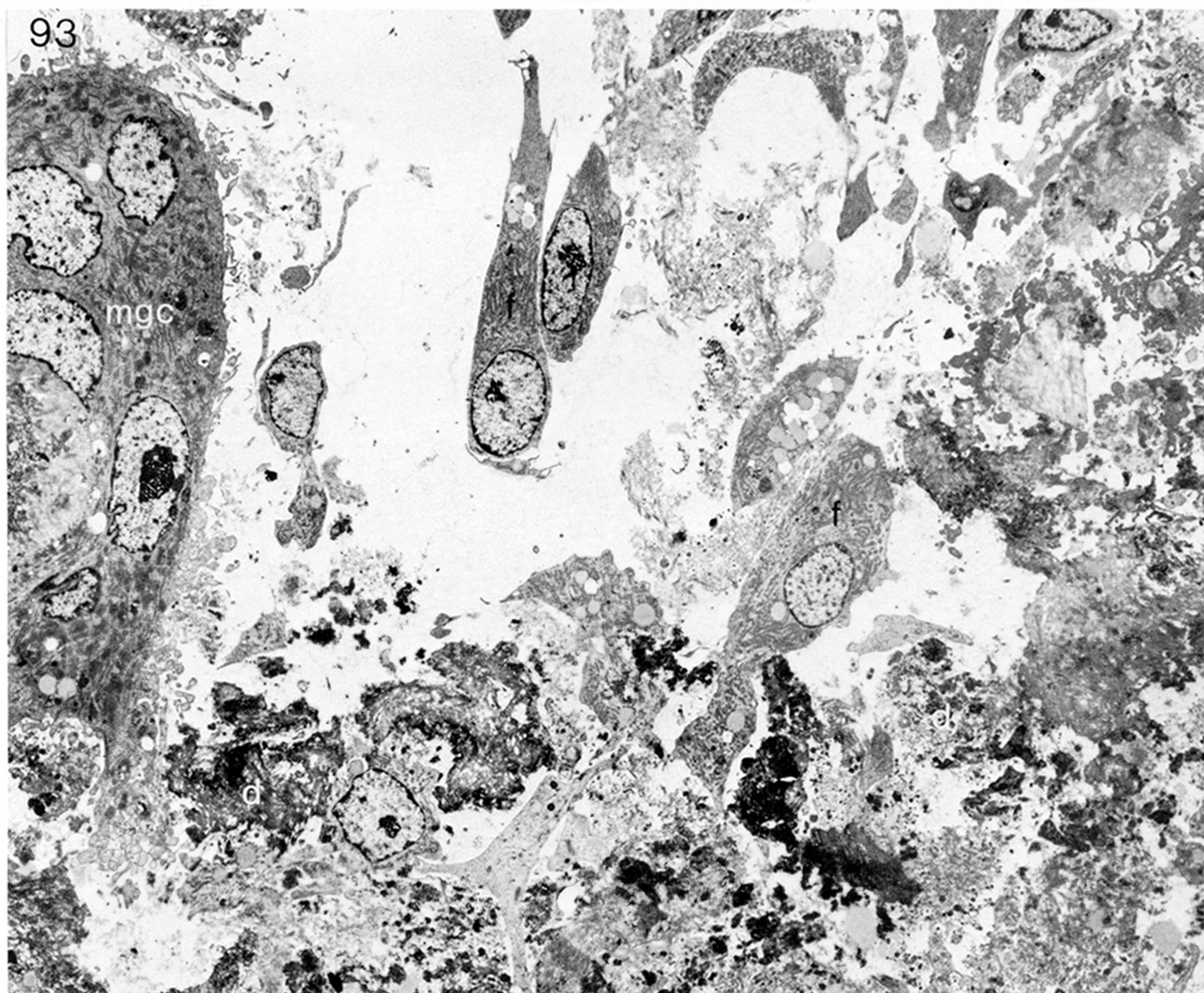
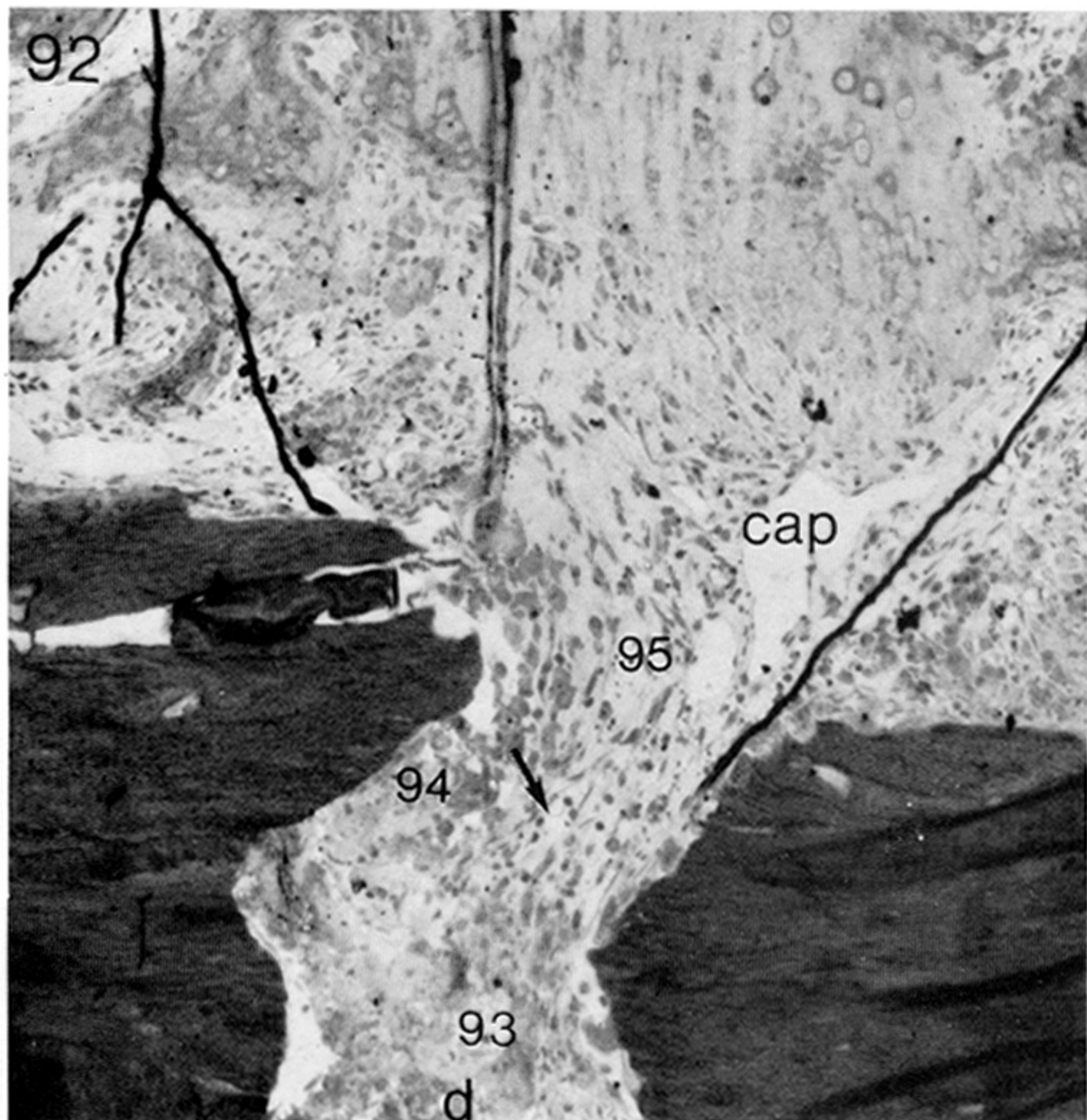
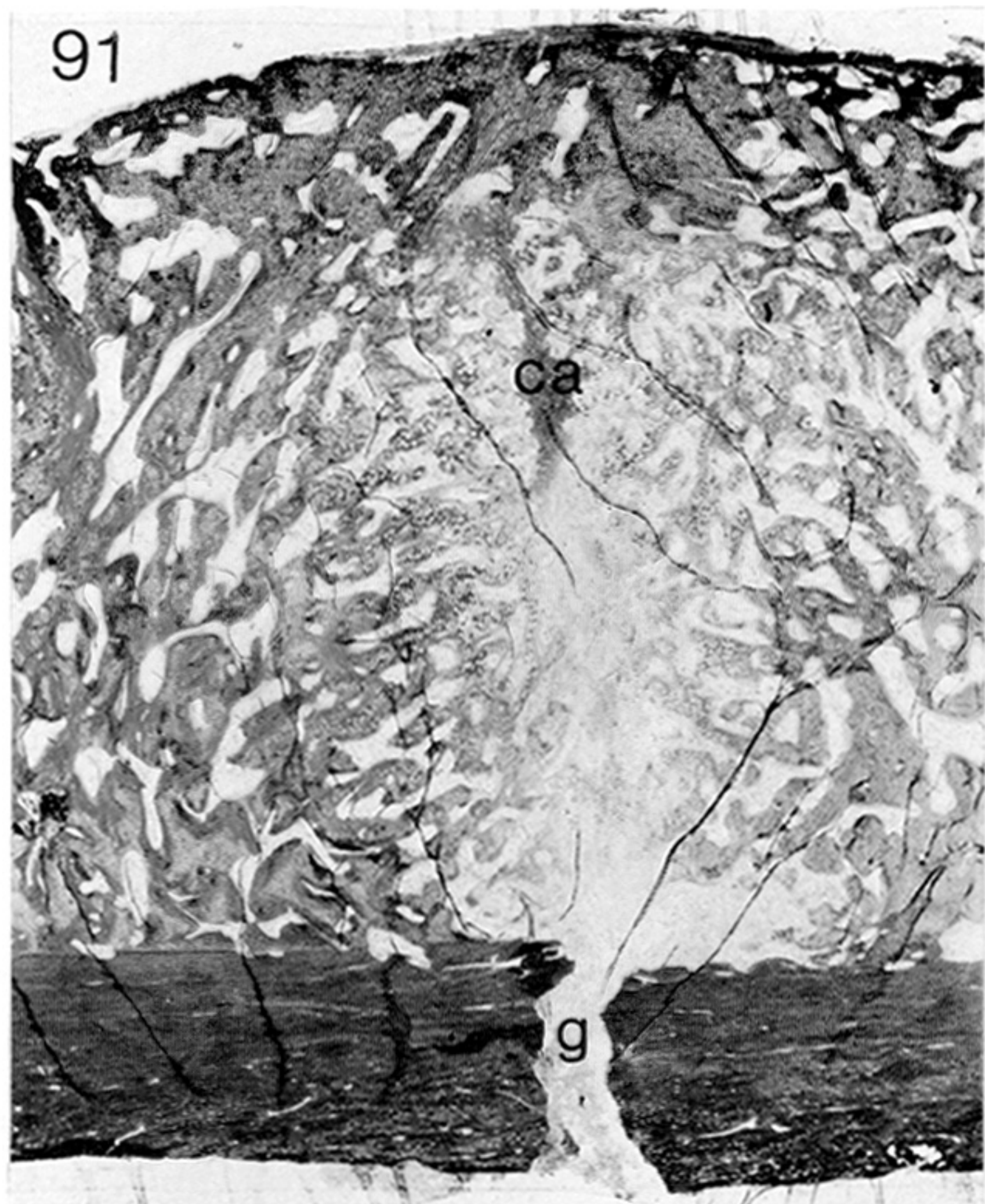


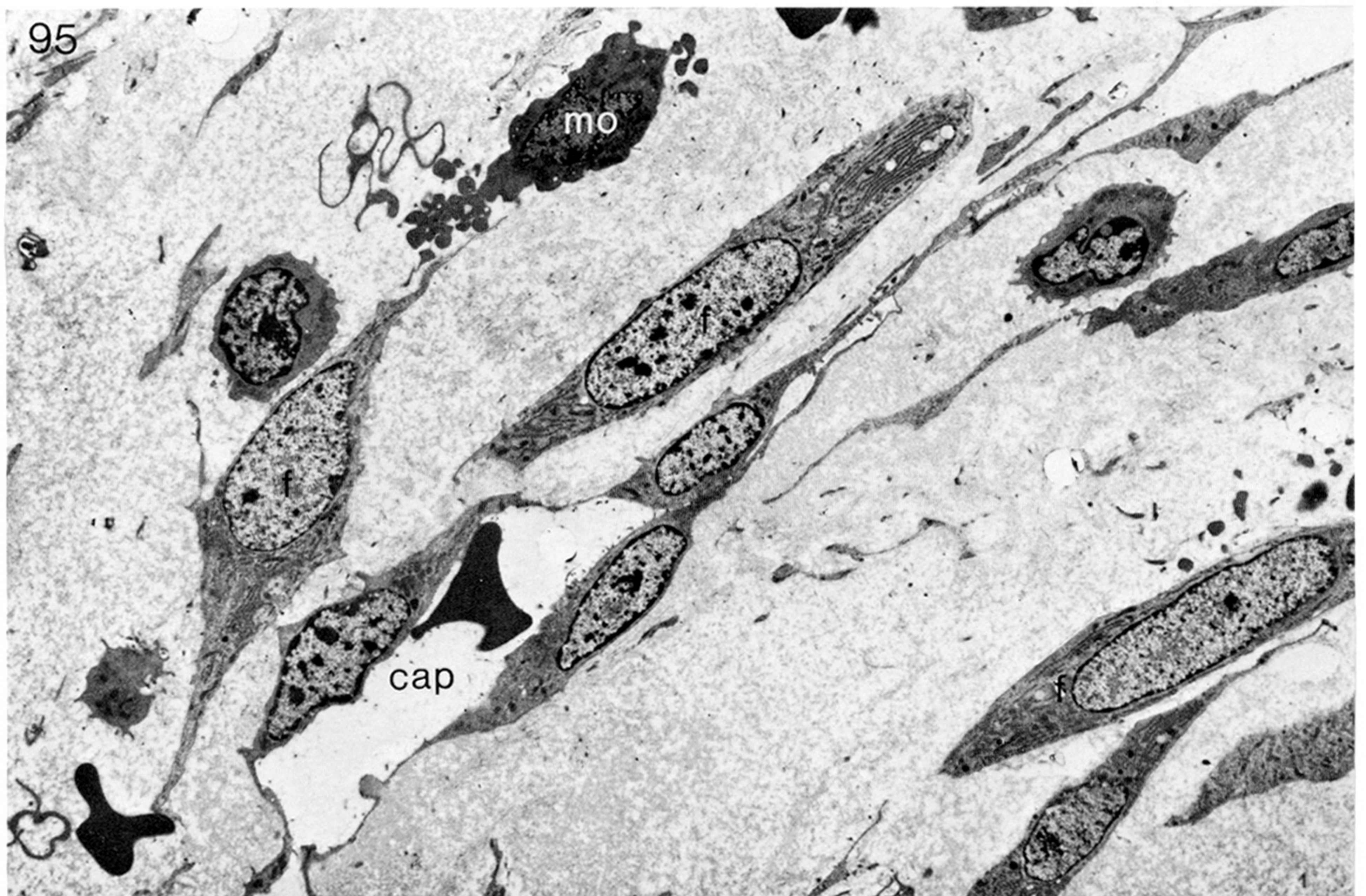
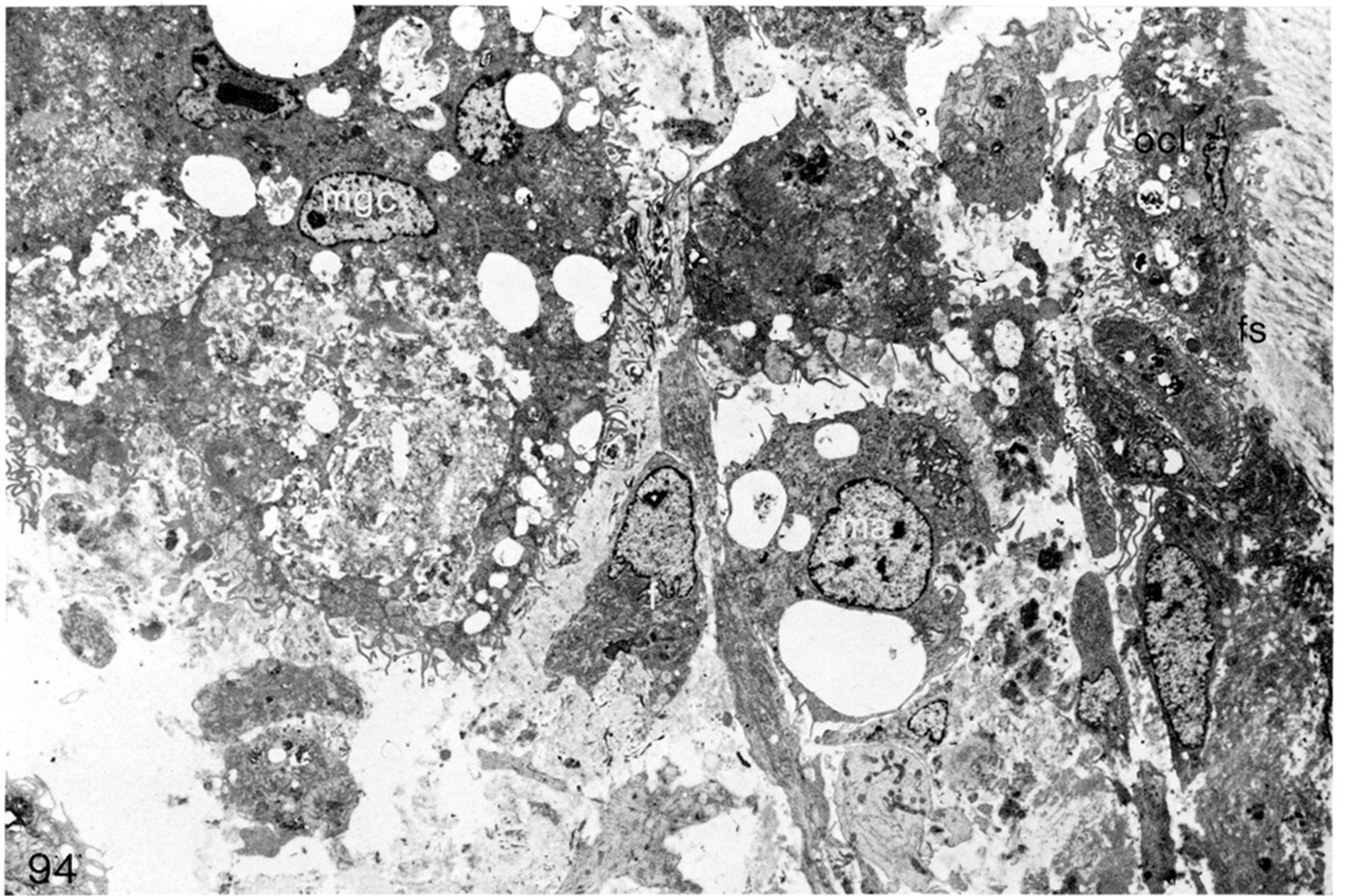
FIGURE 90. This montage of electron micrographs shows a region of endochondral ossification in the callus in figure 75 (= 90). The cartilage matrix, with hypertrophied chondrocytes (ch), is being resorbed by a series of cells, chondroclasts (chl) and mononuclear cells (arrows). Capillaries (cap) are invading the eroded areas, followed by osteoblasts (ob) laying down new bone (nb). (Magn.  $\times 1400$ .)





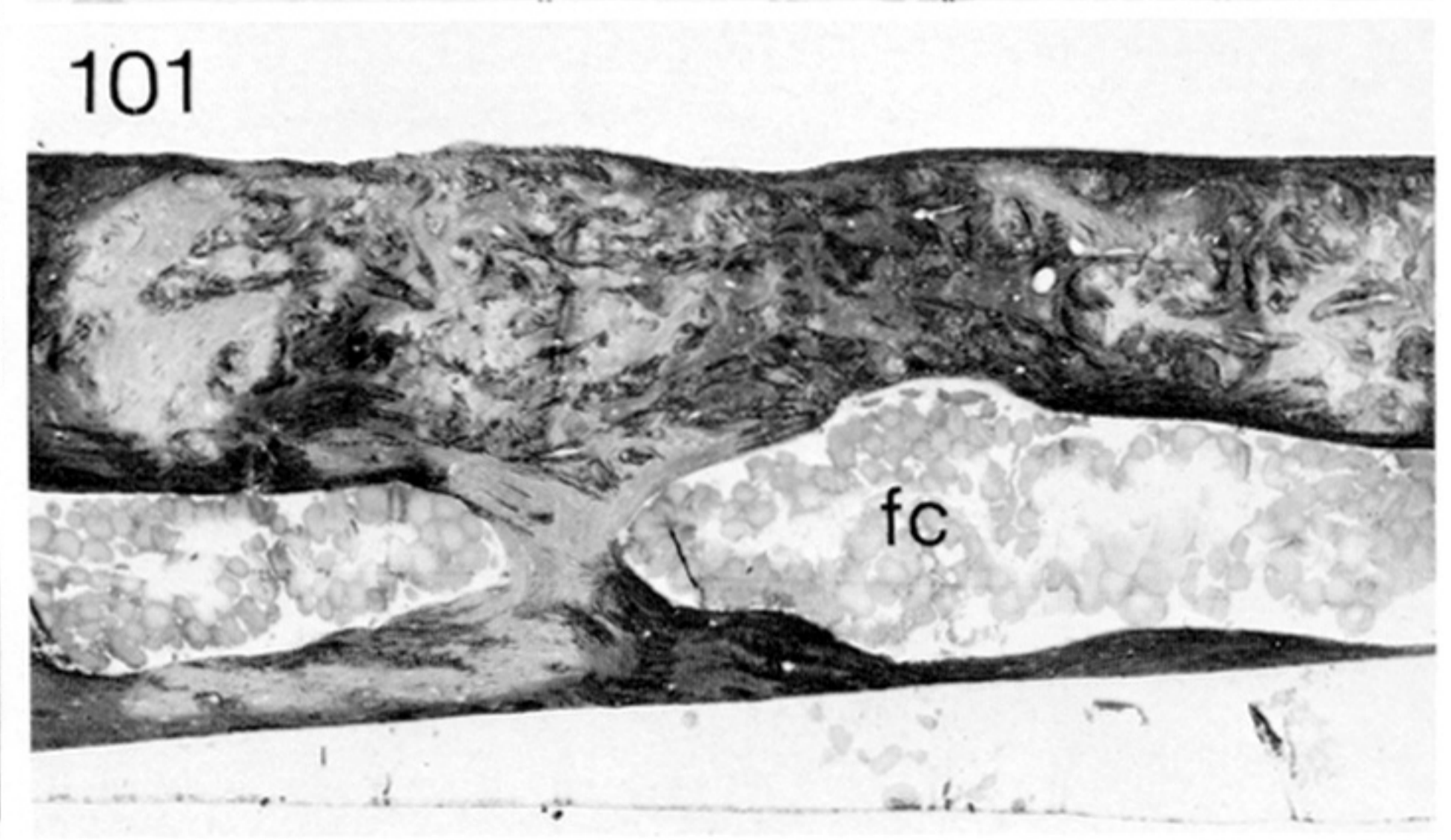
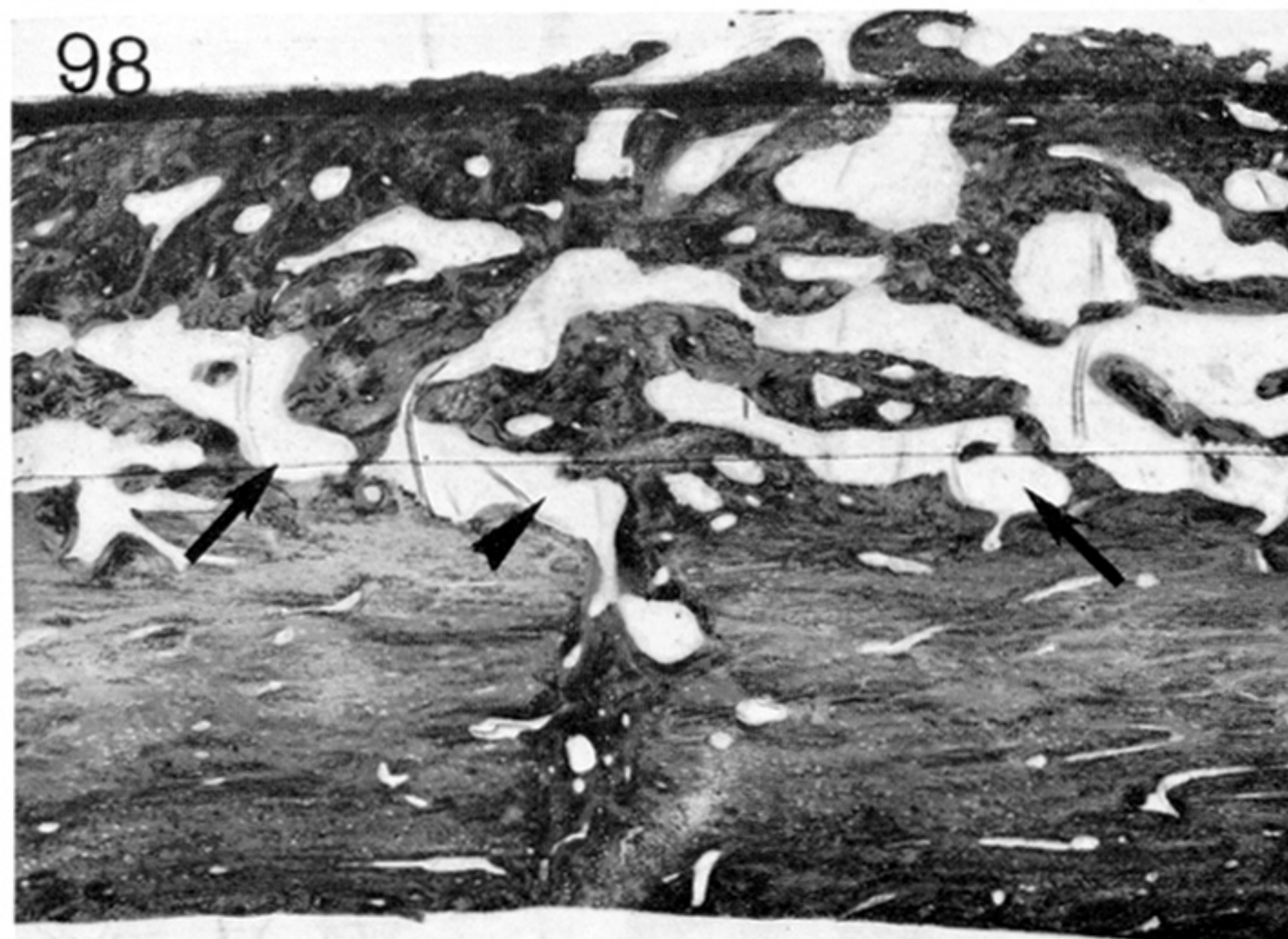
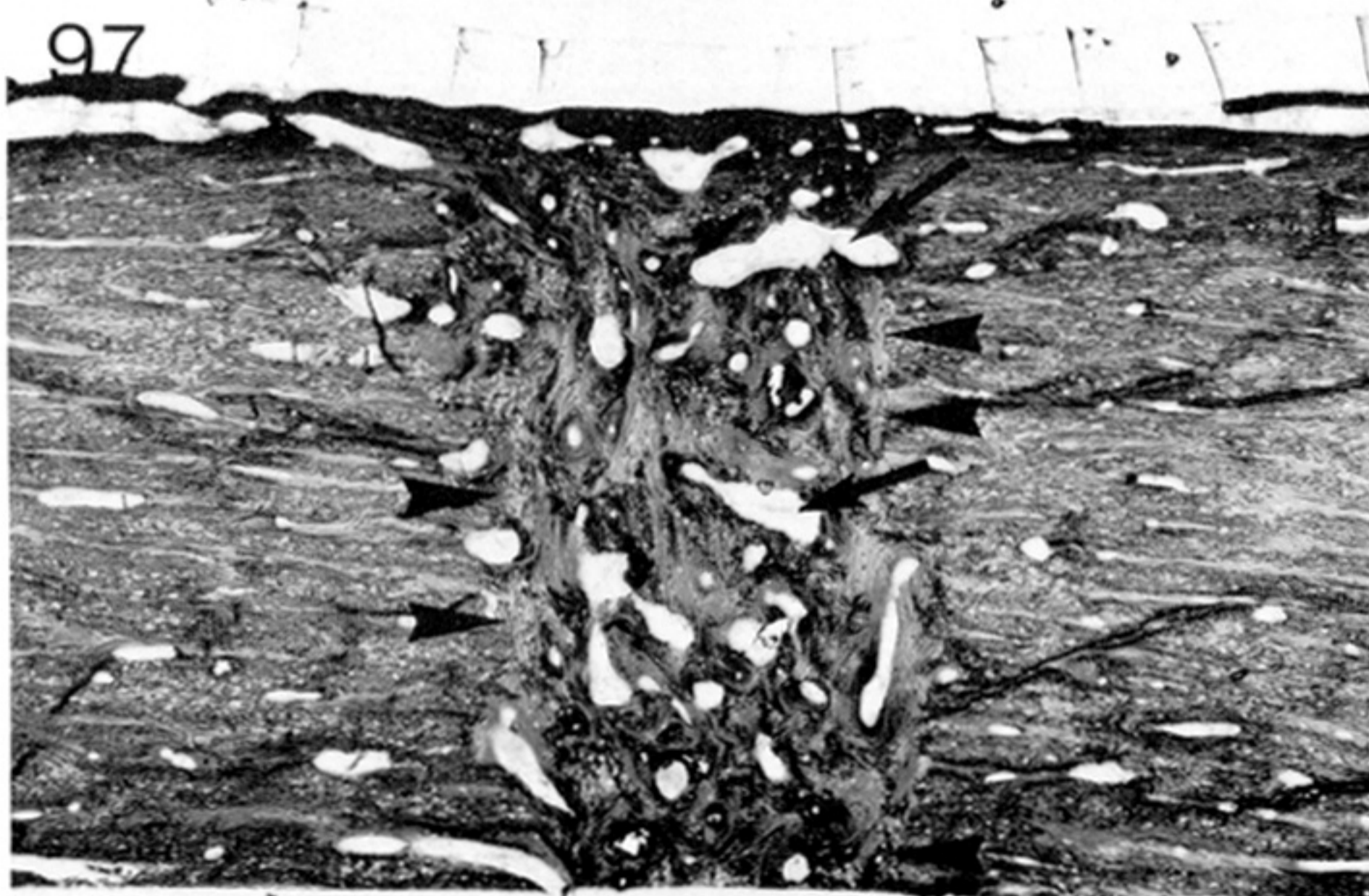
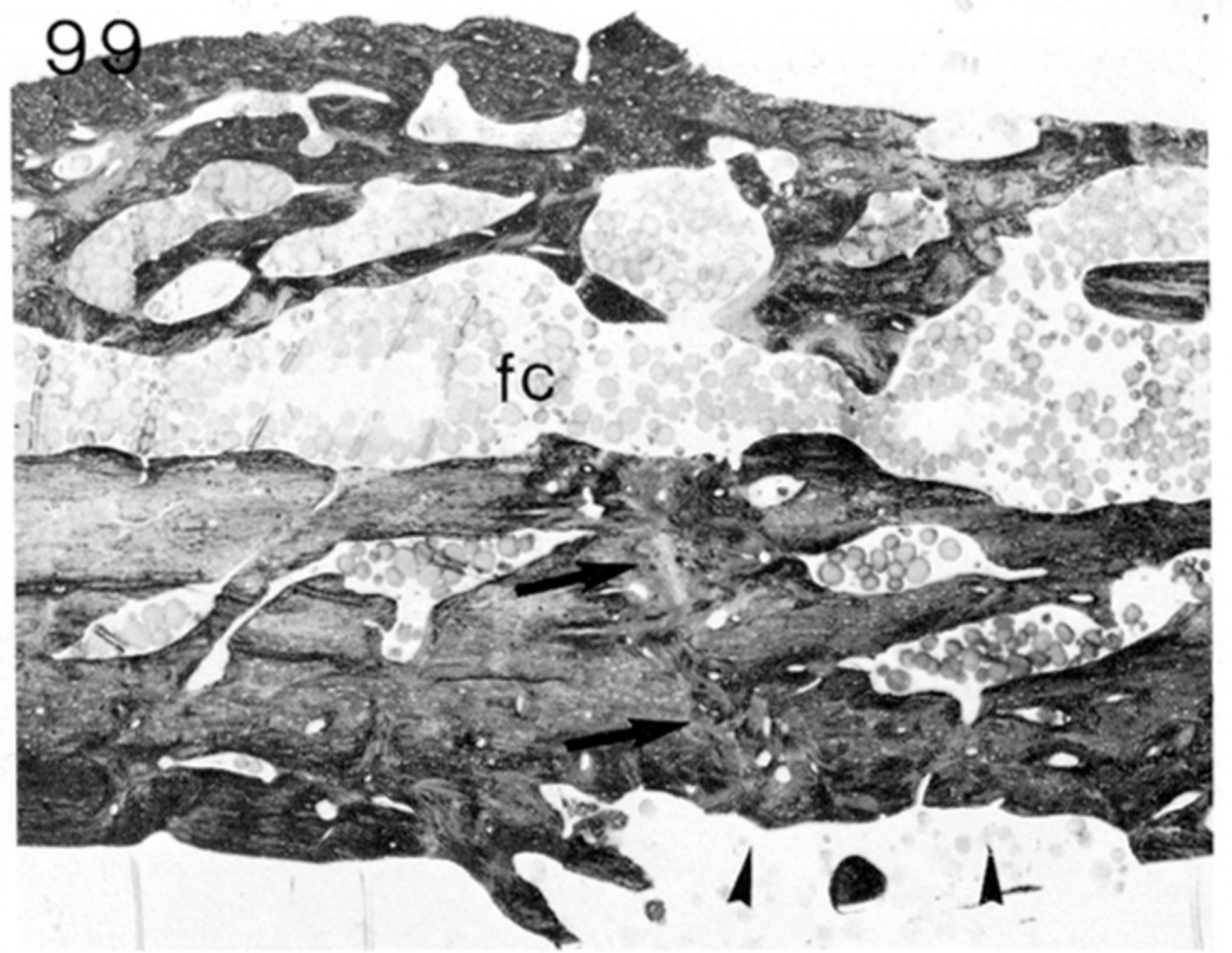
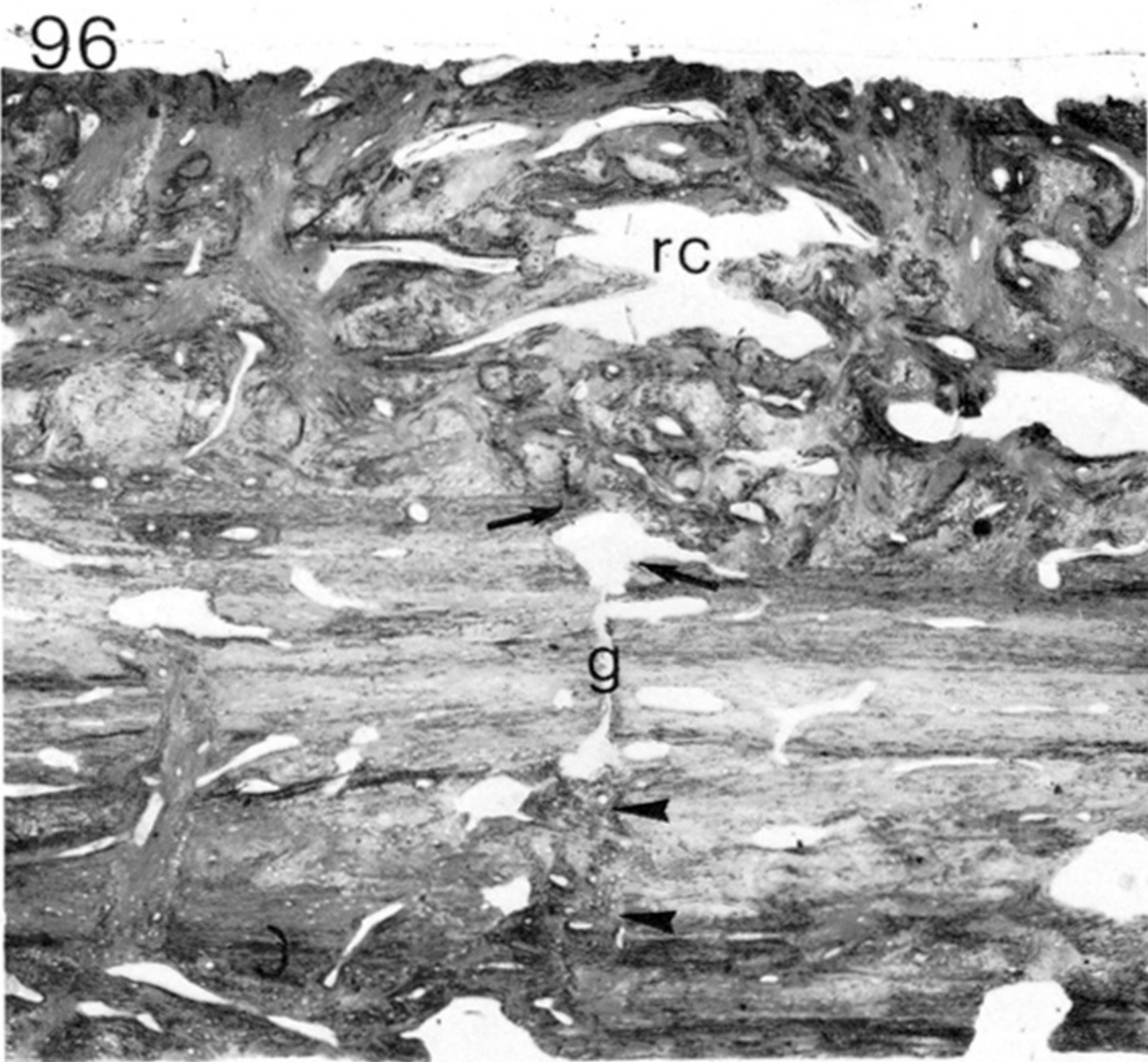
FIGURES 91-93. For description see facing plate 28.





FIGURES 94 AND 95. For description see facing plate 28.





FIGURES 96-102. For description see opposite.